University of Southampton

Faculty of Engineering and Physical Sciences

National Centre for Advanced Tribology at Southampton

Effect of lubrication on tribological properties of PEEK and PEEK composites

by

Go Tatsumi

Thesis for the degree of Doctor of Philosophy

November 2021

University of Southampton

Abstract

Faculty of Engineering and Physical Sciences

National Centre for Advanced Tribology at Southampton}

Doctor of Philosophy

Effect of lubrication on tribological properties of PEEK and PEEK composite

by

Go Tatsumi

Polymers and polymer-based composites are becoming the preferred materials in many tribological applications due to their advantages such as lightweight, reduced noise and self-lubricating properties. In terms of green technology, reducing weight by replacing metallic parts for polymeric ones is a very promising way to improve fuel efficiency in the automotive industry. Poly-Ether-Ether-Ketone (PEEK) and its composites have superior mechanical properties and higher thermal stability than other conventional polymers which make them suitable for tribological applications operating under severe conditions. Lubrication has the potential to reduce further friction and wear. However, the tribological behaviour of PEEK and its composites under lubrication has been less reported than under dry conditions, and a solid understanding of the lubrication mechanism is still lacking. Therefore, the aim of this study is to elucidate the effect and mechanism of lubrication on the tribological properties of PEEK and its composites.

Tribological tests were mainly performed on PEEK-steel and PEEK composites-steel contacts using a Mini Traction Machine (MTM) which simulates the sliding-rolling contact motion as encountered in gears, one of the main expected applications of this study. In addition to pure PEEK, carbon fibre reinforced (CFR) PEEK and glass fibre reinforced (GFR) PEEK as typical PEEK composites were investigated paired with steel counterparts. Base oils with/without lubricant additives, namely organic friction modifiers (OFMs) and anti-wear (AW) additives, were applied as test lubricants. To further investigate the mechanism of action, after-test specimens were analysed using various surface analysis techniques e.g., 3D surface profilometer, nanoindentation, Electron Probe Micro Analysis (EPMA), X-ray Photoelectron Spectroscopy (XPS) and Raman spectroscopy.

The results indicate that the polymer transfer film that formed on the steel counterparts is the dominant factor controlling the tribological properties of the PEEK-steel and PEEK composites-steel contacts, especially when the steel has a rough surface. The polymer transfer films are assumed to act as protective films, thus preventing the direct contact of the relatively soft polymer surfaces with the hard asperities of the steel surfaces and so reducing the wear of the polymers. Although this contribution of polymer transfer films has been previously found in dry conditions, this study reveals their significance under lubrication and the mechanism of action. Furthermore, the novelty of this study is that essential but little-known knowledge such as the effect and working mechanism of lubricant oil viscosity and lubricant additives (OFMs and AW additives) on tribological properties of the PEEK-steel and PEEK composites-steel contacts, was discussed based on the tribological test results and surface analyses of after-test specimens.

Table of Contents

Table of Contents ..... **i**

Table of Tables ..... **vii**

Table of Figures ..... **ix**

Research Thesis: Declaration of Authorship ..... **xxv**

Acknowledgements ..... **xxvii**

Definitions and Abbreviations ..... **xxix**

Chapter 1 Introduction **33**

1.1 Back ground 33

1.2 Aims and objectives 34

1.3 Thesis outline 35

Chapter 2 Literature Review **37**

2.1 Tribology of polymers 37

2.1.1 Introduction 37

2.1.2 Polymers for tribological applications 39

2.1.3 Factors influencing the tribology of polymers 44

2.1.4 Tribology of PEEK and PEEK composites 47

2.2 Lubrication of polymers 56

2.2.1 Introduction 56

2.2.2 Lubrication regime 58

2.2.3 Lubricants and lubricant additives 60

2.2.4 Factors influencing the lubrication of polymers 65

2.2.5 Lubrication of PEEK and PEEK composites 68

2.3 Summary 76

Chapter 3 Methodology **79**

3.1 Materials 79

3.1.1 Polymer specimens 79

3.1.2 Steel specimens 80

3.1.3 Lubricants 81

3.1.3.1 Base oils 81
3.1.3.2 Lubricant additives 82
3.2 Tribological testing 85
3.2.1 Test rig 85
3.2.2 Test configurations 85
3.2.3 Test profiles 86
3.3 Surface analyses 89
3.3.1 Surface profilometer 89
3.3.2 Nanoindentation 90
3.3.3 EPMA 91
3.3.4 XPS 91
3.3.5 Raman spectroscopy 92
3.4 Summary 92
Chapter 4 Base oil lubrication of PEEK 93
4.1 Results: Comparison of dry and base oil lubrication 93
4.1.1 Friction and wear performance 93
4.1.2 Surface analyses 97
4.1.2.1 Nanoindentation 97
4.1.2.2 EPMA 98
4.1.2.3 XPS 100
4.1.3 Testing with preconditioned steel balls 102
4.2 Results: Effect of lubricant oil viscosity 104
4.2.1 Friction and wear performance 105
4.2.2 Surface analyses 107
4.2.2.1 Nanoindentation 108
4.2.2.2 EPMA 109
4.3 Discussion 111
4.3.1 Hardness modification of polymer surface 111
4.3.2 Polymer transfer films on steel counterparts 113

4.3.3 Working mechanism of base oil lubrication....115
4.4 Summary....118
Chapter 5 Effect of lubricant additives on lubrication of PEEK....121
5.1 Results: Effect of organic friction modifiers....121
5.1.1 Friction and wear performance....122
5.1.2 Surface analyses....127
5.1.2.1 Nanoindentation....127
5.1.2.2 EPMA....129
5.1.2.3 Raman spectroscopy....131
5.1.3 Testing in PEEK-PEEK and steel-steel contacts....132
5.2 Results: Effect of anti-wear additives....135
5.2.1 Friction and wear performance....135
5.2.2 Surface analyses....140
5.2.2.1 EPMA of polymer transfer films....140
5.2.2.2 EPMA of AW additive reaction films....142
5.2.3 Tests with AW additives on PEEK-PEEK and steel-steel contacts....144
5.3 Discussion....147
5.3.1 Working mechanism of OFMs....147
5.3.2 Working mechanism of AW additives....151
5.4 Summary....154
Chapter 6 Base oil lubrication of PEEK composites....157
6.1 Results: Comparison of dry and base oil lubrication....157
6.1.1 Friction and wear performance....157
6.1.2 Surface analyses....159
6.1.2.1 3D Profilometry....160
6.1.2.2 Nanoindentation....161
6.1.2.3 EPMA....163
6.1.3 Testing with base oil containing wear debris....166

6.2 Results: Effect of lubricant oil viscosity 169
6.2.1 Friction and wear performance 170
6.2.2 Surface analyses 174
6.2.2.1 3D Profilometry 174
6.2.2.2 EPMA 176
6.3 Discussion 178
6.3.1 Hardness modification of polymer surface 179
6.3.2 Polymer transfer films on steel counterparts 180
6.3.3 Working mechanism of base oil lubrication of PEEK composites 181
6.4 Summary 186
Chapter 7 Effect of lubricant additives on lubrication of PEEK composites 189
7.1 Results: Effect of organic friction modifiers 189
7.1.1 Friction and wear performance 189
7.1.2 Surface analyses 193
7.1.2.1 3D Profilometry 194
7.1.2.2 EPMA 195
7.1.3 Testing at higher temperature 197
7.2 Results: Effect of anti-wear additives 203
7.2.1 Friction and wear performance 203
7.2.2 Surface analyses 207
7.2.2.1 EPMA of polymer transfer films 208
7.2.2.2 EPMA of AW additive reaction films 209
7.2.3 Testing at higher temperature 211
7.3 Discussion 217
7.3.1 Working mechanism of OFMs 217
7.3.2 Working mechanism of AW additives 220
7.4 Summary 221
Chapter 8 Conclusions and future work 223

8.1 Conclusions.....223
8.2 Future work.....229

Appendix A Oil film thickness estimation 231

List of References 235

Table of Tables

Table 2.1. Tribological characteristics of polymers (adapted from [2]) 42

Table 2.2. Transfer layer efficiency factor at different temperatures (adapted from [19]) 47

Table 2.3. Thermal properties of the pure PEEK, CFR PEEK and GFR PEEK (reproduced from [89]) 49

Table 2.4. API base oil classification (source: https://www.api.org/) 61

Table 2.5. Types of lubricant additives (reproduced from [100]) 62

Table 2.6. Interactive features of various lubricant additives (reproduced from [101]) 62

Table 3.1. The typical properties of polymers used in this study 80

Table 3.2. Properties of base oils used in this study 82

Table 3.3. Test oil formulations with OFMs 84

Table 3.4. Test oil formulations with AW additives 84

Table 3.5. Standard test conditions of constant speed routine 87

Table 3.6. Standard test conditions of Stribeck routine 89

Table 8.1. Impact of SRR, oil viscosity, OFM and AW additive on tribological properties of PEEK and PEEK composites when paired with smooth and rough steel 228

Table of Figures

Figure 1.1. Thesis structure 36

Figure 2.1. Economic savings through tribology (in £ million at 1965 values) (adapted from [41]) 37

Figure 2.2. Key technologies for the reduction of CO_2 emissions (adapted from [42]) 38

Figure 2.3. Classification of plastics (polymers) (adapted from [44]) 39

Figure 2.4. Moulded polymer gear made of PEEK (adapted from [48]) 39

Figure 2.5. Seal rings made of polymers (polytetrafluoroethylene, PEEK and rubber) and steel (adapted from [49]) 40

Figure 2.6. Polymer ball bearings (left) and Polymer bearing cages (right) (adapted from [50]) 40

Figure 2.7. Schematic structure of hybrid bushings (lower right) and their use in various automotive locations, including shock absorbers (lower left) (adapted from [51]) 40

Figure 2.8. Polymer pyramid with regard to cost, performance and formability (adapted from [3]) 41

Figure 2.9. Microstructure of polymer composites with fillers (adapted from [3]) 42

Figure 2.10. Facture surface of polymer composites with fillers (adapted from [66]) 43

Figure 2.11. Typical forms of plastic gear failure (adapted from [12]) 43

Figure 2.12. Ambient temperature effects on (a) wear rates and (b) transition torques of POM gears to composite gears (adapted from [75]) 44

Figure 2.13. (a) Effect of cooling on the wear resistance of PP gears to steel gears and (b) PP gear tooth thickness reduction during testing (adapted from [14]) 45

Figure 2.14. Optical images of the worn teeth profiles with an increasing number of cycles at controlled temperatures (adapted from [17]) 45

Figure 2.15. Running-in (left) and steady-state friction (right) with dynamic balance of polymer film (adapted from [56]) 46

Figure 2.16. Friction stages between polymer/steel pairs (adapted from [56]) 46

Figure 2.17. Schematic illustration of the contact modes of polymer composites against steel counterparts (adapted from [84]) 47

Figure 2.18. Chemical structure of PEEK 48

Figure 2.19. Scheme of the PEEK synthesis in diphenylsulfone (adapted from [87]) 48

Figure 2.20. Effect of fibre content on the tensile properties of CFR PEEK (left) and GFR PEEK (right) (adapted from [88]) 49

Figure 2.21. Appearance of PEEK transfer film formed on the steel ball (adapted from [90]) .. 50

Figure 2.22. Wear volumes in different sliding motions (adapted from [91]) 50

Figure 2.23. PEEK transfer films formed on the steel counter surface in different sliding motions (adapted from [91]) 51

Figure 2.24. Wear test results for PEEK on mild steel with different roughness (adapted from [92]) 52

Figure 2.25. Specific wear rates of PEEK as a function of steel roughness. The sliding direction was parallel (II) and perpendicular (⊥) to the steel roughness (adapted from [93])52

Figure 2.26. Friction coefficients (left) and wear rates (right) of PEEK composites paired with steel as a function of content of carbon fibres (adapted from [20]) 53

Figure 2.27. Friction coefficients under different contact configuration (adapted from [94]) .. 53

Figure 2.28. (a) Schematic of test apparatus and (b) designations of fibre orientations (adapted from [95]) 54

Figure 2.29. Wear rates in the three orientations as a function of apparent pressure (adapted from [95]) 54

Figure 2.30. Friction coefficients and wear rates as a function of content of PTFE (adapted from [20]) 55

Figure 2.31. Schematic of the lubricating of PTFE (adapted from [20]) 55

Figure 2.32. Friction coefficients (left) and wear rates (rights) of the PEEK composites with MoS_2 and WS_2 (adapted from [96]) 56

Figure 2.33. Wear rates of different materials sliding on stainless steel. Full lines, water lubricated; dotted lines, unlubricated. (adapted from [30]) 57

Figure 2.34. Friction coefficients and wear rates for PPO, PEEK and PTFE in dry and lubricated conditions (adapted from [25]) 58

Figure 2.35. Schematics of lubrication regimes (adapted from [98]) 58

Figure 2.36. Lubricant film parameter (h/σ) (upper) and friction coefficient (lower) as a function of ηN/P (Stribeck curve) (adapted from [98]).....60

Figure 2.37. Typical chemical structures contained in mineral oils : (a) straight paraffin, (b) branched paraffin, (c) naphthene, and (d) aromatic (adapted from [99]).....61

Figure 2.38. Schematic of the adsorption of OFM on a metallic surface (adapted from [98])....63

Figure 2.39. Schematic of OFM molecular layer on a metallic surface (adapted from [99]).....63

Figure 2.40. Structure of ZDDP (adapted from [113]).....64

Figure 2.41. Schematic of structure and composition of ZDDP reaction film (adapted from [39])64

Figure 2.42. Schematic of TCP decomposition and film formation on steel (adapted from [114])64

Figure 2.43. PA66 gear life under dry and lubricated condition; the circled area indicates the presence of thermal failures of polymer gears (adapted from [122]) 65

Figure 2.44. Effect of water additions following unlubricated sliding (adapted from [30]) 66

Figure 2.45. Effect of diesel injection following unlubricated sliding (adapted from [124]) 66

Figure 2.46. Tribological performance of PPS composites under dry and diesel lubricated conditions (adapted from [28]) 67

Figure 2.47. Friction coefficients and wear rates of epoxy composites under oil lubrication (adapted from [125]) 68

Figure 2.48. Friction coefficients (left) and wear rates (right) of PEEK composite under dry and water lubrication (adapted from [26]) 69

Figure 2.49. Friction coefficients and wear rates of pure PEEK (left) and GFR PEEK (right) under dry and water lubrication (adapted from [27]) 69

Figure 2.50. Friction coefficients (left) and wear rates (right) of CFR PEEK under dry, pure water and sea water lubrication (adapted from [126]) 70

Figure 2.51. Friction coefficients and wear rates of pure PEEK (left) and PEEK composite (right) as a function of diesel flow rate (adapted from [33]) 71

Figure 2.52. Wear volumes of St50, pure PEEK and PEEK Composite paired with steel under engine oil lubrication (adapted from [33]) 71

Figure 2.53. Wear rates of PPS and PEEK under dry and water lubrication (adapted from [31]) 72

Figure 2.54. Hardness of PEEK (upper) and PPS (lower) at the sliding area (adapted from [31]) 72

Figure 2.55. Polymer transfer films (TFLs) thickness distribution on wear-tracks under (a) dry and (b) water lubrication (adapted from [32]) 73

Figure 2.56. Hardness as a function of indentation load on worn PEEK wear-tracks after dry and water lubricated test as well as original PEEK surface (adapted from [32]) ... 73

Figure 2.57. Friction coefficients (left) and wear rates (right) of PEEK composite paired with Si_3N_4 under dry and water lubrication (adapted from [129]) 74

Figure 2.58. Wear rates of CFR PEEK paired with different material counterparts (adapted from [34]) 75

Figure 2.59. SE images of the wear track on W-DLC under (a) dry and (b) water lubrication (adapted from [34]) 75

Figure 3.1. Appearance of polymer specimens (Pure PEEK ball and pure PEEK, CFR PEEK and GFR PEEK plates) 80

Figure 3.2. Appearance of steel specimens 81

Figure 3.3. Chemical structures of hydrocarbons contained in PAO 82

Figure 3.4. Chemical structures of OFMs used in this study 83

Figure 3.5. Chemical structures of AW additives used in this study 84

Figure 3.6. Photograph of MTM 85

Figure 3.7. MTM (a) set-up appearance and configurations of (b) polymer-steel, (c) polymer-polymer and (d) steel-steel 86

Figure 3.8. Constant speed routine sequence 87

Figure 3.9. Stribeck routine sequence 88

Figure 3.10. Example of Stribeck curve 88

Figure 3.11. Typical appearance of after-test polymer plate 89

Figure 4.1. Friction coefficients in dry and PAO4 lubricated conditions 94

Figure 4.2. Low magnification optical images of after-test PEEK plates in (a, b) dry and (c, d) PAO4 lubricated conditions 94

Figure 4.3. High magnification optical images of after-test PEEK plates in (a, b) dry and (c, d) PAO4 lubricated conditions 95

Figure 4.4. Wear profiles of PEEK plates in (a, b) dry and (c, d) PAO4 lubricated conditions 95

Figure 4.5. Friction coefficients averaged during last ten minutes and SWRs of PEEK plates 96

Figure 4.6. Nanoindentation hardness of after-test PEEK plates in (a, b) dry and (c, d) PAO4 lubricated conditions 97

Figure 4.7. Nanoindentation hardness of after-test PEEK plates at 2 μm depth 98

Figure 4.8. Optical images of after-test steel balls in (a, b) dry and (c, d) PAO4 lubricated conditions 99

Figure 4.9. EMPA carbon maps of after-test steel balls in (a, b) dry and (c, d) PAO4 lubricated conditions 100

Figure 4.10. XPS C1s spectrum of unused PEEK plate 101

Figure 4.11. XPS C1s spectra of after-test steel balls in (a, b) dry and (c, d) PAO4 lubricated conditions 101

Figure 4.12. EPMA carbon maps of (a) preconditioned steel ball and (b, c) after-test steel balls with preconditioned steel balls 102

Figure 4.13. Friction coefficients with new and preconditioned rough steel balls in dry and PAO4 lubricated conditions 103

Figure 4.14. Friction coefficients averaged during last ten minutes and SWRs of PEEK plates 104

Figure 4.15. Friction coefficients with smooth steel balls 105

Figure 4.16. Optical images of after-test PEEK plates paired with smooth steel balls lubricated with (a) PAO2, (b) PAO4, and (c) PAO10 106

Figure 4.17. Friction coefficients with rough steel balls 106

Figure 4.18. Optical images of after-test PEEK plates paired with rough steel balls lubricated with (a) PAO2, (b) PAO4 and (c) PAO10 107

Figure 4.19. Wear profiles of PEEK plates paired with rough steel balls lubricated with (a) PAO2, (b) PAO4 and (c) PAO10 107

Figure 4.20. Nanoindentation hardness of after-test PEEK plates paired with smooth steel balls lubricated with (a) PAO2, (b) PAO4 and (c) PAO10 108

Figure 4.21. Nanoindentation hardness of after-test PEEK plates paired with rough steel balls lubricated with (a) PAO2, (b) PAO4 and (c) PAO10 109

Figure 4.22. SE images of after-test rough steel balls lubricated with (a) PAO2, (b) PAO4 and (c) PAO10 110

Figure 4.23. EPMA carbon maps of after-test rough steel balls lubricated with (a) PAO2, (b) PAO4 and (c) PAO10 110

Figure 4.24. Relationship between nanoindentation hardness of after-test PEEK plates and friction coefficients; the optical images show the wear tracks on PEEK plates111

Figure 4.25. Schematics of base oil permeation on low and higher damage PEEK surface 112

Figure 4.26. Relationship between nanoindentation hardness of PEEK plates and wear volumes; the side graphs show the wear profiles of PEEK plates 113

Figure 4.27. Schematic of PEEK transfer film formation/removal in dry condition 114

Figure 4.28. Schematic of PEEK transfer film formation/removal in base oil lubricated condition 114

Figure 4.29. Friction coefficients of PEEK-steel contact as a function of Lambda ratios 116

Figure 4.30. Schematic of removal (through wear) and compression of PEEK asperities..... 116

Figure 4.31. Friction coefficients of PEEK-steel contact as a function of modified Lambda ratios117

Figure 4.32 Schematic of contact surfaces lubricated with different grades of PAOs 118

Figure 5.1. Stribeck curves with smooth steel balls at 50% SRR for PAO4 and PAO4 + OFMs. 123

Figure 5.2. Stribeck curves with smooth steel balls at 200% SRR for PAO4 and PAO4 + OFMs123

Figure 5.3. Stribeck curves with rough steel balls at 50% SRR for PAO4 and PAO4 + OFMs....124

Figure 5.4. Stribeck curves with rough steel balls at 200% SRR for PAO4 and PAO4 + OFMs..124

Figure 5.5. Optical images of after-test PEEK plates paired with rough steel balls at 50% SRR and lubricated with (a) PAO4 and (b-d) PAO4 + OFMs.....125

Figure 5.6. Optical images of after-test PEEK plates paired with rough steel balls at 200% SRR and lubricated with (a) PAO4 and (b-d) PAO4 + OFMs.....125

Figure 5.7. Wear profiles of PEEK plates paired with rough steel balls at 50% SRR and lubricated with (a) PAO4 and (b-d) PAO4 + OFMs.....126

Figure 5.8. Wear profiles of PEEK plates paired with rough steel balls at 200% SRR and lubricated with (a) PAO4 and (b-d) PAO4 + OFMs.....126

Figure 5.9. Nanoindentation hardness of after-test PEEK plates paired with smooth steel balls lubricated with (a, c) PAO4 and (b, d) PAO + OSa 128

Figure 5.10. Nanoindentation hardness of after-test PEEK plates paired with rough steel balls lubricated with (a, c) PAO4 and (b, d) PAO + OSa 128

Figure 5.11. SE images of after-test rough steel balls lubricated with (a, c) PAO4 and (b, d) PAO4 + OSa.....129

Figure 5.12. EMPA carbon maps of after-test rough steel balls lubricated with (a, c) PAO4 and (b, d) PAO4 + OSa.....130

Figure 5.13. Peaks for Raman modes of PEEK.....131

Figure 5.14. Raman spectra of after-test rough steel balls lubricated with (a, c) PAO4 and (b, d) PAO4 + OSa 132

Figure 5.15. Stribeck curves in PEEK-PEEK contact at 50% SRR for PAO4 and PAO4 + OFMs .133

Figure 5.16. Stribeck curves in PEEK-PEEK contact at 200% SRR for PAO4 and PAO4 + OFMs 133

Figure 5.17. Stribeck curves in steel-steel contact at 50% SRR for PAO4 and PAO4 + OFMs...134

Figure 5.18. Stribeck curves in steel-steel contact at 200% SRR for PAO4 and PAO4 + OFMs.134

Figure 5.19. Stribeck curves with smooth steel balls at 50% SRR for PAO4 and PAO4 + AW additives.....136

Figure 5.20. Stribeck curves with smooth steel balls at 200% SRR for PAO4 and PAO4 + AW additives 136

Figure 5.21. Stribeck curves with rough steel balls at 50% SRR for PAO4 and PAO4 + AW additives 137

Figure 5.22. Stribeck curves with rough steel balls at 200% SRR for PAO4 and PAO4 + AW additives 137

Figure 5.23. Optical images of after-test PEEK plates paired with rough steel balls at 50% SRR lubricated with (a) PAO4 and (b, c) PAO4 + AW additives 138

Figure 5.24. Optical images of after-test PEEK plates paired with rough steel balls at 200% SRR lubricated with (a) PAO4 and (b, c) PAO4 + AW additives 138

Figure 5.25. Wear profiles of PEEK plates paired with rough steel balls at 50% SRR lubricated with (a) PAO4 and (b, c) PAO4 + AW additives..... 139

Figure 5.26. Wear profiles of PEEK plates paired with rough steel balls at 200% SRR lubricated with (a) PAO4 and (b, c) PAO4 + AW additives 139

Figure 5.27. SE images of after-test rough steel balls lubricated with (a, c) PAO4 and (b, d) PAO4 + ZDDP 141

Figure 5.28. EMPA carbon maps of after-test rough steel balls lubricated with (a, c) PAO4 and (b, d) PAO4 + ZDDP 141

Figure 5.29. (a, d) SE images and corresponding EPMA (b, e) phosphorus and (c, f) sulphur maps of after-test rough steel balls lubricated with PAO4 + ZDDP 143

Figure 5.30. (a, d) SE images and corresponding EPMA (b, e) phosphorus and (c, f) sulphur maps of after-test PEEK plates lubricated with PAO4 + ZDDP 144

Figure 5.31. Stribeck curves in PEEK-PEEK contact at 50% SRR for PAO4 and PAO4 + AW additives 145

Figure 5.32. Stribeck curves in PEEK-PEEK contact at 200% SRR for PAO4 and PAO4 + AW additives 145

Figure 5.33. Stribeck curves in steel-steel contact at 50% SRR for PAO4 and PAO4 + AW additives 146

Figure 5.34. Stribeck curves in steel-steel contact at 200% SRR for PAO4 and PAO4 + AW additives 147

Figure 5.35. Schematic effect of a sarcosine derivative of fatty acids on a metal surface 148

Figure 5.36. Impact of OFM on friction coefficients of PEEK-smooth steel contact at 200% SRR149

Figure 5.37. Proposed mechanism of lubrication with OFM in PEEK-smooth steel contact 151

Figure 5.38. Proposed mechanism of lubrication with OFM in PEEK-rough steel contact 151

Figure 5.39. Proposed mechanism of lubrication with AW additive in PEEK-smooth steel contact 152

Figure 5.40. Proposed mechanism of lubrication with AW additive in PEEK-rough steel contact154

Figure 6.1. Friction coefficients in dry and PAO4 lubricated conditions.....158

Figure 6.2. Optical images of after-test polymer plates in (a, c) dry and (b, d) PAO4 lubricated conditions 159

Figure 6.3. Wear profiles of polymer plates in (a, c) dry and (b, d) PAO4 lubricated conditions159

Figure 6.4. Optical images of wear tracks on polymer plates in (a, c) dry and (b, d) PAO4 lubricated conditions 161

Figure 6.5. 3D surface profiles of wear tracks on polymer plates in (a, c) dry and (b, d) PAO4 lubricated conditions 161

Figure 6.6. Optical images of new polymer plates and wear tracks on polymer plates in (a, c) dry and (b, d) PAO4 lubricated conditions.....162

Figure 6.7. Nanoindentation hardness maps of (a, c) new polymer plates and (b, d) wear tracks on polymer plates in PAO4 lubricated condition.....163

Figure 6.8. Optical images of after-test steel balls paired with CFR and GFR PEEK in (a, c) dry and (b, d) PAO4 lubricated conditions.....164

Figure 6.9. SE images of after-test steel balls paired with CFR and GFR PEEK in (a, c) dry and (b, d) PAO4 lubricated conditions 165

Figure 6.10. EMPA carbon maps of after-test steel balls paired with CFR and GFR PEEK in (a, c) dry and (b, d) PAO4 lubricated conditions.....165

Figure 6.11. Optical image of dispersed CFR PEEK wear debris contained in PAO4 oil 166

Figure 6.12. PAO4 oil containing CFR PEEK wear debris..... 166

Figure 6.13. Friction coefficients in wear debris PAO4 lubricated condition 167

Figure 6.14. (a) Optical image and (b) wear profile of polymer plate in wear debris PAO4 lubricated condition 168

Figure 6.15. (a) Optical image and (b) 3D surface profile of wear tracks on polymer plate in wear debris PAO4 lubricated condition 168

Figure 6.16. (a) SE image and (b) EPMA carbon map of after-test steel balls in wear debris PAO4 lubricated condition 169

Figure 6.17. Friction coefficients of CFR PEEK paired with smooth steel balls and lubricated with PAOs 170

Figure 6.18. Optical images of after-test CFR PEEK plates paired with smooth steel balls and lubricated with (a) PAO2, (b) PAO4 and (c) PAO10..... 171

Figure 6.19. Friction coefficients of GFR PEEK paired with smooth steel balls and lubricated with PAOs 171

Figure 6.20. Optical images of after-test GFR PEEK plates paired with smooth steel balls and lubricated with (a) PAO2, (b) PAO4 and (c) PAO10..... 171

Figure 6.21. Friction coefficients of CFR PEEK paired with rough steel balls and lubricated with PAOs 172

Figure 6.22. Friction coefficients of GFR PEEK paired with rough steel balls and lubricated with PAOs 172

Figure 6.23. Optical images of after-test CFR PEEK plates paired with rough steel balls and lubricated with (a) PAO2, (b) PAO4 and (c) PAO10..... 173

Figure 6.24. Wear profiles of CFR PEEK plates paired with rough steel balls and lubricated with with (a) PAO2, (b) PAO4 and (c) PAO10 173

Figure 6.25. Optical images of after-test GFR PEEK plates paired with rough steel balls and lubricated with (a) PAO2, (b) PAO4 and (c) PAO10..... 174

Figure 6.26. Wear profiles of GFR PEEK plates paired with rough steel balls and lubricated with (a) PAO2, (b) PAO4 and (c) PAO10 174

Figure 6.27. Optical images of wear tracks on CFR PEEK plates paired with rough steel balls and lubricated with (a) PAO2, (b) PAO4 and (c) PAO10 175

Figure 6.28. 3D surface profiles of wear tracks on CFR PEEK plates paired with rough steel balls and lubricated with (a) PAO2, (b) PAO4 and (c) PAO10 175

Figure 6.29. Optical images of wear tracks on GFR PEEK plates paired with rough steel balls and lubricated with (a) PAO2, (b) PAO4 and (c) PAO10 176

Figure 6.30. 3D surface profiles of wear tracks on GFR PEEK plates paired with rough steel balls and lubricated with (a) PAO2, (b) PAO4 and (c) PAO10 176

Figure 6.31. SE images of after-test rough steel balls paired with CFR PEEK and lubricated with (a) PAO2, (b) PAO4 and (c) PAO10 177

Figure 6.32. EPMA carbon maps of after-test rough steel balls paired with CFR PEEK and lubricated with (a) PAO2, (b) PAO, and (c) PAO10 177

Figure 6.33. SE images of after-test rough steel balls paired with GFR PEEK and lubricated with (a) PAO2, (b) PAO4 and (c) PAO10 178

Figure 6.34. EPMA carbon maps of after-test rough steel balls paired with GFR PEEK and lubricated with (a) PAO2, (b) PAO4 and (c) PAO10 178

Figure 6.35. Hardness distribution of new polymer plates and wear tracks on polymer plates for (a) CFR PEEK and (b) GFR PEEK in PAO4 lubricated conditions 179

Figure 6.36. Schematic of contact surfaces in dry and base oil lubricated conditions 181

Figure 6.37. Friction coefficients of (a) CFR PEEK-steel and (b) GFR PEEK-steel contacts as a function of modified Lambda ratios 182

Figure 6.38. Friction coefficients of polymer-steel contacts as a function of modified Lambda ratios 183

Figure 6.39. Wear volumes of polymer plates as a function of modified Lambda ratios 184

Figure 6.40. Schematic of contact surfaces depending on the modified Lambda ratios 185

Figure 6.41. SE images of the inner surfaces of (a) CFR PEEK and (b) GFR PEEK plates 186

Figure 7.1. Stribeck curves of CFR PEEK paired with smooth steel balls for PAO4 and PAO4 + OFMs 190

Figure 7.2. Stribeck curves of GFR PEEK paired with smooth steel balls for PAO4 and PAO4 + OFMs 190

Figure 7.3. Stribeck curves of CFR PEEK paired with rough steel balls for PAO4 and PAO4 + OFMs 191

Figure 7.4. Stribeck curves of GFR PEEK paired with rough steel balls for PAO4 and PAO4 + OFMs 191

Figure 7.5. Optical images of after-test CFR PEEK plates paired with rough steel balls for (a) PAO4 and (b-d) PAO4 + OFMs 192

Figure 7.6. Optical images of after-test GFR PEEK plates paired with rough steel balls for (a) PAO4 and (b-d) PAO4 + OFMs 192

Figure 7.7. Wear profiles of CFR PEEK plates paired with rough steel balls for (a) PAO4 and (b-d) PAO4 + OFMs 193

Figure 7.8. Wear profiles of GFR PEEK plates paired with rough steel balls for (a) PAO4 and (b-d) PAO4 + OFMs 193

Figure 7.9. Optical images of wear tracks on polymer plates with rough steel balls for (a, c) PAO4 and (b, d) PAO4 + OSa 195

Figure 7.10. 3D surface profiles of wear tracks on polymer plates with rough steel balls for (a, c) PAO4 and (b, d) PAO4 + OSa 195

Figure 7.11. SE images of after-test rough steel balls paired with CFR and GFR PEEK lubricated with (a, c) PAO4 and (b, d) PAO4 + OSa 196

Figure 7.12. EPMA carbon maps of after-test rough steel balls paired with CFR and GFR PEEK lubricated with (a, c) PAO4 and (b, d) PAO4 + OSa 197

Figure 7.13. Stribeck curves of pure PEEK paired with rough steel balls for PAO4 and PAO4 + OSa at ambient temperature (approximately 25 °C) and 80 °C 198

Figure 7.14. Stribeck curves of CFR PEEK paired with rough steel balls for PAO4 and PAO4 + OSa at ambient temperature (approximately 25 °C) and 80 °C 199

Figure 7.15. Stribeck curves of GFR PEEK paired with rough steel balls for PAO4 and PAO4 + OSa at ambient temperature (approximately 25 °C) and 80 °C.....199

Figure 7.16. Optical images of after-test polymer plates paired with rough steel balls and lubricated with (a, c, e) PAO4 and (b, d, f) PAO4 + OSa at 80 °C.....200

Figure 7.17. Wear profiles of after-test polymer plates paired with rough steel balls and lubricated with (a, c, e) PAO4 and (b, d, f) PAO4 + OSa at 80 °C.....201

Figure 7.18. SE images of after-test rough steel balls lubricated with (a, c, e) PAO4 and (b, d, f) PAO4 + OSa at 80 °C.....202

Figure 7.19. EPMA carbon maps of after-test rough steel balls lubricated with (a, c, e) PAO4 and (b, d, f) PAO4 + OSa at 80 °C.....202

Figure 7.20. Stribeck curves of CFR PEEK paired with smooth steel balls for PAO4 and PAO4 + AW additives.....204

Figure 7.21. Stribeck curves of GFR PEEK paired with smooth steel balls for PAO4 and PAO4 + AW additives.....204

Figure 7.22. Stribeck curves of CFR PEEK paired with rough steel balls for PAO4 and PAO4 + AW additives.....205

Figure 7.23. Stribeck curves of GFR PEEK paired with rough steel balls for PAO4 and PAO4 + AW additives.....205

Figure 7.24. Optical images of after-test CFR PEEK plates paired with rough steel balls lubricated with (a) PAO4 and (b, c) PAO4 + AW additives.....206

Figure 7.25. Optical images of after-test GFR PEEK plates paired with rough steel balls lubricated with (a) PAO4 and (b, c) PAO4 + AW additives.....206

Figure 7.26. Wear profiles of CFR PEEK plates paired with rough steel balls lubricated with (a) PAO4 and (b, c) PAO4 + AW additives.....207

Figure 7.27. Wear profiles of GFR PEEK plates paired with rough steel balls lubricated with (a) PAO4 and (b, c) PAO4 + AW additives.....207

Figure 7.28. SE images of after-test rough steel balls lubricated with (a, c) PAO4 and (b, d) PAO4 + ZDDP.....208

Figure 7.29. EMPA carbon maps of after-test rough steel balls lubricated with (a, c) PAO4 and (b, d) PAO4 + ZDDP 209

Figure 7.30. (a, d) SE images and corresponding EPMA (b, e) phosphorus and (c, f) sulphur maps of after-test rough steel balls lubricated with PAO4 + ZDDP 210

Figure 7.31. (a, d) SE images and corresponding EPMA (b, e) phosphorus and (c, f) sulphur maps of after-test polymer plates lubricated with PAO4 + ZDDP 210

Figure 7.32. Stribeck curves of pure PEEK paired with rough steel balls for PAO4 and PAO4 + ZDDP at ambient temperature (approximately 25 °C) and 80 °C 211

Figure 7.33. Stribeck curves of CFR PEEK paired with rough steel balls for PAO4 and PAO4 + ZDDP at ambient temperature (approximately 25 °C) and 80 °C 212

Figure 7.34. Stribeck curves of GFR PEEK paired with rough steel balls for PAO4 and PAO4 + ZDDP at ambient temperature (approximately 25 °C) and 80 °C 212

Figure 7.35. Optical images of after-test polymer plates paired with rough steel balls and lubricated with (a, c, e) PAO4 and (b, d, f) PAO4 + ZDDP at 80 °C 213

Figure 7.36. Wear profiles of after-test polymer plates paired with rough steel balls and lubricated with (a, c, e) PAO4 and (b, d, f) PAO4 + ZDDP at 80 °C 213

Figure 7.37. SE images of after-test rough steel balls lubricated with PAO4 and PAO4 + ZDDP at 80 °C 214

Figure 7.38. EPMA carbon maps of after-test rough steel balls lubricated with (a, c, e) PAO4 and (b, d, f) PAO4 + OSa at 80 °C..... 215

Figure 7.39. (a, d, g) SE images and corresponding EPMA (b, e, h) phosphorus and (c, f, i) sulphur maps of after-test rough steel balls lubricated with PAO4 + ZDDP at 80 °C. 216

Figure 7.40. (a, d, g) SE images and corresponding EPMA (b, e, h) phosphorus and (c, f, i) sulphur maps of after-test PEEK plates lubricated with PAO4 + ZDDP at 80 °C..... 216

Figure 7.41. Schematic of contact surfaces in polymer-smooth steel contacts lubricated with PAO and PAO + OFM 218

Figure 7.42. Schematic of contact surfaces in polymer-rough steel contacts lubricated with PAO and PAO + OFM 219

Figure 7.43. Schematic of contact surfaces in polymer-rough steel contacts lubricated with PAO and PAO + OFM at high temperature.....220

Research Thesis: Declaration of Authorship

Print name: Go Tatsumi

Title of thesis: Effect of lubrication on tribological properties of PEEK and PEEK composite

I declare that this thesis and the work presented in it are my own and has been generated by me as the result of my own original research.

I confirm that:

1. This work was done wholly or mainly while in candidature for a research degree at this University;
2. Where any part of this thesis has previously been submitted for a degree or any other qualification at this University or any other institution, this has been clearly stated;
3. Where I have consulted the published work of others, this is always clearly attributed;
4. Where I have quoted from the work of others, the source is always given. With the exception of such quotations, this thesis is entirely my own work;
5. I have acknowledged all main sources of help;
6. Where the thesis is based on work done by myself jointly with others, I have made clear exactly what was done by others and what I have contributed myself;
7. Parts of this work have been published as:

Articles:

[1] G. Tatsumi, M. Ratoi, Y. Shitara, K. Sakamoto, and B. G. Mellor, “Effect of Lubrication on Friction and Wear Properties of PEEK with Steel Counterparts”, Tribol. Online, vol. 14, no. 5, pp. 345–352, 2019.

[2] G. Tatsumi, M. Ratoi, Y. Shitara, K. Sakamoto, and B. G. Mellor, “Effect of organic friction modifiers on lubrication of PEEK-steel contact”, Tribol. Int., 151, 106513, 2020.

[3] G. Tatsumi, M. Ratoi, Y. Shitara, S. Hasegawa, K. Sakamoto, and B. G. Mellor, “Mechanism of oil-lubrication of PEEK and its composites with steel counterparts”, Wear, 486-487, 204085, 2021.

Conferences:

[1] G. Tatsumi, M. Ratoi, Y. Shitara, K. Sakamoto, and B. G. Mellor, “Effect of lubricants on friction properties of the steel/PEEK contact”, 74th STLE Annual Meeting and Exhibition (Nashville, US, 2019)

[2] G. Tatsumi, M. Ratoi, Y. Shitara, K. Sakamoto, and B. G. Mellor, “Effect of Lubrication in Sliding/Rolling Contact of PEEK Composites with Steel Counterparts”, European Conference on Tribology 2019 (Vienna, Austria, 2019)

[3] G. Tatsumi, M. Ratoi, Y. Shitara, K. Sakamoto, and B. G. Mellor, “Friction of PEEK with Steel Counterparts in EHL and Mixed Lubrication”, 46th Leeds-Lyon Symposium on Tribology (Lyon, France, 2019)

[4] G. Tatsumi, M. Ratoi, Y. Shitara, K. Sakamoto, and B. G. Mellor, “Effect of Lubrication on Friction and Wear Properties of PEEK with Steel Counterparts”, International Tribology Conference Sendai 2019 (Sendai, Japan, 2019)

[5] G. Tatsumi, “Effect of lubrication on tribological properties of polymeric materials”, 28th Mission of Tribology Research (London, UK, 2019)

[6] G. Tatsumi, M. Ratoi, Y. Shitara, K. Sakamoto, and B. G. Mellor, “Effect of Friction Modifiers on the Lubrication of Polymeric Materials with Steel Counter Parts”, 22nd International Colloquium Tribology (Esslingen, Germany, 2020)

Signature: .....Date:23/11/2021.....

Acknowledgements

Firstly, I would like to express my deepest gratitude to my supervisors, Dr Monica Ratoi and Dr Brian G Mellor, for their continuous support during my PhD study. Their expertise and insightful feedback pushed me to sharpen my thinking and raised my work to a higher level. The Covid-19 pandemic, which raged during the time of my PhD study, made life difficult for both students and supervisors, however, they always offered encouragement and kindly provided me with the best environment.

My deepest gratitude also extends to Dr Yuji Shitara for his guidance and assistance from the very beginning of my overseas study project. In addition to his technical support, he has provided me with a wealth of connections, not only in the field of tribology, which were essential to my study.

Part of the experimental work presented in this thesis was performed using the facilities of the Central Research Laboratory of ENEOS Corporation, Japan. Help from the following in carrying out the analyses and for the support in interpreting the data is gratefully acknowledged: Mr Shinji Hasegawa (Lubricant R&D Dept., ENEOS Corporation) – nanoindentation, Analytical Technology Group (R&D Solution Centre, ENEOS Corporation) – EPMA/XPS.

I would like to thank my sponsor, ENEOS Corporation, for giving me the opportunity to study in the UK as a PhD student. Their financial support and the comprehensive assistance provided from the staff involved allowed me to concentrate on my PhD study and so I was able to gain a lot of valuable experience.

I would like to thank the members of nCATS and my colleagues in Room 4061 of Building 7, University of Southampton, namely Dr Fatih Yanar, Mr Emanuele Zappia, Mr Saad Alshammari and Mr Madan Pal. They were always kind, friendly and helpful. It has been my privilege to work with them.

I would like to offer special thanks to the following colleagues of ENEOS Corporation, Mr Osamu Kurosawa, Mr Akira Yaguchi, Mr Kiyomi Sakamoto and the members of the Grease group. Although I left for my PhD study when they were under considerable pressure, they were always positive and supportive. My gratitude also extends to Dr Koji Hoshino, Dr Yasushi Onumata, Dr Kazumi Sakai and Mr Tadashi Oshio who had experienced overseas studies before me. Thanks to the valuable information they shared with me in advance, I was able to prepare appropriately for my project.

Finally, I would like to express my sincere gratitude to my wife Misa for her support, patience and encouragement. During my two years in Southampton, she gave birth, in Japan, to our babies, Jin

(in 2018) and Ema (in 2020). It must have been tough for her. Additionally, thanks to her great support I was able to finish writing up this thesis after I returned to Japan.

Definitions and Abbreviations

AlN.....Aluminium nitride

API.....American Petroleum Institute

AW.....Anti-wear

CF.....Carbon fibre

CFR.....Carbon fibre reinforced

EDX.....Energy Dispersive X-ray spectrometry

EHL.....Elastohydrodynamic lubrication

EP.....Extreme pressure

EPMA.....Electron Probe Micro Analysis

FM.....Friction modifier

FTIR.....Fourier-transform infrared spectroscopy

GF.....Glass fibre

GFR.....Glass fibre reinforced

ICI.....Imperial Chemical Industries

MoS_2.....Molybdenum disulphide

MTM.....Mini traction machine

NP.....Nano particle

OAc.....Oleic acid

OAm.....Olyel amine

OFM.....Organic friction modifier

OSa.....N-oleoyl sarcosine

PE.....Polyethylene

PA.....Polyamides or Nylon

PAEK.....Poly-aryl-ether-ketone

PAO.....Poly-α-olefin

PBI.....Polybenzimidazole

PDMS ..... Poly-dimethyl siloxane

PEEK ..... Poly-ether-ether-ketone

PET ..... Polyesters

POM ..... Polyoxymethylene or Polyacetal

PP ..... Polypropylene

PPO ..... Polyphenylene oxide

PPP ..... Polyparaphenylene

PS ..... Polystyrene

PTFE ..... Polytetrafluoroethylene

PVC ..... Polyvinyl chloride

SE ..... Secondary Electron

SRR ..... Sliding-rolling Ratio

SWR ..... Specific wear rate

TCP ..... Tricresyl phosphate

TFL ..... Transfer film layer

VI ..... Viscosity Index

WDX ..... Wavelength Dispersive X-ray spectroscopy

WS_2 ..... Tungsten disulphide

XPS ..... X-ray Photoelectron Spectroscopy

ZDDP ..... Zinc dialkyldithiophosphate

Symbols

h ..... Oil film thickness

μ ..... Friction coefficient

Λ ..... Lubricant film parameter, Lambda ratio

P ..... Pressure

Ra ..... Arithmetic average of the roughness profile

σ .....Composite surface roughness

Ts.....Tensile strength

V .....Velocity

Chapter 1 Introduction

1.1 Back ground

Polymers are becoming preferred materials in many tribological applications such as gears, seals and bearings. Compared with metals, polymers have advantages such as lightweight, reduced noise and self-lubricating properties which make their use in automotive, aerospace, medical, industrial applications highly desirable [1–6]. In terms of green technology, reducing weight by replacing metallic parts for polymeric ones is a very promising way to improve fuel efficiency [7–11]. However, the mechanical strength and thermal stability of polymers are lower than those of metals, and therefore they tend to fail from, for example, wear, local melting and pitting when used in severe conditions [12–17]. Due to these shortcomings the use of polymers is restricted to applications in comparatively mild conditions; therefore, there is an increasing demand to improve the tribological properties of polymers.

Among the various types of polymers which have been developed and used for tribological applications, Poly-Ether-Ether-Ketone (PEEK) has superior mechanical properties and higher thermal stability which make it suitable for applications operating under severe conditions [2,3,18,19]. For further improvement of its tribological performance, PEEK composites with specific fillers such as carbon/glass fibres and solid lubricants (e.g. graphite, PTFE and MoS_2) have been extensively investigated and their working mechanisms discussed [20–24]. Nevertheless, most of the studies mentioned above were performed mainly under dry conditions relying on the self-lubricating properties of PEEK and its composites.

However, lubrication also has the potential to improve further the tribological performance of polymers. In most tribological applications with steel parts lubrication, which reduces friction and wear by mitigating the direct contact of the two sliding surfaces, is essential to ensure their efficient operation and durability. For polymer applications, some research groups have reported that friction and wear were reduced under lubricated conditions compared with dry conditions [25–29]. On the other hand, negative effects of lubrication, especially on the wear of polymers have also been reported [30–32]. Despite hardness modification of polymer surfaces and polymer transfer films on steel counterparts being proposed as the key factors in understanding their behaviour, these factors have not been fully investigated in previous studies and the reason why lubrication can have opposite effects on the tribological performance of polymers remains unclear. In the lubrication of PEEK and its composites, positive and negative effects have been also reported and a clear understanding of their mechanisms is still lacking [26,27,31–35]. In addition, previous

studies mainly used water or fuel lubrication, and little is known of the effect of oil lubrication and especially of lubricant additives commonly added to lubricants for improving tribological performance.

Lubricants in tribological applications with steel parts are basically formulated from various types of base oils and additives depending on the purpose they are used for, and their formulation optimization relies much on the fundamental knowledge of their effect and working mechanism which has been historically well investigated [36–40]. While the lubrication mechanism of PEEK and its composites may be partly the same as that of steel, they should be different in many ways due to the large difference in mechanical properties and reactivity of steel and polymer. Bearing in mind the growing demand for improvement in the tribological properties of PEEK and its composites and the lack of fundamental knowledge of their lubrication, there is an urgent need to investigate the effect of lubrication on the tribological properties of PEEK and its composites, and its working mechanism.

1.2 Aims and objectives

The aim of this study is to elucidate how lubrication influences the tribological properties of PEEK and its composites and its working mechanism. To obtain fundamental knowledge of lubrication, the effect of base oil lubrication and lubricant additives were investigated stepwise for pure PEEK and PEEK composites, respectively. From the various types of lubricant additives, organic friction modifiers (OFMs) and anti-wear (AW) additives were focused on because of their strong influence on tribological properties. Carbon fibre reinforced (CFR) PEEK and glass fibre reinforced (GFR) PEEK were used in this study as they are the most typical PEEK composites.

The main objectives of this work are to clarify the followings:

- The effect and working mechanism of base oil lubrication on the tribological properties of PEEK
- The effect and working mechanism of lubricant additives (OFMs and AW additives) on the lubrication of PEEK
- The effect and working mechanism of base oil lubrication on the tribological properties of CFR PEEK and GFR PEEK
- The effect and working mechanism of lubricant additives (OFMs and AW additives) on the lubrication of CFR PEEK and GFR PEEK

The knowledge obtained in this study is essential to be able to formulate suitable lubricants for the tribological applications envisaged for PEEK and its composites. Furthermore, this study could contribute to helping to understand the tribological properties of other polymers under lubrication, because the fundamental mechanism of action is expected to be common. The formulated lubricants will help to improve the efficiency and durability of the systems by reducing friction and wear, thus promoting the adoption of polymer applications in green technologies so as to reduce weight by the replacement of metallic gears for polymeric ones in automobiles where numerous gears transmit engine/motor power to the wheels, thus contributing to reducing CO_2 emission.

1.3 Thesis outline

This thesis is divided into eight chapters summarized as follows:

- Chapter 1 introduces this study and includes its background, aims and objectives,
- Chapter 2 reviews the literature to understand the research context,
- Chapter 3 summarizes the materials and experimental methods applied in this study,
- Chapter 4 contains experimental results of base oil lubrication of PEEK and discusses the mechanism of action,
- Chapter 5 investigates the effect of lubricant additives, organic friction modifiers (OFMs) and anti-wear (AW) additives, on the lubrication of PEEK,
- Chapter 6 covers base oil lubrication of PEEK composites namely carbon fibre reinforced (CFR) PEEK and glass fibre reinforced (GFR) PEEK,
- Chapter 7 investigates the effect of OFMs and AW additives on the lubrication of CFR PEEK and GFR PEEK,
- Chapter 8 summarizes the conclusions of the experimental results and the discussions contained in chapters 4, 5, 6 and 7, and presents future work arising from this study.

The thesis structure is schematically illustrated in Figure 1.1.

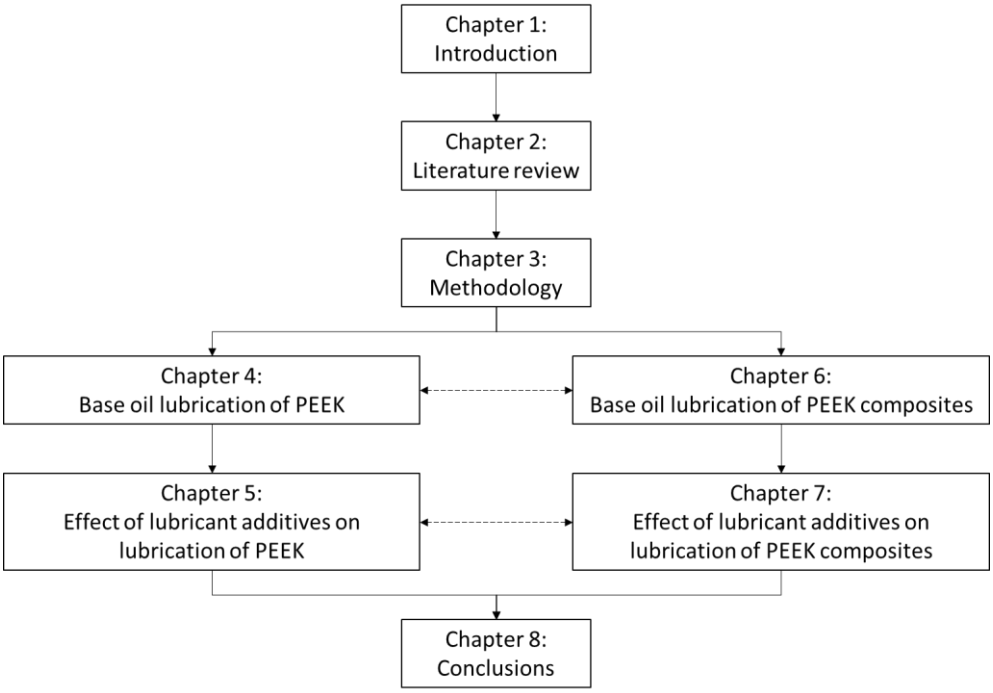

Figure 1.1. Thesis structure

Chapter 2 Literature Review

This chapter reviews the literature relevant to understanding the research context of the studied topic. Section 2.1 gives an overview of polymers in tribological applications and their tribology under dry conditions. Section 2.2 reviews existing research related to the lubrication of polymers and includes in depth section on PEEK and PEEK composites.

2.1 Tribology of polymers

2.1.1 Introduction

The word of "tribology" was derived from "tribos", the Greek word for "rubbing". It was coined by Peter Jost, and became widely used following his report published in 1966 [41]. The concept was defined as "The science and technology of interacting surfaces in relative motion – and of associated subjects and practices", focusing on the research of friction, wear, and lubrication. According to his report, much money was lost through unnecessary wear, friction and connected breakdowns. Additionally, if greater attention was paid to tribology, approximately 500 million pounds (at 1965 values) could be saved annually in the U.K. alone, as shown in Figure 2.1.

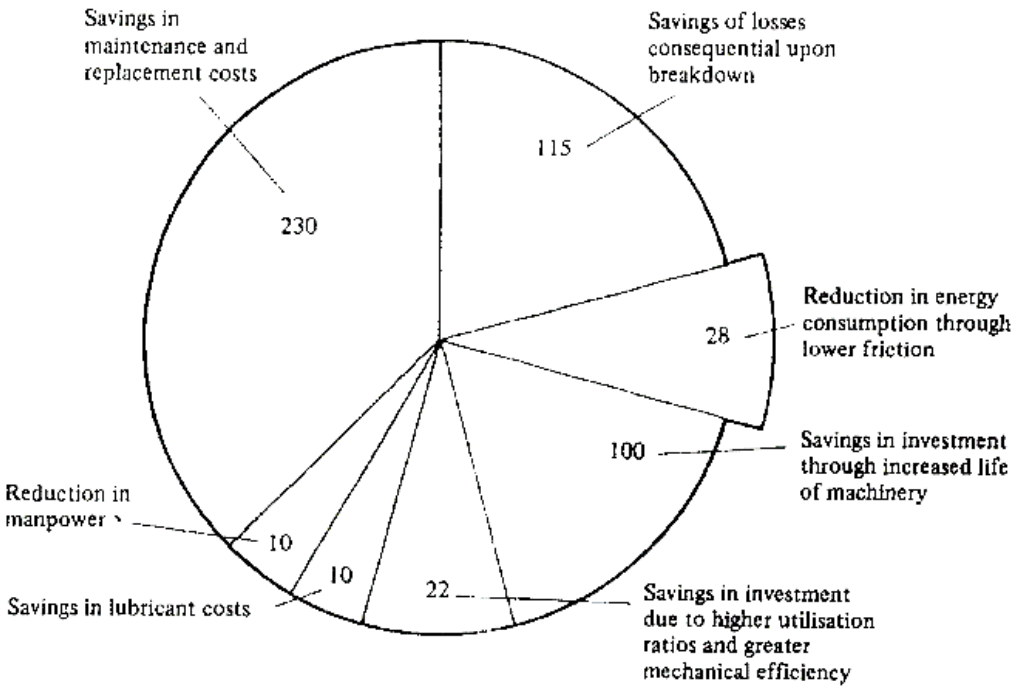

Figure 2.1. Economic savings through tribology (in £ million at 1965 values) (adapted from [41])

Recently, the significance of tribology is increasing because of not only economic issues but also environmental concerns. Figure 2.2 shows the International Energy Agency (IEA) estimation of key technologies for the reduction of CO_2 emissions in order to limit global warming to 2 °C above pre-industrial levels by 2050 [42]. Tribology is mainly expected to contribute to the area of "End-use energy efficiency" which has the largest weighting (38%). Holmberg and Erdemir reported that by taking advantage of the new surface, materials, and lubrication technologies, energy losses due to friction and wear could potentially be reduced by 40% in the long term (15 years) and by 18% in the short term (8 years).

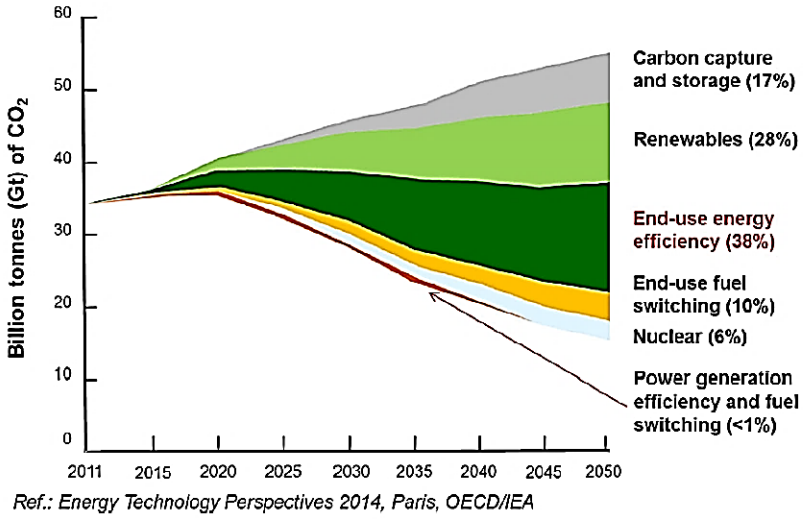

Figure 2.2. Key technologies for the reduction of CO_2 emissions (adapted from [42])

The term "polymer" was derived from "polys", the Greek word for "many", and "meros", for "part", and was first introduced by Jöns Jakob Berzelius in 1833 [43]. It is basically synonymous with "resin" and "plastic", and means a material consisting of large molecules made up by structural units bound together by covalent bonds. Polymers are obtained through the polymerization processes where monomers react with each other and form large molecules. There is a wide range of polymers, and they are classified in terms of their compositions, structures, properties, and chemical reaction processes. Figure 2.3 shows an example of the classification of polymers (plastics) focused on the macromolecular structure and the temperature-dependent physical properties [44]. Thermoplastics have linear or branched macromolecule chains and are used in applications where stiffness and toughness are needed. Elastomers and thermosets have crosslinking-macromolecule chains, the lower crosslinking in the elastomers providing their elasticity. Compounds are composed

of several base materials. This composition can be achieved on a physical basis (e.g., polymer blends or composite materials) or on a chemical basis (copolymers).

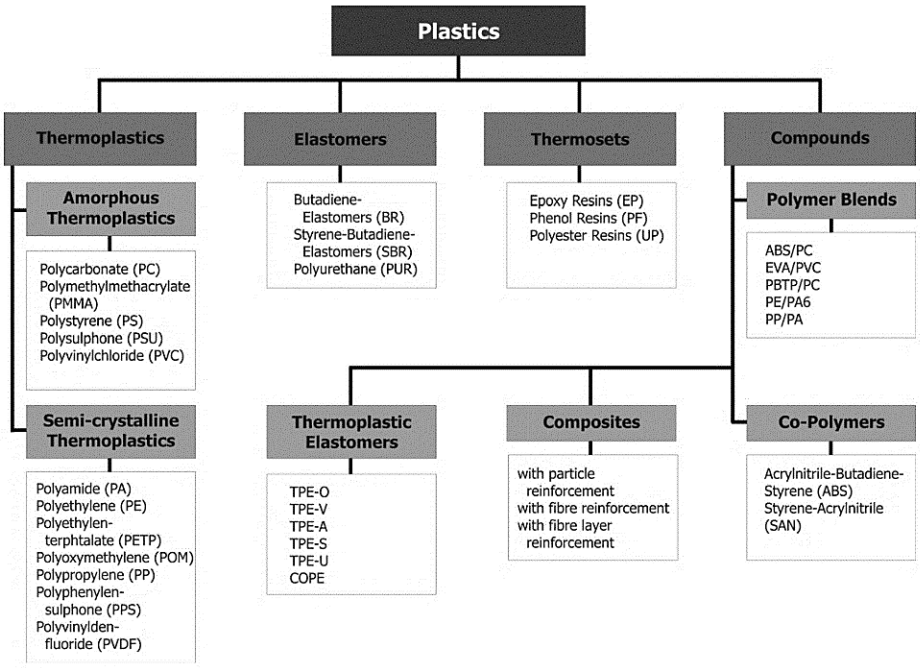

Figure 2.3. Classification of plastics (polymers) (adapted from [44])

2.1.2 Polymers for tribological applications

Polymers are becoming preferred materials in many tribological applications such as gears, seals and bearings. Compared with metals, polymers have advantages such as lightweight, reduced noise and self-lubricating properties which make their use in automotive, aerospace, medical, industrial applications highly desirable [1–6,45–47]. Figure 2.4, Figure 2.5 and Figure 2.6 show some examples of polymers used in tribological applications [48–50].

Figure 2.4. Moulded polymer gear made of PEEK (adapted from [48])

Figure 2.5. Seal rings made of polymers (polytetrafluoroethylene, PEEK and rubber) and steel (adapted from [49])

Figure 2.6. Polymer ball bearings (left) and Polymer bearing cages (right) (adapted from [50])

Polymers are also used as hybrid materials with metals. Figure 2.7 shows an example of hybrid bushings [51]. By incorporating a polymer material into a porous metal layer, a low friction matrix with favourable tribological properties, load carrying properties and thermal conductivity of metals can be obtained.

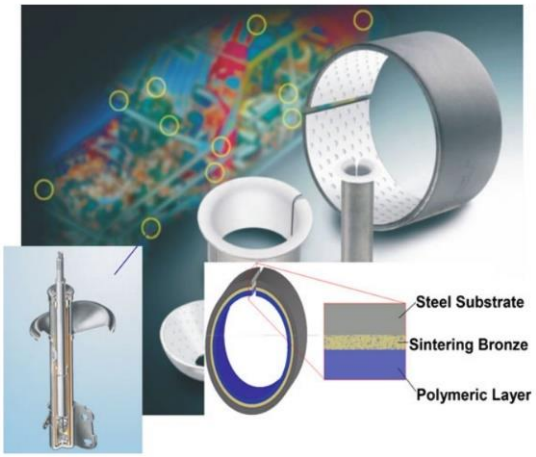

Figure 2.7. Schematic structure of hybrid bushings (lower right) and their use in various automotive locations, including shock absorbers (lower left) (adapted from [51])

Typical polymers used in tribological applications can be schematically arranged in a pyramid on the basis of their physical properties, operating temperature ranges and cost, as shown in Figure 2.8 [3]. The "Commodity Polymers" of PS (Polystyrene), PVC (Polyvinyl Chloride), PP (Polypropylene), and PE (the various forms of Polyethylene) are relatively weak materials with Tensile Strengths, Ts, of the order of 20 MPa. Ts is measured as the maximum stress that a polymer can support without breaking when being stretched. They have limited operating temperature ranges of up to 100 °C, but are produced internationally because of their cheap cost, (<£1/kg). The "Engineering Polymers" such as PA (Polyamides, 'Nylon'), POM (Polyoxymethylene or Polyacetal) and PET (Polyesters) have higher strengths of the order of 75 MPa with continuous operating temperatures of up to 110/120 °C and a cost range up to £10/kg. The "High Performance" polymers have a higher level of physical properties, higher melting points and very good resistance to degradation and cost up to £100/kg. This class merges into the 'Ultra-high Performance Polymers', with very high melting points, higher strength such as the polyaramids and the PAEK (Poly-aryl-ether-ketone) family which includes PEEK (Poly-ether-ether-ketone), with Ts up to 100 MPa, melting point around 343 °C and a usable temperature range to 250 °C, with prices beginning in the region of £100/kg [52].

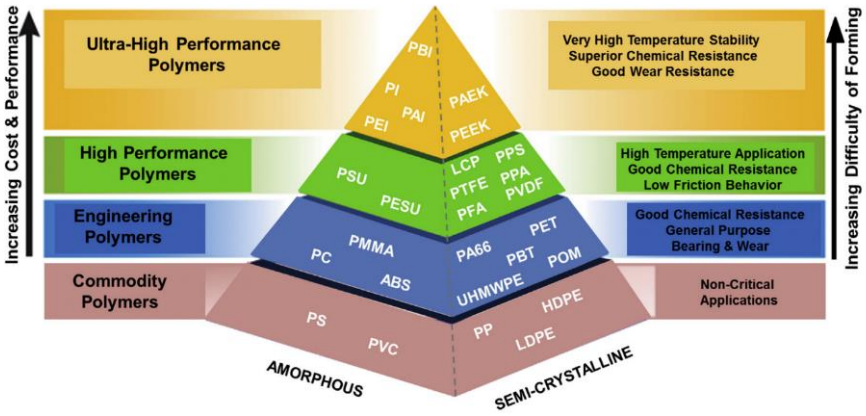

Figure 2.8. Polymer pyramid with regard to cost, performance and formability (adapted from [3])

A number of papers have been published on the tribological properties of polymers in dry conditions [53–62]. An overview of the tribological characteristics of various polymers used in tribological applications is also shown in Table 2.1 [2] where "÷" indicates the range of values. Operational temperature ranges depend mainly on their melting temperatures. Most polymers give friction coefficients μ (μ = F/N, where F frictional force and N the normal force) of 0.1 to 0.5 in dry conditions, while fluoroplastics such as polytetrafluoroethylene, PTFE, provide remarkably lower friction coefficients of 0.01 to 0.05. Due to the low mechanical strength of PTFE, it is commonly

used as composite materials with various fillers added to improve its strength. PTFE is also applied as antifriction fillers in other polymers.

Table 2.1. Tribological characteristics of polymers (adapted from [2])

Material	Friction coefficient	Operation temperature [°C]	Advantages	Disadvantages
Aliphatic polyamides	0.2 ÷ 0.5	– 40 ÷ + 85	Low wear and high fatigue resistance	Water sorption, high coefficient of friction
Aromatic polyamides	0.1 ÷ 0.3	– 100 ÷ + 200	Low wear, high fatigue resistance and heat stability	High cost, water sorption
Fluoroplastics	0.01 ÷ 0.05	– 269 ÷ + 260	Low friction, resistance to aggressive media	Creep and low mechanical strength
Polycarbonate	0.2 ÷ 0.5	– 60 ÷ + 125	Rigidity and resistance to aggressive media	Low fatigue strength
Polyacetals	0.1 ÷ 0.3	– 50 ÷ + 120	High wear and fatigue resistance	Abrasive effect due to high rigidity
Polyolefins	0.1 ÷ 0.3	– 100 ÷ + 100	High resistance to aggressive media	Low mechanical strength
Polyalkylene terephthalate	0.1 ÷ 0.3	– 20 ÷ + 115	Resistance to aggressive media and heat resistance	Sensitivity to hot water
Thermoplastic elastomers	0.3 ÷ 0.6	– 60 ÷ + 120	High elasticity and resistance to ambience	High friction and low mechanical strength
Polyetherether ketone	0.2 ÷ 0.4	– 30 ÷ + 250	High heat and ambient resistance, and γ-radiation.	High cost
Polyphenylene sulfide	0.2÷ 0.5	– 30 ÷ + 220	High wear and fatigue resistance	High cost

In terms of wear resistance, polymer composites with fillers such as glass fibres and carbon fibres are effective in improving the mechanical properties. Additionally, solid lubricants such as graphite, PTFE and MoS_2 are typically incorporated to improve tribological performance [3,23,29,63,64]. Reinforcement fibres and solid lubricants are used solely or in combinations to achieve a desirable performance for their intended use. Figure 2.9 shows an example of the microstructure of polymer composites with fillers [3]. Recently, various types of inorganic nano-particles (NPs) such as Al_2O_3, ZnO, SiO_2, and TiO_2 have been investigated as solid lubricants for polymer composites [51,65–67]. As shown in Figure 2.10, the size of NPs is much smaller than that of the reinforcement fibres or solid lubricants [66].

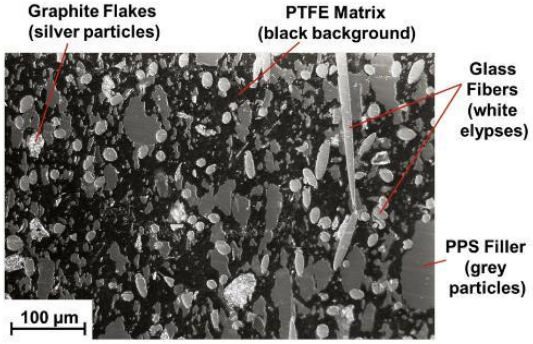

Figure 2.9. Microstructure of polymer composites with fillers (adapted from [3])

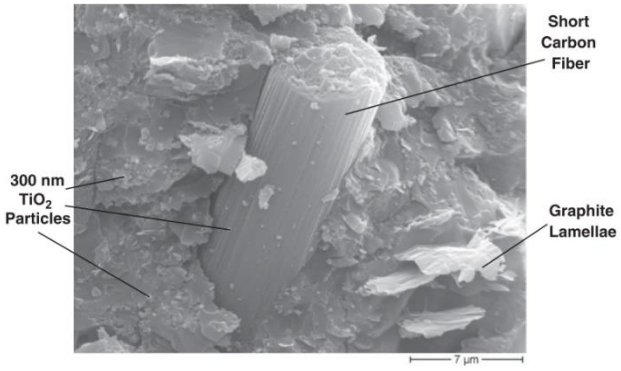

Figure 2.10. Facture surface of polymer composites with fillers (adapted from [66])

Some previous studies have focused on polymer parts such as gears and bearings [68–73]. Figure 2.11 shows the typical forms of polymer gear failure [12]. Polymer gears usually fail due to cracking at the root, wear, cracking at the pitch circle and pitting. A pitch circle is the imaginary circle that rolls with a pitch circle of a mating gear, and their radius is equal to the distance from the centre of the gears to the contact point of the circles. With the exception of wear, the other failure modes are considered to be some form of fatigue failure. Among these failures, cracking at the pitch circle is unique to polymers. This is explained by the high temperatures at the pitch circle which leads to a decrease in the strength of polymers. In fact, Terashima et al. (1986) investigated the failure modes of a polymer (improved 6-nylon) gear paired with a steel gear, and found that most of the failures (62%) were cracking near pitch points [74]. They also found that the temperature at the pitch point was higher than at the tooth root by 15–20 °C.

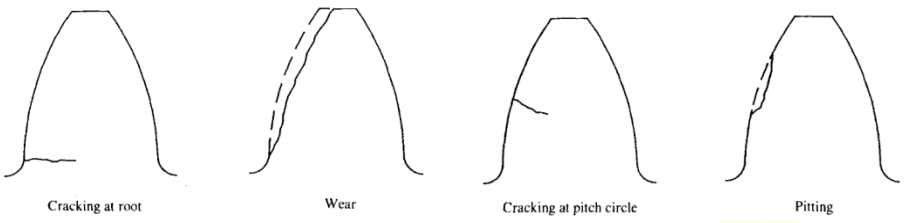

Figure 2.11. Typical forms of plastic gear failure (adapted from [12])

2.1.3 Factors influencing the tribology of polymers

(a) Heat

The tribological properties of polymers are very sensitive to heat because of their lower thermal stabilities compared to metals. Figure 2.12 shows the wear rates of POM gears to composite gears, which consist of 55% nylon, 30% glass fibres and 15% PTFE, as a function of torque for ambient temperatures and the torques at which the transition from low to high wear occurs [75]. Increasing the ambient temperature reduces the transition torque, and the torque/temperature curve appears to cross the zero-torque line close to the melting point of acetal (175 °C). This indicates the sudden increase in wear rate is due to the gear surface temperature reaching the material melting temperature under the tribological condition. Mertens and Senthilvelan reported the effect of cooling on the wear resistance of PP gears to steel gears [14]. A temperature drop of 10 to 20 °C is observed when the compressed air is delivered near the gear mesh region during the test. As shown in Figure 2.13 with increased load, gear tooth wear increased due to the higher contact pressure, while air cooling improved wear resistance especially at high loads associated with higher frictional heat. Kalin and Kupec reported the dominant effect of temperature on the fatigue behaviour of POM gears in contact with steel gears (Ra roughness of 0.60 µm) [17]. As shown in Figure 2.14, temperature changes the fatigue life and damage of POM gears dramatically: the fatigue life at 30 °C is up to four times longer than that at 70 °C and up to two times longer than that at 50 °C. Thus, heat greatly affects the tribological properties of polymers at least when tested in dry conditions. In addition to the low thermal stability of polymers, the heat conduction of polymers is much lower than metals, and therefore frictional heat accumulates on the polymer surface, causing thermal failures [72]. This is the reason why polymers are commonly used paired with steel counterparts which have good heat transfer characteristics.

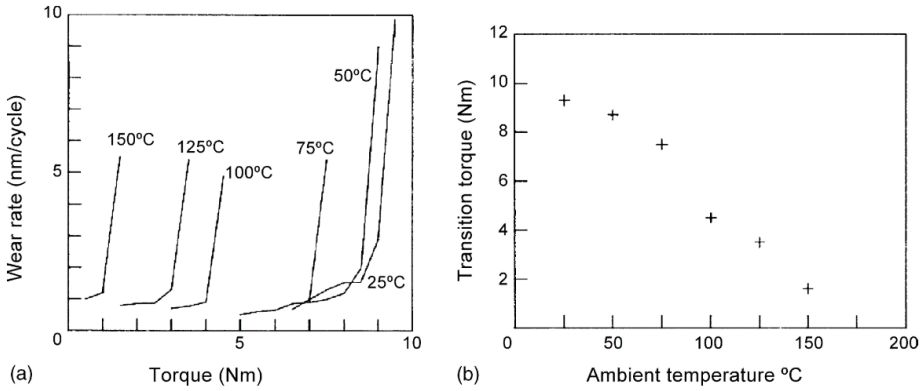

Figure 2.12. Ambient temperature effects on (a) wear rates and (b) transition torques of POM gears to composite gears (adapted from [75])

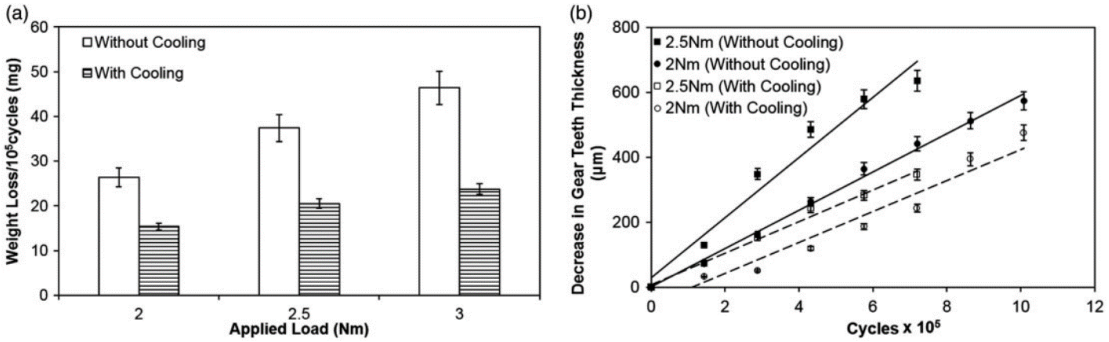

Figure 2.13. (a) Effect of cooling on the wear resistance of PP gears to steel gears and (b) PP gear tooth thickness reduction during testing (adapted from [14])

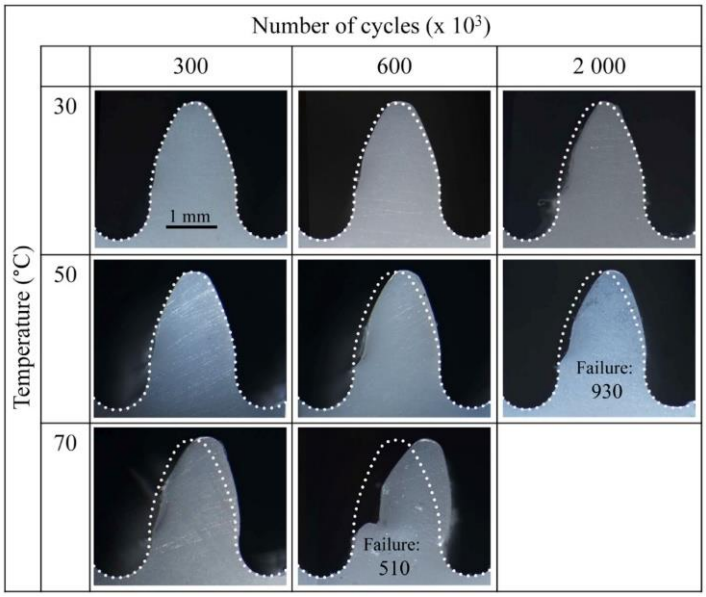

Figure 2.14. Optical images of the worn teeth profiles with an increasing number of cycles at controlled temperatures (adapted from [17])

(b) Polymer transfer films on the steel counterparts

As described above, polymers are commonly used with steel counterparts because of the good heat transfer characteristics of steel. Therefore, numerous studies have investigated the friction and wear properties of polymer/steel contacts under dry conditions [2–4,54,56,61,76–79]. One of the key factors reported for the favourable tribological properties exhibited under dry conditions is the formation of polymer transfer films on steel counterparts [80–84]. They act as protective films avoiding the direct contact of polymers with the hard asperities of steel and thus reduce wear as

shown in Figure 2.15 [56]. Figure 2.16 shows an example of the behaviour of the friction coefficient as a function of sliding distance [56]. The transfer film is gradually formed on the steel counterpart during the initial running-in stage. As the transfer film forms, the friction coefficient increases due to the adhesion at the polymer/polymer contact which is greater than at the polymer/steel contact. At greater sliding distances a steady state develops, and the friction coefficient becomes stable from μ_{max} at the transition state to μ_{av} shown in Figure 2.16.

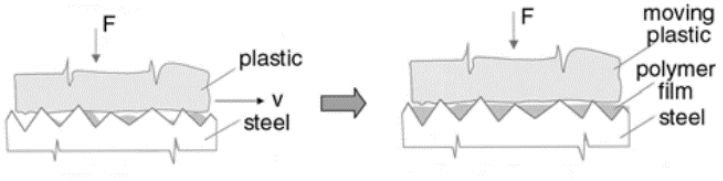

Figure 2.15. Running-in (left) and steady-state friction (right) with dynamic balance of polymer film (adapted from [56])

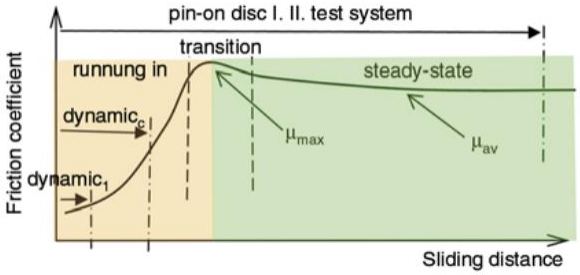

Figure 2.16. Friction stages between polymer/steel pairs (adapted from [56])

Kurdi et al. investigated the effect of temperature on the formation of the polymer transfer films formed on steel counterparts [19]. Table 2.2 summarizes the values of the transfer layer efficiency factor, the ratio of the average thickness of polymer transfer films to the Ra surface roughness of steel counterpart, at different temperatures. The dependency on temperature depends on the polymer type: pure PEEK and PEEK composites with TiO_2 fillers show higher values of transfer layer efficiency factors at higher temperature, while polyparaphenylene (PPP) provides lower values as temperature increases. The values for polybenzimidazole (PBI) are less influenced by the test temperature. The authors suggested that heat caused softening of the polymer surfaces and as a result, there was an increase in the amount of film that adhered on the steel counterpart, especially in the case of PEEK and PEEK composites which show more ductile behaviour at higher temperature.

Table 2.2. Transfer layer efficiency factor at different temperatures (adapted from [19])

Sample	At 23 °C	At 150 °C	At 210 °C
Pure PEEK	0.45	0.97	1.01
PEEK + 5%TiO_2	0.62	0.87	0.91
PEEK + 10%TiO_2	0.59	0.77	0.88
PEEK + 15%TiO_2	0.33	0.49	0.54
PPP	0.41	0.18	0.17
PBI	0.78	0.73	0.72

Chang et al. reported that in the contact of polymer composites with steel, polymer transfer films still played an important role, mitigating the contact between steel and "hard" fillers such as glass fibres or carbon fibres exposed on the surface of the polymer composites [84]. As shown in Figure 2.17, contact modes can be designated as follows depending on the thickness and distribution of the transfer films; hard-on-hard (rigid fillers against asperities of steel), hard-on-soft (rigid fillers against polymeric transfer films) and soft-on-soft (polymer against polymeric transfer films).

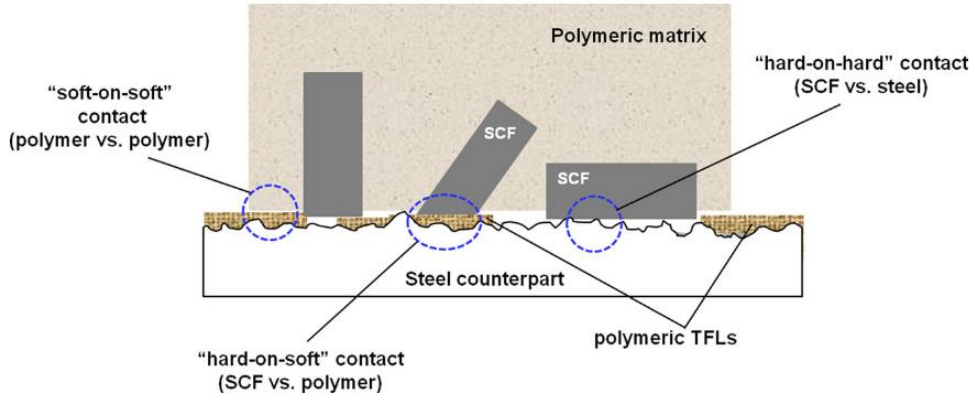

Figure 2.17. Schematic illustration of the contact modes of polymer composites against steel counterparts (adapted from [84])

2.1.4 Tribology of PEEK and PEEK composites

(a) PEEK and PEEK composites

Poly-ether-ether-ketone (PEEK) is considered as one of the most promising polymers for tribological applications because of its superior mechanical properties and higher thermal stability than other

conventional polymers [5]. PEEK is a semi-crystalline polymer with a melting point of approximately 340 °C and a glass transition temperature of approximately 140 °C, whose aromatic ring backbone (Figure 2.18) provides the desirable properties of PEEK [85,86].

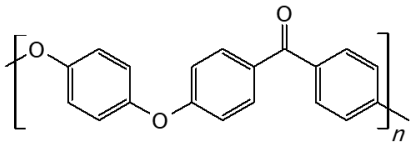

Figure 2.18. Chemical structure of PEEK

There are various methods to synthesis PEEK, but the nucleophilic substitution reaction is the most widely applied route for commercial production. Figure 2.19 shows the scheme developed by Imperial Chemical Industries (ICI) and now manufactured by Victrex, following a management buyout of the PEEK polymer business of ICI [87]. The reaction was carried out by polycondensation of equimolar amounts of the aromatic halide 4,4'-difluorobenzophenone and bisphenol hydroquinone in solvent diphenylsulfone with a catalyst of potassium carbonate. The reactants were heated with stirring between the temperatures of 180 °C to 320 °C. The resulting solid reaction product is washed with acetone, water, and finally acetone/methanol solution.

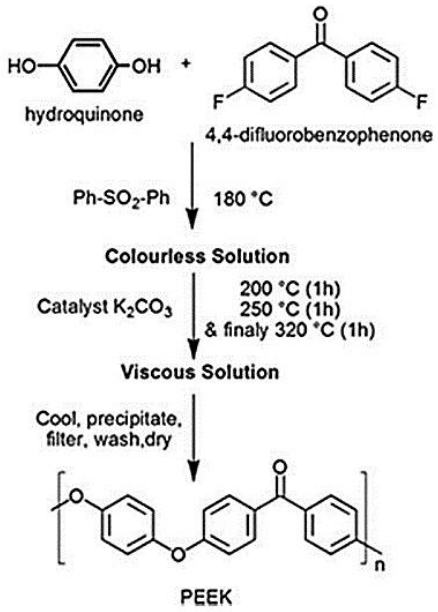

Figure 2.19. Scheme of the PEEK synthesis in diphenylsulfone (adapted from [87])

PEEK is often used as fibre reinforced PEEK composites such as carbon fibre reinforced (CFR) PEEK and glass fibre reinforced (GFR) PEEK to further improve the mechanical properties. Figure 2.20 shows the effect of fibre content on the tensile properties of CFR PEEK and GFR PEEK [88]. For both PEEK composites, the tensile strength and modulus increase as the weight content of fibres increases from 0 to 15%. On the other hand, the addition of reinforcement fibres does not affect the thermal stability or degree of crystallinity of the materials as reported in Table 2.3 [89].

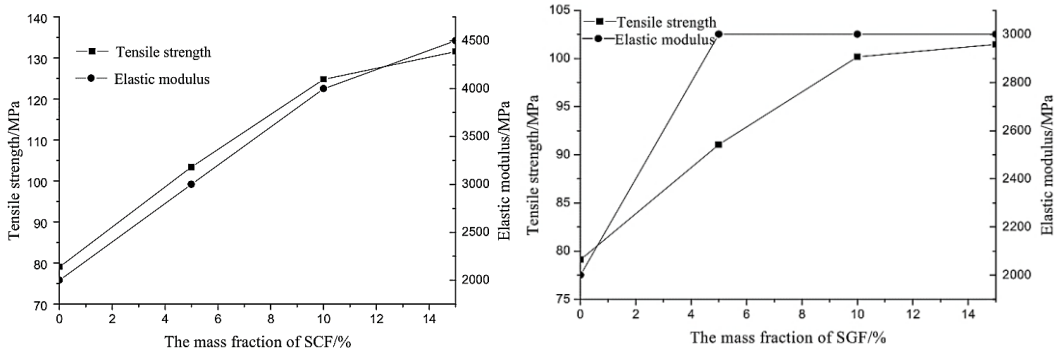

Figure 2.20. Effect of fibre content on the tensile properties of CFR PEEK (left) and GFR PEEK (right) (adapted from [88])

Table 2.3. Thermal properties of the pure PEEK, CFR PEEK and GFR PEEK (reproduced from [89])

	Pure	Reinforced Carbon fibres (CF)			Glass fibres (GF)		
Thermal properties		+10%	+20%	+30%	+10%	+20%	+30%
Melting temperature (°C)	331.2	329.6	326.9	326.0	329.5	329.4	329.5
Melting enthalpy (Jg^{-1})	34.0	31.4	27.7	26.1	31.1	28.0	24.5
Crystallinity degree (%)	29	30	30	32	29	30	30

(b) Tribology of PEEK and PEEK composites

The tribological properties of PEEK with steel counterparts have been extensively investigated under dry conditions and the transfer films are reported to affect strongly their tribological behaviour. In-situ observation of the PEEK wear process with steel and sapphire counterparts (Ra steel roughness of less than 0.02 μm) was reported by Puhan and Wong who proposed that PEEK

wear debris produced by ploughing of the asperities of the counter surface (steel) re-entered the contact and became trapped between the asperities of the counter surfaces by compression, so forming the PEEK transfer films on the counter surfaces (Figure 2.21) [90]. Laux and Schwartz investigated the influence of sliding motions on wear behaviour and transfer film formation [91]. They reported that there is a significant difference in the wear volume of PEEK with steel (Ra roughness of 0.5 µm) depending on the sliding motion (Figure 2.22). The reciprocating motions (indicated as "RC" and "RL") results in lower wear volumes of PEEK. In addition, they provided more continuous PEEK transfer films than the sliding motion in a single direction (indicated as "VVC") (Figure 2.23). The authors assumed that the reciprocating motion enables both sides of the steel asperities to be covered with PEEK transfer films, while the one direction sliding motion keeps the trailing edge of the steel asperities exposed and capable of abrading PEEK. The tribological mechanism aspects described in this section were obtained in dry conditions, but they could also be relevant for lubricated conditions, and contribute to the understanding of the mechanism of lubrication in PEEK-steel contacts.

Figure 2.21. Appearance of PEEK transfer film formed on the steel ball (adapted from [90])

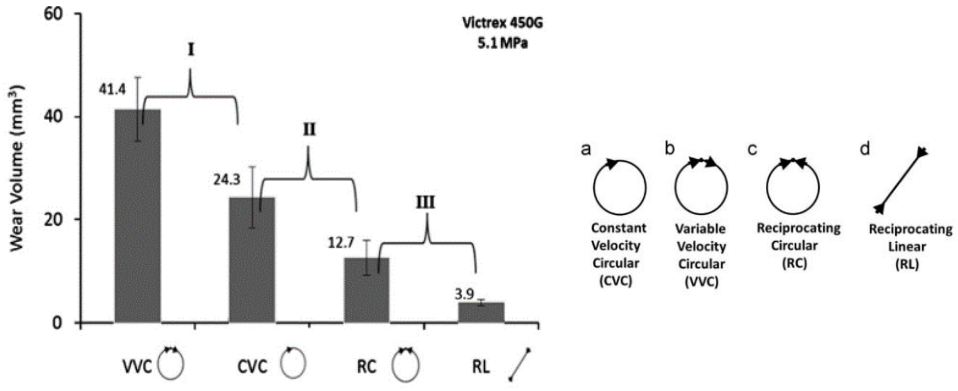

Figure 2.22. Wear volumes in different sliding motions (adapted from [91])

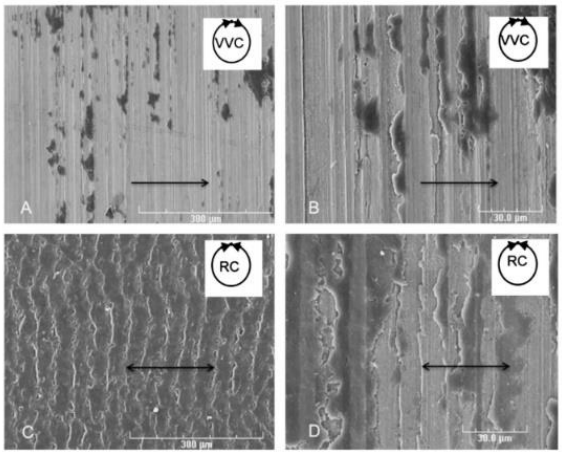

Figure 2.23. PEEK transfer films formed on the steel counter surface in different sliding motions (adapted from [91])

The roughness of steel counterparts has been reported as an important factor in the tribological performance of PEEK/steel contacts. Figure 2.24 shows the effect of the surface roughness of the steel disc on the wear factor (specific wear rate) of PEEK in the pin-on-disc configuration [92]. Specific wear rate (SWR, w_s) is defined as the wear volume (V) per sliding distance (D) and per load (L) and calculated according to Equation 2-1:

$$SWR = \frac{V}{D \times L} \qquad \text{(Eq. 2-1)}$$

The results indicated that the wear of PEEK is dependent on the surface roughness of steel, and a relative minimum wear occurs in a specific root mean square (RMS) roughness range between 0.1-0.2 μm. Interestingly, the morphology of the wear debris changed with surface roughness from a sheet-like or platelet form (indicative of delamination) to smaller-sized, irregularly torn particles (indicative of abrasion). Friedrich et. al investigated the influence of steel roughness orientation in the block on ring test (Figure 2.25) [93]. When the sliding direction was parallel to the steel roughness orientation, SWRs (w_s) of PEEK blocks became larger depending on the Ra values of steel rings. By contrast, the specific wear rates of PEEK were almost constant regardless of steel roughness when the sliding direction was perpendicular to the steel roughness orientation. Placette et.al also reported a similar effect of steel roughness orientation on the wear of PEEK in linear reciprocating tests [65].

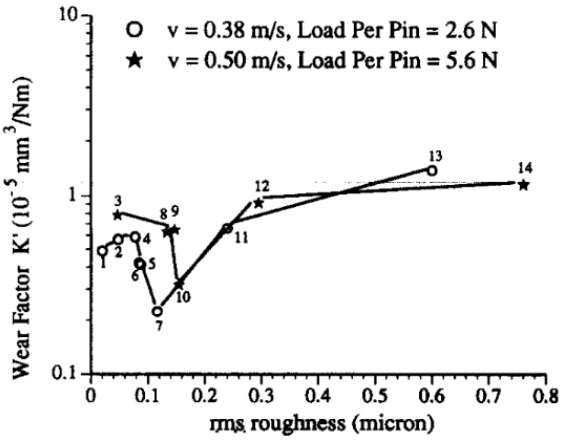

Figure 2.24. Wear test results for PEEK on mild steel with different roughness (adapted from [92])

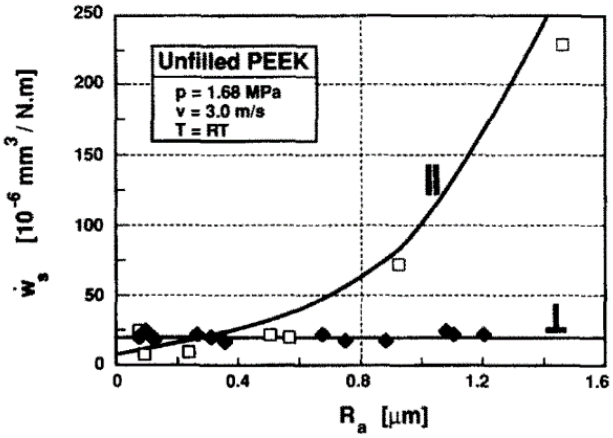

Figure 2.25. Specific wear rates of PEEK as a function of steel roughness. The sliding direction was parallel (II) and perpendicular (⊥) to the steel roughness (adapted from [93])

The effect of the type and volume of reinforcement fibres contained in PEEK composites on the tribological behaviour has been investigated in some depth. Figure 2.26 shows the improvement achieved by carbon fibres in PEEK composites [20]. The specific wear rate of PEEK composites paired with steel (Ra roughness of 0.2-0.3 μm) was reduced by approximately one order of magnitude when at least 10 vol.% of CF was added. A similar trend was observed with the friction coefficient. Pei et al. investigated the friction and wear mechanism of carbon fibre reinforced (CFR) PEEK using different contact configurations in a triboindentor (Figure 2.27) [94]. Sliding of a fibre on the surface of CF (indicated in Figure 2.27 as "Against CF") or sliding between two fibres (indicated in Figure 2.27 as "Against CF/PEEK/CF") led to the friction coefficient being at a lower value. These results suggested that carbon fibres bear the load, thereby reducing the shear contribution to friction of the polymer matrix in CFR PEEK. In addition to the type and volume, the orientation of the

reinforcement fibres strongly affects the tribological properties of PEEK composites with steel (Ra roughness of 0.3 µm), as reported by Zhang et al. [95]. The effects of fibre orientation, which were tested in parallel (P-orientation), anti-parallel (AP-orientation) and normal (N-orientation) relative to the sliding direction, on the tribological behaviour was investigated (Figure 2.28 and Figure 2.29). Under higher pressures, the wear rates in the antiparallel orientation (the perpendicular orientation) were notably lower than those in the normal and parallel-orientations. The authors concluded that the shear stress of the PEEK matrix is reduced by carbon fibres more effectively in the antiparallel orientation than in the other orientations. The results of these studies run in dry conditions suggest that the distribution and orientation of the reinforced fibres are important factors which should also be investigated under lubrication.

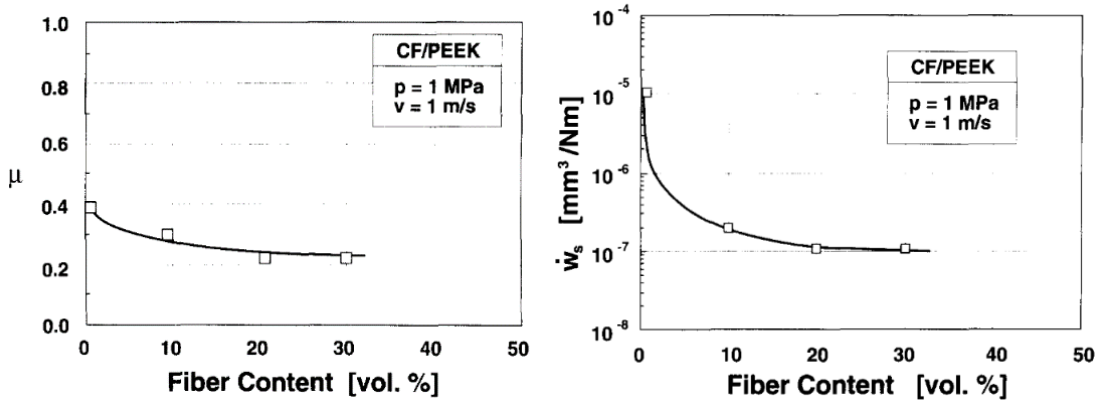

Figure 2.26. Friction coefficients (left) and wear rates (right) of PEEK composites paired with steel as a function of content of carbon fibres (adapted from [20])

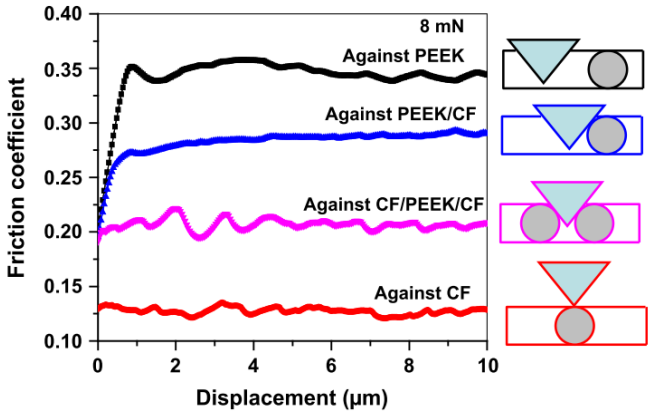

Figure 2.27. Friction coefficients under different contact configuration (adapted from [94])

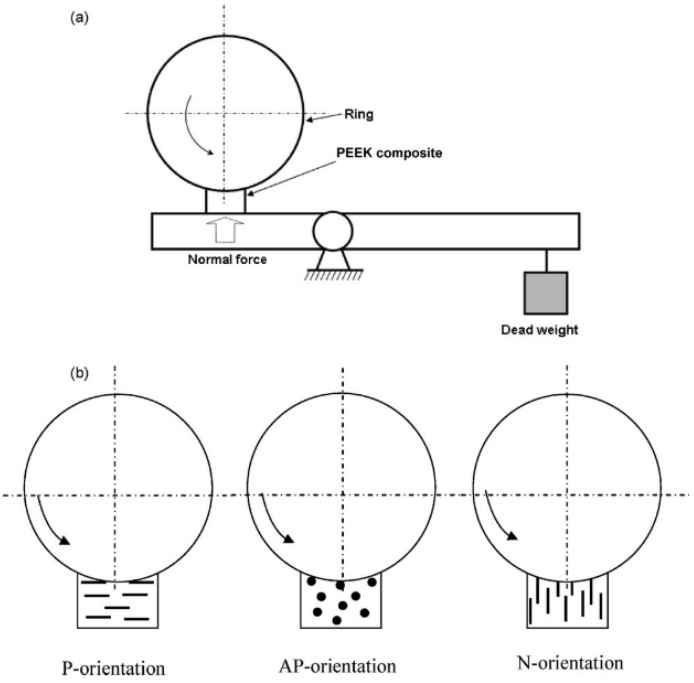

Figure 2.28. (a) Schematic of test apparatus and (b) designations of fibre orientations (adapted from [95])

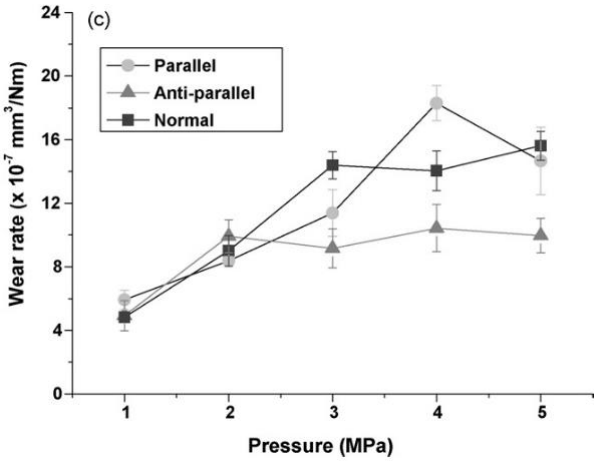

Figure 2.29. Wear rates in the three orientations as a function of apparent pressure (adapted from [95])

Solid lubricants such as graphite and PTFE further enhance the tribological properties of PEEK composites. The tribological behaviour of PEEK-PTFE blends with steel counterparts (Ra roughness of 0.2-0.3 μm) was investigated by Lu and Friedrich [20] (Figure 2.30). Both the wear rates and the friction coefficients exhibit minimum values at PTFE volumes of 10 to 20%. The friction reducing effect of PTFE is considered to be due to the formation of a lubricating transfer film of PTFE on the

steel counterparts (Figure 2.31), but with a higher PTFE content this phase becomes continuous so that the poor wear resistance of PTFE dominates the performance of the blends. The performance of MoS_2 and WS_2 as solid lubricants for PEEK composites paired with stainless steel (Ra roughness of 0.030 ± 0.005 μm) was reported by Zalaznik et al [96]. Figure 2.32 shows friction coefficients and wear rates of the PEEK composites with micro/nano MoS_2 and WS_2. Friction coefficients showed lower values at higher concentrations of solid lubricants. Wear volumes were improved with low concentrations (0.5 wt.% and 1 wt.%) of micro MoS_2, nano MoS_2 and nano WS_2. Based on the results that the composites with a higher hardness had a much better wear performance than the composites with a lower hardness, the authors concluded that the wear behaviour was closely related to the hardness of the PEEK composites. Kalin et al reported that a similar relationship between wear behaviour and hardness was observed for the PEEK composites with graphene and carbon nanotube nanoparticles [97].

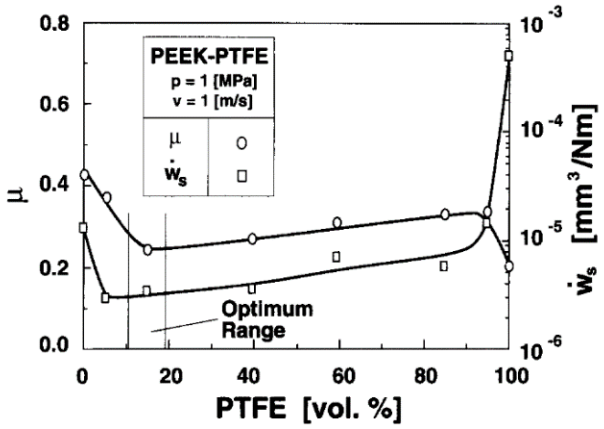

Figure 2.30. Friction coefficients and wear rates as a function of content of PTFE (adapted from [20])

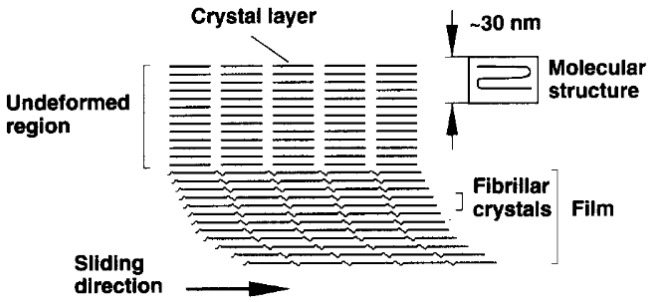

Figure 2.31. Schematic of the lubricating of PTFE (adapted from [20])

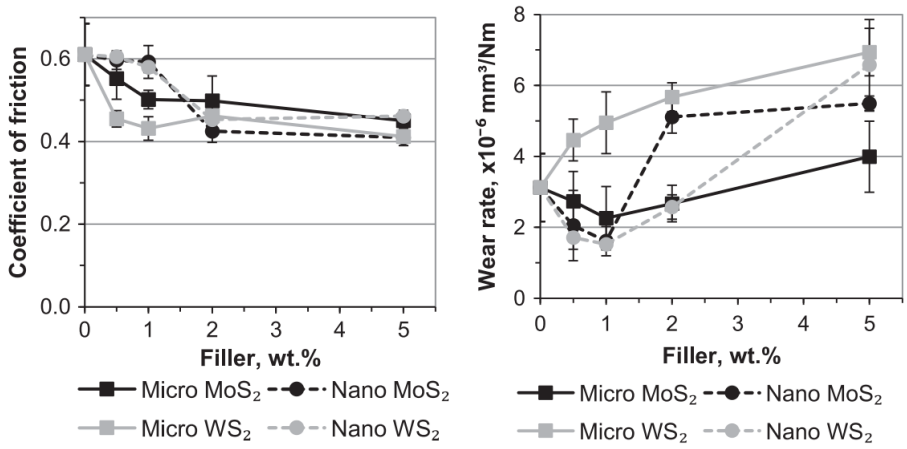

Figure 2.32. Friction coefficients (left) and wear rates (rights) of the PEEK composites with MoS_2 and WS_2 (adapted from [96])

2.2 Lubrication of polymers

2.2.1 Introduction

The term "lubrication" is usually used for two different situations: solid lubrication and fluid lubrication. In both cases, lubricants (solid or fluid) are used to reduce friction and/or wear in a contact between two surfaces. In this study the focus is mainly on fluid lubrication.

In comparison to metals, one of the advantages of polymers is their self-lubricating properties. Therefore, they are widely used with steel counterparts under dry conditions. On the other hand, in some applications, e.g., water/fuel pumps, polymers are used under fluid lubricated conditions by default. In general, lubrication has a positive effect as it prevents the direct contact of two surfaces and basically reduces friction and wear. In addition, fluid lubrication effectively removes frictional heat from the contact surfaces which is expected to improve tribological performance. However, this is not always true of polymers and both positive and negative effects of fluid lubrication have been reported as detailed below.

Figure 2.33 shows wear rates of different materials sliding on stainless steel (roughness of approximately 0.15 µm) under dry and water lubricated conditions, reported by Lancaster [30]. All the materials based on polymers exhibited higher wear rates under the water lubricated condition than under the dry condition. It was argued that water lubrication inhibited the formation of transfer films on the steel surface thus increasing the wear rates of polymers. A similar negative effect has been reported also for the lubrication of PEEK which will be described in section 2.2.5.

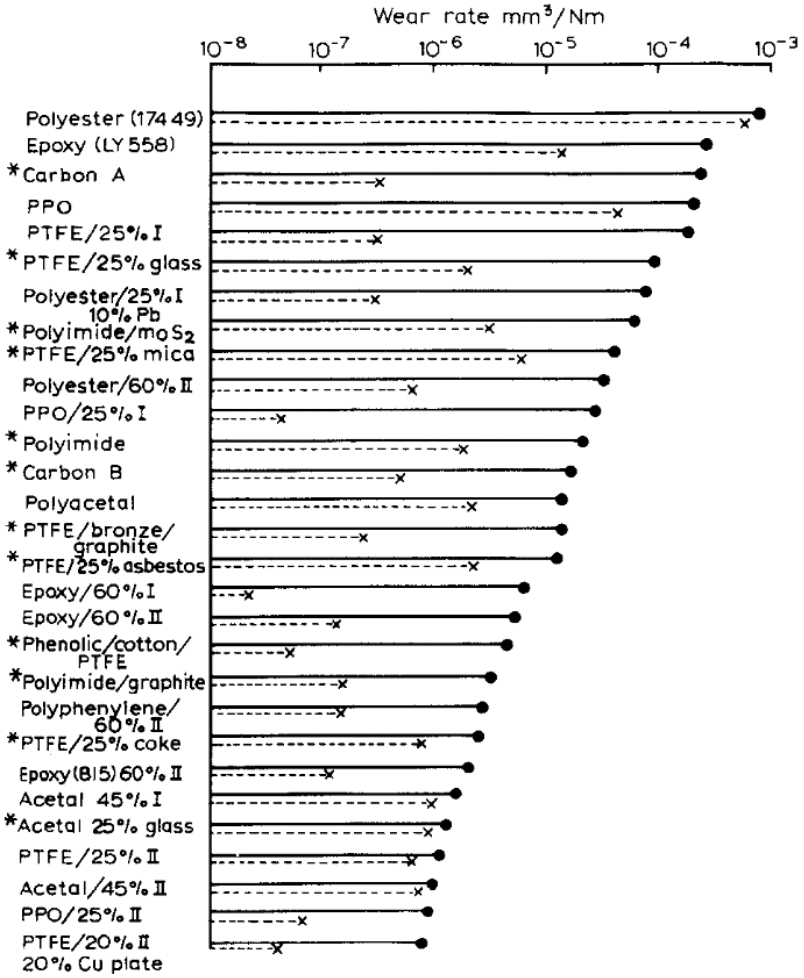

Figure 2.33. Wear rates of different materials sliding on stainless steel. Full lines, water lubricated; dotted lines, unlubricated. (adapted from [30])

On the other hand, a positive effect of lubrication with poly-dimethyl siloxane (PDMS) was reported as shown in Figure 2.34 [25]. Despite the low viscosity of PDMS (10 cSt), lubrication improved both friction and wear for all polymers tested (polyphenylene oxide (PPO), PEEK and PTFE) in contact with steel counterparts (Ra roughness of 0.10 µm). The authors pointed out that the positive effect of lubrication was especially seen at high speeds, due to the transition from boundary or mixed lubrication regime to elastohydrodynamic lubrication (EHL) or hydrodynamic lubrication regime. In this case, no negative effect was shown even at low speeds, governed by boundary or mixed lubrication regime. Note that lubrication regimes will be described more in section 2.2.2.

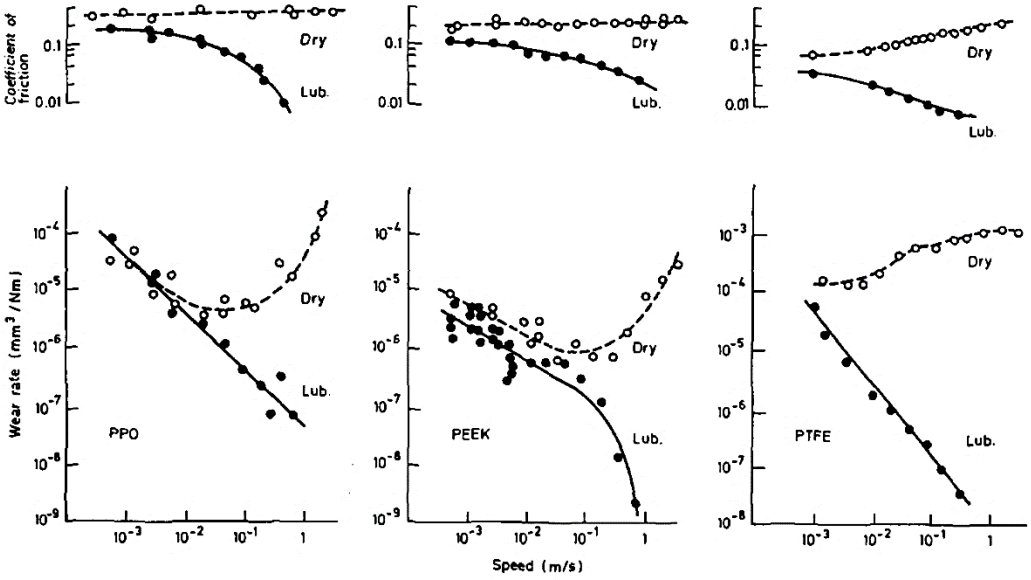

Figure 2.34. Friction coefficients and wear rates for PPO, PEEK and PTFE in dry and lubricated conditions (adapted from [25])

2.2.2 Lubrication regime

Lubrication regimes are generally classified into the following four regimes: (a) Hydrodynamic lubrication, (b) Elastrohydrodynamic lubrication, (c) Mixed lubrication, and (d) Boundary lubrication. The schematics of these lubrication regimes are shown in Figure 2.35 [98].

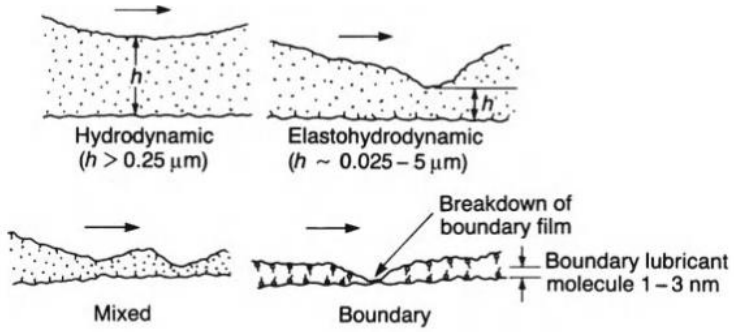

Figure 2.35. Schematics of lubrication regimes (adapted from [98])

(a) Hydrodynamic lubrication

Hydrodynamic lubrication is sometimes called fluid-film lubrication and referred to as the ideal lubricated contact condition because the fluid films are normally many times thicker than the

roughness of the two surfaces, which means solid contacts do not occur. Therefore, the friction coefficient in the HD regime can be as small as 0.001.

(b) Elastrohydrodynamic lubrication

Elastohydrodynamic lubrication (EHL) is a part of hydrodynamic lubrication in which the elastic deformation of the contacting surfaces plays an important role. EHL readily occurs in highly pressured contacts, such as the point contacts of ball bearings and the line contacts of roller bearings and of gear teeth. At highly pressured contacts, both the viscosity of the lubricant and elastic deformation of the bodies in contact can change dramatically and influence film thickness.

(c) Mixed lubrication

The transition regime between hydrodynamic lubrication and boundary lubrication is known as mixed lubrication in which two lubrication regimes combine. There are more frequent solid contacts, but a portion of the two surface remains supported by a partial hydrodynamic film.

(d) Boundary lubrication

Boundary lubrication is the regime in which the solid surfaces are so close together that surface interaction between monomolecular or multimolecular films of lubricants and the solid asperities dominates the contact. The friction coefficient in boundary lubrication can approach high levels (about 0.1 or much higher).

The representative friction curves in these four regimes are described in the so-called Stribeck curve shown in Figure 2.36 [98]. Friction coefficients are plotted as a function of the product of dynamic viscosity "η" and rotational speed in revolutions per unit second "N" divided by the load per unit projected area "P (pressure)". The lubrication regimes are commonly identified by a lubricant film parameter "Λ", also called Lambda ratio. Lambda ratio is calculated from Equations 2-1 and 2-2:

$$\Lambda = h/\sigma \qquad \text{(Eq. 2-1)}$$

$$\sigma = \sqrt{(\sigma_1{}^2 + \sigma_2{}^2)} \qquad \text{(Eq. 2-2)}$$

where h is the oil film thickness under operating conditions, σ is the composite surface roughness, and σ_1 and σ_2 are the surface roughness of the two contact surfaces.

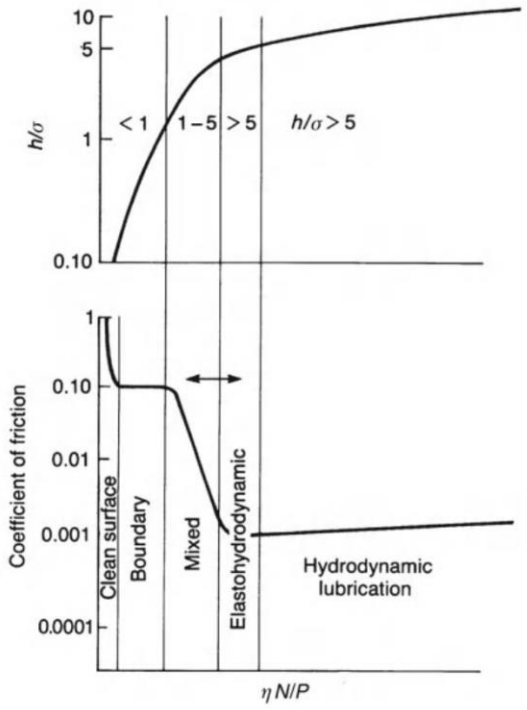

Figure 2.36. Lubricant film parameter (h/σ) (upper) and friction coefficient (lower) as a function of ηN/P (Stribeck curve) (adapted from [98])

2.2.3 Lubricants and lubricant additives

(a) Lubricants

Lubricants basically consist of base oils and additives. Various types of base oils and additives are used depending on the purpose the lubricants are used for. Table 2.4 shows the classifications of base oils by the American Petroleum Institute (API) (https://www.api.org/). Base oils are classified into five groups according to their ingredients and performance characteristics. The Viscosity Index (VI) characterizes the viscosity-temperature behaviour of a lubricant. A higher VI value indicates a more stable viscosity to temperature variations. Group I to III base oils are mineral oils commonly used as base stocks for lubricants because of their low cost. They are refined from crude oil and classified depending on the remaining sulphur contents and ratios of saturated-hydrocarbons. Typical chemical structures contained in mineral oils are shown in Figure 2.37 [99]. Group IV consists of synthetic poly-alpha-olefins (PAOs). They are expensive compared to mineral oils, but the use of synthetic oil has increased gradually, especially in more specialized applications such as in the automotive industry. PAO is synthesized by oligomerization of a monomer with a straight carbon chain with an unsaturated carbon atom at one end of the chain (α-olefin). PAOs in the market are basically a mixture of oligomers with different chain lengths such as dimer, trimer and

so on. The viscosity of PAOs depends on the ratios and type of oligomers and is available as several grades. All base oils, not included in Group I to IV, such as silicones, naphthenics, polyalkylene glycols and organic esters are included in Group V.

Table 2.4. API base oil classification (source: https://www.api.org/)

Group	Sulphur, %		Saturates, %	Viscosity Index
I	>0.03	and/or	<90	80-119
II	≤0.03	And	≥90	80-119
III	≤0.03	And	≥90	≥120
IV	All poly-alpha-olefins (PAOs)			
V	All base oils not included in Groups I-IV			

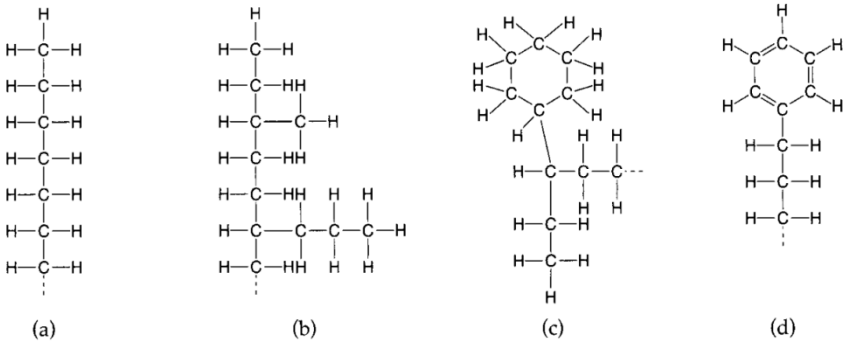

Figure 2.37. Typical chemical structures contained in mineral oils : (a) straight paraffin, (b) branched paraffin, (c) naphthene, and (d) aromatic (adapted from [99])

(b) Lubricant additives

Lubricant additives are added to base stocks in quantities of a few weight percent to improve their lubricity and lifespan [38,100,101]. There are various types of lubricant additives as shown in Table 2.5 [100]. They work chemically and/or physically at the interfaces between different phases or in bulk lubricants. Minami depicted the interactive features of various lubricant additives in Table 2.6 [101]. In terms of the working function, extreme pressure (EP) additives, anti-wear (AW) additives and friction modifiers (FMs) are listed as tribo-improvers which reduce friction and wear. They work chemically/physically on the interface, mitigating direct contacts of the two sliding surfaces by

forming adsorption films and/or reaction films. Although other additives also influence the tribological properties to some extent, the effect of EP additives, AW additives and FMs is much higher than that of other additives.

Table 2.5. Types of lubricant additives (reproduced from [100])

Additive	Use
Antioxidant	Prevent oil decomposition
Lubricity additive	Reduce friction and wear at moderate temperature
Extreme pressure agent	Reduce friction wear at high temperature
Pour-point depressant	Decrease low-temperature use limit
Viscosity index improver	Lower the viscosity-temperature coefficient
Rust inhibitor	Protect metal surfaces against corrosion
Detergent	Prevent formation of sludges and varnishes
Dispersant	Keep insoluble decomposition products in suspension
Foam inhibitor	Break foams

Table 2.6. Interactive features of various lubricant additives (reproduced from [101])

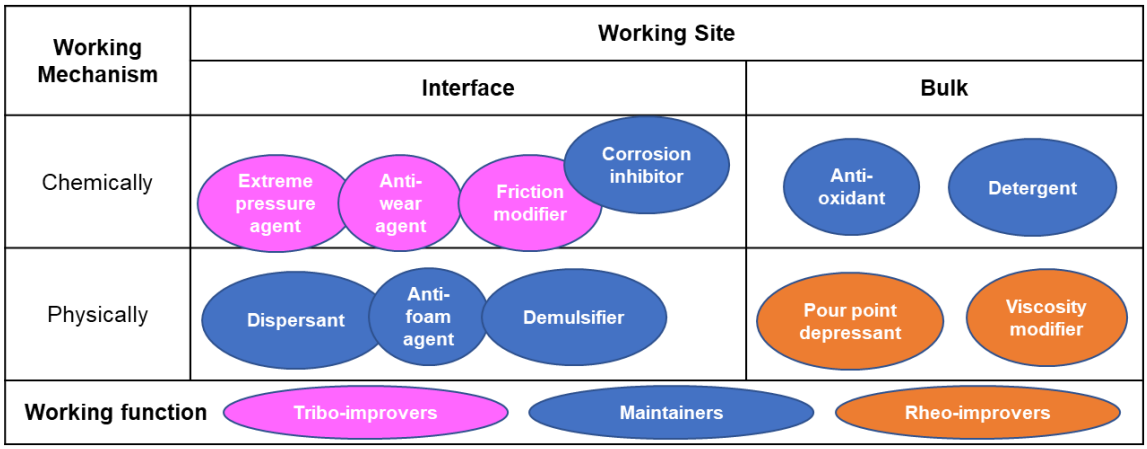

Organic friction modifiers (OFMs) are historically some of the most essential lubricant additives [40,102]. OFMs are surfactant-like molecules generally consisting of long hydrocarbon chains (usually more than 10 carbon atoms) with polar groups (e.g., alcohol, amine, amide and carboxylic

acid groups) at their ends. The effect of OFMs has been extensively investigated in steel-steel contacts [103–111], and the working mechanism proposed was that OFMs adsorb or chemically react on the polar steel surfaces to form dense monolayers or thick reacted viscous layers, thus preventing direct contact between two sliding surfaces and mitigating friction and wear. Figure 2.38 and Figure 2.39 show examples of the adsorption of OFMs with polar groups on a surface and the formation of durable films [98,99]. As can be seen from these schematics the effects of OFMs depend on their chemical structures and the tribological conditions such as surface materials, contact pressure, sliding speed and temperature, therefore when lubricants are formulated it is important to choose suitable OFMs from the many chemical structures available.

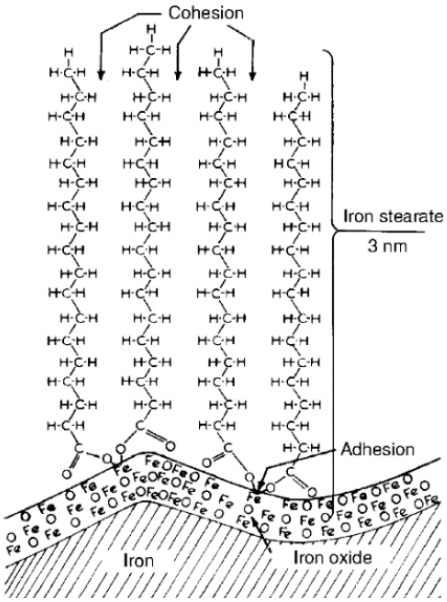

Figure 2.38. Schematic of the adsorption of OFM on a metallic surface (adapted from [98])

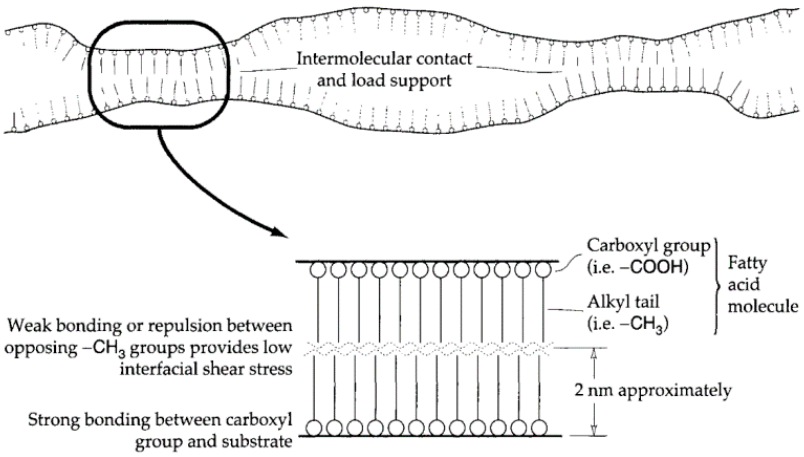

Figure 2.39. Schematic of OFM molecular layer on a metallic surface (adapted from [99])

EP additives and AW additives are also essential additives especially for the lubricants used under severe conditions such as in automobiles. Among the various types of EP/AW additives, Zinc dialkyldithiophosphate (ZDDP) and tricresyl phosphate (TCP) are the most standard additives widely used in lubricants for many applications and an enormous number of studies on their effect and working mechanism in steel-steel contacts has been reported [39,112–116]. ZDDP contains phosphorus and sulphur atoms in its structure (Figure 2.40), and therefore has characteristics of both EP additive and AW additives. Sulphur atoms in ZDDP play a distinctive role in preventing seizure as an EP additive. ZDDP also act as an AW additive by forming reaction films consisting of phosphorus atoms on the steel surface as shown in Figure 2.41 [39]. Although the reaction mechanism of ZDDP is complicated and multiple processes have been proposed, they basically need the decomposition of ZDDP to work. This also applies to the working mechanism of TCP which functions as an AW additive (Figure 2.42) [114].

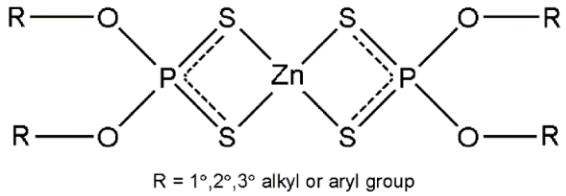

Figure 2.40. Structure of ZDDP (adapted from [113])

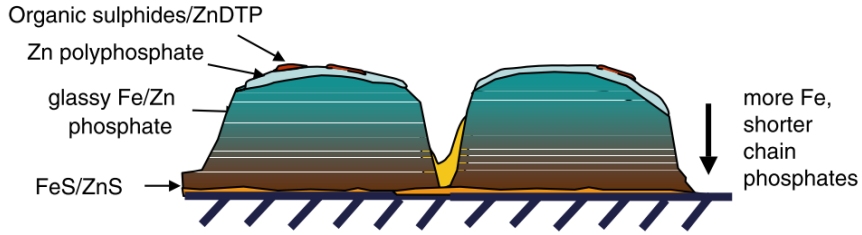

Figure 2.41. Schematic of structure and composition of ZDDP reaction film (adapted from [39])

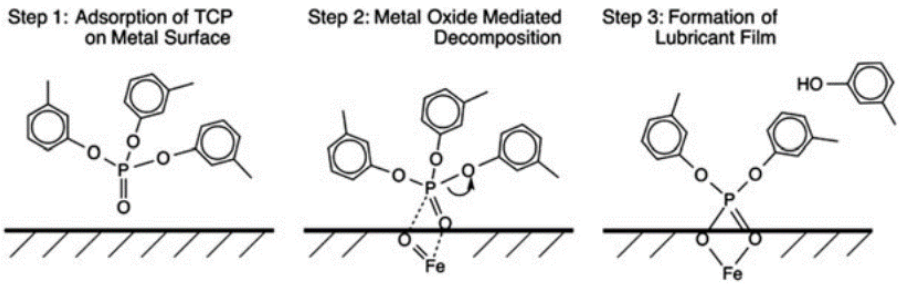

Figure 2.42. Schematic of TCP decomposition and film formation on steel (adapted from [114])

Despite the large number of studies reported on the effect and working mechanism of lubricant additives described above, most of these studies have been limited to metal-metal contacts, especially steel-steel contacts.

2.2.4 Factors influencing the lubrication of polymers

(a) Heat

As described in section 2.1.3, heat causes an unfavourable effect on the tribological properties of polymers because of their lower thermal stabilities compared to metals. In addition, due to the low thermal conductivity of polymers, frictional heat accumulates on the polymer surface, causing thermal failures. One of the advantage of lubricating polymers is that it will effectively remove frictional heat from the contact surfaces [32,117–123]. Sarita and Senthilvelan reported that polymer (PA66) gear life was longer under lubrication with gear oil compared to under dry condition [122]. Based on the result that cracking near pitch points, which is caused by a decrease in polymer tensile strength with the frictional heat, was not observed under lubricated conditions (Figure 2.43), the authors concluded that lubrication dissipates the frictional heat effectively, thus achieving a longer polymer gear life.

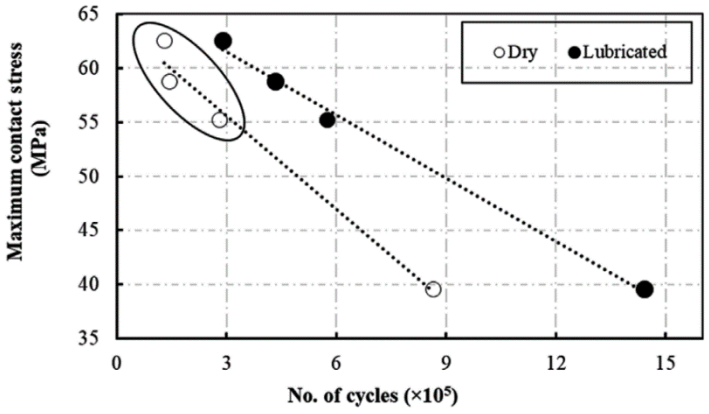

Figure 2.43. PA66 gear life under dry and lubricated condition; the circled area indicates the presence of thermal failures of polymer gears (adapted from [122])

(b) Polymer transfer films on steel counterparts

As mentioned in section 2.1.3 and section 2.1.4, the formation of polymer transfer films on steel counterparts is considered to be the key to reducing the friction and wear of polymers with steel

counterparts in dry conditions. It is therefore assumed that the negative effect of lubrication mainly results from the inhibition of transfer film formation on the steel counterparts. Figure 2.44 shows the wear volumes of epoxy composites in contact with steel (roughness of approximately 0.15 µm) plotted as a function of revolutions reported by Lancaster [30]. Water additions following unlubricated sliding caused the rapid increase of wear volumes. The author mentioned that these results indicate that transfer films formed in dry conditions were removed by the addition of water within a few revolutions and the wear rates then increased markedly. Zhang et al. also reported the addition of diesel onto the wear track of PEEK composites paired with steel (Ra of 0.25 µm) caused the friction coefficient to increase significantly due to the removal of the transfer film as shown in Figure 2.45 [124].

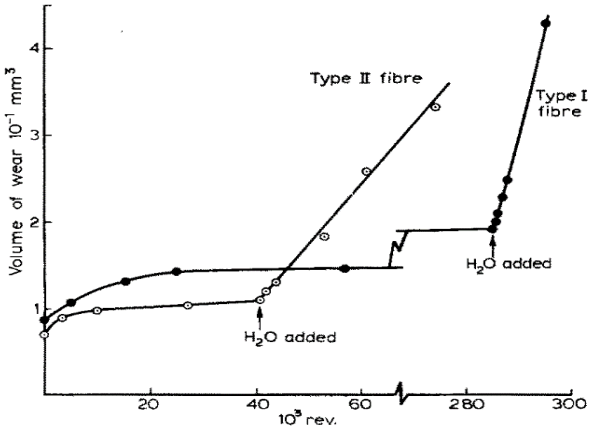

Figure 2.44. Effect of water additions following unlubricated sliding (adapted from [30])

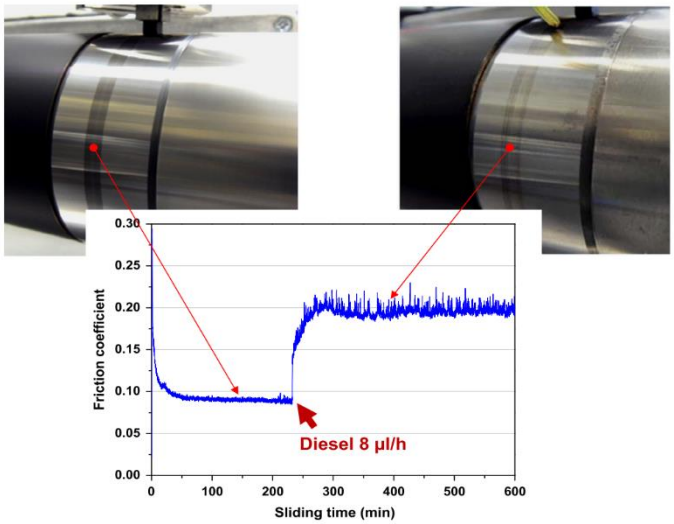

Figure 2.45. Effect of diesel injection following unlubricated sliding (adapted from [124])

Zhang et al. reported the positive effect of diesel lubrication on the friction and wear of poly phenylene sulfide (PPS) composites and observed the presence of some films on steel counterparts (Figure 2.46) [28]. PPS composites were rubbed against a dry, diesel pre-wetted and diesel continuously lubricated rings (Ra roughness of approximately 0.2 µm). Interestingly, the prewetted ring showed the lowest friction and wear of all the PPS composites tested. Continuous lubrication with diesel showed higher friction and wear than prewetted, but less that observed under dry conditions. Optical images of the steel surfaces after the tests indicated that the presence of diesel inhibited the formation of the film on the steel counter face. Nevertheless, some film formation was observed under lubricated conditions. Based on the EDX analysis of the film, the authors proposed that the superior tribological performance with prewetted steel rings was due to the combined effects of both a diesel film (liquid) and a tribofilm formed by the solid lubricants of tungsten disulphide (WS_2) and aluminium nitride (AlN) nano particles (NPs) contained in the PPS composites. On the other hand, Zhao et al. reported that the addition of solid lubricants of PTFE and graphite, and SiO_2 NPs did not change the friction coefficients and wear rates much of short glass fibre (SGF) reinforced epoxy composites under oil lubrication with poly-alpha-olefin (PAO) (Figure 2.47) [125].

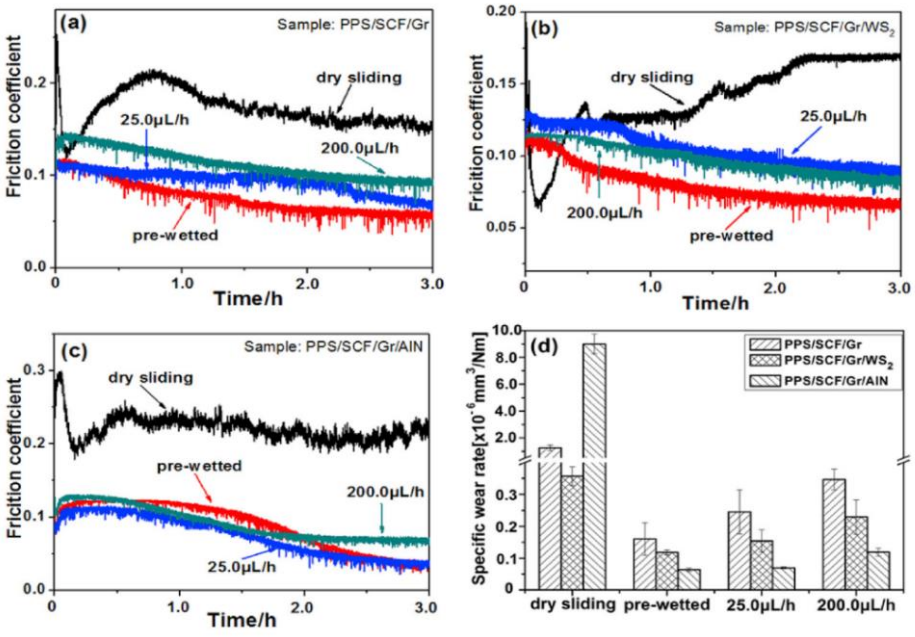

Figure 2.46. Tribological performance of PPS composites under dry and diesel lubricated conditions (adapted from [28])

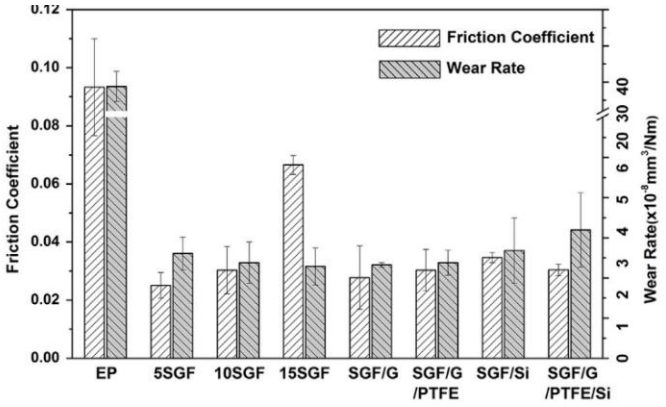

Figure 2.47. Friction coefficients and wear rates of epoxy composites under oil lubrication (adapted from [125])

2.2.5 Lubrication of PEEK and PEEK composites

Similar to other polymers, positive and negative effects of lubrication on the tribological performance of PEEK and PEEK composites have been reported by several groups as follows.

(a) Positive effect of lubrication

Jia et al. reported the positive effect of lubrication for the tribological contact of carbon fibre and PTFE reinforced PEEK composite with steel counterparts (Ra roughness of 0.1 μm) [26]. Figure 2.48 shows the friction coefficients and wear rates of PEEK composites under dry and water lubrication at various loads. The friction coefficients under dry conditions and loads above 500 N exhibited lower values than those under water lubrication because of the action of the solid lubricant PTFE contained in the PEEK composite. By contrast, wear rates under water lubrication were lower than those for the dry conditions over the whole range of loads studied. The worn surfaces of the steel counterparts were investigated by XPS. Interestingly, the peaks assigned to iron fluoride appeared on the surface only under dry condition and almost no iron fluoride was observed on the surface under water lubrication. The authors concluded that the role of the solid lubricant, PTFE, would have less effect on the tribological behaviour of polymers under water lubrication than under dry conditions, while the cooling and boundary lubricating effects of water would dominate the tribological behaviour.

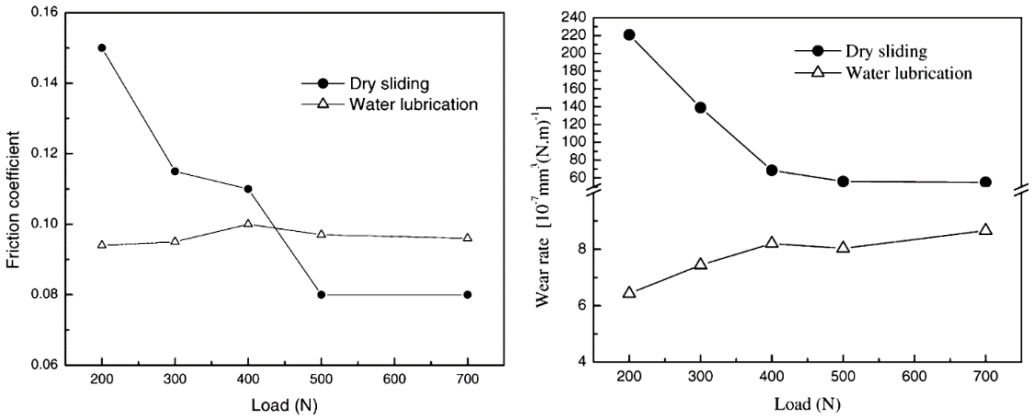

Figure 2.48. Friction coefficients (left) and wear rates (right) of PEEK composite under dry and water lubrication (adapted from [26])

The positive effect of lubrication on the contact of pure PEEK and glass fibre reinforced (GFR) PEEK with steel counterparts (roughness of 0.28-0.35 µm) was also reported by Sumer et al. [27]. Figure 2.49 shows the friction coefficients and wear rates under dry and water lubrication. Water lubrication reduced friction and wear for both pure PEEK and GFR PEEK, while the change in the combined pressure and speed factor (PV factor) influenced less the tribological behaviour. For both pure PEEK and GFR PEEK under water lubrication, polymer transfer films on steel were hardly observed in the optical images of the steel counterparts, implying that water lubrication inhibited the formation of transfer films. The authors assumed that the cooling effect of water prevented thermal degradation (melting) of the PEEK and PEEK composite, thus improving tribological performance.

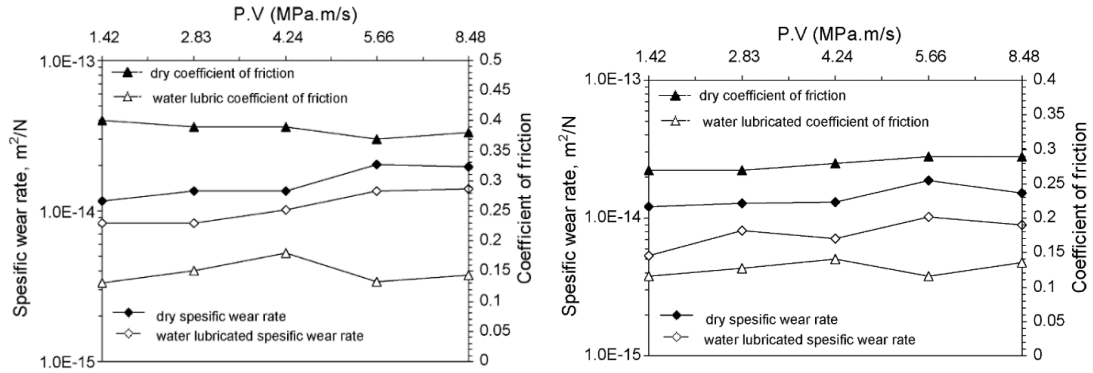

Figure 2.49. Friction coefficients and wear rates of pure PEEK (left) and GFR PEEK (right) under dry and water lubrication (adapted from [27])

Chen et al. reported that lubrication with pure and sea water improved the tribological performance of the carbon fibre reinforced (CFR) PEEK with steel (Ra roughness of approximately 0.1 µm) [126]. Figure 2.50 shows friction coefficients and wear rates of CFR PEEK under dry, pure water and sea water lubrication. Transfer films were not observed on the steel surfaces under pure and sea water lubrication. The authors noted that the better tribological performance under pure and sea water lubrication relied on their cooling effect eliminating much frictional heat. Interestingly, the wear rate under sea water lubrication was much smaller than under pure water lubrication, despite the film thickness being almost the same. Based on the previous study using XPS analysis [127], the authors proposed that the superior lubrication of sea water originated from the deposition of Ca^{2+} and Mg^{2+} in the form of $CaCO_3$ and $Mg(OH)_2$ on the sliding surface.

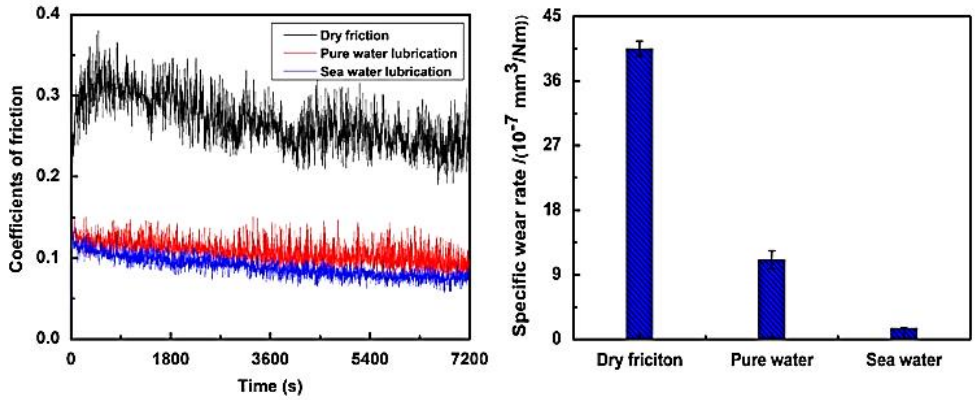

Figure 2.50. Friction coefficients (left) and wear rates (right) of CFR PEEK under dry, pure water and sea water lubrication (adapted from [126])

Apart from water lubrication, Zhang et al. investigated the tribological behaviour of pure PEEK and PEEK composites with multiple fillers i.e. short carbon fibres, solid lubricants and ceramic particles under diesel and engine oil lubrication (Figure 2.51) [33]. In comparison with the dry condition, diesel lubrication showed a positive effect for the pure PEEK-steel contact, and a negative effect for the PEEK composite-steel contact (100Cr6 bearing steel, Ra roughness of 0.2-0.3 µm). Under diesel lubrication the polymer transfer film observed on the steel counterparts rubbed with pure PEEK was thicker than that on the steel counterparts rubbed with PEEK composite, indicating the importance of the transfer films for obtaining better tribological behaviour. The authors also compared wear volumes of St50 (low alloy steel), pure PEEK and the PEEK composite with steel counterparts as shown in Figure 2.52. The PEEK composite showed a better wear performance than St50 and pure PEEK. The authors conjectured that the enhanced abrasion resistance of the PEEK composite due to the reinforcing fibres is beneficial to its wear resistance. In addition, the authors

assumed that films were produced by PEEK transfer and tribo-chemical reactions, but no chemical analysis was carried out to confirm that.

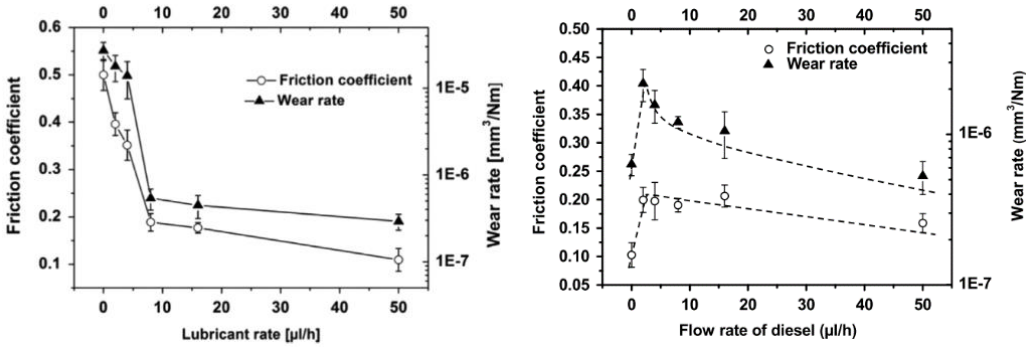

Figure 2.51. Friction coefficients and wear rates of pure PEEK (left) and PEEK composite (right) as a function of diesel flow rate (adapted from [33])

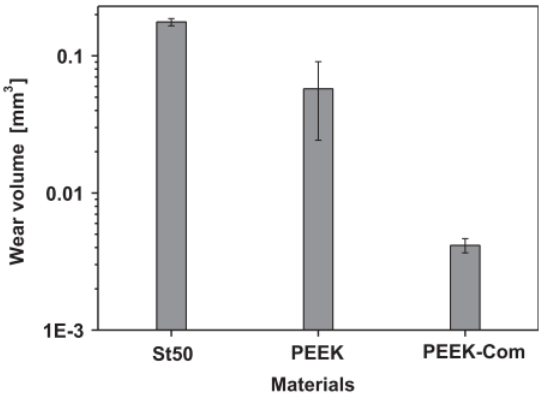

Figure 2.52. Wear volumes of St50, pure PEEK and PEEK Composite paired with steel under engine oil lubrication (adapted from [33])

(b) Negative effect of lubrication

Yamamoto et al. reported the negative effect of lubrication on PEEK as well as PPS [31]. Figure 2.53 shows wear rates of PPS and PEEK with steel counterparts (average roughness of 0.8 µm) under dry and water lubrication. Water lubrication increased the wear rates of both polymers, but PEEK showed a greater deterioration than PPS. To explain the difference of wear rates between the two polymers, the authors noted that sulphur atoms in the PPS structure contributes to its greater ability to form a polymer transfer film on the steel counterparts compared to PEEK. In addition, the authors pointed out that the hardness modification of the polymer surfaces was another factor affecting tribological behaviour. Figure 2.54 shows the surface hardness of the polymers at the

sliding area measured using a micro Vickers hardness tester. Under water lubrication, the hardness of the sliding surface of PEEK significantly decreased, but not that of PPS. The authors confirmed that the hardness of PEEK was not decreased just by immersion in water and concluded that the reduction in hardness promoted the wear of PEEK under water lubrication. The authors also assumed that this softening was due to the water molecules attacking the carbonyl groups contained in the PEEK molecule, as this did not occur in PPS. Similar softening of PEEK in water lubricated conditions were reported by Yamaguchi and Hokkirigawa [128]. However, no investigation was carried out to demonstrate this hypothesis by using less polar lubricants such as oils.

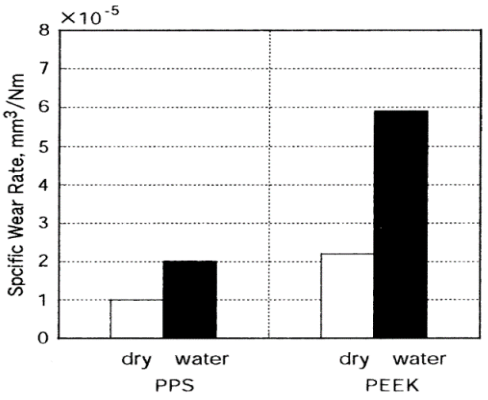

Figure 2.53. Wear rates of PPS and PEEK under dry and water lubrication (adapted from [31])

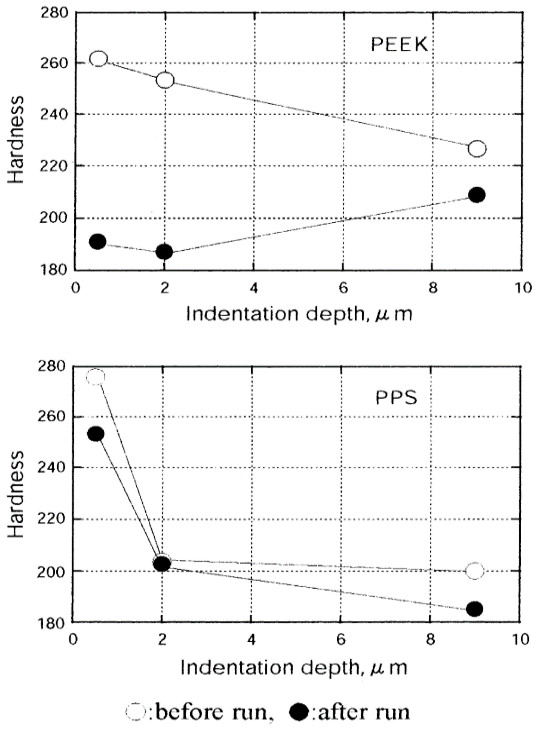

Figure 2.54. Hardness of PEEK (upper) and PPS (lower) at the sliding area (adapted from [31])

The negative effect of lubrication was also reported by Kurdi et al. [32] who investigated the tribological behaviour of pure PEEK and PEEK composites with TiO_2 nanoparticles under dry and water lubrication, followed by the characterization of the thickness of the polymer transfer films (transfer film layers (TFLs)) by a nanoindentation technique. Water lubrication inhibited the formation of transfer films for both pure PEEK and PEEK composites (Figure 2.55), and also increased the wear rates of these polymers. The authors also reported a softening of the PEEK after the sliding tests. Similar to the results reported by Yamamoto et al. [31], the hardness of the worn PEEK wear track under water lubrication was lower than that under dry conditions as shown in Figure 2.56. However, Fourier-transform infrared spectroscopy (FTIR) analysis indicated no significant differences between the worn PEEK wear track under water lubrication and the original PEEK surface. These results did not support the hypothesis of water molecules attacking the carbonyl groups from the PEEK molecule proposed by Yamamoto et al. [31].

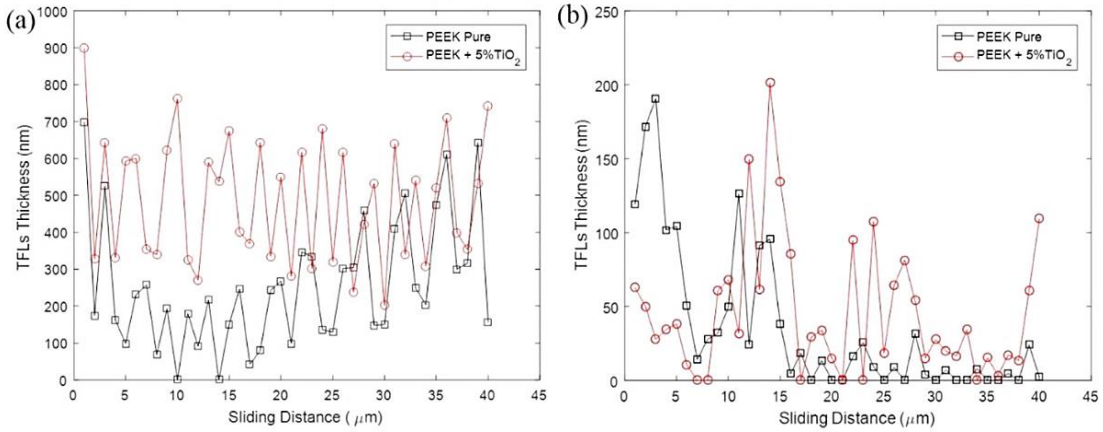

Figure 2.55. Polymer transfer films (TFLs) thickness distribution on wear-tracks under (a) dry and (b) water lubrication (adapted from [32])

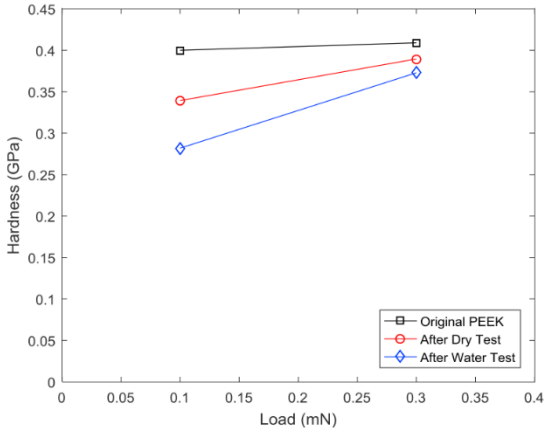

Figure 2.56. Hardness as a function of indentation load on worn PEEK wear-tracks after dry and water lubricated test as well as original PEEK surface (adapted from [32])

The studies mentioned so far in this section investigated PEEK and/or PEEK composites against steel counterparts but the negative effects of lubrication on PEEK composites have also been reported with counterparts of various materials. Wang et al. reported the tribological behaviour of the PEEK composite with PTFE against Si_3N_4 ceramic (roughness of 0.014 µm) [129]. Figure 2.57 shows the friction coefficients and wear rates of the PEEK composite with Si_3N_4 ceramic under dry and water lubrication at different loads and sliding velocities. Under most conditions, water lubrication increased wear rates compared with the dry condition, while similar values for friction coefficients were observed. As described above, in most cases of PEEK-steel and PEEK composites-steel, transfer films were thinner under lubricated conditions than dry conditions. On the other hand, the authors of this study noted that transfer films on Si_3N_4 ceramic counterparts were thicker under water lubrication than under dry conditions. Note that compared with the roughness of steel counterparts described above (in a range of 0.1-1 µm), the roughness of Si_3N_4 ceramic counterpart (0.014 µm) was very low. This implies that the roughness of counterparts can affect the tribological behaviour of PEEK and PEEK composite under lubrication as well as under dry conditions.

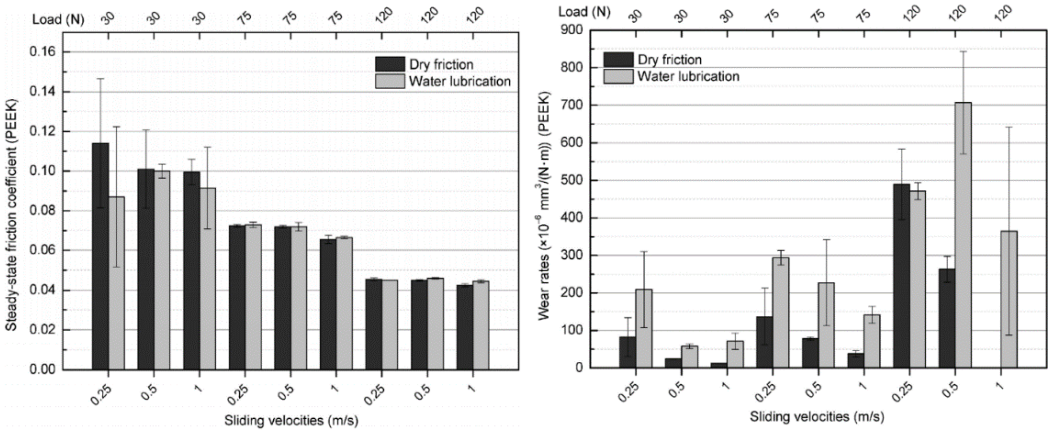

Figure 2.57. Friction coefficients (left) and wear rates (right) of PEEK composite paired with Si_3N_4 under dry and water lubrication (adapted from [129])

Jacobs et al. reported that water lubrication shows positive or negative effect on the wear of CFR PEEK depending on the counterpart materials (Rz roughness of 0.1-0.5 µm) [34]. Figure 2.58 shows the wear rates of CFR PEEK against different material surfaces under dry and water lubrication. Notably, water lubrication reduced wear rates with the alumina (Al_2O_3) and the tungsten doped diamond like carbon (W-DLC), while it notably increased with steel (X5CrNi18-10 and plasma-nitrided X5CrNi18-10). W-DLC under water lubrication delivered the best result for wear rates, producing a particularly smooth surface of the wear track after sliding (Figure 2.59). Al_2O_3 also gave

a smooth surface under lubrication due to the tenacious transfer filling the pores on the surface. Contrary to Al_2O_3, silicon nitride (Si_3N_4) increased the wear rate under water lubrication. The authors postulated that Si_3N_4 forms a thin SiO_2 surface layer which is beneficial in dry conditions but susceptible to stress corrosion cracking causing the growth of a crack in a corrosive environment such as under water lubrication. Therefore, the wear process of Si_3N_4 was promoted under water lubrication which does not happen with Al_2O_3. However, no chemical analysis was carried out to demonstrate this hypothesis.

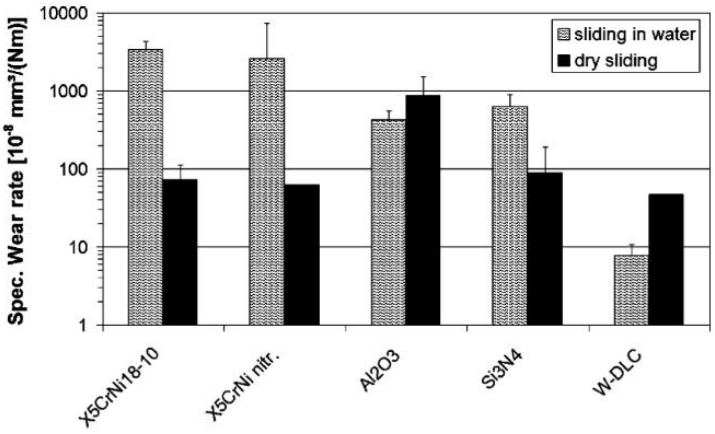

Figure 2.58. Wear rates of CFR PEEK paired with different material counterparts (adapted from [34])

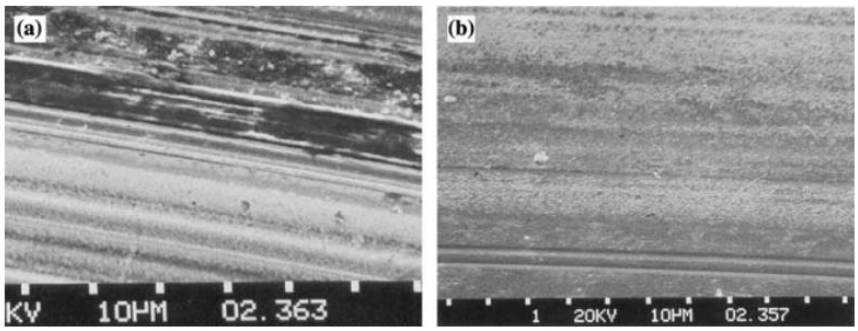

Figure 2.59. SE images of the wear track on W-DLC under (a) dry and (b) water lubrication (adapted from [34])

2.3 Summary

This chapter reviewed the literature relevant to understanding the research context of the studied topic. Firstly, an overview of polymers for tribological applications and their tribology under dry conditions was conducted by focusing on the factors influencing their tribological behaviour. Secondly, existing research related to the lubrication of polymers was reviewed with a special emphasis being placed on PEEK and PEEK composites.

From the extensive studies of the tribological performance of polymers under dry conditions against steel counterparts, steel being necessary to avoid thermal failures of polymers caused by frictional heat accumulating on the contact surface, there is a general consensus that polymer transfer films on steel counterparts play an important role in determining performance. They act as protective films avoiding the direct contact of the polymers with the hard asperities of the steel and thus reduce wear. The formation of transfer films is affected by various factors such as the composition of the polymers, surface topography of the steel counterparts and tribological conditions. Most of the previous studies of polymer tribology have focused on improving the tribological performance by incorporating specific fillers such as reinforcement fibres (carbon fibres, glass fibres, etc) and solid lubricants (graphite, PTFE, WS_2 particles, etc) and their effects on friction and wear performance have been evaluated.

Both a positive and negative effect of lubrication on the tribological performance of polymer-steel contacts have been reported. A positive effect is plausibly derived from:

(1) Mitigating direct contact of the two surfaces by the formation of a lubricant fluid film
(2) Removing frictional heat from the contact surfaces

On the other hand, a negative effect may arise from:

(1) Inhibition of the formation of polymer transfer films on steel counterparts
(2) Softening of the surfaces of polymers

In PEEK-steel and PEEK composite-steel contacts, the overall effect of lubrication may be determined by the balance between the positive and negative effects mentioned above. However, as discussed in section 2.1.4 and section 2.2.5, there are many factors affecting this balance (e.g., contact motion, surface roughness of steel counterparts, lubricant properties, polymer transfer films and/or reaction films on counterparts, hardness modification of polymer surface), and these have been considered separately. However, the working mechanism of the lubrication of PEEK and PEEK composites still remains unclear. Moreover, most of previous studies were performed under water lubrication, and the effect of lubricant additives commonly used in oil lubricants for

improving tribological performance has been little investigated. Due to these limitations, a solid understanding of lubrication mechanism of PEEK and PEEK composites is still lacking.

Based on the findings of this literature review and the gaps in knowledge identified, this thesis will therefore address the following points using the methodology described in Chapter 3:

(1) Comparison of different contact motions (i.e., sliding and sliding-rolling contacts)
(2) Comparison of smooth and rough steel counterparts
(3) Effect of lubricant viscosity
(4) Effect of lubricant additives
(5) Concomitant investigation of two key factors (i.e., polymer transfer films on steel and hardness modification of the polymer surface)
(6) Concomitant investigation of pure PEEK and PEEK composites

Chapter 3 Methodology

This chapter summarizes the materials and experimental methods applied in this study. These methods are designed to elucidate the effect and working mechanism of lubrication on the tribological properties of PEEK and its composites. Tribological tests were mainly performed on PEEK-steel and PEEK composites-steel contacts using a Mini Traction Machine (MTM) which simulates the sliding-rolling contact motion as encountered in gears, one of the main expected applications of this study. In addition to pure PEEK, carbon fibre reinforced (CFR) PEEK and glass fibre reinforced (GFR) PEEK, as typical PEEK composites, were investigated paired with steel counterparts. Base oils with/without lubricant additives were used as test lubricants. To further investigate the mechanism of action, after-test specimens were analysed using various surface analysis techniques for example 3D surface profilometer, nanoindentation, Electron Probe Micro Analysis (EPMA), X-ray Photoelectron Spectroscopy (XPS) and Raman spectroscopy, focusing especially on the hardness of the polymers and the formation of polymer transfer films on the steel counterparts which both plausibly have impacts on the tribological behaviour of polymer-steel contacts.

3.1 Materials

3.1.1 Polymer specimens

Polymer specimens for tribological tests were prepared as plates and balls (Figure 3.1). Plate specimens $40 \times 40 \times 2$ mm were injection moulded from commercially available pure PEEK (Solvay® KT-820 NT, Solvay) and PEEK composites, carbon fibre reinforced (CFR) PEEK (Solvay® KT-820 CF30, Solvay) and glass fibre reinforced (GFR) PEEK (Solvay® KT-820 GF30, Solvay). 30 wt.% of carbon fibre and glass fibre are blended for CFR PEEK and GFR PEEK, respectively. These fibres are distributed randomly inside the plate specimens. The features of the fibres embedded in the PEEK matrix will be further discussed in section 6.3.3. Typical properties of each material adapted from the supplier's catalogue (https://www.solvay.com/) are summarized in Table 3.1. The specific gravities of CFR PEEK and GFR PEEK are higher than that of pure PEEK due to the reinforced fibres. The values of Young's modulus and Poisson's ratios are used to calculate contact pressures employed in the tribological testing. The higher values of Young's modulus (stiffness in the longitudinal direction) for CFR PEEK and GFR PEEK lead to higher contact pressures, as discussed later in section 3.2.3. Pure PEEK balls (Ketron® 1000, Mitsubishi Chemical Advanced Materials) with a diameter of 12.7 mm

(half inch) were purchased and drilled to fit the test rig. The values of Ra surface roughness of pure PEEK specimens were approximately 0.05 μm for plates and 0.1 μm for balls, respectively. The values of Ra surface roughness of PEEK composite plates were approximately 0.2 μm for both CFR PEEK and GFR PEEK. PEEK composite plates were slightly rougher than pure PEEK plates due to the fibres blended; they were used without polishing. Pristine polymer plates and balls were used for each test and cleaned with a hydrocarbon-mix solvent (FASTCLEAN 201, CRC Industries UK Ltd) and isopropanol prior to testing.

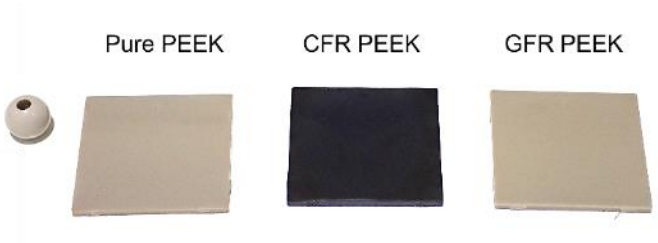

Figure 3.1. Appearance of polymer specimens (Pure PEEK ball and pure PEEK, CFR PEEK and GFR PEEK plates)

Table 3.1. The typical properties of polymers used in this study

	Pure PEEK	**CFR PEEK**	**GFR PEEK**
Polymer sources	Solvay® KT-820 NT	Solvay® KT-820 CF30	Solvay® KT-820 GF30
Fibre types	none	Carbon fibre	Glass fibre
Fibre contents, wt.%	none	30	30
Specific gravities	1.30	1.41	1.53
Young's modulus, GPa	3.8	22.8	11.4
Poisson's ratios	0.33	0.42	0.34

3.1.2 Steel specimens

Steel balls (AISI 52100) with a diameter of 12.7 mm (half inch) and discs (AISI 52100) were obtained from PCS Instruments Ltd (Figure 3.2). These steel specimens had smooth surfaces (Ra roughness of 0.01-0.02 μm). As described in Chapter 2, most of the previous studies on PEEK-steel and PEEK composites-steel contacts were performed using rougher steel, with roughness in the range 0.1-1

μm. As the surface roughness of steel counterparts plays an important role in determining the lubrication regime, in order to evaluate the tribological performance over a wide range of lubrication regime (from hydrodynamic lubrication to mixed and boundary lubrication), rough steel balls were also prepared from the smooth balls by shot blasting to a Ra roughness of approximately 0.5 μm. Note that this value is representative of the roughness of steel parts used for practical applications such as gears. Pristine steel balls and discs were used for each test and cleaned with a hydrocarbon-mix solvent (FASTCLEAN 201, CRC Industries UK Ltd) and isopropanol prior to the test.

Figure 3.2. Appearance of steel specimens

3.1.3 Lubricants

3.1.3.1 Base oils

Base oils with/without lubricant additives were employed as test lubricants in this study. Poly-α-olefin (PAO) oils were used as base oils. These PAO oils are synthesized by oligomerization of a monomer with a straight carbon chain with an unsaturated carbon atom at one end of the chain (α-olefins). PAOs in the market are basically a mixture of oligomers with different chain lengths such as dimer, trimer etc. (Figure 3.3). The viscosity of PAO oils depend on the ratios and type of oligomers and are available as several grades. PAO oils with different viscosity grades, PAO2, PAO4 and PAO10 were selected for the tests in this study. The detailed properties of each PAO oil are summarized in Table 3.2. Generally, the figures numbered after PAO indicate the kinematic viscosity, a measure of resistance to the liquid moving, at 100 °C for the oil. For example, the kinematic viscosity of PAO4 at 100 °C is 3.9 cSt (almost 4 cSt). It should be noted that commercial lubricants commonly consist of low-cost mineral oils, and only high-end products use more expensive PAO oils because of their superior performance. In this study, synthetic PAO oils were chosen as base oils so as to eliminate any influence from contaminants contained in mineral oils. This is often the case for fundamental studies on lubrication mechanisms, and the knowledge obtained from using PAO oils can be generalized to systems using mineral oils. The majority of the tests in this study was conducted with PAO4, but PAO2 and PAO10 were used to investigate the effect of lubricant oil

viscosity which is one of the most important factors when lubricant formulations are designed. Note that the range of viscosity between PAO2 to PAO10 covers most of the lubricants on the market. The density and pressure-viscosity coefficient for each PAO oil are also summarized in Table 3.2. These values along with the kinematic viscosities will be used to calculate the oil film thickness under tribological testing in Chapter 4 and 6.

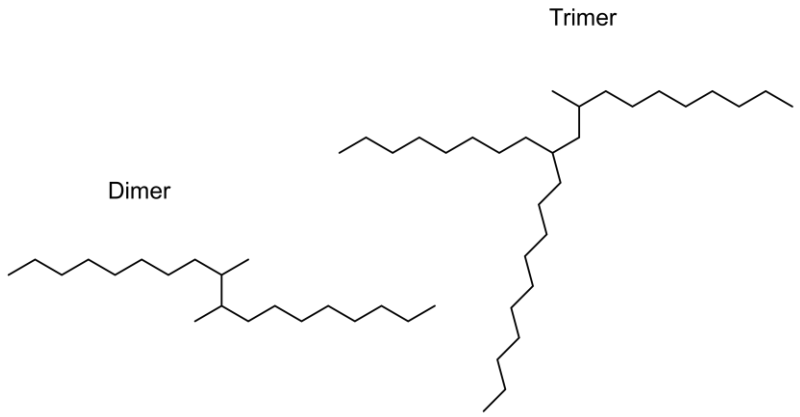

Figure 3.3. Chemical structures of hydrocarbons contained in PAO

Table 3.2. Properties of base oils used in this study

	PAO2	**PAO4**	**PAO10**
Density, g/cm^3 - 15 °C	0.798	0.819	0.836
Kinematic viscosity, cSt - 25 °C - 40 °C - 100 °C	 8 5.0 1.7	 31 17.5 3.9	 136 65.1 9.8
Pressure-viscosity coefficient, GPa^{-1} - 25 °C	15	19	22

3.1.3.2 Lubricant additives

Lubricant additives are added to base stocks in quantities of a few weight percent to improve their lubricity and lifespan [38,100,101]. As described in section 2.2.3, there are various types of lubricant additives, and they work chemically or physically at the interfaces between the different phases or in bulk lubricants. Additives which reduce friction and wear are the most important additives in lubricant formulations. By adsorbing and/or reacting on surfaces and forming films, they work in mixed and boundary lubrication conditions preventing direct contact of the two sliding surfaces.

This study mainly focuses on the additives which are known to strongly affect the tribological properties of steel-steel contacts, namely organic friction modifiers (OFMs) and anti-wear (AW) additives. As described in section 2.2.3, extreme pressure (EP) additives are also commonly added to the lubricants used in steel-steel contacts. However, as EP additives prevent seizure between nascent steel surfaces by forming iron sulphide, EP additives are expected to have less influence on polymer-steel contacts and therefore they were not studied in this thesis.

(a) Organic friction modifiers (OFMs)

OFMs are surfactant-like molecules generally consisting of long hydrocarbon chains (usually more than 10 carbon atoms) with polar groups at their ends. To investigate the effect and working mechanism of OFMs, three types of OFMs which have been widely used in the commercial lubricants namely oleylamine (OAm), oleic acid (OAc) and N-oleoyl sarcosine (OSa), were used in this study. The chemical structures of these OFMs are shown in Figure 3.4. They were chosen to have similar types of hydrocarbon moieties, but different polar groups. This study used these OFMs of technical grade which contain a small amount of different hydrocarbon structures as impurities. However, the composition of these hydrocarbon impurities is similar in the three OFMs, hence the main difference between the three OFMs is their polar groups. The OFMs were added at 1.0 wt.% to PAO4 as listed in Table 3.3.

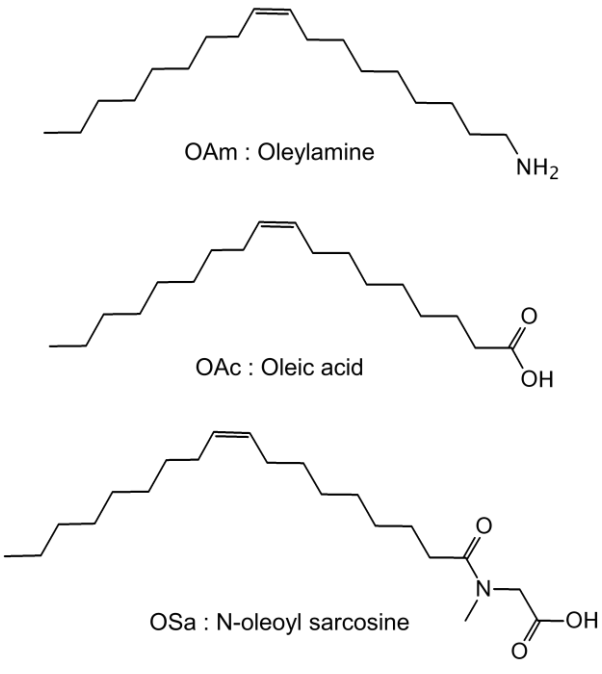

Figure 3.4. Chemical structures of OFMs used in this study

Table 3.3. Test oil formulations with OFMs

Lubricant	**Composition**
PAO4 + OAm	PAO4 + 1wt.% Oleylamine
PAO4 + OAc	PAO4 + 1wt.% Oleic acid
PAO4 + OSa	PAO4 + 1wt.% N-oleoyl sarcosine

(b) Anti-wear (AW) additives

AW additives generally contain phosphorus and/or sulphur atoms in their structures. Two types of typical anti-wear (AW) additives, Zinc dialkyldithiophosphate (ZDDP) and tricresyl phosphate (TCP) were used in this study. Their chemical structures are shown in Figure 3.5. The ZDDP employed was a so-called 'secondary ZDDP' which has higher reactivity than a 'primary ZDDP' [39]. Although this study used industrial grade ZDDP and TCP which contains a small amount of other chemicals, they mainly consist of the structures shown in Figure 3.5. Both AW additives were added at 1.0 wt.% to PAO4 as listed in Table 3.4.

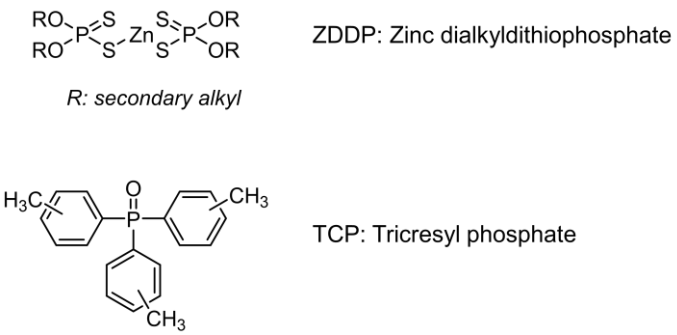

Figure 3.5. Chemical structures of AW additives used in this study

Table 3.4. Test oil formulations with AW additives

Lubricant	**Composition**
PAO4 + ZDDP	PAO4 + 1wt.% Zinc dialkyldithiophosphate
PAO4 + TCP	PAO4 + 1wt.% Tricresyl phosphate

3.2 Tribological testing

3.2.1 Test rig

Tribological tests were carried out using a Mini Traction Machine (MTM) from PCS Instruments Ltd which has been widely used to investigate lubrication under tribological test conditions simulating those present in actual components such as cams, gears and bearing [116,130,131]. The rig consists of a test chamber, a control unit, and a PC with data logging software (Figure 3.6). The standard set-up is a ball-on-disc configuration. The ball is loaded against the surface of the disc and the ball and disc are driven independently so as to be able to create a mixed sliding-rolling contact. By keeping the ball stationary and rotating only the disc a pure-sliding contact can be achieved. The frictional force between the ball and disc is measured by a force transducer. The friction coefficient is automatically calculated by the MTM software following the equation $\mu = F/N$ where F frictional force and N the normal force (contact load). Additional sensors measure the applied load, lubricant temperature, electrical contact resistance (ECR) between the specimens, and the relative wear between them. Because of electrical insulation of polymers, the ECR sensor was turned off in this study.

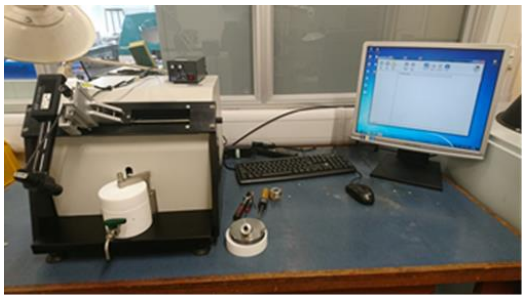

Figure 3.6. Photograph of MTM

3.2.2 Test configurations

This study mainly focused on the polymer-steel contact using a pair consisting of a steel ball and a polymer plate which was placed on top of a bespoke MTM disc and secured in place with a nut (Figure 3.7 (a, b)). To investigate the mechanism of lubrication with lubricant additives described in section 5.1.3 and section 5.2.3, polymer-polymer and steel-steel contacts were also studied using a polymer ball and plate and a steel ball and plate pairs, respectively (Figure 3.7 (c, d)). The standard configuration in this study was set to the sliding-rolling contact motion as encountered in gears, one of the main expected applications. As described in Chapter 2, the tribological performance of

PEEK-steel and PEEK composites-steel contacts depends on contact motion. Therefore, in some cases tribological tests were performed under two different types of contact motion: sliding and sliding-rolling. In the sliding condition, the ball is kept stationary and only the disc is rotated. In the sliding-rolling condition, the ball and disc are driven independently to create a mixed sliding-rolling contact with a slide-roll ratio (SRR) of 50% which represents the standard testing condition of this study. SRR is defined as the ratio of the sliding speed (u_{disc} - u_{ball}) to the entrainment speed ((u_{disc} + u_{ball})/2), where u_{disc} and u_{ball} are the speeds of the disc and the ball with respect to the contact. SRRs in actual gears vary depending on the design of the gear teeth, but the 50% SRR applied in this study is in the range typically found in gear applications [132,133]. In sliding conditions, the SRR is calculated as 200%.

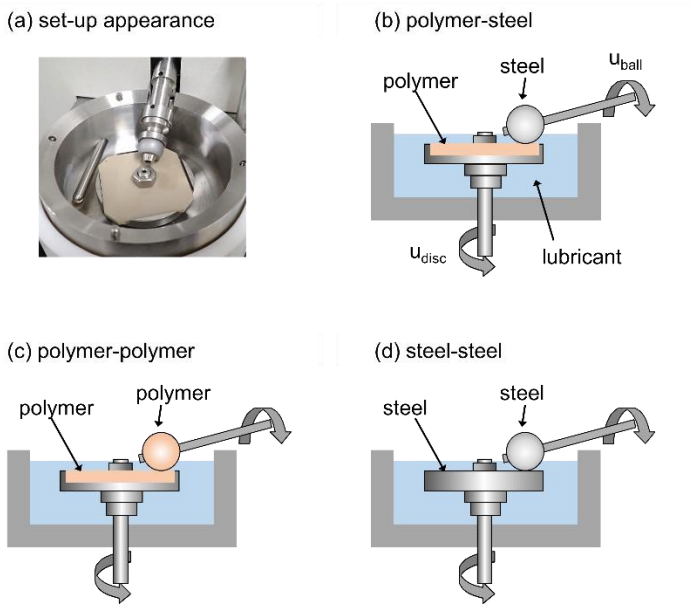

Figure 3.7. MTM (a) set-up appearance and configurations of (b) polymer-steel, (c) polymer-polymer and (d) steel-steel

3.2.3 Test profiles

Two measurement routines, a constant speed routine and a Stribeck routine, were adopted in this study. As the constant speed routine is more useful in comparing wear performance under various conditions, this was mainly used in this study of base oil lubrication. The Stribeck routine generates Stribeck curves, representing friction coefficient values as a function of entrainment speed. Stribeck curves are useful in assessing frictional performance over a wide range of lubrication regimes (from hydrodynamic lubrication to mixed and boundary lubrication), and, therefore, valuable in

investigating the effect of lubricant additives which are expected to work in mixed to boundary lubrication.

(a) Constant speed routine

In the constant speed routine, the entrainment speed along with other test conditions (e.g., load, SRR, temperature) are kept constant during the entire testing period (Figure 3.8). Friction coefficient values during testing are recorded every 10 seconds. It was mainly used to evaluate the effect of base oil lubrication on friction and wear performance. The standard test conditions for the constant speed routine are summarized in Table 3.5, but each parameter was changed as appropriate to investigate the effect of individual parameters. In some cases, the averaged friction coefficient values, along with the standard deviations, recorded during the last ten minutes of testing are used to compare the frictional performance. The entrainment speed of 0.5 m/s is typical of the low to middle speed range envisaged for gear applications. The applied load of 50 N leads to the maximum Hertzian contact pressure (Pmax) of: 0.16 GPa in PEEK-steel, 0.53 GPa in CFR PEEK-steel and 0.33 GPa in GFR PEEK-steel, respectively. These contact pressures were at higher values compared to previous studies of polymer-steel contacts, because one of the expected advantages of oil-lubrication is to increase the contact pressures possible in polymer applications.

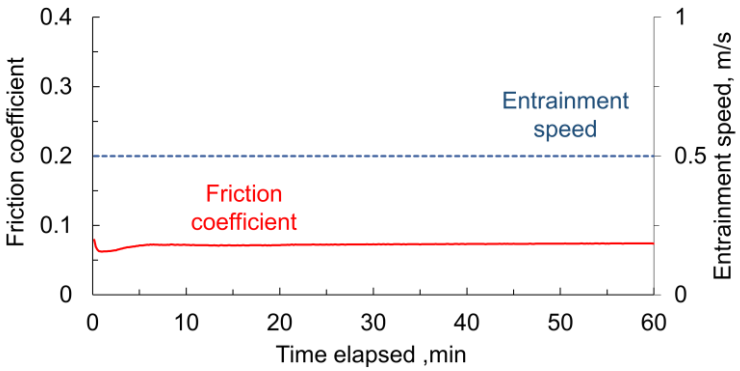

Figure 3.8. Constant speed routine sequence

Table 3.5. Standard test conditions of constant speed routine

Load	50 N
Entrainment speed	0.5 m/s
SRR	50%
Temperature	Ambient (approximately 25 °C)
Testing time	60 minutes

(b) Stribeck routine

In the Stribeck routine, the entrainment speed is gradually increased up to 1 m/s and is maintained for 60 seconds at each speed, while the other parameters are kept constant. To allow for run-in, the speed cycle is repeated three times consecutively as shown in Figure 3.9. Stribeck curves are given by the averaged friction coefficients, along with the standard deviations, over the last 20 seconds at each entrainment speed during the 3rd cycle as shown in Figure 3.10. Error bars designate ± one standard deviation. This routine was mainly used to evaluate the effect of lubricant additives on friction and wear performance. The standard test condition of the Stribeck routine is summarized in Table 3.6, but each parameter is changed as required. In the standard test condition, the applied load of 50 N leads to maximum Hertzian contact pressures (Pmax) as follows: 0.16 GPa in PEEK-steel, 0.53 GPa in CFR PEEK-steel and 0.33 GPa in GFR PEEK-steel, respectively.

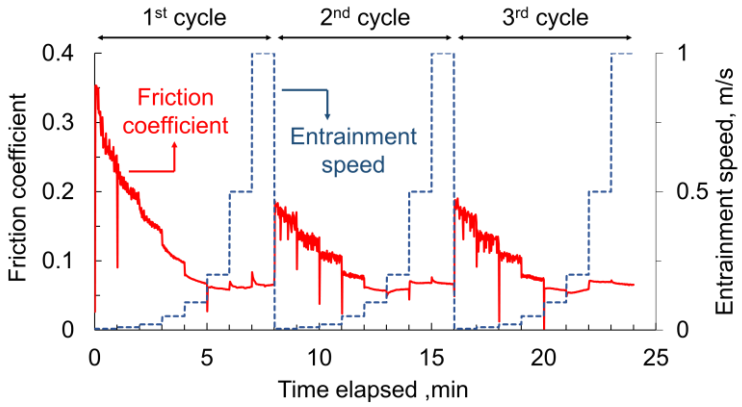

Figure 3.9. Stribeck routine sequence

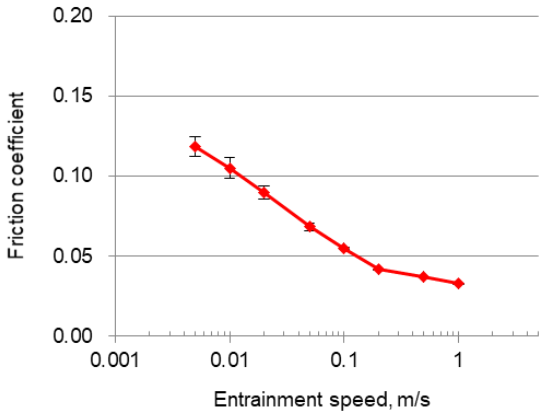

Figure 3.10. Example of Stribeck curve

Table 3.6. Standard test conditions of Stribeck routine

Load	50 N
Entrainment speed	0.005 - 1.0 m/s
SRR	50%
Temperature	Ambient (approximately 25 °C)
Testing time	60 seconds at each speed (approximately 25 minutes in total)

3.3 Surface analyses

3.3.1 Surface profilometer

Stylus profilometers (Intra Touch, Taylor Hobson Ltd. and SURFCOM 1500 DX2, Tokyo Seimitsu Co., Ltd.) were used to measure wear profiles on after-test polymer plates. When tested in the constant speed routine described in section 3.2.3, wear volumes of polymer plates (V) were calculated from the wear profiles using Equations 3-1 and 3-2:

$$A = \int_a^b f(x)\,dx \approx \sum_{k=1}^{n} (a_k - a_{k-1}) \frac{f(a_{k-1}) + f(a_k)}{2} \qquad \text{(Eq. 3-1)}$$

$$V = A \times \pi D \qquad \text{(Eq. 3-2)}$$

where A is the worn area of the cross section calculated by the trapezoidal rule and D is the diameter of the wear track on the polymer plate. Figure 3.11 shows the typical appearance of an after-test polymer plate. Although the variation in the wear profiles with position on the tracks was slight, profiles were measured at four positions (0, 90, 180, 270 degrees), followed by calculation of the wear volumes and their standard deviations.

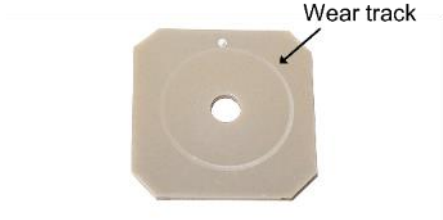

Figure 3.11. Typical appearance of after-test polymer plate

In this study most of the tests in the constant speed routine were conducted in the standard test conditions of 50% SRR, but some tests were performed at 100% SRR. When comparing wear performance tested under different SRRs, the specific wear rate (SWR) is commonly used. SWR is defined as the wear volume (V) per sliding distance (D) and per load (L) and calculated according to Equation 3-3:

$$SWR = \frac{V}{D \times L} = \frac{V}{(u_d - u_b) \times t \times L} \quad \text{(Eq. 3-3)}$$

where u_d and u_b are the speeds of the disc and the ball with respect to the contact, and t is the testing time. Note that the sliding distance in the constant speed routine (described in section 3.3.3) depends not only on entrainment speed and testing time but also on SRR, because while the entrainment speed is maintained constant, the sliding speed changes with SRR. For example, if tested at the same entrainment speed of 0.5 m/s but at different SRRs of 50% and 100%, the sliding speeds are calculated as 0.25 and 0.5 m/s. As a result, the sliding distance of the 100% SRR test is twice that of the 50% SRR test.

3D surface profiles were generated with an Alicona InfiniteFocus G4 (Alicona Imaging GmbH), with the Focus-Variation technique. The Focus-Variation technique works by moving a focal plane over a surface and collecting optical images and 3D data which can then be used to generate 3D surface profiles with the vertical resolution depending on the lens objective. The optical images and 3D surface profiles were obtained using a 50 × objective with a vertical resolution of 20 nm.

3.3.2 Nanoindentation

Nanoindentation measurements were performed with an iNano nanoindenter, (NANOMECHANICS, Inc.). Two methods: continuous stiffness measurement (CSM) and hardness mapping measurement were used in this study.

(a) Continuous stiffness measurement

To evaluate the hardness of polymer surfaces as a function of indentation depth, the continuous stiffness measurement (CSM) technique [134–136] with a Berkovich tip was employed by applying a small, sinusoidally varying signal on top of a DC signal driving the indenter. The hardness at each indentation depth was determined by analysing the response of amplitude and phase. The frequency and displacement amplitude values were 110 Hz and 1 nm, respectively. Under a load range of 0 to 50 mN, a target depth of 3 μm and a strain rate of 0.01 s^{-1}, sixteen indents at least 50

μm apart were made inside the wear track for each polymer plate. The average hardness at each indentation depth and its standard deviation were then calculated.

(b) Hardness mapping measurement

As discussed in section 2.1.4, exposed "hard" reinforcement fibres on the contact surfaces of PEEK composites are assumed to play an important role. Hardness mapping measurement with a Berkovich tip was used to investigate the distribution of carbon fibres and glass fibres on the wear tracks of after-test PEEK composites plates. Under a load of 1 mN, a target depth of 0.5 μm and a strain rate of 1 s^{-1}, 6,400 indents (80 × 80) were made at 5 μm intervals, producing a hardness map of an area 400 × 400 μm. Compared to continuous stiffness measurement, the accuracy of hardness mapping measurements is considered to be lower due to the shallower depth and faster strain rate. However, the accuracy is acceptable considering that the main purpose of the hardness mapping technique is to investigate the distribution of exposed carbon fibres and glass fibres which have much higher hardness than the PEEK matrix.

3.3.3 EPMA

Electron Probe Micro Analysis (EPMA) was carried out on the wear tracks on the steel balls after tribological tests using a JXA-8530F (JEOL Ltd.) to investigate the polymer transfer films and/or reaction films formed by AW additives. Test specimens were gently rinsed with a hydrocarbon solvent and dried before measurement. The EPMA is equipped with Wavelength Dispersive X-ray spectroscopy (WDX) which counts the number of X-rays of a specific wavelength diffracted by a crystal, therefore it has higher resolution than Energy Dispersive X-ray spectrometry (EDX) and is suitable for element mapping [137,138]. The secondary electron (SE) images and elemental maps for elements such as carbon, phosphorus and sulphur were acquired with a 15-kV beam at 100 nA current.

3.3.4 XPS

X-ray Photoelectron Spectroscopy (XPS) was carried out on the polymer transfer films found on the steel balls after tribological testing using a PHI 5000 VersaProbe III (Ulvac-Phi, Inc.) to investigate the nature of these films. Test specimens were gently rinsed with a hydrocarbon solvent and dried

before measurement. The XPS spectra were obtained using a monochromatic A1 Kα source. The C 1s detailed scan was performed with a spot size of 100-μm diameter.

3.3.5 Raman spectroscopy

Raman spectroscopy was performed on the polymer transfer films found on the steel balls after tribological tests using a Renishaw inViaTM Raman spectrometer (Renishaw plc) to investigate the nature of these films. Raman spectroscopy is a useful technique for analysing polymers as it gives characteristic spectra of their molecular structures based upon the inelastic scattering of photons from the samples [139–142]. The Raman spectra were obtained between 700 cm^{-1} and 1800 cm^{-1} from 100 scans of 1 second each with a 785 nm laser, using a 20 × objective.

3.4 Summary

This chapter summarizes the materials and experimental methods applied in this study. Tribological tests using a Mini Traction Machine (MTM) were designed to investigate the effect of lubrication on the tribological properties of PEEK and its composites. In addition to pure PEEK, carbon fibre reinforced (CFR) PEEK and glass fibre reinforced (GFR) PEEK were investigated paired with steel counterparts under dry and base oils with/without lubricant additives. To further investigate the mechanism of action, after-test specimens were analysed using various surface analysis techniques principally to determine the hardness of the polymers in and around the wear track and the nature of the polymer transfer films on the steel counterparts which both may have an impact on the tribological behaviour of polymer-steel contacts.

Chapter 4 Base oil lubrication of PEEK

This chapter covers the base oil lubrication of PEEK which is the most basic condition of this study. The effect of base oil lubrication on friction and wear properties of pure PEEK paired with steel counterpart were investigated in comparison with the dry conditions. The tribological tests were followed by surface analyses on the after-test specimens. The effect of lubricant oil viscosity, one of the most important parameters of lubrication, was also investigated.

4.1 Results: Comparison of dry and base oil lubrication

As reviewed in chapter 2, polymers for tribological applications are widely used in dry conditions and the lubrication does not always improve their friction and wear performance. This section aimed to investigate the effect of base oil lubrication on the friction and wear properties of pure PEEK paired with a steel counterpart and elucidate its mechanism of lubrication.

The detailed methodology was described in Chapter 3. In this section, PAO4 and rough steel balls with a Ra roughness of approximately 0.5 µm were used as a test oil and steel specimens, respectively. The tribological testing was carried out using a MTM with the constant speed routine as described in section 3.2.3. The test conditions were based on the standard conditions in Table 3.5, but the 100% SRR tests were added to the 50% SRR tests to investigate the effect of lubrication under more severe conditions.

4.1.1 Friction and wear performance

The most important and desirable outputs from the tribological testing are lower friction and wear, and the lubrication is expected to contribute to achieving these. The friction performance of the tribological tests is illustrated in Figure 4.1. Friction coefficient values are plotted as a function of time. Regardless of SRR, a significant friction reduction was achieved in the PAO4 lubricated tests compared to the dry ones. In dry conditions, the friction coefficients are above 0.2 for both 50% and 100% SRRs, while the ones in PAO4 lubricated conditions are below 0.1 for both SRRs. Notably, for both dry and lubricated contacts, friction was lower for 100% SRR than for 50% SRR.

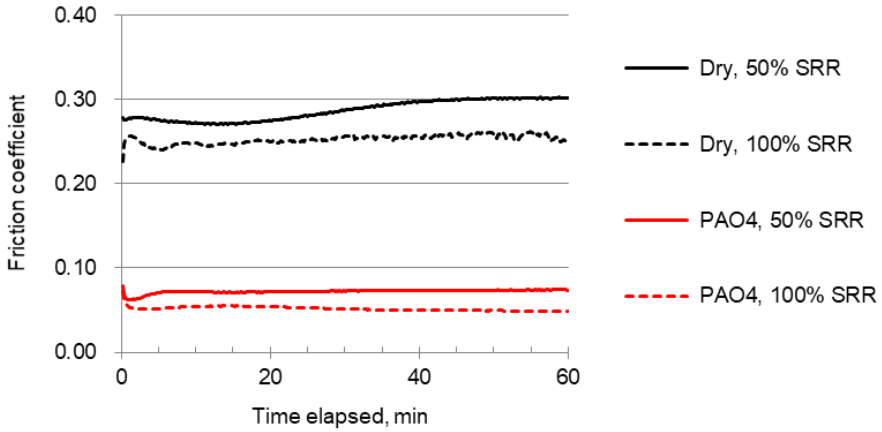

Figure 4.1. Friction coefficients in dry and PAO4 lubricated conditions

To investigate the wear mechanism of PEEK plates, optical images of the wear tracks under two magnifications were analysed (Figure 4.2 and Figure 4.3). The wear performance can be estimated from the low magnification images (Figure 4.2), but the wear performance was discussed in more detail based on the results of wear profiles later in this section. The high magnification images (Figure 4.3) show that the appearance of the wear tracks is different, especially in the case of two specimens: the dry 50% SRR and PAO4 50% SRR. The wear track on the dry 50% SRR plate showed small marks characteristic of adhesive or fatigue wear. By contrast, the wear track of the PAO4 50% SRR showed sets of parallel ridges, a characteristic pattern of abrasion as observed by Schallamach for the abrasive wear of rubber [143–145].

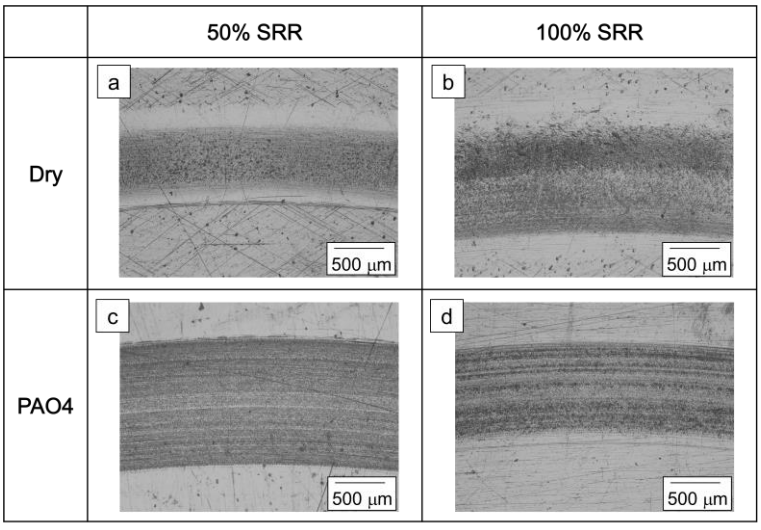

Figure 4.2. Low magnification optical images of after-test PEEK plates in (a, b) dry and (c, d) PAO4 lubricated conditions

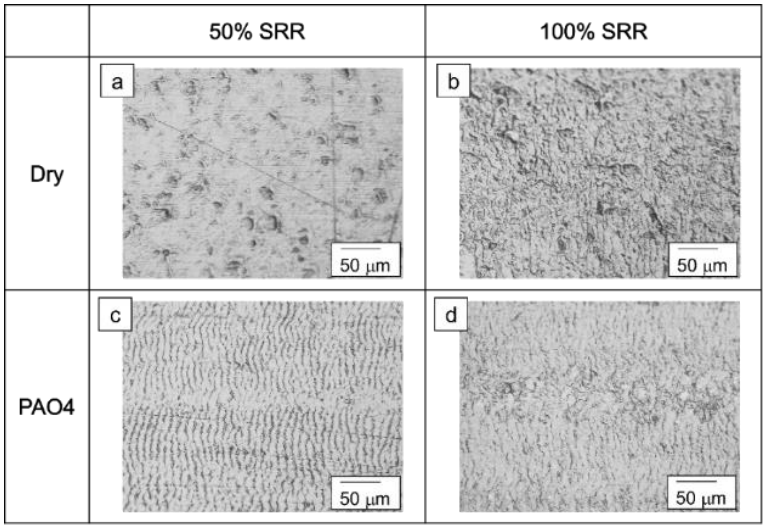

Figure 4.3. High magnification optical images of after-test PEEK plates in (a, b) dry and (c, d) PAO4 lubricated conditions

The wear profiles of the PEEK plates in Figure 4.4 show their wear performance more directly. In dry conditions, the 100% SRR wear volume was much higher than at 50% despite showing the lower friction. In the case of lubricated contacts, the wear trend was opposite to the dry ones, with 100% SRR resulting in lower wear than 50% SRR. The PAO4 50% SRR plate shows the largest wear volume in all conditions. Further steps will be taken to elucidate the lubrication mechanism and the results will be corroborated and discussed in section 4.3.2.

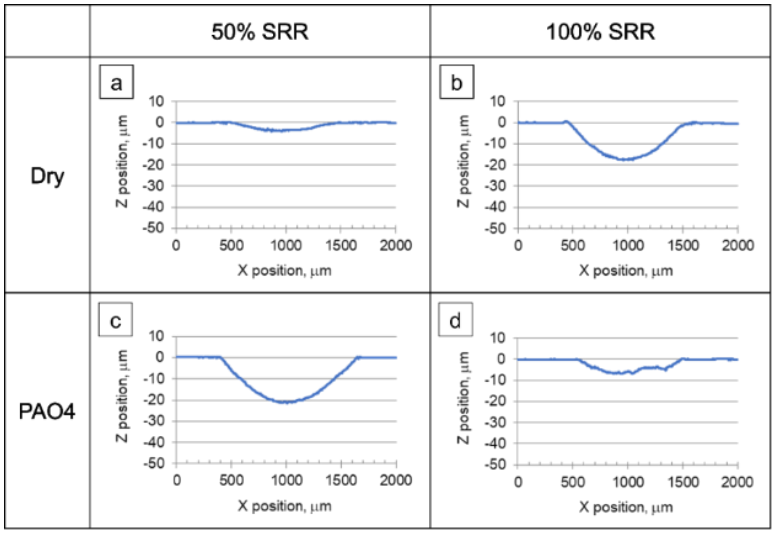

Figure 4.4. Wear profiles of PEEK plates in (a, b) dry and (c, d) PAO4 lubricated conditions

When comparing the wear performance tested under different SRRs it is worth noting that the sliding distance depends on SRR because the sliding speed changes with SRR even if the entrainment speed is maintained constant. Therefore, to compare wear performance more precisely, the specific wear rates (SWRs) were calculated for each condition by following the steps described in section 3.3.1. Figure 4.5 compares the SWRs and the averaged friction coefficient values recorded during the last ten minutes of testing. Error bars designate ± one standard deviation calculated by following the procedure described in sections 3.2.3 and 3.3.1. The wear performance derived from SWRs shows a different trend from the friction coefficients. In dry conditions, the 100% SRR wear rate was higher than at 50% despite showing the lower friction. In the case of lubricated contacts, the wear trend was opposite to the unlubricated ones, with 100% SRR resulting in much lower wear than 50% SRR. The SWRs were dramatically improved from above 3 x 10^{-5} $mm^3/(N•m)$ in PAO4 50% SRR to below 1 x 10^{-5} $mm^3/(N•m)$ in PAO4 100% SRR. Additionally, while lubrication exerted a negative effect on wear at 50% SRR, below 1 x 10^{-5} $mm^3/(N•m)$ in dry 50% SRR to above 3 x 10^{-5} $mm^3/(N•m)$ in PAO4 50% SRR, it had a positive effect at 100% SRR, above 1 x 10^{-5} $mm^3/(N•m)$ in dry 100% SRR to below 1 x 10^{-5} $mm^3/(N•m)$ in PAO4 100% SRR. As a result, almost no correlation was seen between friction and wear results. This indicates that base oil lubrication effectively reduces friction, but it does not lead to an improvement in wear performance, and there are other factors which govern wear performance. The working mechanism of base oil lubrication will be discussed later in section 4.3 taking into account the results of surface analyses investigated in section 4.1.2 and the additional tests with preconditioned steel balls in section 4.1.3.

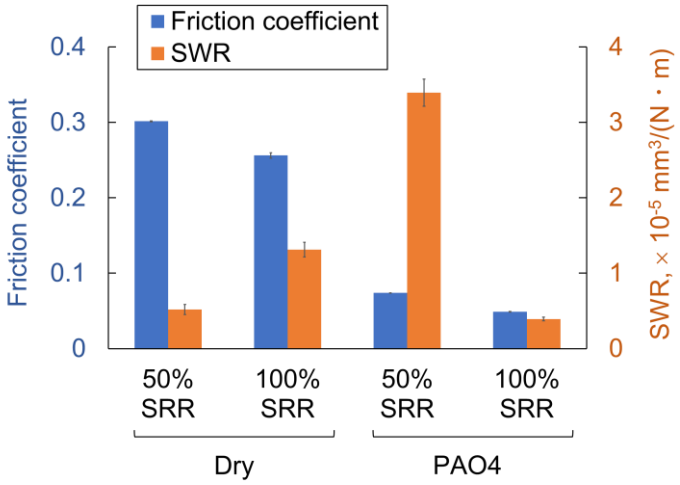

Figure 4.5. Friction coefficients averaged during last ten minutes and SWRs of PEEK plates

4.1.2 Surface analyses

As discussed in section 2.2.3, lubrication can affect the hardness of PEEK and the formation of transfer films on steel counterparts which both plausibly have impacts on tribological behaviour. Therefore, to understand the working mechanism of lubrication these two factors were carefully investigated by nanoindentation, EPMA and XPS.

4.1.2.1 Nanoindentation

The hardness of after-test PEEK plates was measured using nanoindentation. The continuous stiffness measurement (CSM) technique described in section 3.3.2 was applied. Hardness measurements were carried out on PEEK plates outside and inside of wear tracks and the hardness values were plotted as a function of indentation depth (Figure 4.6). Error bars designate ± one standard deviation calculated by following the procedure described in section 3.3.2. In all tests, hardness showed high values at indentation depth values <0.5 µm. These values are thought to be attributed to a phenomenon known as indentation size effect, and not regarded as physically significant because they are distorted by the inadequacies in the procedures applied to provide corrections for the imperfections in the tip geometry [136,146].

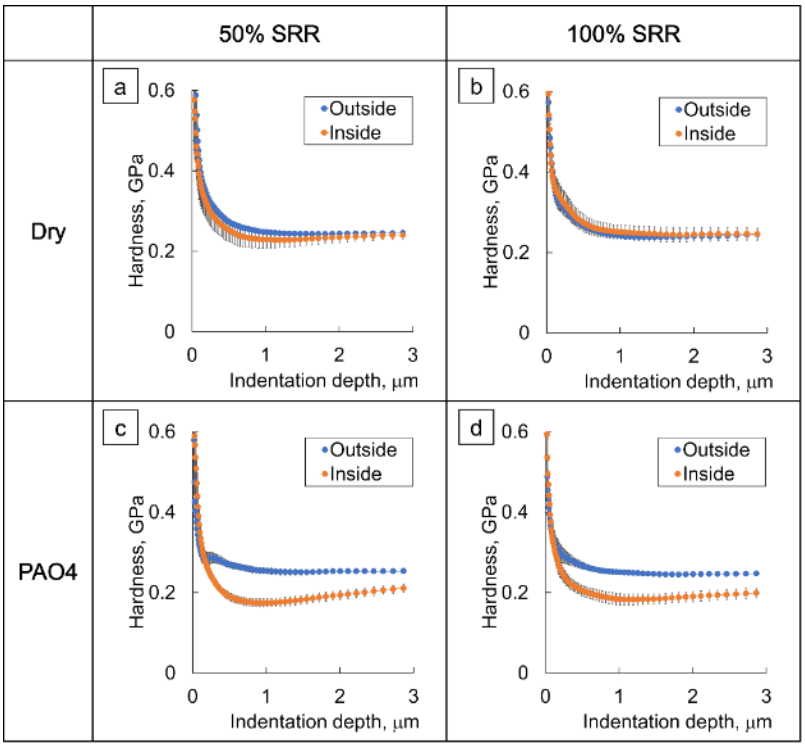

Figure 4.6. Nanoindentation hardness of after-test PEEK plates in (a, b) dry and (c, d) PAO4 lubricated conditions

The hardness at 2 μm indentation depth for the four specimens are graphically summarized in Figure 4.7. The hardness values for the specimens used in the dry 50% and 100% SRR tests are very similar inside and outside of the wear track. By contrast, the PAO4 lubricated specimens show a significant decrease in hardness (of approximately 23%) inside the wear tracks for both 50% and 100% SRR tests. This implies that lubrication with PAO4 reduced the hardness of the PEEK plates, regardless of SRR. Interestingly, lubrication with PAO4 (a non-polar solvent) caused softening of PEEK as previously reported in the case of lubrication with water (a polar solvent) [31]. Outside of the wear tracks the hardness of the plate tested in dry conditions is similar to the new plates described in section 3.3.2. Outside of the wear tracks the hardness showed almost the same value for all specimens including the ones lubricated with PAO4. This indicates that the softening of PEEK did not occur only by immersion in PAO4. Noticeably, the hardness of plates from 50% and 100% SRR tests showed almost the same values in dry and lubricated conditions respectively, a trend opposite to that seen for the wear performance. This implies that softening of PEEK by lubrication with PAO4 was not the main cause of the high wear rate of the PEEK plate in the PAO4 50% SRR test. In fact, the PAO4 100% SRR test showed the lowest wear rate despite the decrease in the hardness of PEEK.

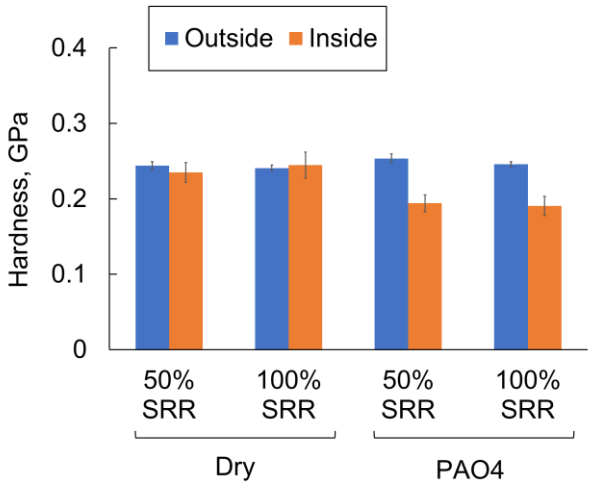

Figure 4.7. Nanoindentation hardness of after-test PEEK plates at 2 μm depth

4.1.2.2 EPMA

To investigate the PEEK transfer films, the wear tracks of the steel balls were analysed after the tribological tests. Optical images of all specimens in Figure 4.8 showed that there was almost no

wear on the steel balls. As the hardness of the steel ball is much higher than that of PEEK plates, it was expected that wear would mainly occur on the PEEK plates. The balls used in the dry tests show the presence of PEEK wear debris outside the wear tracks, especially abundant with 100% SRR. In lubricated tests, the wear debris would be flushed out by PAO4, but small amounts of wear debris were still observed as white residuals/marks just outside of wear tracks. The Ra roughness of the wear tracks on steel balls did not show significant difference between the PAO4 50% and 100% tests (approximately 0.35 μm for both tests), while these Ra values are lower than that of the unused shot-blasted ball (approximately 0.5 μm). In addition, the Ra value of the wear track on the steel ball for the dry 50% test was approximately 0.3 μm.

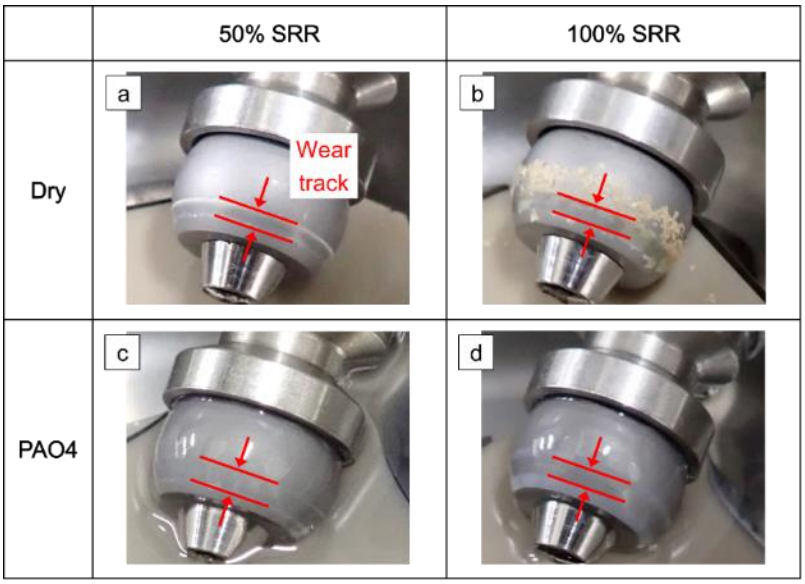

Figure 4.8. Optical images of after-test steel balls in (a, b) dry and (c, d) PAO4 lubricated conditions

The visual evaluation of the amount of PEEK transfer films on the wear track was found to be challenging, so EPMA carbon mapping was employed for further analysis by following the procedure described in section 3.3.3. EPMA carbon maps on after-test steel balls are shown in Figure 4.9. The carbon amount is indicated by the colour scale on the map. A clear difference between the steel ball wear tracks can be observed depending on the conditions. In addition, for each of the two testing conditions a good correlation can be seen between the wear performance (Figure 4.5) and the carbon amount on the wear track of steel balls (Figure 4.9). Larger amounts of carbon distributed as a uniform layer were detected on the wear tracks of the steel balls used in the dry 50% SRR test and PAO4 100% SRR test. These testing conditions also led to low SWRs of PEEK plates. The PAO4 100% SRR PEEK plate showed the lowest SWR despite the dry 50 % steel ball

wear track showing much higher carbon amount. This was thought to be due to the combined effect of PEEK transfer film and oil lubrication which will be discussed in detail in section 4.3.3. A reduced amount of carbon was detected on the steel ball wear track from the PAO4 50% SRR test which showed a very high wear volume of the PEEK plate. The wear track of the steel ball used in the dry 100% SRR test showed non-uniform coverage with carbon varying between high and low concentrations. The reason why the tribological test conditions influence the amount of PEEK transfer films will be further discussed in section 4.3.2 in combination with the results of testing with preconditioned steel balls investigated in section 4.1.3.

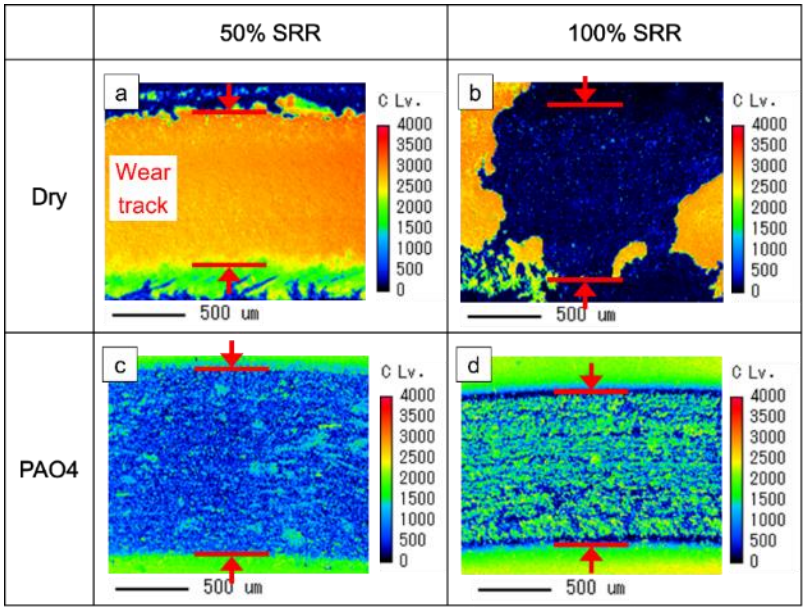

Figure 4.9. EMPA carbon maps of after-test steel balls in (a, b) dry and (c, d) PAO4 lubricated conditions

4.1.2.3 XPS

The presence of carbon detected with EPMA is supposedly related to PEEK transfer films on steel ball wear tracks, but this assumption is questionable in the case of PAO4 lubricated balls. To confirm the assumption, XPS analysis of C 1s spectra was recorded on steel ball wear tracks. As Figure 4.10 and Figure 4.11 show, C 1s spectra in all tests, except for the PAO4 50% SRR, showed almost identical peak curves which matched well the spectra recorded on an unused PEEK plate and the literature reported PEEK spectra [147]. A small difference in spectra is seen for the PAO4 50 %SRR wear track which can be due to the very low carbon presence on the steel ball. Therefore, from the XPS results it can be concluded that EPMA carbon maps are a valid analysis of PEEK transfer films on steel ball wear tracks. Moreover, a good correlation is seen between the EPMA detected carbon

amount on steel ball wear tracks and the wear volumes of PEEK plates. This indicates that the presence of a PEEK transfer film on the steel ball is a key factor not just for dry conditions but also for lubricated ones.

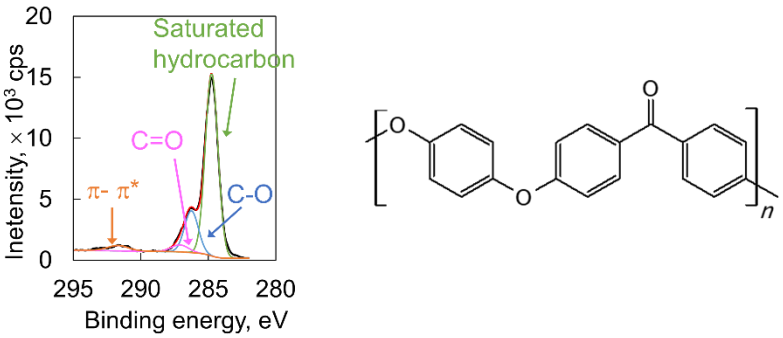

Figure 4.10. XPS C1s spectrum of unused PEEK plate

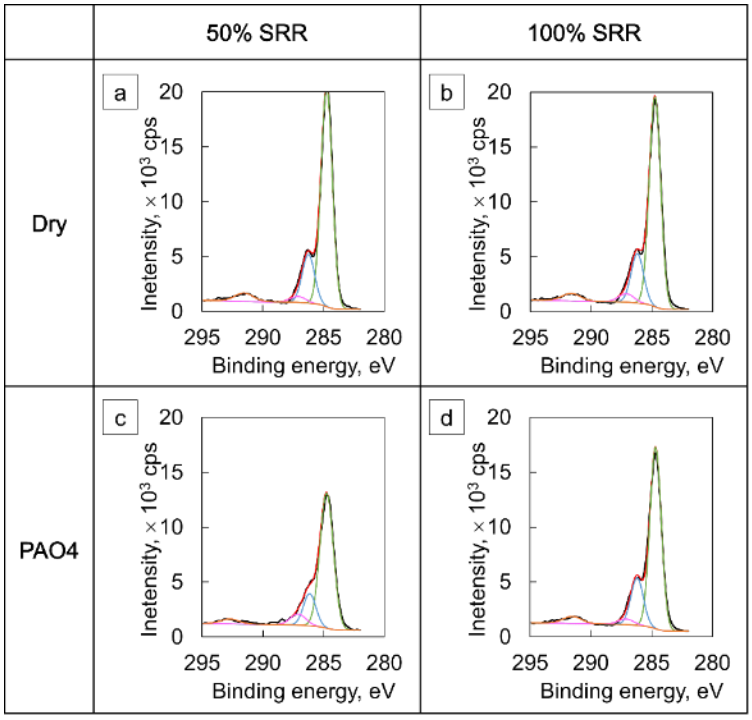

Figure 4.11. XPS C1s spectra of after-test steel balls in (a, b) dry and (c, d) PAO4 lubricated conditions

4.1.3 Testing with preconditioned steel balls

In dry conditions, the increase in SRR from 50% to 100% mean the higher sliding speed accelerated film removal and led to a non-uniform transfer film as seen in the EPMA carbon map of the dry 100% SRR test (Figure 4.9 (b)). Similar to the previous reports for water lubrication, PAO4 inhibited the formation of transfer films in the 50% SRR test (Figure 4.9 (a)), causing direct contact between the PEEK surface and asperities of the counter steel surface. This explains the difference in surface patterns in Figure 4.3. The dry 50% SRR test shows a specific pattern on the PEEK plate (Figure 4.3 (a)) and a thick PEEK transfer film on the steel surface which bears the hallmarks of adhesive wear or fatigue wear that can take place in the PEEK/PEEK contact. By contrast, the PAO4 50% SRR test showed an abrasion pattern on PEEK (Figure 4.3 (c)) and a thin PEEK transfer film on the ball wear track indicating abrasive wear in the PEEK/steel contact which resulted in the most significant wear loss from all tests. The presence and thickness of PEEK transfer films on the steel counterpart are determined by the formation and removal process and thus can be significantly influenced by the tribological test conditions (SRR).

However, it was still unclear as to why the variation of SRR in the PAO4 lubricated tests resulted in significant differences in PEEK transfer film thicknesses. A plausible explanation could be that the SRR influences/controls the formation and removal process of PEEK transfer films and lubrication with PAO4 can inhibit not only the formation but also the removal of films.

To investigate why poorer PEEK transfer films resulted from the dry 100% SRR and PAO4 50% SRR tests, additional testing was carried out using preconditioned steel balls. Run-in dry 50% SRR tests were carried out for 10 minutes (testing conditions identical to those used for the previous dry tests) to achieve a uniform PEEK transfer films on the steel ball wear track as seen in Figure 4.9 (a). The EPMA carbon map of the 10 minutes preconditioned steel ball is shown in Figure 4.12 (a).

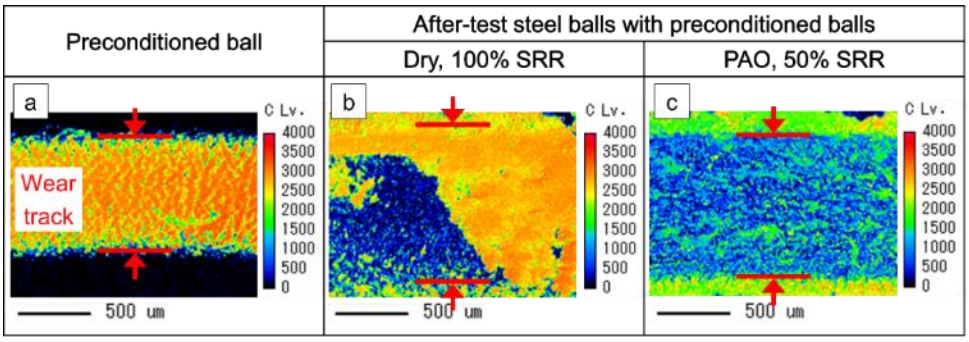

Figure 4.12. EPMA carbon maps of (a) preconditioned steel ball and (b, c) after-test steel balls with preconditioned steel balls

The preconditioned balls were then paired with unused PEEK plates and tested in dry 100% SRR and PAO4 50% SRR for 60 minutes. The friction coefficients of these tests are shown in Figure 4.13 and compared with the results obtained with new balls. In dry conditions, the friction coefficients with the preconditioned ball and new disc started from lower values than those with the new ball and new disc but in a short time (less than 10 minutes) converged to the same level as the wear track on the PEEK disc started to form. The EPMA carbon map of the after-test steel ball in Figure 4.12 (b) showed a non-uniform coverage of the wear track similar to the test with the new ball in Figure 4.9 (b). These results indicate that the formation and removal of PEEK transfer films in dry 100% SRR tests were very fast and the preconditioned ball did not have a significant effect. By contrast, the preconditioning of the ball significantly reduced friction in the PAO4 50% SRR test. Friction coefficient values with the preconditioned ball were half those with the new ball for 20 minutes and stabilized at a lower level for the rest of the test.

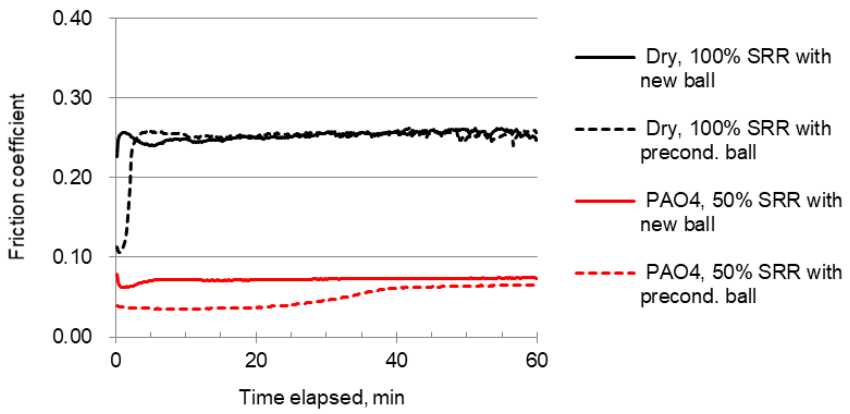

Figure 4.13. Friction coefficients with new and preconditioned rough steel balls in dry and PAO4 lubricated conditions

Moreover, the wear of the PEEK plate decreased drastically with the preconditioning of the ball in the PAO4 50% SRR test. Figure 4.14 summarizes friction coefficients averaged during the last ten minutes of testing and the SWRs of PEEK plates. Error bars designate ± one standard deviation calculated by following the procedure described in sections 3.2.3 and 3.3.1. The SWRs in the dry 100% SRR tests show almost same values of about 1 x 10^{-5} $mm^3/(N•m)$ for the new ball and the preconditioned ball, while the SWRs in PAO 50% SRR tests decreased from above 3 x 10^{-5} $mm^3/(N•m)$ with the new ball to below 1 x 10^{-5} $mm^3/(N•m)$ with the preconditioned ball. In the PAO

50% SRR tests, the PEEK transfer film with the preconditioned ball, Figure 4.12 (c), was slightly thicker than that with the new ball, Figure 4.9 (c). These results indicate that lubrication with PAO4 suppressed the speed of the removal of PEEK films, and thus the initial film formed through preconditioning was reasonably stable during the test. The mechanism of action of PEEK transfer films on steel balls and the working mechanism of lubrication will be further discussed in sections 4.3.2 and 4.3.3.

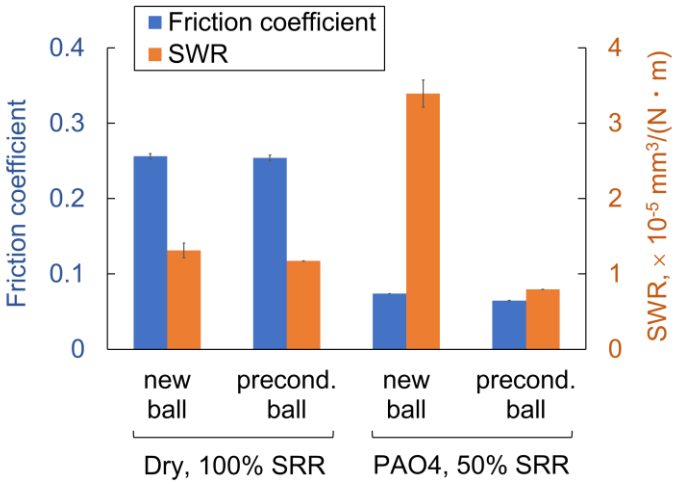

Figure 4.14. Friction coefficients averaged during last ten minutes and SWRs of PEEK plates

4.2 Results: Effect of lubricant oil viscosity

As reviewed in chapter 2, most previous studies of lubrication of PEEK were conducted with water as a lubricant and hence they did not cover the effect of lubricant oil viscosity. In terms of designing the lubricants suitable for each application, the lubricant oil viscosity is one of the most important parameters. Therefore, this section aimed to investigate the effect of lubricant oil viscosity.

The detailed methodology was described in chapter 3. In this section, PAOs with different viscosity grades, PAO2, PAO4 and PAO10 were used as test oils (Table 3.2). Note that the range of viscosity between PAO2 to PAO10 covers most of lubricants in the market. Additionally, the steel balls with smooth surfaces (Ra roughness of 0.01-0.02 μm) and rough surfaces (Ra roughness of approximately 0.5 μm) were used as described in section 3.1.2. The combination of PAOs with different viscosity grades and the steel balls with different surface roughness enables the tribological tests in this section to cover a wide range of lubrication regime (from hydrodynamic

lubrication to mixed and boundary lubrication). The tribological testing was carried out using a MTM with the constant speed routine as described in section 3.2.3. The test conditions were based on the standard conditions in Table 3.5.

4.2.1 Friction and wear performance

(a) PEEK-smooth steel contact

As mentioned in section 4.1.1, friction and wear performance are the most important outputs from the tribological testing. Figure 4.15 shows that the friction coefficients of PEEK-smooth steel contact lubricated with PAO2, PAO4 and PAO10. PAO4 and PAO10 gave almost the same and very low values of friction coefficients of approximately 0.02 during the entire period of testing. PAO2 resulted in a slightly higher friction than that of PAO4 and PAO10, but the values of friction coefficients were still low, approximately 0.03.

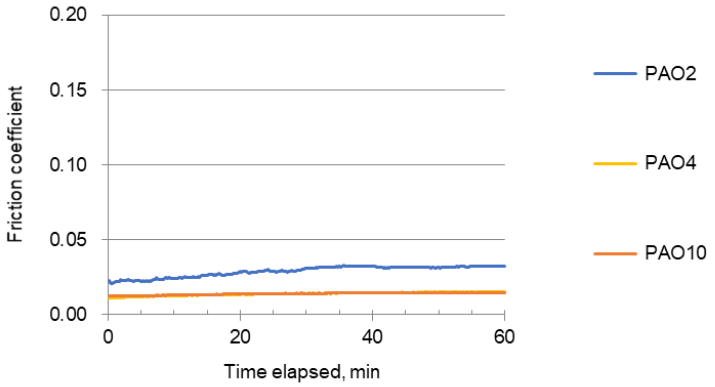

Figure 4.15. Friction coefficients with smooth steel balls

Optical images of after-test PEEK plates are presented in Figure 4.16. The damage on the wear tracks was well correlated with their friction performance. PAO2 lubricated plate had the most damage (although still small) on the wear tracks, while there was less damage on the plates lubricated with PAO4 and PAO10. The wear volumes of the PEEK plates were very low and were hardly observed by the stylus profilometer for all of after-test PEEK plates paired with smooth steel. Considering the friction and wear performance, the lubrication regimes of PEEK-smooth steel contact lubricated with PAO2, PAO4 and PAO10 is estimated as mixed to hydrodynamic lubrication. In these regimes, lubricant oil films separate the contact surfaces fully or partially, giving low friction

and wear. The lubrication regimes are significant to understand the working mechanism of lubrication, therefore it will be further discussed in section 4.3.3 with the results of PEEK-rough steel contact.

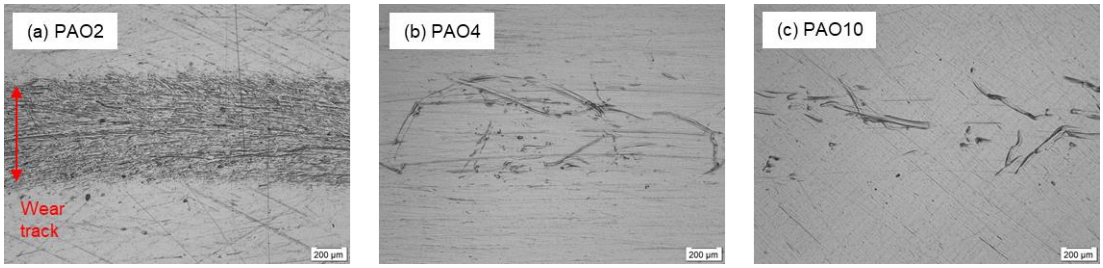

Figure 4.16. Optical images of after-test PEEK plates paired with smooth steel balls lubricated with (a) PAO2, (b) PAO4, and (c) PAO10

(b) PEEK-rough steel contact

Figure 4.17 illustrates the friction coefficients of the PEEK-rough steel contact lubricated with PAO2, PAO4 and PAO10. Regardless of the viscosity grades of PAO, the friction coefficients show higher values than those of the PEEK-smooth steel contact (Figure 4.15). Furthermore, the friction performance shows a completely different trend compared with the PEEK-smooth contact. In the PEEK-rough steel contact, the friction coefficient values of PAO2 were the lowest, while PAO10 gave much higher friction coefficients than PAO4.

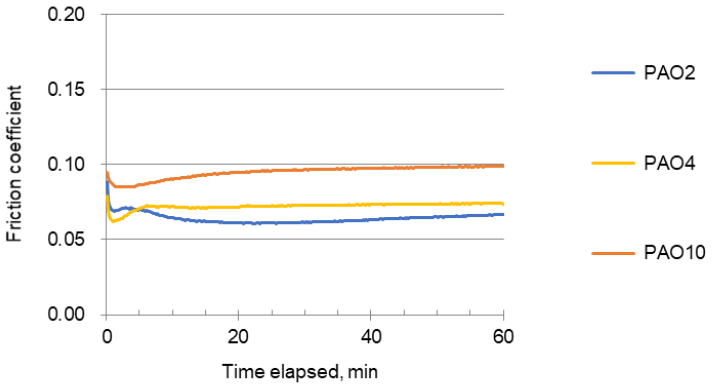

Figure 4.17. Friction coefficients with rough steel balls

Figure 4.18 and Figure 4.19 present optical images and wear profiles of after-test PEEK plates. It is notable that the wear volume became higher as the lubricant oil viscosity increases, resulting in the highest wear volume when lubricated with PAO10 (Figure 4.19 (c)). This is well correlated with the friction performance reported in Figure 4.17, but these results cannot be interpreted through the lubrication regimes estimated from the lubricant oil viscosity because higher viscosity oils theoretically are predicted to give milder lubrication regimes with lower friction and wear.

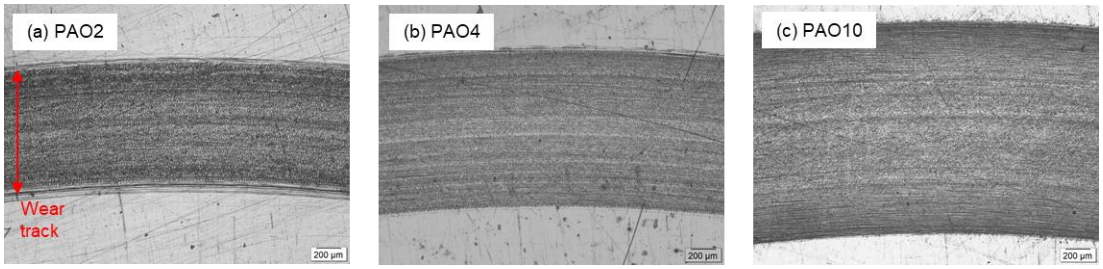

Figure 4.18. Optical images of after-test PEEK plates paired with rough steel balls lubricated with (a) PAO2, (b) PAO4 and (c) PAO10

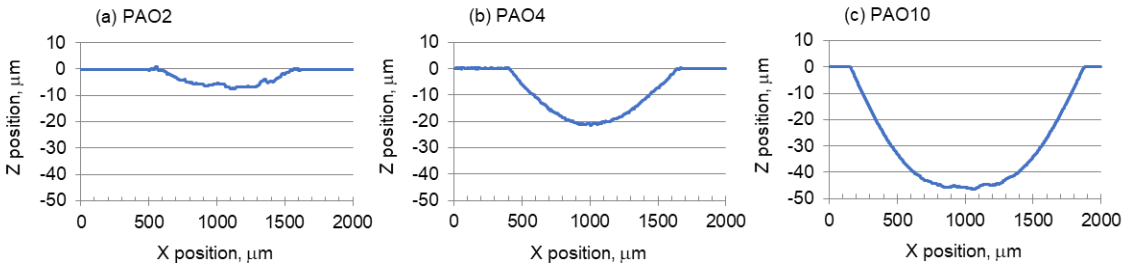

Figure 4.19. Wear profiles of PEEK plates paired with rough steel balls lubricated with (a) PAO2, (b) PAO4 and (c) PAO10

4.2.2 Surface analyses

The friction and wear performance when lubricated with different viscosity grades indicate that apart from lubrication regimes there will be key factors which govern the tribological behaviour of PEEK-steel contact. As investigated in section 4.1.2, the hardness of PEEK plates and PEEK transfer films on steel balls were also investigated in order to understand the mechanism of action.

4.2.2.1 Nanoindentation

The hardness of after-test PEEK plates was measured using nanoindentation. Similar to section 4.1.2.1, the continuous stiffness measurement (CSM) technique described in section 3.3.2 was applied. Hardness measurements were carried out inside the wear tracks and the hardness values were plotted as a function of indentation depth and compared with those of a new plate. Note that the hardness at indentation depth values <0.5 µm was not used in the discussion to eliminate the indentation size effect (ISE) as mentioned in section 4.1.2.1.

Figure 4.20 shows the results of nanoindentation of after-test PEEK plates paired with smooth steel balls. The hardness values for the after-test PEEK plate lubricated with PAO2 decreased compared to the new plate. When lubricated with PAO4 and PAO 10, the after-test PEEK plates gave the same hardness as the new plate. As investigated in section 4.1.2.1, the hardness outside the wear tracks gave similar values to the new plate, indicating that the softening of PEEK did not occur just by immersing it in the lubricant.

The results of nanoindentation of after-test PEEK plates paired with rough steel balls are shown in Figure 4.21. The softening of PEEK was observed regardless of the viscosity grades of PAOs. Interestingly, the wear tracks of PAO2, PAO4 and PAO10 gave almost the same hardness values despite the large difference in the friction and wear performance (Figure 4.17 and Figure 4.19). Considering that the less damaged wear tracks rubbed with smooth steel balls under lubrication with PAO4 and PAO10 (Figure 4.16 (b, c)) gave the same hardness as the new plate, the softening of PEEK may possibly only occur under severe lubrication regimes. The mechanism of hardness modification of PEEK will be further discussed in section 4.3.1. Having said that, these results lead to the same conclusion as that presented in section 4.1.2.1 which is softening of PEEK by lubrication with PAOs was not the main parameter which governs the tribological properties of PEEK-steel contacts.

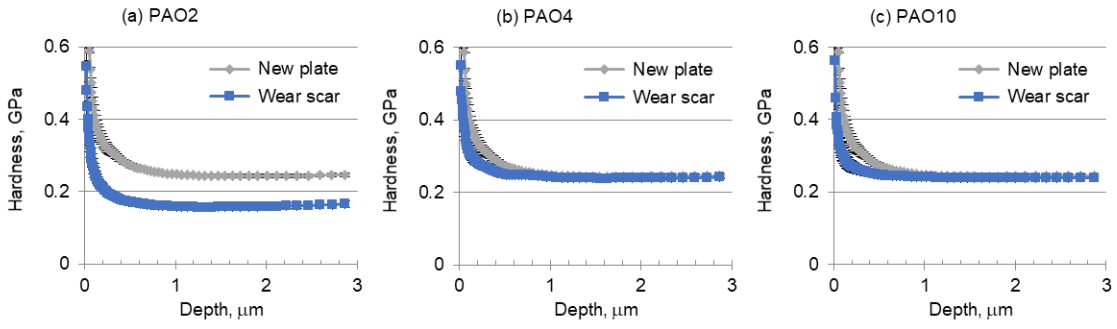

Figure 4.20. Nanoindentation hardness of after-test PEEK plates paired with smooth steel balls lubricated with (a) PAO2, (b) PAO4 and (c) PAO10

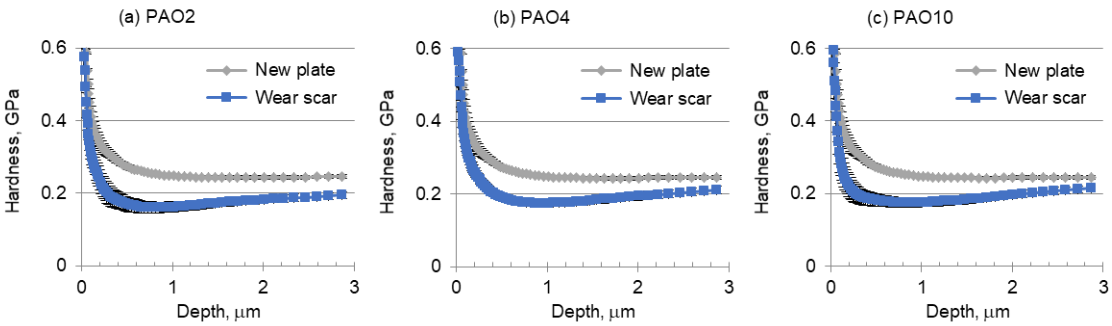

Figure 4.21. Nanoindentation hardness of after-test PEEK plates paired with rough steel balls lubricated with (a) PAO2, (b) PAO4 and (c) PAO10

4.2.2.2 EPMA

To investigate the PEEK transfer films, the wear tracks of the steel balls were analysed by EPMA carbon mapping following the procedure described in section 3.3.3. The PEEK transfer films were investigated only on the rough steel balls because they were entrapped between the asperities of steel surfaces and therefore more noticeable than those on the smooth steel balls. The PEEK transfer films on smooth steel balls proved difficult to detect because they were easily removed from smooth surfaces at the end of tests.

Figure 4.22 and Figure 4.23 show SE images and EPMA carbon maps of rough steel balls paired with PEEK plates when lubricated with PAO2, PAO4 and PAO10. SE images of all specimens showed that there was almost no wear on the steel balls. The widths of the wear tracks on the steel balls vary with the oils tested, and correspond to those of the paired PEEK plates. The corresponding wear profiles of the PEEK plates are shown in Figure 4.19. In terms of the carbon amounts detected from the wear tracks in EPMA carbon maps, the steel balls lubricated with low viscosity PAOs showed larger amounts of carbon. The presence of carbon detected with EPMA is related to PEEK transfer films as confirmed by the investigation using XPS in section 4.1.2.3. The amounts of carbon from EPMA carbon maps detected on the wear tracks of steel balls are well correlated with the tribological properties of the PEEK-rough steel contact (Figure 4.17 and Figure 4.19). The PAO2 test where the amount of carbon was high gave lower friction and wear, while the PAO10 test where the amount of carbon was low gave higher friction and wear. These results strongly indicate that the presence of a PEEK transfer film on the steel ball is a key factor in controlling the tribological performance of the PEEK-rough steel contact as investigated by the comparison of dry and lubricated conditions in section 4.1.

In terms of the effect of lubricant oil viscosity on the PEEK transfer films, PAO2 with lower viscosity leads to much amount of transfer films than PAO4 or PAO10. As discussed in section 4.1.3, the amount of the PEEK transfer films on the steel counterpart is determined by the formation and removal process and thus can be influenced by the tribological test conditions. The lubricant oil viscosity plausibly affects the balance between the formation and removal of PEEK transfer films. It can be expected that with a lower viscosity oil like PAO2 where the lubrication regime is more severe the formation of the PEEK transfer film is more facilitated. The mechanism of action of PEEK transfer films on steel balls and the working mechanism of lubrication will be further discussed in sections 4.3.2 and 4.3.3.

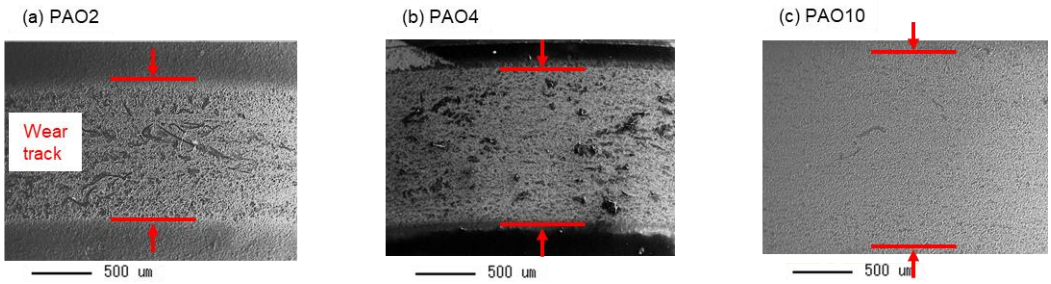

Figure 4.22. SE images of after-test rough steel balls lubricated with (a) PAO2, (b) PAO4 and (c) PAO10

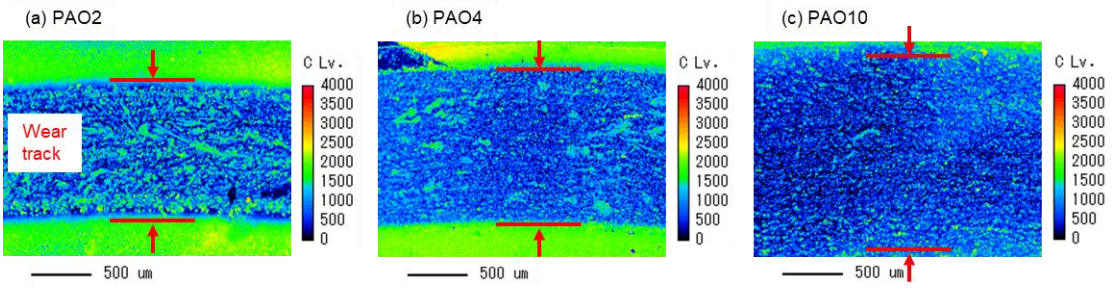

Figure 4.23. EPMA carbon maps of after-test rough steel balls lubricated with (a) PAO2, (b) PAO4 and (c) PAO10

4.3 Discussion

The experimental results investigated in sections 4.1 and 4.2 provide a series of insights to understand the working mechanism of base oil lubrication of PEEK-steel contact. Based on the results obtained, this section further discusses the two factors considered by previous studies to play decisive roles in this type of tribological contacts, namely: hardness modification of PEEK and PEEK transfer films on steel. Finally, the working mechanism of base oil lubrication of PEEK-steel contact will be discussed in detail.

4.3.1 Hardness modification of polymer surface

As reviewed in section 2.2.3, lubrication can have a negative effect on the tribological properties of PEEK-steel contact and some previous studies considered the softening of PEEK as the key factor causing it. In this study, the softening of PEEK was also observed to depend on the test conditions. Figure 4.24 depicts the relationship between hardness of after-test PEEK plates and friction coefficients, with illustrative examples of optical images of the plates. The after-test PEEK plates were separated into two groups: low damage and higher damage surfaces. Interestingly, those with a higher damage surface showed a significant reduction of PEEK hardness compared to the new plate. On the other hand, PEEK plates with a low damage surface showed almost the same values of PEEK hardness as that of the new plate.

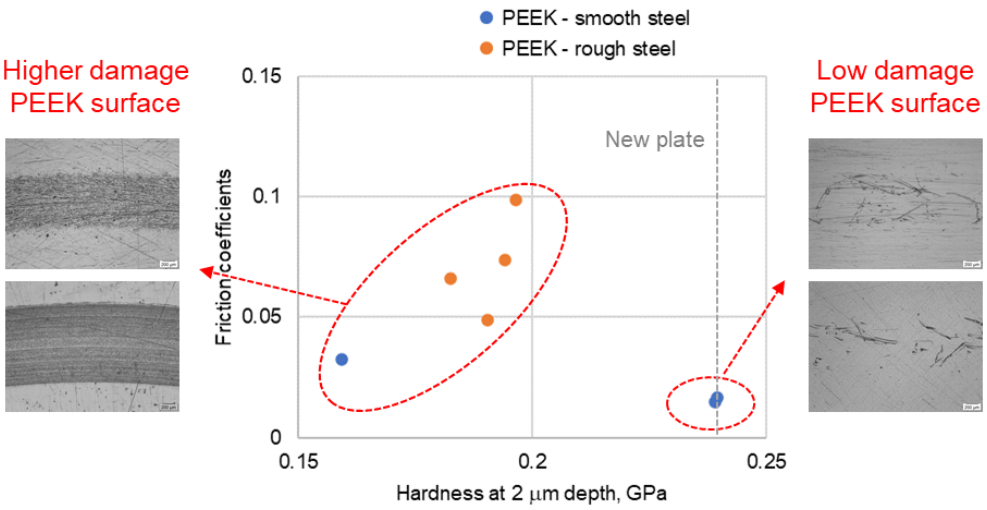

Figure 4.24. Relationship between nanoindentation hardness of after-test PEEK plates and friction coefficients; the optical images show the wear tracks on PEEK plates

In terms of the softening mechanism, a previous study using water as lubricant postulated that it was caused by the interaction between water molecules and the carbonyl group in the PEEK molecular structure [31]. However, lubrication with PAO (a non-polar solvent) caused a similar softening of PEEK to that with water lubrication (a polar solvent), which implies that the softening mechanism of PEEK is related to the permeation of lubricant molecules (in this case the base oil) into PEEK surfaces. Figure 4.25 shows the schematics of the base oil permeation on low and higher damage PEEK surfaces. Base oil molecules cannot penetrate into the low damage surface, while the scratches (possibly cracks) formed on the higher damage surface can facilitate this. In this model the smaller molecules contained in a lower viscosity oil like PAO2 are plausibly easy to penetrate and cause the softening of PEEK.

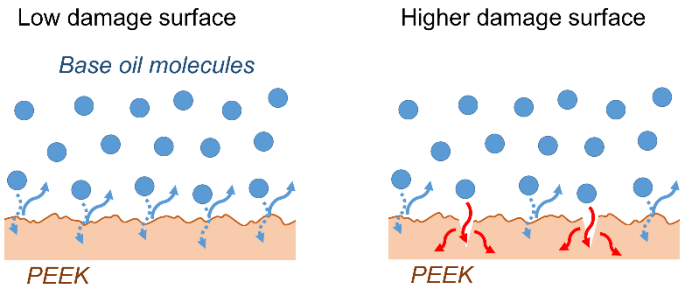

Figure 4.25. Schematics of base oil permeation on low and higher damage PEEK surface

It is notable that all PEEK plates tested with rough steel showed a wide range of wear volumes but the difference in PEEK hardness was not so large (Figure 4.26). Looking at the details, the tests that gave larger (deeper) wear tracks showed smaller reductions of PEEK hardness, while the tests that gave smaller (shallower) wear showed higher reductions of PEEK hardness. Considering that softening of PEEK occurred at comparatively shallow depths (< a few μm), deeper wear of PEEK surface (> 10 μm) can remove the volume of reduced hardness material. On the other hand, PEEK plates with only slight wear but with damage show the effect of base oil permeation manifested by a lower PEEK hardness.

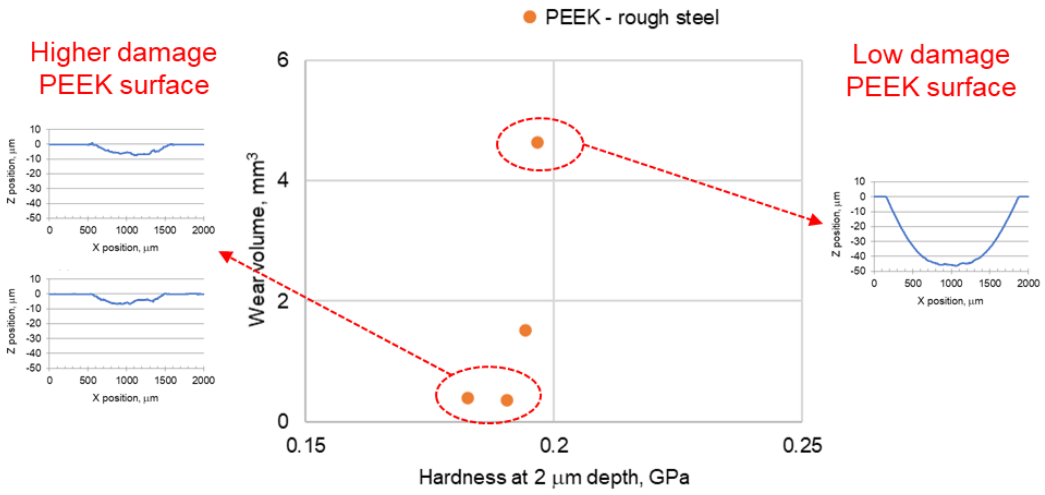

Figure 4.26. Relationship between nanoindentation hardness of PEEK plates and wear volumes; the side graphs show the wear profiles of PEEK plates

As investigated in section 4.1.2.1, the hardness modification caused by base oil lubrication was not the main factor controlling the tribological behaviour of lubricated PEEK-steel contact. The discussion above supports the argument that the hardness modification of PEEK by base oil lubrication does not govern the tribological performance but is the consequence of the lubricant permeation of damaged wear surfaces.

4.3.2 Polymer transfer films on steel counterparts

The experimental results investigated in Chapter 4 indicate that the PEEK transfer film on the steel counterpart is the dominant factor controlling the tribological properties of the PEEK-steel contact, especially in the PEEK-rough steel contact as mentioned in sections 4.1.2.2 and 4.2.2.2. The PEEK transfer films are assumed to act as protective films, thus avoiding the direct contact of the relatively soft PEEK surfaces with the hard asperities of the steel surfaces and so reducing the wear of PEEK. This contribution of PEEK transfer films has been previously found in dry conditions, as described in section 2.1.3. This study reveals their significance under lubrication.

Figure 4.27 and Figure 4.28 present schematics of the formation and removal of PEEK transfer films in dry and base oil lubricated conditions. As investigated in section 4.1, base oil lubrication inhibits both the formation and removal of PEEK transfer films, and the balance between these processes is controlled by the severity of the tribological conditions e.g. SRR. Base oil lubrication inhibits the formation of a PEEK transfer film on the steel counter surface, thus causing direct contact between

PEEK and steel in mild testing conditions. Within the severe conditions (e.g. high SRR), the speeds of the formation and removal processes are both accelerated, and their balance changes significantly compared to the mild conditions. The results using preconditioned steel balls, investigated in section 4.1.3 indicate that base oil lubrication effectively suppresses the removal of PEEK transfer films once they formed, and therefore the film formation overtakes the removal in the test with severe conditions. Severe conditions include not only high SRR but also low base oil viscosity as investigated in section 4.2. This explains why the test with the low viscosity PAO2 gave a larger amount of PEEK transfer films and better tribological performance than the tests with the higher viscosity PAO4 and PAO10. Additionally, the combination of the PEEK transfer film and the oil film contributes to mitigating the direct contact of surfaces and results in the lowest friction coefficients and PEEK wear rates.

	Dry	
	Mild condition	Severe condition
Schematic	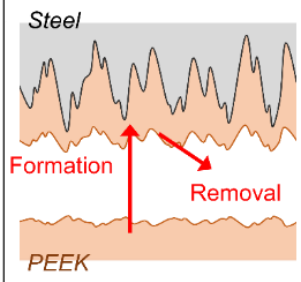	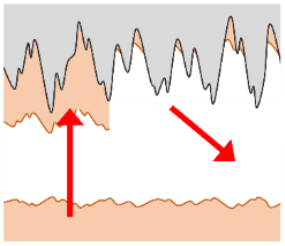
Formation speed	Medium	High
Removal speed	Medium	High

Figure 4.27. Schematic of PEEK transfer film formation/removal in dry condition

	Base oil lubrication	
	Mild condition	Severe condition
Schematic	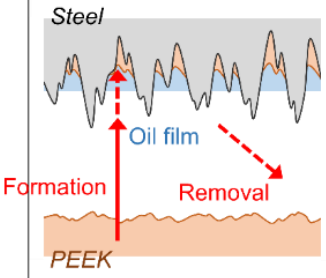	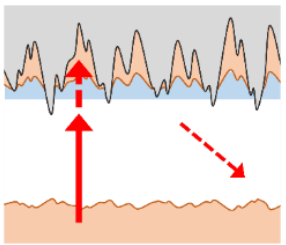
Formation speed	Very low	Low
Removal speed	Low	Low

Figure 4.28. Schematic of PEEK transfer film formation/removal in base oil lubricated condition

Previous studies which investigated dry testing of PEEK have also reported that tribological test conditions affected the balance of formation and removal of PEEK transfer films on steel counterparts [19,91,148,149]. This study clarifies the effects of lubrication by showing the impact of lubrication not only on the formation but also the removal of films.

4.3.3 Working mechanism of base oil lubrication

The concept of lubrication regime is very important in understanding the mechanism of lubrication. The lubrication regimes are commonly identified by a lubricant film parameter "Λ", also called Lambda ratio. Lambda ratio is calculated Equations 4-1 and 4-2:

$$\Lambda = h/\sigma \quad \text{(Eq. 4-1)}$$

$$\sigma = \sqrt{({\sigma_1}^2 + {\sigma_2}^2)} \quad \text{(Eq. 4-2)}$$

where h is the oil film thickness under operating conditions, σ is the composite surface roughness, and σ_1 and σ_2 are the surface roughness of the two contact surfaces. Figure 4.29 shows the friction coefficients of PEEK-smooth steel and PEEK-rough steel contacts investigated in sections 4.1 and 4.2 as a function of Lambda ratios for each testing conditions. For the determination of the Lambda ratios, the values of the oil film thickness were estimated from the expression presented by Hamrock and Dowson [150,151] described in Appendix A. Friction coefficients are expected to gradually increase around Lambda ratios of 1-5 corresponding to mixed lubrication, then rapidly increase at ratios <1 corresponding to boundary lubrication. However, the friction coefficients of PEEK-steel contacts in Figure 4.29 did not match such a typical trend. More specifically, the friction coefficients of PEEK-smooth steel contacts showed lower values than expected from the corresponding Lambda ratios, and the friction coefficients of PEEK-rough steel contacts surprised by gradually decreasing with lower Lambda ratios.

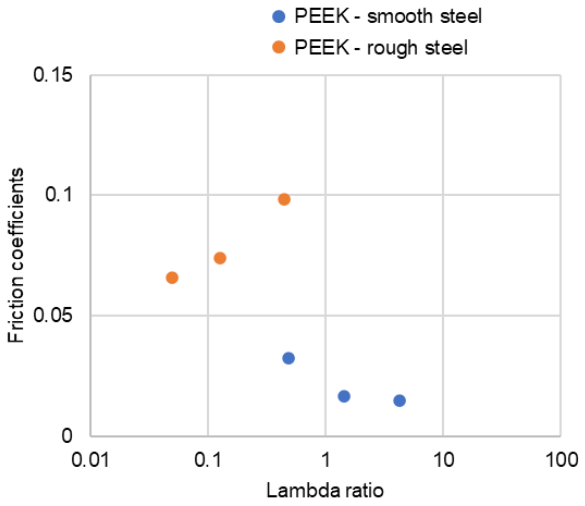

Figure 4.29. Friction coefficients of PEEK-steel contact as a function of Lambda ratios

Plausible explanations for these discrepancies are the overestimation of composite roughness in PEEK-smooth steel contacts and the effect of PEEK transfer films in PEEK-rough steel contacts. In the estimation of the composite roughness by following Eq. 4-2, the surface roughness of pristine specimens of PEEK and steel were used. However, taking into account the large difference in hardness and stiffness between PEEK and steel, the actual roughness of the PEEK wear track surface can be modified by removal (through wear) and/or compression of PEEK asperities (Figure 4.30).

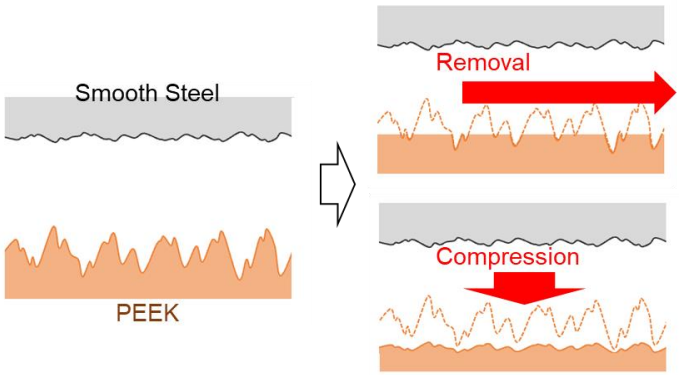

Figure 4.30. Schematic of removal (through wear) and compression of PEEK asperities

Based on the assumption that the composite roughness of PEEK and steel contacts are governed by the roughness of steel surface, the Lambda ratio was recalculated as the modified Lambda ratio "Λ_{mod}" by Equation 4-3:

$$\Lambda_{mod} = h/\sigma_{steel} \quad \text{(Eq. 4-3)}$$

where h is the oil film thickness under operating conditions and σ_{steel} is the surface roughness of steel specimens. For example, the Lambda ratio for PAO2 test is calculated as approximately 0.5 using the composite roughness, while the modified Lambda ratios using only steel roughness instead of composite roughness is calculated as approximately 2. The friction coefficients of PEEK-steel contacts were replotted as a function of the modified Lambda ratios in Figure 4.31. Now, the friction coefficients of PEEK-smooth steel contacts well matched the expected trend that friction coefficients gradually increase around Lambda ratios of 1-5 corresponding to mixed lubrication. This means that the working mechanism of base oil lubrication in PEEK-smooth steel contact basically follows the traditional theory where lower Lambda ratios (<3) are linked to higher friction coefficients, although minor modification is required. Note that there was almost no effect on the plots of PEEK-rough steel contacts, because their values of the composite roughness were already governed by the rough steel balls.

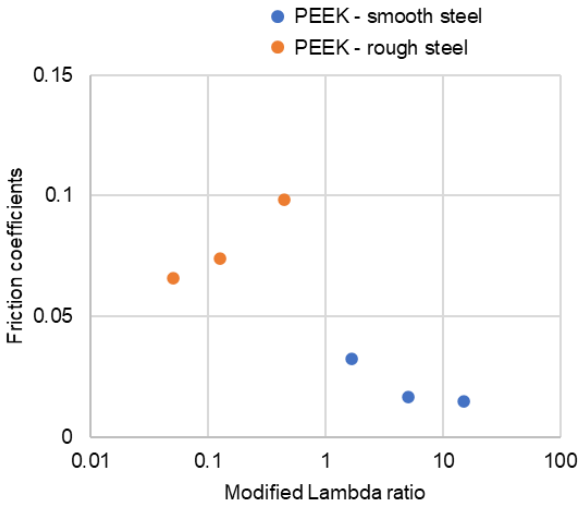

Figure 4.31. Friction coefficients of PEEK-steel contact as a function of modified Lambda ratios

The reason why the friction coefficients of PEEK-rough steel contacts gradually decreased with lower Lambda ratios is presumably related to the PEEK transfer films. As discussed in section 4.3.2, under lubrication, the amount of PEEK transfer films becomes more in severe conditions. Figure 4.32 shows the schematic of contact surfaces lubricated with different grades of PAOs. The PAO2 test with the lower Lambda ratio gave thicker transfer films and better tribological performance than the PAO4 and PAO10 tests with the higher Lambda ratios. Additionally, the combination of the

PEEK transfer film and the oil film contributes to mitigating the direct contact of surfaces and results in the lowest friction coefficients and the lowest wear of PEEK.

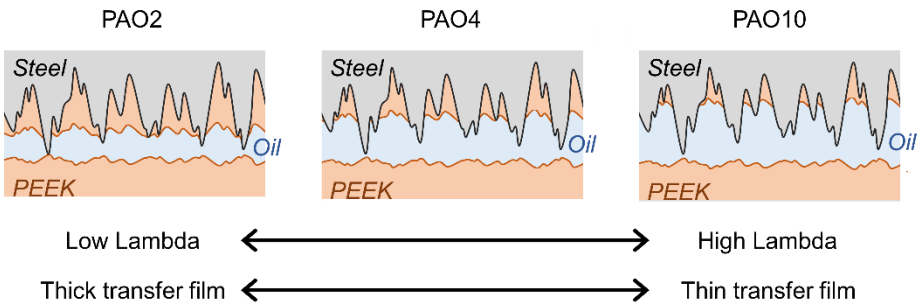

Figure 4.32 Schematic of contact surfaces lubricated with different grades of PAOs

As discussed in this section, the working mechanism of base oil lubrication depends on the surface roughness of steel counterparts. In PEEK-smooth steel contacts, the working mechanism of base oil lubrication basically follows the traditional theory after taking into account the modification of the surface roughness by removal (through wear) and/or compression of PEEK asperities. On the other hand, the working mechanism of base oil lubrication in PEEK-rough steel contacts does not follow the traditional theory due to the PEEK transfer films on steel counterparts. This indicates that when investigating the effect of lubricant additives in Chapter 5 the PEEK transfer films can be a key factor to understand the working mechanism.

4.4 Summary

In the absence of lubricant additives, base oil lubrication is the most basic way of lubrication. Therefore, it is considered to be a suitable start to this study of oil lubrication of PEEK. In this chapter, friction and wear properties of pure PEEK paired with steel counterpart under base oil lubrication were investigated by tribological testing and surface analyses of after-test specimens.

Firstly, tribological testing using a MTM was performed under dry and PAO4 oil lubricated conditions. Surface analyses of after-test specimens with nanoindentation, EPMA and XPS were

carried out by focusing on two key factors, the hardness modification of PEEK and the formation of PEEK transfer films on steel counterparts. The following conclusions have been drawn:

(1) Compared with dry conditions, lubrication with PAO4 reduced the friction of the PEEK-steel contact regardless of the operating conditions (i.e. SRR). By contrast, lubrication has a positive or negative effect on wear of PEEK depending on SRR;

(2) Lubrication with PAO4 had a softening effect on the wear track of PEEK, but no correlation was established with the wear performance;

(3) The thickness of PEEK transfer films on the steel counter surfaces was the main parameter that controlled PEEK wear in not only dry conditions but also lubricated conditions;

(4) Lubrication with PAO4 inhibited not only the formation but also the removal of the PEEK transfer films. This explains why lubrication can play both a positive or negative role on the wear of PEEK depending on the operating conditions.

Secondly, the effect of base oil viscosity which is one of the most important parameters of lubrication was investigated by using PAOs with different viscosities, PAO2, PAO4 and PAO10. The pure PEEK plates were paired with smooth and rough steel balls. The conclusions:

(1) The effect of base oil viscosity shows different trends depending on the roughness of the steel counterparts. In PEEK-smooth steel contacts, PAOs with higher viscosity gave lower friction and less damage on the PEEK surfaces, while in PEEK-rough steel contacts they resulted in higher friction and greater wear of PEEK;

(2) The softening of PEEK wear tracks was observed in some conditions, but little correlation was found with their tribological performance;

(3) The amounts of PEEK transfer films on steel counterparts were well correlated with the tribological properties of the PEEK-rough steel contact. PAOs with lower viscosity gave much amount of transfer films, resulting in better tribological performance.

Considering the two factors proposed in previous studies to play decisive roles in PEEK-steel contacts, hardness modification of PEEK and PEEK transfer films on steel balls, the working mechanism of base oil lubrication of PEEK has been discussed in detail and is summarized below:

(1) Hardness modification of PEEK is caused by the permeation of base oil molecules through the damaged surface and does not directly affect the tribological properties of the PEEK-steel contact;

(2) Base oil lubrication inhibits both the formation and removal of the PEEK films. The balance between these processes is controlled by the severity of the tribological conditions, causing both a positive or negative effect on the tribological properties of PEEK;

(3) The working mechanism of base oil lubrication depends on the surface roughness of the steel counterparts. In PEEK-smooth steel contacts, the working mechanism of base oil lubrication basically follows the traditional theory where lower Lambda ratios (<3) are linked to higher friction coefficients after taking into account the modification of the surface roughness by removal (through wear) and/or compression of PEEK asperities. However, the base oil lubrication of PEEK-rough steel contacts does not follow the traditional theory due to the PEEK transfer films formed on the steel counterparts.

Chapter 5 Effect of lubricant additives on lubrication of PEEK

In this chapter, the effect of lubricant additives on the lubrication of PEEK paired with steel counterparts is investigated. Lubricant additives are added to base oils in quantities of a few weight percent to improve their properties e.g. lubricity, lifespan [38,100,101]. Among the various types of lubricant additives, this study focused on the ones which have been known to strongly affect tribological properties namely, organic friction modifiers (OFMs) and anti-wear (AW) additives, because they are essential in formulating optimal lubricants and developing ideally suited PEEK-based systems for tribological applications. These two classes of additives are also ubiquitously used in lubricants for applications like engines and transmissions where the PEEK-steel contacts are envisaged to replace the existent steel-steel contacts.

Tribological testing was performed with lubricants containing OFMs and AW additives, followed by surface analyses on the after-test specimens. In addition, tribological testing with polymer-polymer and steel-steel pairs was also performed to investigate the working mechanism of lubricant additives.

5.1 Results: Effect of organic friction modifiers

This section investigates the effect of OFMs on the friction and wear performance of pure PEEK paired with a steel counterpart. As described in section 3.1.3.2, OFMs are surfactant-like molecules generally consisting of long hydrocarbon chains with polar groups at their ends. Three types of OFMs, oleylamine (OAm), oleic acid (OAc) and N-oleoyl sarcosine (OSa), which have been widely used in the commercial lubricants, were included in this study.

The detailed methodology was described in Chapter 3. The OFMs were added at 1.0 wt.% to PAO4 as listed in Table 3.3. The tribological testing was carried out using a MTM with the Stribeck routine described in section 3.2.3. Stribeck curves are useful in estimating the frictional performance over a wide range of entrainment speeds and hence lubrication regimes (from hydrodynamic lubrication to mixed and boundary lubrication). This makes them valuable in investigating the effect of OFMs which are expected to work in mixed to boundary lubrication. The tests were carried out in the standard conditions listed in Table 3.6, but 200% SRR (sliding) tests were also performed in addition to 50% SRR (sliding-rolling) tests to investigate the effect of lubrication under more severe

conditions. Additionally, steel balls with smooth surfaces (Ra of 0.01-0.02 μm) and rough surfaces (Ra of approximately 0.5 μm) were employed as described in section 3.1.2.

5.1.1 Friction and wear performance

(a) PEEK-smooth steel contact

As shown for the case of base oil lubrication in section 4.1, the severity of the operating condition (e.g. SRR) has a significant impact on the tribological behaviour of the PEEK-steel contact. Therefore, Stribeck routine tests were performed at 50% and 200% SRRs. The Stribeck curves for the PEEK-smooth steel contact lubricated with PAO4 and PAO4 + OFMs are presented in Figure 5.1 and Figure 5.2. In the Stribeck curves, the lubrication regime changes from hydrodynamic lubrication to boundary lubrication as the entrainment speed is reduced. This means the effect of OFMs is expected to be clearer at lower entrainment speeds (<0.1 m/s) where the lubricant films are very thin (< 50 nm). Indeed, the results show that the addition of OFMs to PAO reduced friction at entrainment speeds below 0.1 m/s. Among the three types of OFMs, a significant friction reduction was achieved at both SRRs by the addition of OSa (N-oleoyl sarcosine). OAm (oleylamine) and OAc (oleic acid) also reduced friction, although their impact was much less than that of OSa. In terms of the impact of the SRR, while PAO4 showed slightly higher friction at 200% SRR (sliding) than 50% SRR (sliding-rolling), the OFMs reduced friction more effectively at 200% SRR. Theoretically, the different values of SRRs used for testing have no effect on the lubrication regime. In this study, the entrainment speeds were the same at 200% SRR (sliding) and 50% SRR (sliding-rolling), and therefore the lubricant film thicknesses were similar. As discussed in section 4.3.3, the lubrication regimes corresponding to the conditions can be estimated from the calculated Lambda ratios. The Lambda ratios of approximately 0.1 to 3 for the PEEK-smooth steel contact indicate that both 200% SRR and 50% SRR tests were performed under the boundary/mixed lubrication regimes. It is also worth mentioning that when the tribological tests were conducted with smooth steel balls, there was almost no wear on the PEEK plates regardless of SRRs or lubricant formulations. In the steel-steel contact, OFMs have been reported to reduce friction by adsorbing or reacting on contact surfaces with their polar groups, thus mitigating the direct contact of the two surfaces in the mixed and boundary lubrication regimes [98,99]. The friction results of PAO4 + OFMs imply that the effect of OFMs, especially OSa, in the PEEK-smooth steel contact is similar to that in the steel-steel contact, although whether OFMs are adsorbed on PEEK is uncertain. Further aspects of the adsorption ability of OFMs on PEEK and steel surfaces are investigated in section 5.1.3.

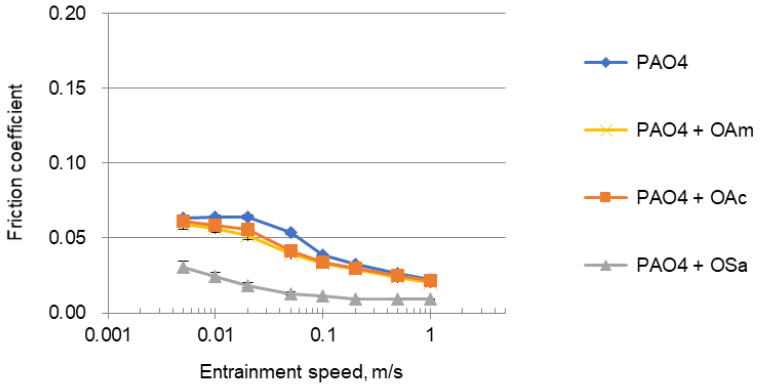

Figure 5.1. Stribeck curves with smooth steel balls at 50% SRR for PAO4 and PAO4 + OFMs

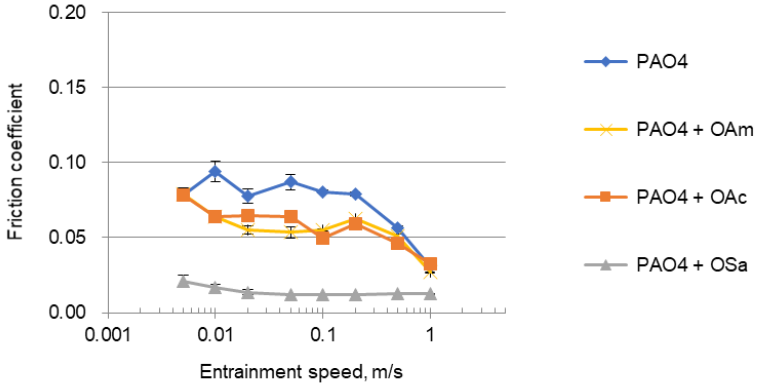

Figure 5.2. Stribeck curves with smooth steel balls at 200% SRR for PAO4 and PAO4 + OFMs

(b) PEEK-rough steel contact

As reported in section 4.2, the tribological properties of the PEEK-steel contact under base oil lubrication showed different trends depending on the surface roughness of the steel counterparts. Therefore, in this chapter, the effect of OFMs in the PEEK-steel contact was also investigated using rough steel balls. The Stribeck curves for this contact lubricated with PAO4 and PAO4 + OFMs are shown in Figure 5.3 and Figure 5.4. The calculated Lambda ratios of below one for the PEEK-rough steel contact in this section indicate that both the 200% SRR and 50% SRR tests were performed in the boundary lubrication regime. Under PAO4 lubrication, the friction coefficients were considerably higher at 50% SRR (from 0.05 up to 0.16) than at 200% SRR (from 0.02 up to 0.12). With the addition of OFMs, their effect was different depending on the SRR. At 200% SRR (sliding), OFMs reduced friction when added to PAO4. By contrast, at 50% SRR (sliding-rolling), OFMs,

especially OSa, increased friction. This friction increasing effect of OSa at 50% SRR was more significant at entrainment speeds above 0.1 m/s.

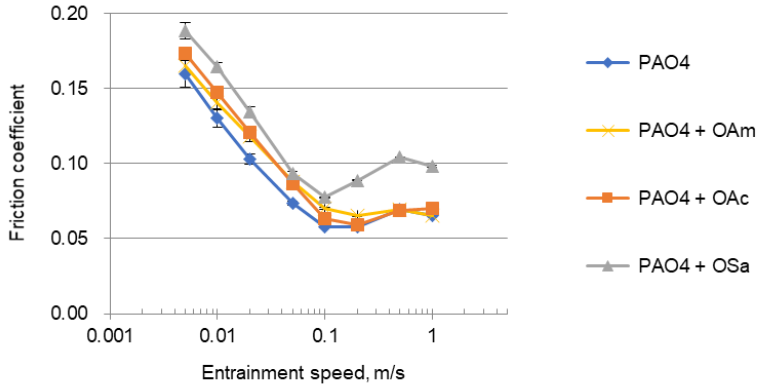

Figure 5.3. Stribeck curves with rough steel balls at 50% SRR for PAO4 and PAO4 + OFMs

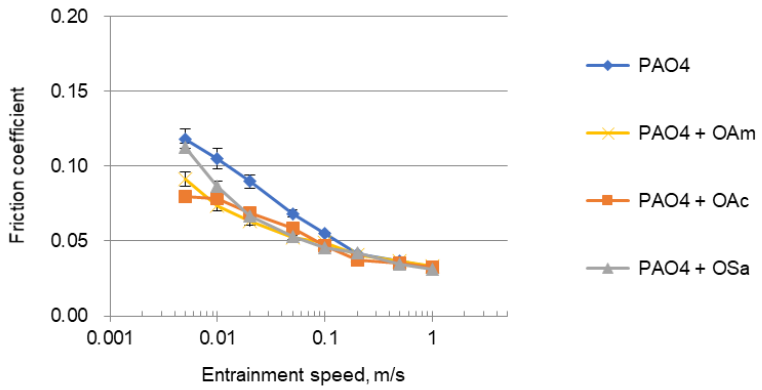

Figure 5.4. Stribeck curves with rough steel balls at 200% SRR for PAO4 and PAO4 + OFMs

The optical images of the after-test PEEK plates are presented in Figure 5.5 and Figure 5.6. The plates tested at 50% SRR showed uniform damage inside the wear tracks, while the ones at 200% SRR gave a non-uniformed damage like with scratches along with the sliding direction. This indicates that the SRR greatly affects the tribological performance and the working mechanism of lubricant additives should be discussed after considering the impact of the SRR. In terms of the effect of OFMs, PAO4 + OSa at 200% SRR provided a distinctively less damaged wear track, although its friction coefficients were similar to those lubricated with PAO4 + OAm and PAO4 + OAc.

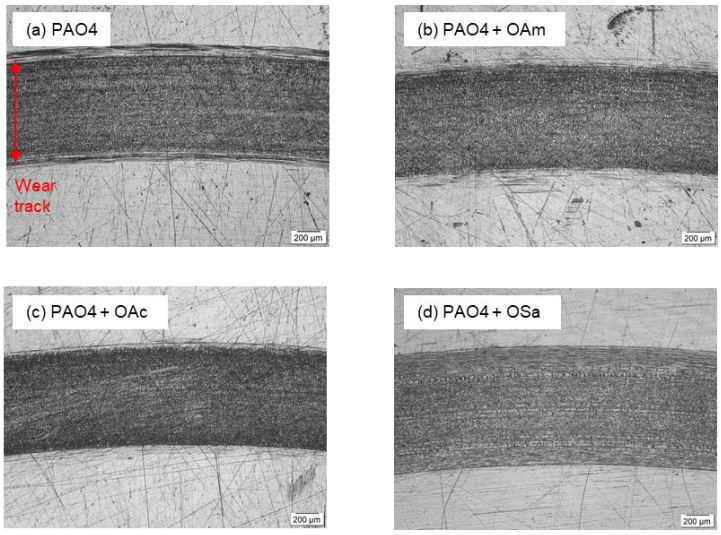

Figure 5.5. Optical images of after-test PEEK plates paired with rough steel balls at 50% SRR and lubricated with (a) PAO4 and (b-d) PAO4 + OFMs

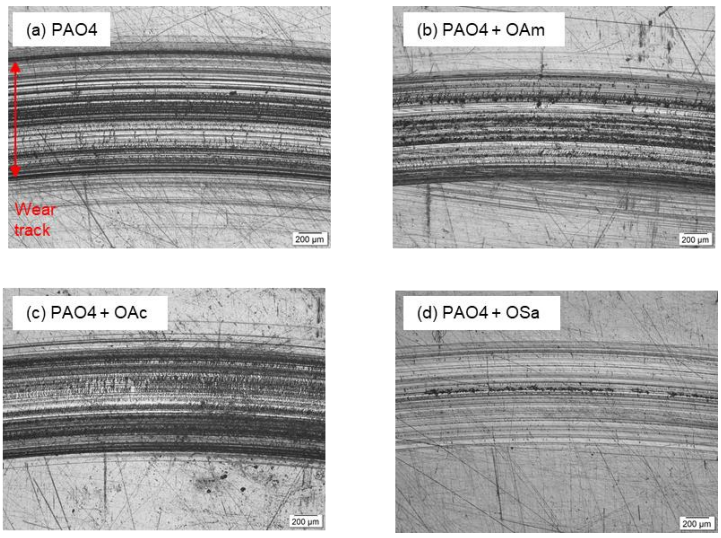

Figure 5.6. Optical images of after-test PEEK plates paired with rough steel balls at 200% SRR and lubricated with (a) PAO4 and (b-d) PAO4 + OFMs

The wear profiles of the after-test PEEK plates in Figure 5.7 and Figure 5.8 show good correlation with the friction results i.e., the tests with the higher friction coefficients led to larger wear volumes of the PEEK plates. The wear volumes of the PEEK plates lubricated with PAO4 were higher at 50% SRR than at 200% SRR (Figure 5.7 (a) and Figure 5.8 (a)), well matching the trend of the friction coefficients as shown in Figure 5.3 and Figure 5.4. Although OAm and OAc did not affect wear, OSa significantly reduced wear at 200% SRR and increased it at 50% SRR (Figure 5.7 (d) and Figure 5.8 (d)), also matching the trend of its frictional performance. Contrary to the constant speed routine

tests used in Chapter 4, in the Stribeck routine tests, the entrainment speeds vary widely during the test and therefore the specific wear rates (SWRs) cannot be readily calculated. Based on the definition of SRR described in section 3.2.2, the wear tracks produced in the 200% SRR tests resulted from a sliding distance four times greater than that in the 50% SRR tests. However, the wear volumes were much larger in the 50% SRR tests than in the 200% SRR tests, indicating other factors apart from the sliding distance-controlled wear performance. The working mechanism will be discussed in section 5.3.1 taking into account the results of surface analyses.

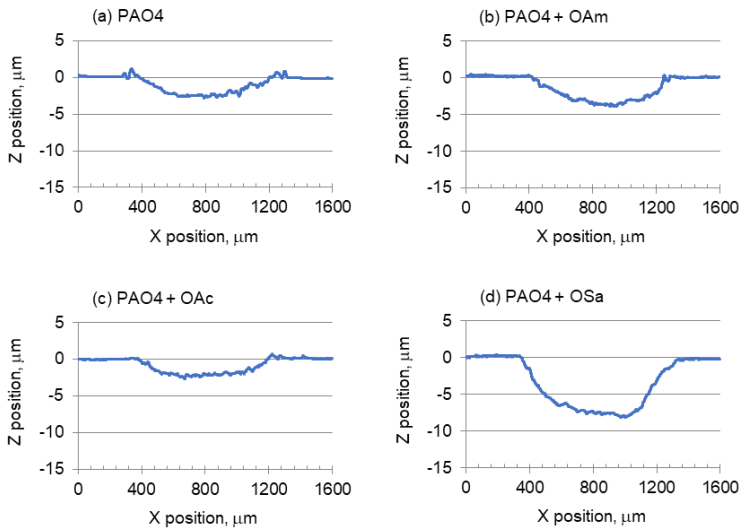

Figure 5.7. Wear profiles of PEEK plates paired with rough steel balls at 50% SRR and lubricated with (a) PAO4 and (b-d) PAO4 + OFMs

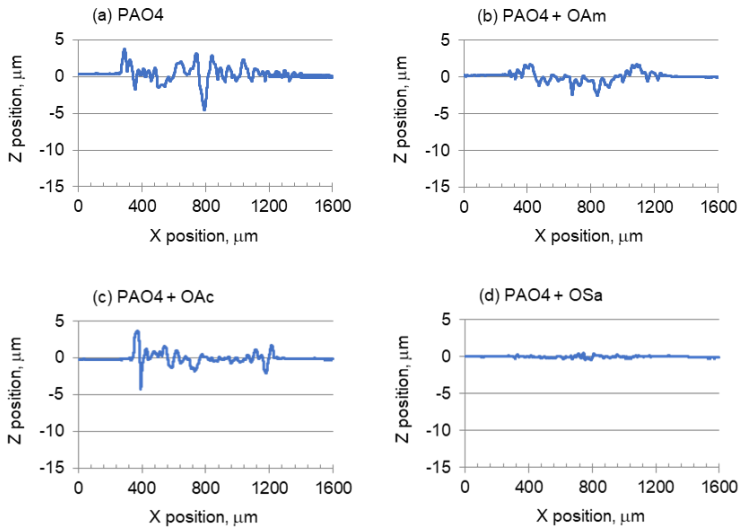

Figure 5.8. Wear profiles of PEEK plates paired with rough steel balls at 200% SRR and lubricated with (a) PAO4 and (b-d) PAO4 + OFMs

5.1.2 Surface analyses

The two key factors which possibly influence the tribological performance of the PEEK-steel contact, i.e., the hardness modification of polymer surfaces and the formation of polymer transfer films on steel counterparts were investigated and discussed in Chapter 4. The effect of OFMs on these factors are investigated in this section.

5.1.2.1 Nanoindentation

The nanoindentation measurements were carried out on the wear tracks of the PEEK plates from the PEEK-steel tests lubricated with PAO4 and PAO4 + OSa, because OSa had the most significant effect on the friction and wear results. The continuous stiffness measurement (CSM) technique described in section 3.3.2 was applied. The hardness values were plotted as a function of indentation depth and compared to those of a new PEEK plate (Figure 5.9 and Figure 5.10). In all tests, the hardness had high values at an indentation depth <0.5 µm. As already mentioned in section 4.1.2.1, these values are thought to be attributed to a phenomenon known as the indentation size effect (ISE), and are not regarded as physically significant. Therefore, the hardness at indentation depth values <0.5 µm was not used in this discussion.

The nanoindentation measurement results indicate that there was no correlation between the hardness of the PEEK surfaces and the friction and wear properties. In the case of the PEEK-smooth steel contact, the hardness of the PEEK plate lubricated with PAO4 was lower at 200% SRR than at 50% SRR (Figure 5.9 (a, c)), while the friction was higher at 200% SRR than at 50% SRR (Figure 5.1 and Figure 5.2). On the other hand, PAO4 + OSa also led to a lower PEEK hardness at 200% SRR than at 50% SRR (Figure 5.9 (b, d)), but showed lower friction at 200% SRR than at 50% SRR (Figure 5.1 and Figure 5.2). A similar discrepancy was also observed for the PEEK-rough steel contacts. At both SRRs, the values of PEEK hardness when lubricated with PAO4 + OSa were higher than those when lubricated with PAO4 (Figure 5.10), although OSa affected friction and wear properties in opposite ways, depending on SRRs i.e. improving friction and wear at 200% SRR (Figure 5.4 and Figure 5.8) and worsening them at 50% SRR (Figure 5.3 and Figure 5.7). The effect of OFMs on the hardness modification of PEEK surfaces will be discussed in detail in section 5.3.1, but the nanoindentation measurement results suggest that the hardness modification of PEEK surfaces did not control the tribological performance of the PEEK-steel contacts lubricated with PAO4 and PAO4 + OFMs and that other factors could play a more important role.

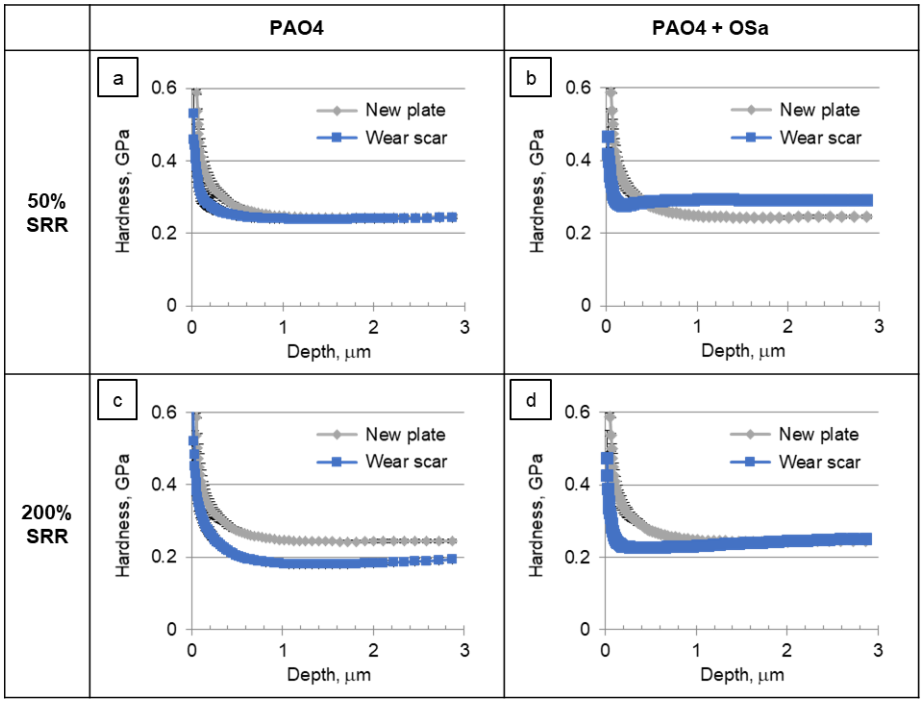

Figure 5.9. Nanoindentation hardness of after-test PEEK plates paired with smooth steel balls lubricated with (a, c) PAO4 and (b, d) PAO + OSa

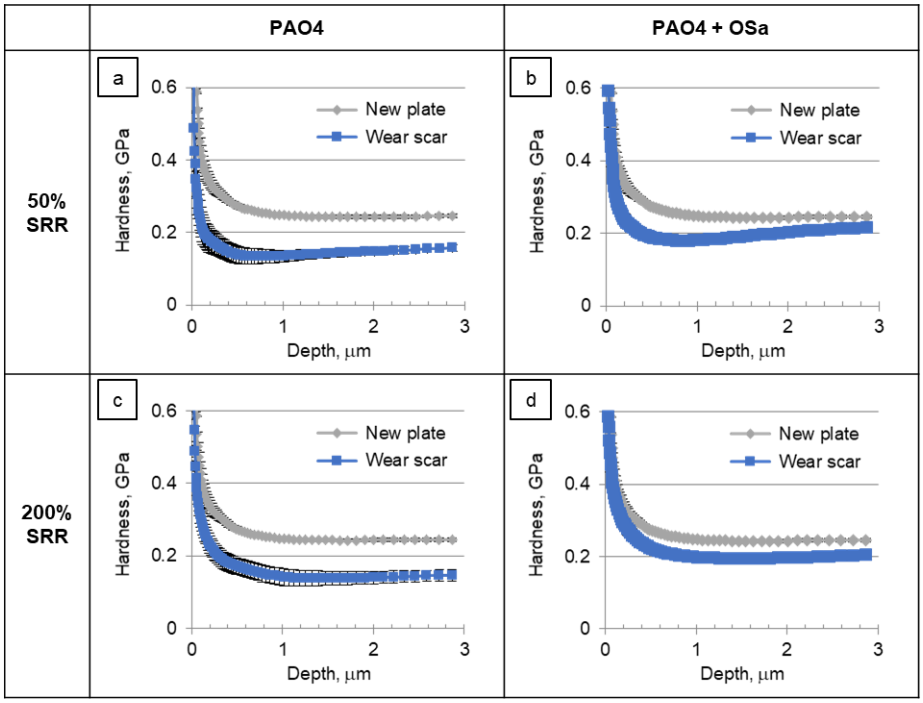

Figure 5.10. Nanoindentation hardness of after-test PEEK plates paired with rough steel balls lubricated with (a, c) PAO4 and (b, d) PAO + OSa

5.1.2.2 EPMA

EPMA of the after-test steel ball specimens, following the procedure described in section 3.3.3, was performed to investigate the presence of PEEK transfer films. The tribological tests were carried out on PEEK-smooth steel and PEEK-rough steel contacts, but the PEEK transfer films were investigated only on the rough steel balls. The PEEK transfer films proved difficult to detect on smooth steel balls as they were easily removed from the smooth surfaces at the end of tests. In PEEK-rough steel contacts, the PEEK transfer films were trapped between asperities on the rough steel surfaces and were more noticeable than those on the smooth steel balls. In addition, for similar reasons to that of the nanoindentation study, this study focused on the specimens tested with PAO4 and PAO4 + OSa.

Secondary Electron (SE) images of all specimens in Figure 5.11 showed that there was almost no wear on the steel balls. As the hardness of a steel ball is much higher than that of a PEEK plate, it was expected that wear would mainly occur on the PEEK plates. The shape of wear scars was different for the 50% SRR (sliding-rolling) and 200% SRR (sliding) tests. In the sliding-rolling tests (50% SRR), the steel balls rotated producing a circumferential wear scar (Figure 5.11 (a, b)), while in the sliding tests (200% SRR), the steel balls were fixed and the wear scars had a round shape (Figure 5.11 (c, d)).

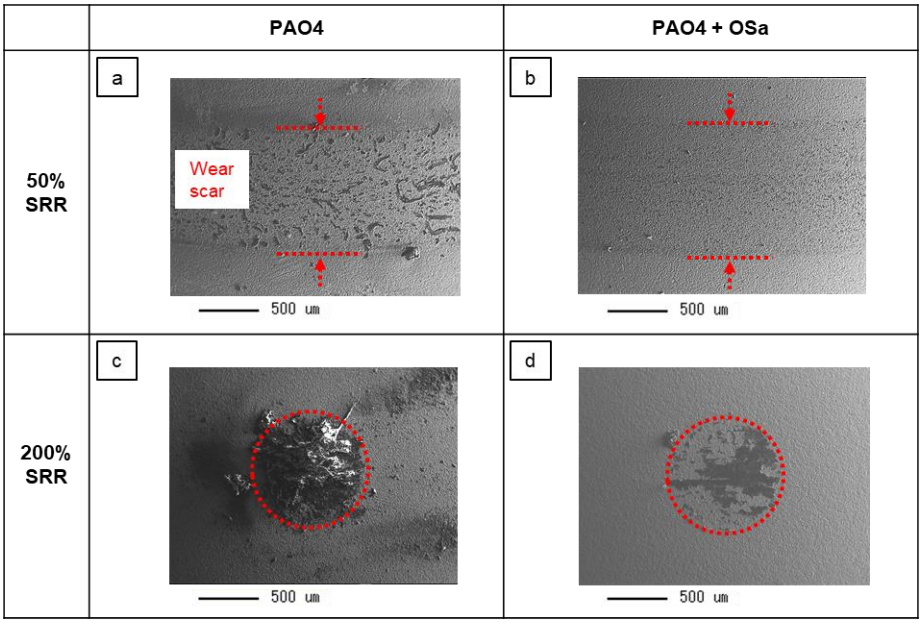

Figure 5.11. SE images of after-test rough steel balls lubricated with (a, c) PAO4 and (b, d) PAO4 + OSa

Although SE images clearly indicate the presence of PEEK transfer films, EPMA carbon mapping was employed to evaluate the amount present (Figure 5.12). The carbon amount is indicated by the colour scale on the map. On the wear scars of the steel balls lubricated with PAO4, larger amounts of carbon were detected at 200% SRR than at 50% SRR (Figure 5.12 (a, c)). By adding OSa, the carbon amount was reduced especially at 50% SRR (Figure 5.12 (b)), and this reduction was observed not only inside the wear scars but also outside. It is noteworthy that the carbon amount on the wear scars of steel balls and the friction and wear properties (Figure 5.3, Figure 5.4, Figure 5.7, Figure 5.8) showed good correlation i.e. a greater amount of carbon on the steel counterparts led to lower friction and wear. This indicates that the presence of a PEEK transfer film on the steel ball is a key factor in controlling the tribological performance of the PEEK-rough steel contact. As investigated in section 5.1.1, OSa had a detrimental effect on friction and wear at 50% SRR. The lower carbon amount on the steel ball lubricated with PAO4 + OSa at 50% SRR (Figure 5.12 (b)) suggests that the amount of the PEEK transfer films was not enough to cover the roughness of the steel ball. This caused abrasive wear by direct contact between the PEEK surface and the large asperities of the steel counterpart. In this case, the adsorption of OSa on the steel surface may have inhibited the formation of a PEEK transfer film. Intriguing, a thick transfer film was formed at 200% SRR even in the PAO4 + OSa lubricated test (Figure 5.12 (d)). This implies that in sliding (200% SRR) conditions the formation of the PEEK transfer film was more dominant than the inhibition by OSa adsorption and thus it controlled the process. The working mechanism of OFM will be discussed in more detail in section 5.3.1.

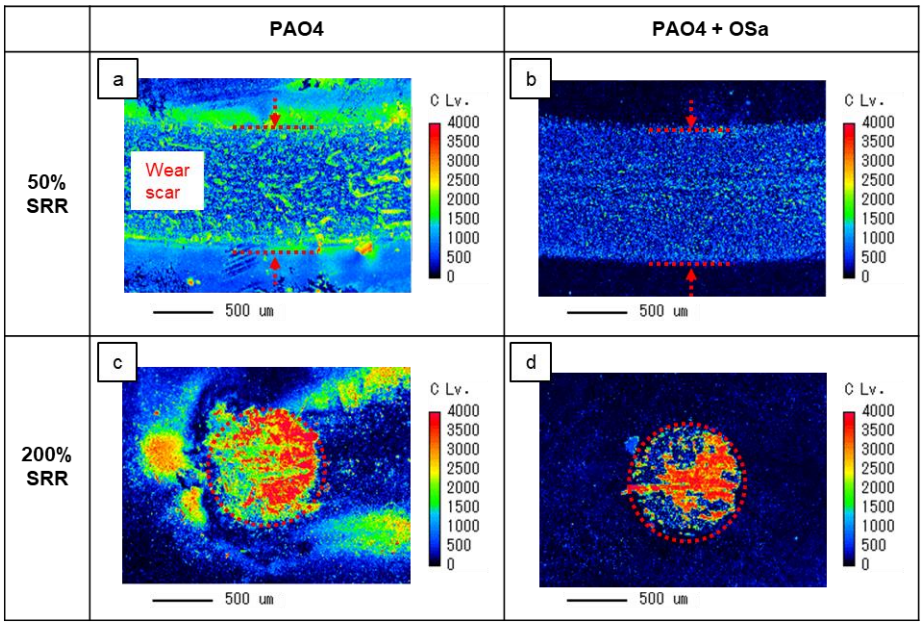

Figure 5.12. EMPA carbon maps of after-test rough steel balls lubricated with (a, c) PAO4 and (b, d) PAO4 + OSa

5.1.2.3 Raman spectroscopy

The presence of carbon detected with EPMA is assumed to be related to PEEK transfer films but to confirm this assumption Raman spectra were recorded on the wear scars of steel balls as shown in Figure 5.14 following the procedure described in section 3.3.5. All spectra display identical peaks (Figure 5.13) which match the Raman spectra of PEEK reported in the literature [90,139,140,142]. A small difference is observed around 1300 cm^{-1} in the spectra for PAO4 and PAO4 + OSa at 50% SRR (Figure 5.14 (a, b)) which could be caused by the steel substrate. From the Raman spectroscopy results it can be thus concluded that EPMA carbon mapping is a valid analysis technique for evaluating the amount of PEEK transfer films on steel balls. In section 4.1.2.3, XPS analysis of C 1s spectra was also used successfully to establish the relationship between the carbon detected with EPMA and the PEEK transfer films, as well as Raman spectra. Thus all these techniques can be used to evaluate the amount of transfer films present.

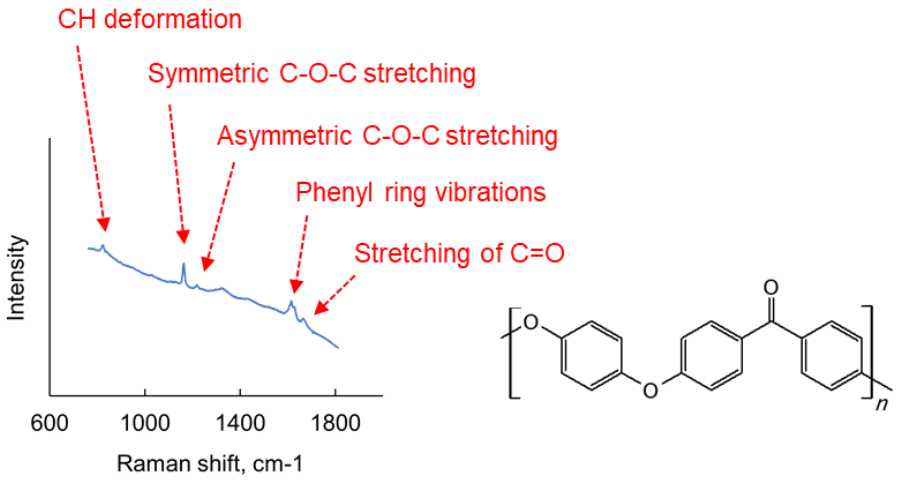

Figure 5.13. Peaks for Raman modes of PEEK

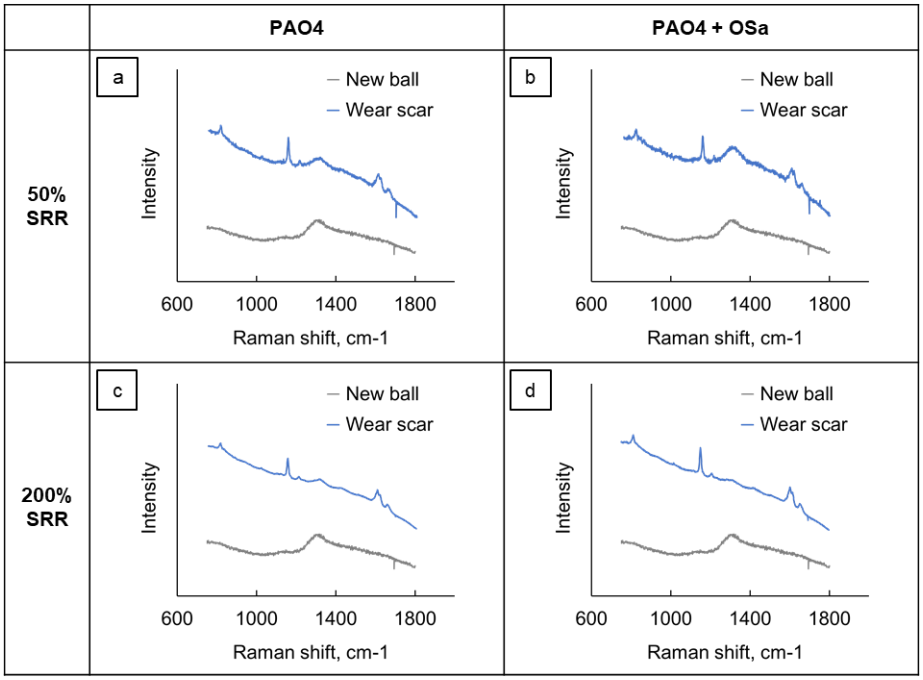

Figure 5.14. Raman spectra of after-test rough steel balls lubricated with (a, c) PAO4 and (b, d) PAO4 + OSa

5.1.3 Testing in PEEK-PEEK and steel-steel contacts

Although this study mainly focused on the PEEK-steel contact, tribological tests using pairs of the same materials (PEEK-PEEK and steel-steel) were performed in this study to investigate the adsorption abilities of OFMs on PEEK and steel surfaces, separately. Ideally, direct observation of OFM adsorption films on the PEEK and steel surfaces using surface analysis techniques such as TOF-SIMS and XPS is desirable. However, OFM adsorption films are thin, unstable and therefore difficult to observe.

The test conditions were the same as for the PEEK-steel contacts investigated in section 5.1.1 except for the applied load in the steel-steel contact. The applied loads were 50 N in the PEEK-steel and PEEK-PEEK contacts, and 5 N (the minimum load of the test equipment) in the steel-steel contact to make the Hertzian contact pressure as similar in value as possible for all material combinations. The maximum Hertzian contact pressure (Pmax) was calculated as 0.16 GPa in PEEK-steel, 0.10 GPa in PEEK-PEEK and 0.68 GPa in steel-steel, respectively.

The Stribeck curves for the PEEK-PEEK contact lubricated with PAO4 and PAO4 + OFMs are shown in Figure 5.15 and Figure 5.16. PAO showed the typical trend of Stribeck curves, where friction coefficients become higher as the entrainment speeds become lower. OSa significantly reduced

friction in the PEEK-PEEK contacts at both 50% and 200% SRRs. OAm and OAc showed the friction reducing effects at 200% SRR but had little effect at 50% SRR.

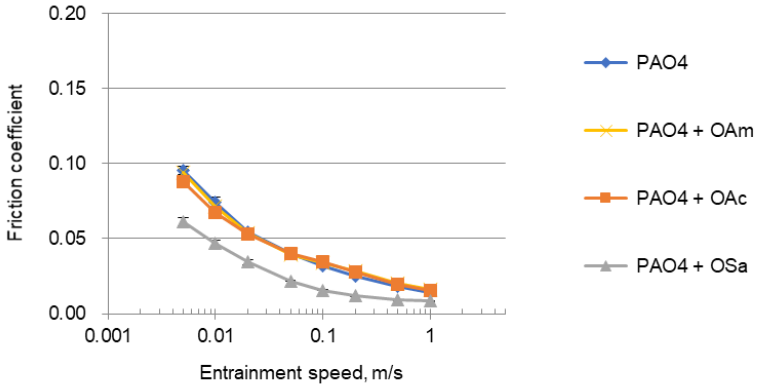

Figure 5.15. Stribeck curves in PEEK-PEEK contact at 50% SRR for PAO4 and PAO4 + OFMs

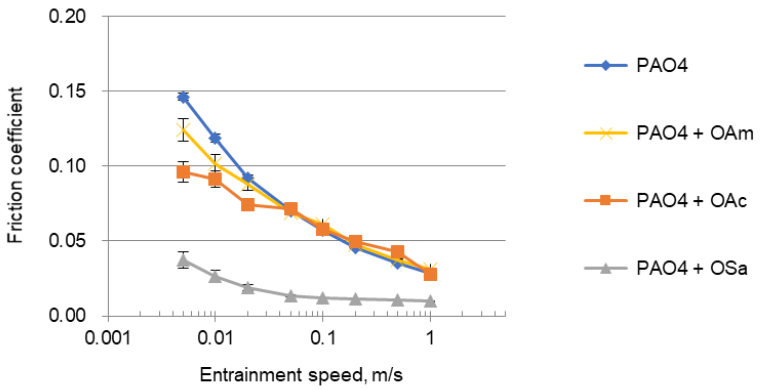

Figure 5.16. Stribeck curves in PEEK-PEEK contact at 200% SRR for PAO4 and PAO4 + OFMs

The Stribeck curves for the steel-steel contact lubricated with PAO4 and PAO4 + OFMs are shown in Figure 5.17 and Figure 5.18. Similar to the PEEK-PEEK contact, PAO4 showed the typical trend of Stribeck curves. At 200% SRR, the friction coefficients of PAO4 increased notably below 0.1 m/s. As mentioned, the contact pressure in the steel-steel contact was higher than that in the PEEK-steel and PEEK-PEEK contacts. Therefore, the lubrication regime was more severe in the steel-steel contact, possibly causing partial seizure at 200% SRR. As a result, the contact surfaces experienced higher wear and became rougher, leading to higher friction coefficients. As expected from previous research on steel-steel contact, the addition of OFMs to PAO4 had an important effect on friction. OSa reduced friction in the steel-steel contact at both 50% and 200% SRRs. The effects of OAm and

OAc were lower than OSa but the friction increase observed for PAO4 below 0.1 m/s was absent for PAO4 + OAm and PAO4 + OAc which indicates that OAm and OAc adsorbed on the steel surfaces and suppressed partial seizure.

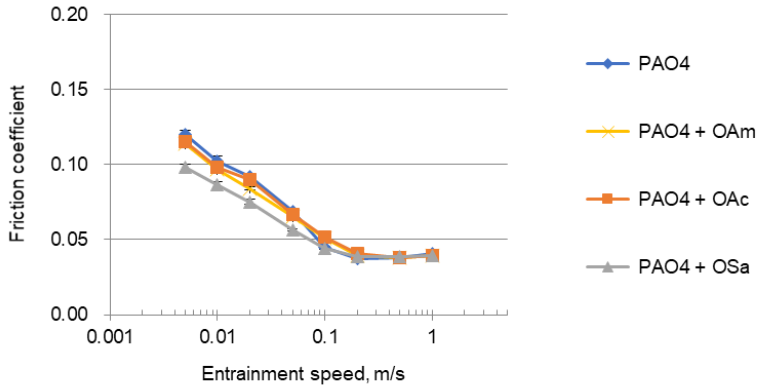

Figure 5.17. Stribeck curves in steel-steel contact at 50% SRR for PAO4 and PAO4 + OFMs

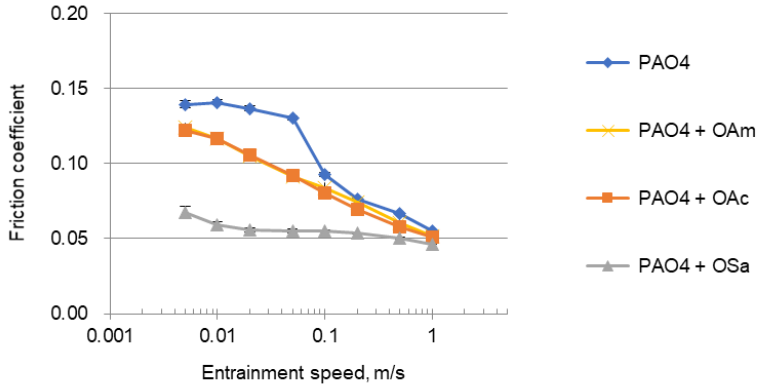

Figure 5.18. Stribeck curves in steel-steel contact at 200% SRR for PAO4 and PAO4 + OFMs

These results imply that OFMs adsorb on both PEEK and steel surfaces. As reported in section 5.1.1, OFMs, especially OSa, had a different effect on the friction and wear properties depending on the surface roughness of the steel counterparts and SRRs. The results of the adsorption behaviour of OFMs investigated in this section will be used to help deduce the working mechanism of OFMs in these testing conditions, presented in section 5.3.1.

5.2 Results: Effect of anti-wear additives

This section investigates the effect of anti-wear (AW) additives on the friction and wear performance of pure PEEK paired with a steel counterpart. The typical anti-wear (AW) additives, Zinc dialkyldithiophosphate (ZDDP) and tricresyl phosphate (TCP), described in section 3.1.3.2, were used in this study.

The detailed methodology was described in Chapter 3. The AW additives were added at 1.0 wt.% to PAO4 as listed in Table 3.4. Similar to the investigation of OFMs presented in section 5.1, the tribological testing was carried out using a MTM with the Stribeck routine as described in section 3.2.3. The test conditions were based on the standard conditions in Table 3.6, but 200% SRR (sliding) tests were also carried out in addition to the 50% SRR (sliding-rolling) tests. Additionally, steel balls with smooth surfaces (Ra of 0.01-0.02 μm) and rough surfaces (Ra of approximately 0.5 μm) were used as described in section 3.1.2. By using the same methodology as that used in section 5.1, the effect of AW additives can be compared with that of OFMs.

5.2.1 Friction and wear performance

(a) PEEK-smooth steel contact

The Stribeck curves, representing friction coefficient values as a function of entrainment speed, in the PEEK-smooth steel contact lubricated with PAO4 and PAO4 + AW additives, ZDDP and TCP, are presented in Figure 5.19 and Figure 5.20. Compared with PAO4, the addition of ZDDP and TCP slightly reduced friction at 200% SRR (sliding), but less influence was identified at 50% SRR (sliding-rolling). As seen in section 5.1, OSa (N-oleoyl sarcosine) notably reduced friction both at 50% and 200% SRRs (Figure 5.1, Figure 5.2), but the effect of ZDDP and TCP was much less than that of OSa and more similar to that of OAm (oleylamine) and OAc (oleic acid). When the tribological tests were conducted with the smooth steel balls, there was almost no wear on the after-test PEEK plates, regardless of SRRs or lubricant formulations. In the steel-steel contact, AW additives have been reported to work by reacting on contact surfaces and forming reaction films with low shear strength, thus mitigating the direct contact of the two surfaces and preventing seizure [39,113–115]. Although the lubrication regimes of the testing conditions applied can be estimated as boundary/mixed lubrication, as described in section 5.1.1, the friction results of PAO4 + AW additives imply that the testing conditions for PEEK-smooth steel contacts were possibly too mild for AW additives to form reaction films for AW additives. Further aspects of the reactivity of AW additives on PEEK and steel surfaces will be investigated in section 5.2.3.

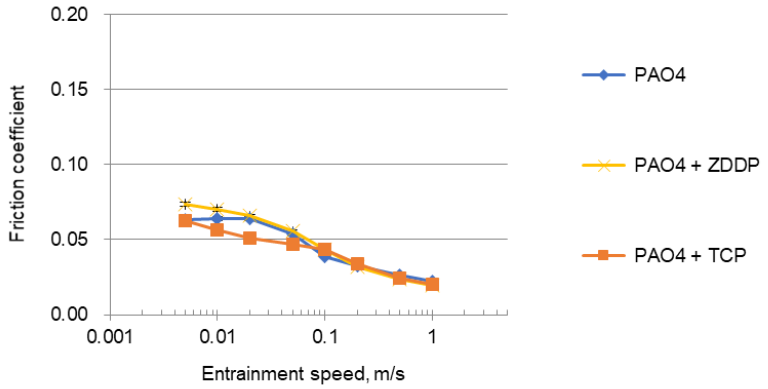

Figure 5.19. Stribeck curves with smooth steel balls at 50% SRR for PAO4 and PAO4 + AW additives

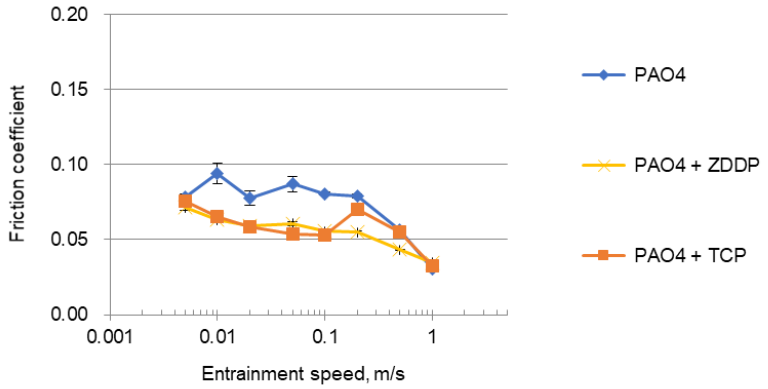

Figure 5.20. Stribeck curves with smooth steel balls at 200% SRR for PAO4 and PAO4 + AW additives

(b) PEEK-rough steel contact

Similar to the investigation of OFMs in section 5.1.1, the effect of AW additives on the PEEK-steel contact was investigated using rough steel balls. The calculated Lambda ratios of below one for the PEEK-rough steel contact in this section indicate that both the 200% SRR and 50% SRR tests were performed in the boundary lubrication regime. The Stribeck curves lubricated with PAO4 and PAO4 + AW additives are shown in Figure 5.21 and Figure 5.22. The addition of ZDDP and TCP to PAO4 slightly increased friction at 50% SRR, while friction decreased at 200% SRR. Similar to the results for the PEEK-smooth steel contacts, the effect of ZDDP and TCP was comparable to those of OAm (oleylamine) and OAc (oleic acid) presented in Figure 5.3 and Figure 5.4.

.

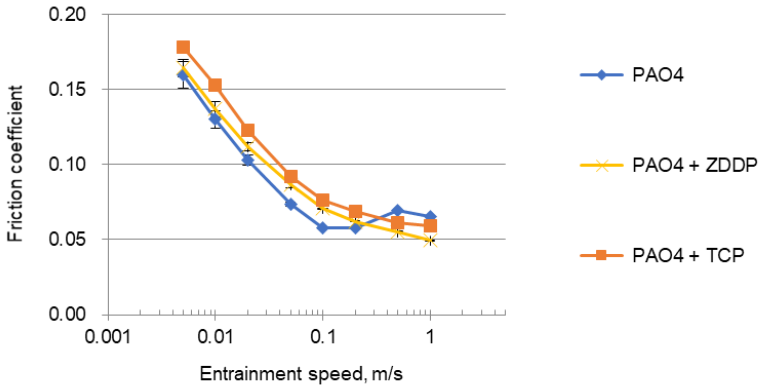

Figure 5.21. Stribeck curves with rough steel balls at 50% SRR for PAO4 and PAO4 + AW additives

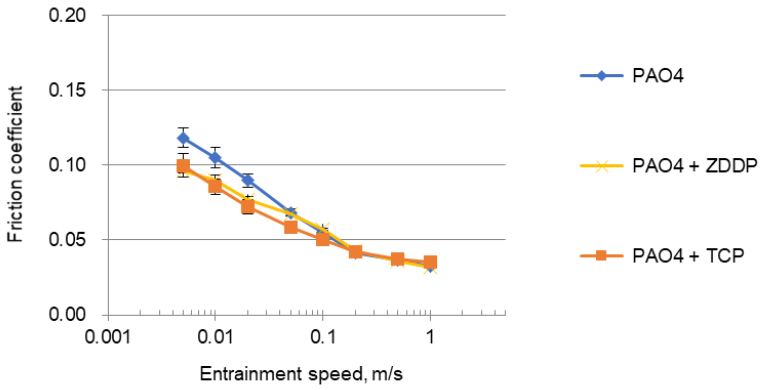

Figure 5.22. Stribeck curves with rough steel balls at 200% SRR for PAO4 and PAO4 + AW additives

The optical images of the after-test PEEK plates are shown in Figure 5.23 and Figure 5.24. The plates tested at 50% SRR had uniform damage inside the wear tracks, while the ones at 200% SRR exhibited non-uniform damage with scratches along the sliding direction. The wear tracks produced by PAO + ZDDP and PAO + TCP had similar appearance to the PAO4 results at both 50% and 200% SRRs. The width of the wear track for PAO + ZDDP at 200% SRR was narrower than that for PAO4, suggesting that ZDDP influenced the wear property to some extent. This was also confirmed by the wear profiles.

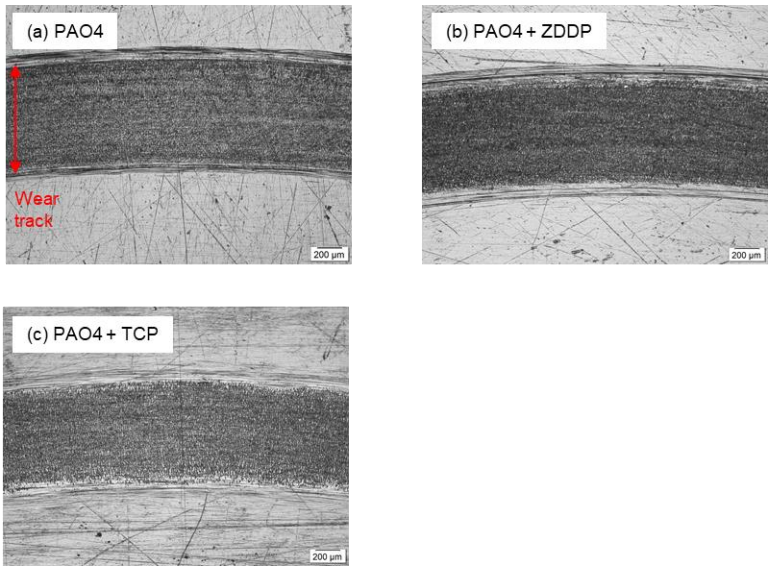

Figure 5.23. Optical images of after-test PEEK plates paired with rough steel balls at 50% SRR lubricated with (a) PAO4 and (b, c) PAO4 + AW additives

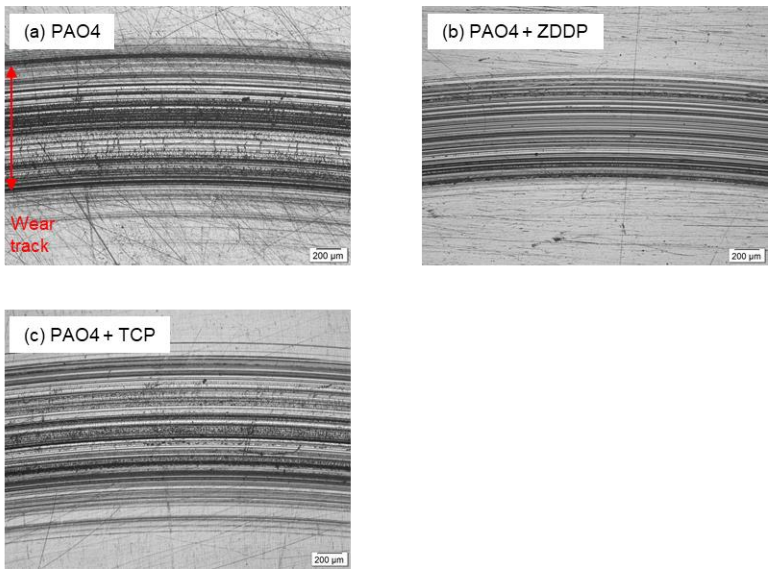

Figure 5.24. Optical images of after-test PEEK plates paired with rough steel balls at 200% SRR lubricated with (a) PAO4 and (b, c) PAO4 + AW additives

The wear profiles of the after-test PEEK plates are presented in Figure 5.25 and Figure 5.26. Similar to that described in section 5.1.1, the wear volumes for PEEK plates lubricated with PAO4 were larger at 50% SRR than at 200% SRR. The wear profiles for PAO4 + ZDDP and PAO4 + TCP were similar to that of PAO4 at both 50% and 200% SRRs, but the width of the wear profile of PAO + ZDDP at 200% SRR (approximately 800 μm) was narrower than that of PAO4 (approximately 1000 μm). Despite OSa being an OFM and not an AW additive, it reduced wear (Figure 5.8(d)) much more

significantly than ZDDP. However, the optical images and the wear profiles suggest that ZDDP influenced wear performance to some extent. The working mechanism will be discussed in section 5.3.2 taking into account the results of surface analyses and the additional tests carried out on PEEK-PEEK and steel-steel contacts.

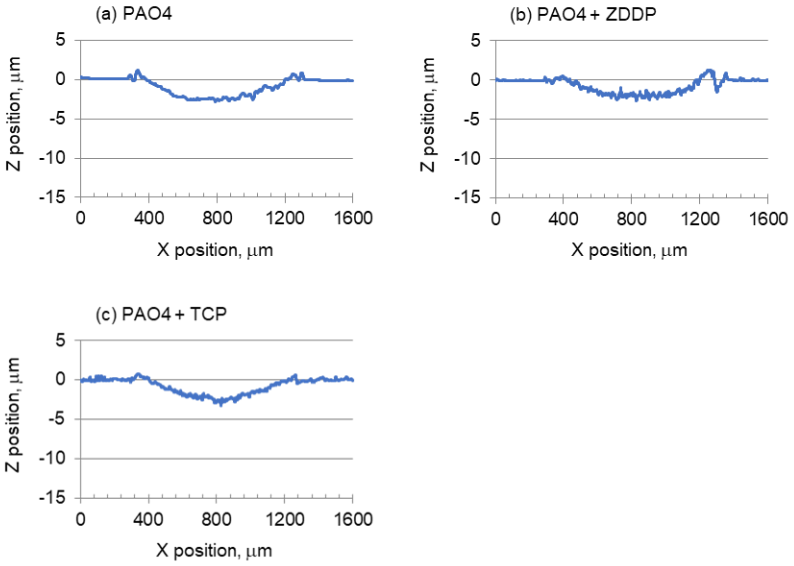

Figure 5.25. Wear profiles of PEEK plates paired with rough steel balls at 50% SRR lubricated with (a) PAO4 and (b, c) PAO4 + AW additives

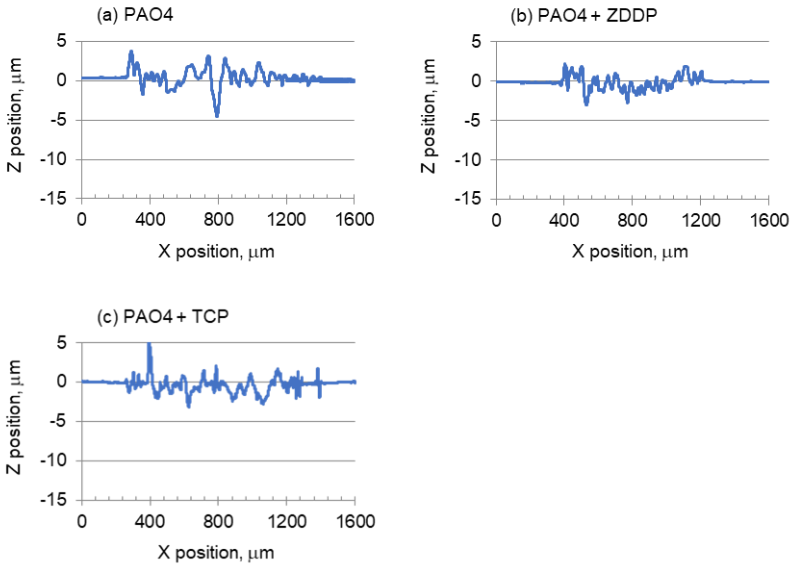

Figure 5.26. Wear profiles of PEEK plates paired with rough steel balls at 200% SRR lubricated with (a) PAO4 and (b, c) PAO4 + AW additives

5.2.2 Surface analyses

The two key factors which possibly influence the tribological performance of the PEEK-steel contact, i.e., the hardness modification of polymer surfaces and the formation of polymer transfer films on steel counterparts, were investigated to clarify the working mechanism of OFMs in section 5.1. However, the hardness modification of polymer surfaces correlated little with tribological performance, and the formation of the polymer transfer films was the dominant factor. Therefore, this section focuses on investigations of polymer transfer films on the steel balls and reaction films formed on the steel balls and the polymer plates taking into account the known working mechanism of AW additives in steel-steel contacts.

5.2.2.1 EPMA of polymer transfer films

EPMA on the after-test steel ball specimens, following the procedure described in section 3.3.3, was performed to investigate the PEEK transfer films. This section focuses on the steel balls in the PEEK-rough steel contact lubricated with PAO4 and PAO4 + ZDDP, because ZDDP showed an improvement in the wear performance, while TCP had less effect, as reported in section 5.2.1.

Secondary Electron (SE) images of the after-test rough steel balls are presented in Figure 5.27. As already mentioned in section 5.1.2.2, the shape of the wear scars for the 50% SRR (sliding-rolling) and 200% SRR (sliding) tests was different because in the sliding-rolling tests (50% SRR) the steel balls rotated, so producing a circumferential wear scar (Figure 5.27 (a, b)), while in the sliding tests (200% SRR) the steel balls were fixed and the wear scars thus had a round shape (Figure 5.27 (c, d)). Compared to PAO4 + OSa, which produced wear scars distinctively different from those lubricated with PAO4 (Figure 5.11), PAO4 + ZDDP had very similar wear scars to PAO4 both at 50% and 200% SRRs.

EPMA carbon mapping was also employed as shown in Figure 5.28. The carbon amount is indicated by the colour scale on the map. Regardless of SRRs, PAO4 + ZDDP gave a larger amount of carbon outside the wear scars than PAO4. However, inside the wear scars, which better reflects tribological performance, both PAO4 and PAO4 + ZDDP at 50% and 200% SRRs produced almost the same amount of carbon. As seen in 5.2.1, the addition of ZDDP slightly improved the wear of the polymer plate at 200% SRR (Figure 5.26 (b)). These results imply that in the case of AW additives, the formation of polymer transfer films on the steel counterparts is not the only factor determining the tribological performance of the PEEK-steel contact and there will be other factors, such as reaction

films formed by these additives. Taking into account the investigation of the reaction films in section 5.2.2.2, the working mechanism of AW additives will be discussed in more detail in section 5.3.2.

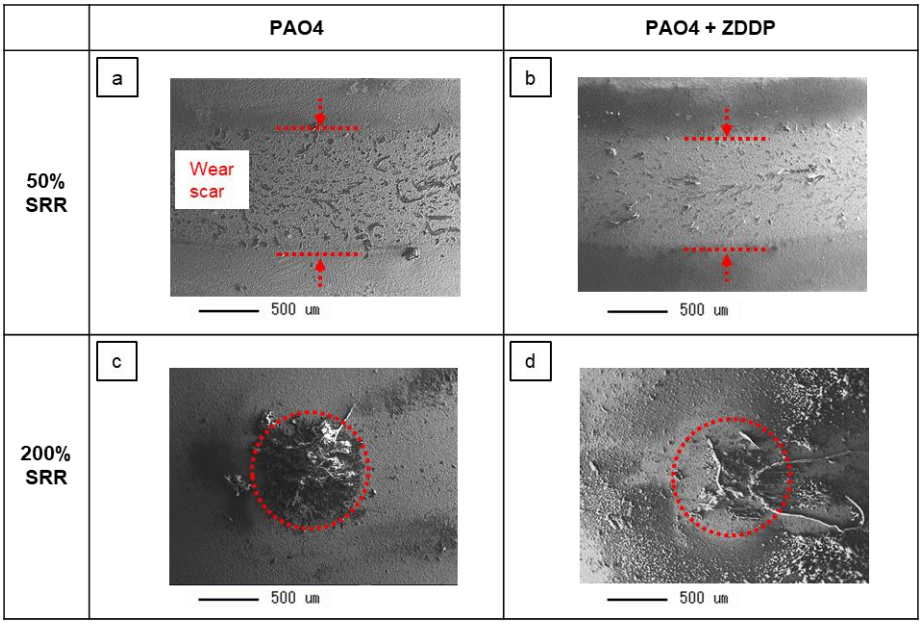

Figure 5.27. SE images of after-test rough steel balls lubricated with (a, c) PAO4 and (b, d) PAO4 + ZDDP

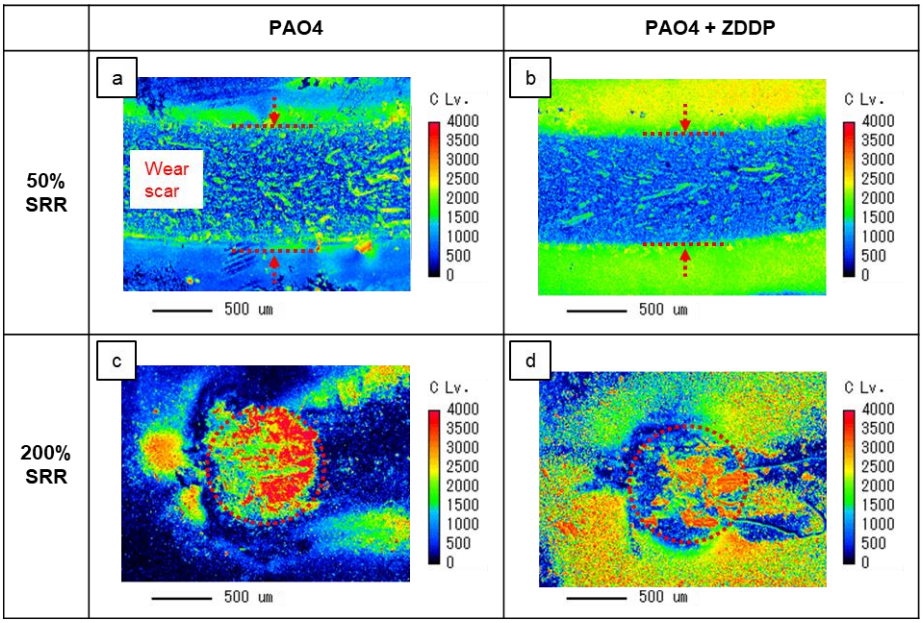

Figure 5.28. EMPA carbon maps of after-test rough steel balls lubricated with (a, c) PAO4 and (b, d) PAO4 + ZDDP

5.2.2.2 EPMA of AW additive reaction films

In steel-steel contacts, AW additives are known to form low shear strength reaction films on the contact surfaces and so prevent direct contact, thus reducing wear. In PEEK-steel contacts, the polymer transfer films work similarly to the reaction films formed in steel-steel contacts. As seen in section 5.2.2.1, PAO4 and PAO4 + ZDDP produced almost the same amount of the polymer transfer films on the steel counterparts but the wear of the polymer plate was slightly improved when lubricated with PAO4 + ZDDP at 200% SRR. However, if ZDDP rection films form on the steel and/or polymer surfaces, these films may contribute to reducing the wear of the polymer plate. ZDDP contains phosphorus and sulphur in its chemical structure and has been reported to form reaction films containing these elements [39]. Therefore, EPMA phosphorus and sulphur mapping was conducted on the after-test steel balls and PEEK plates from the PEEK-rough steel contact tests at 50% and 200% SRRs following the procedure described in section 3.3.3. Although, as seen in section 5.2.1, ZDDP reduced friction in the PEEK-smooth steel contact at 200% SRRs, the EPMA phosphorus and sulphur mapping was only conducted on specimens tested with the PEEK-rough steel contacts. This was because almost no wear was detected on the PEEK plates tested in the PEEK-smooth steel contacts regardless of SRRs or lubricant formulations as already mentioned and therefore the effect of ZDDP was indiscernible.

Figure 5.29 shows the SE images and corresponding EPMA phosphorus and sulphur maps of the after-test rough steel balls lubricated with PAO4 + ZDDP. The phosphorus and sulphur amounts are indicated by the colour scales on the maps. Note that the maximum ranges of the scales of the phosphorus and sulphur maps are much lower than that of the carbon maps in Figure 5.28. At both 50% and 200% SRRs, the amount of phosphorus and sulphur was very low compared to the amount of carbon (Figure 5.28 (c, d)). This indicates there was almost no ZDDP reaction film on the steel surface regardless of SRRs.

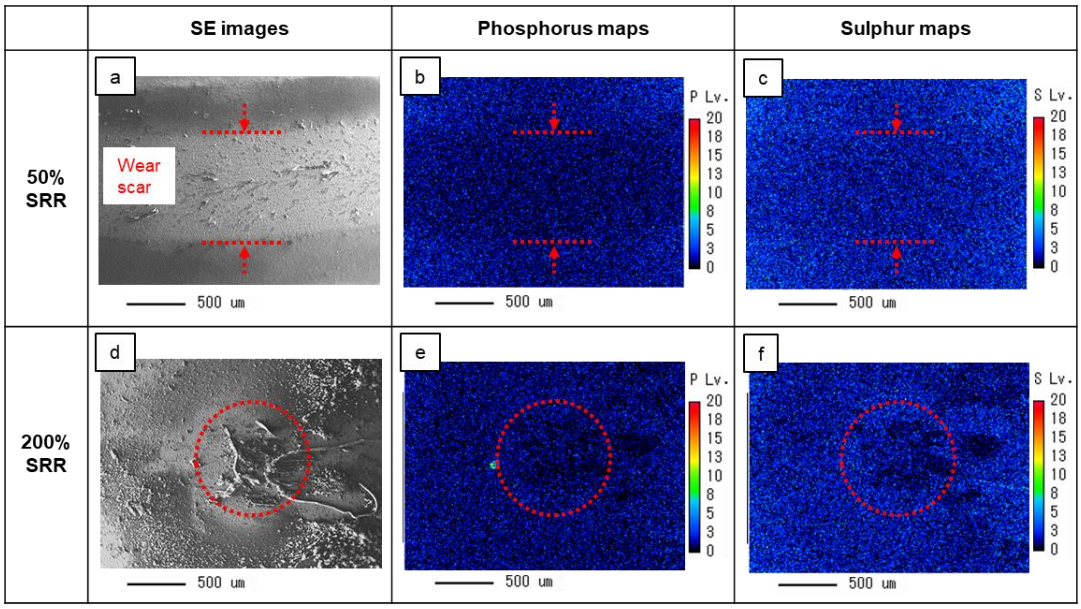

Figure 5.29. (a, d) SE images and corresponding EPMA (b, e) phosphorus and (c, f) sulphur maps of after-test rough steel balls lubricated with PAO4 + ZDDP

The EPMA phosphorus and sulphur maps were also obtained for the after-test PEEK plates as shown in Figure 5.30. Phosphorus and sulphur were observed to be present in very low amount on the wear tracks produced in the tests at 200% SRR (Figure 5.30 (e, f)). As described in section 3.3.3, the specimens were gently rinsed with a hydrocarbon solvent before EPMA measurements. Therefore, the phosphorus and sulphur detected arose from the substances attached to the PEEK surfaces, assumed to be the ZDDP reaction film. Interestingly, phosphorus and sulphur were only detected on the wear tracks tested at 200% SRR (Figure 5.30 (e, f)), and were not observed on the steel counter surface (Figure 5.29 (e, f)). These results suggest that the ability to form a ZDDP reaction film at ambient temperature depends on the type of surface (chemistry and roughness). In addition, section 5.2.1 reported that the effect on friction and wear performance depends on the types of AW additive, implying that the ability to form a reaction film also depends on the type of AW additives, however, this section only considered ZDDP. Therefore, to estimate the reaction film formation ability of AW additives on PEEK and steel surfaces, additional tests in PEEK-PEEK and steel-steel contacts were conducted and the results are presented in section 5.2.3.

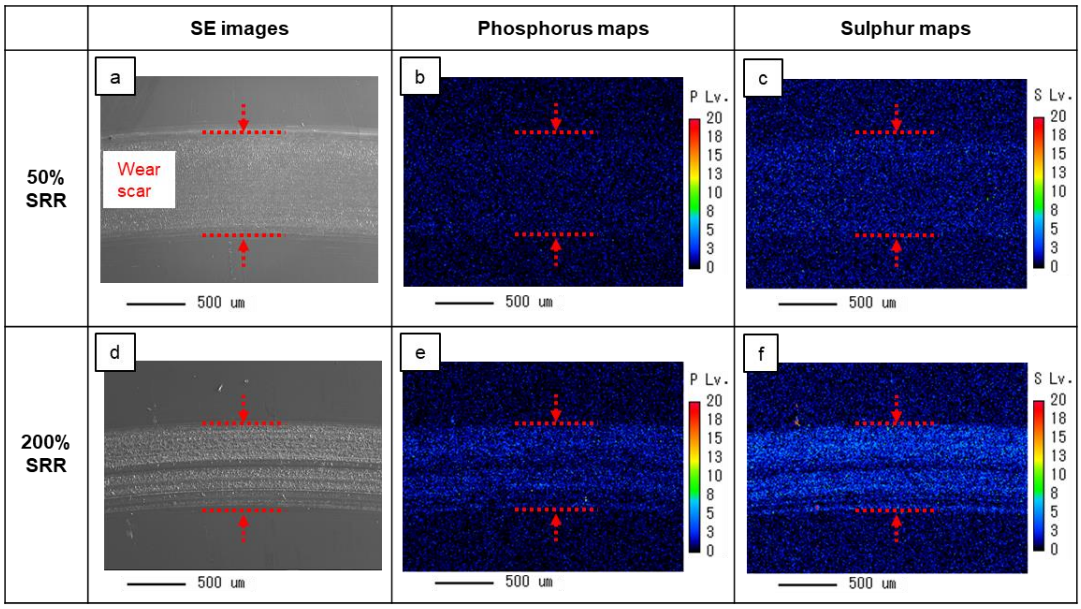

Figure 5.30. (a, d) SE images and corresponding EPMA (b, e) phosphorus and (c, f) sulphur maps of after-test PEEK plates lubricated with PAO4 + ZDDP

5.2.3 Tests with AW additives on PEEK-PEEK and steel-steel contacts

This section aims to estimate the reaction film formation ability of AW additives on PEEK and steel surfaces by evaluating the effect of AW additives on PEEK-PEEK and steel-steel contacts, respectively. Although the reaction film formation ability of AW additives, especially of ZDDP, in steel-steel contacts has been well investigated [39,113–115], it was also investigated in this section in parallel with the investigation on the PEEK-PEEK contact to ensure that the testing conditions employed were as close as possible for the three contact pairs.

The test conditions were the same as in the PEEK-steel contacts investigated in section 5.2.1 except for the applied loads. The applied loads were 50 N in the PEEK-steel and PEEK-PEEK contacts, and 5 N (the minimum load of the test equipment) in the steel-steel contact so as to make the Hertzian contact pressure as similar in value as possible for all material combinations. The maximum Hertzian contact pressure (Pmax) was calculated as 0.16 GPa in PEEK-steel, 0.10 GPa in PEEK-PEEK and 0.68 GPa in steel-steel, respectively. Steel specimens (balls and discs) with smooth surfaces (Ra of 0.01-0.02 μm) were used in this section.

The Stribeck curves for the PEEK-PEEK contact lubricated with PAO4 and PAO4 + AW additives are shown in Figure 5.31 and Figure 5.32. PAO4 + ZDDP and PAO4 + TCP exhibited almost identical curves to PAO4 regardless of SRRs. As reported in section 5.1.3, the OFMs showed a friction reducing effect in the PEEK-PEEK contact, suggesting that OFMs had the ability to form adsorption

films on PEEK surfaces. If ZDDP and TCP form reaction films on the PEEK surfaces, the friction coefficients are expected to change with respect to those found for lubrication with only PAO4. However, the almost identical friction curves of PAO4 and PAO4 + AW additives indicate that ZDDP and TCP did not form any films on the PEEK surface in the PEEK-PEEK contact. This indicates that the ability of AW additives to form reaction films on the PEEK surface was also low in the PEEK-steel contact tested in section 5.2.1.

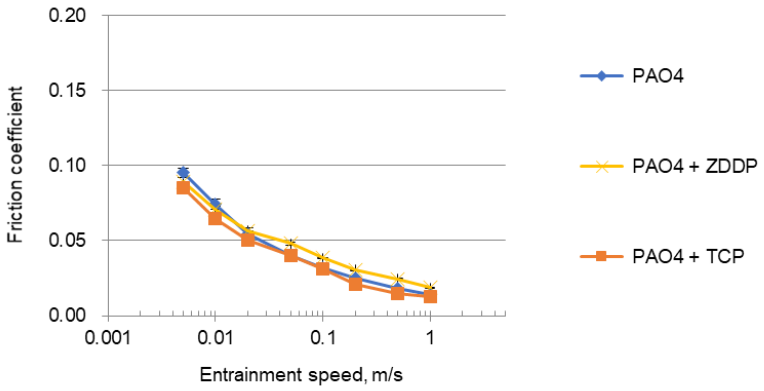

Figure 5.31. Stribeck curves in PEEK-PEEK contact at 50% SRR for PAO4 and PAO4 + AW additives

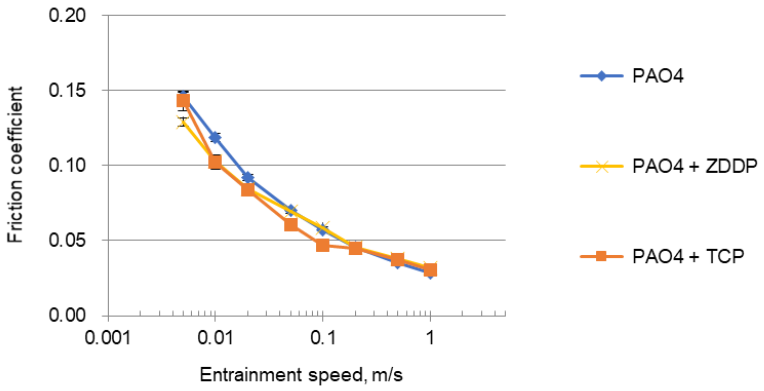

Figure 5.32. Stribeck curves in PEEK-PEEK contact at 200% SRR for PAO4 and PAO4 + AW additives

The Stribeck curves for the steel-steel contact lubricated with PAO4 and PAO4 + AW additives are shown in Figure 5.33 and Figure 5.34. Compared to PAO4, PAO4 + ZDDP gave lower friction at 50% SRR and higher friction at 200% SRR. PAO4 + TCP showed almost the same friction as PAO4 at 50% and slightly lower friction at 200% SRR. These results can be explained by the reactivity of AW additives. At 50% SRR, ZDDP which has higher reactivity, formed a reaction film which then

prevented direct contacts between sliding surfaces, thus reducing friction compared to PAO4. TCP, with lower reactivity, did not form a reaction film and thus showed similar friction to PAO4. As mentioned in section 5.1.3, at 200% SRR the friction coefficients of PAO4 increased substantially below 0.1 m/s due to the partial seizure in the boundary lubrication regime. Although the reactivity of TCP was not high enough to form a reaction film at 50% SRR, it did react to form a reaction film at 200% SRR, preventing seizure and reducing friction. Under 200% SRR, ZDDP increased friction over the entire range of the entrainment speeds. Ratoi et al. have reported that at high SRRs the addition of ZDDP to the base oil increases friction in mixed and boundary lubrication regimes and this can be explained by the rapid formation of a rough and irregular ZDDP reaction film on the wear track [152]. When a thin ZDDP reaction film is formed, it prevents direct contact between sliding surfaces and reduces friction. By contrast, when a rough, thick and irregular ZDDP reaction film is formed, the lubrication regime moves more to boundary, increasing friction in not only the boundary lubrication regime but also in the mixed lubrication regime. The difference in the effect of the AW additives at 50% and 200% SRRs is explained by the activation energy required to form reaction films. Based on the results from PEEK-PEEK and steel-steel contacts, the reaction film formation ability of AW additives is found to be much higher on the steel surface than on the PEEK surface. This was expected due to the increased polarity and reactivity towards AW additives exhibited by steel. The working mechanism of AW additives will be discussed in more detail in section 5.3.2.

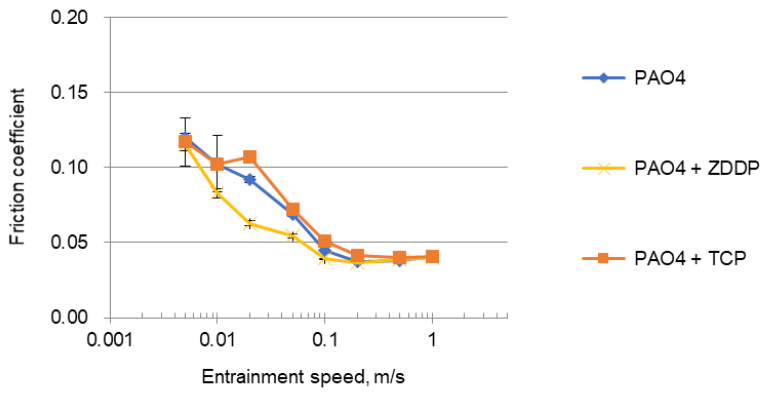

Figure 5.33. Stribeck curves in steel-steel contact at 50% SRR for PAO4 and PAO4 + AW additives

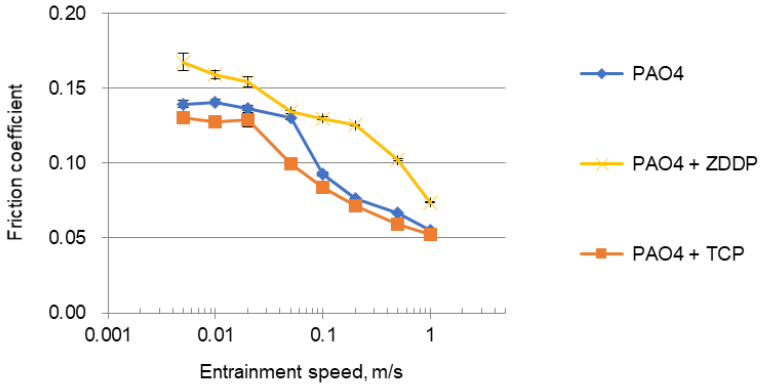

Figure 5.34. Stribeck curves in steel-steel contact at 200% SRR for PAO4 and PAO4 + AW additives

5.3 Discussion

As reported in sections 5.1, OFMs, especially OSa, greatly affected the friction and wear properties of the PEEK-steel contact. The results in section 5.2 show that the effect of AW additives, especially ZDDP, on tribological performance was limited compared to that of OFMs. Based on the experimental results of tribological testing and surface analyses, this section discusses the working mechanisms of OFMs and AW additives.

5.3.1 Working mechanism of OFMs

As reported in section 5.1.1, the effect of OFMs on the friction and wear properties of the PEEK-steel contact depended on SRRs and the surface roughness of the steel specimens. Although OFM (OSa) affected the hardness of PEEK surfaces, as shown in section 5.1.2.1, no correlation was found between the PEEK hardness and the tribological performance of the PEEK-steel contact. Therefore, it is assumed that the friction and wear properties of the PEEK-steel contact under lubrication with OFMs are mainly controlled by the adsorption of OFMs on the contact surfaces and the formation of the PEEK transfer films on the steel surfaces. Therefore, these factors will be discussed separately, then the mechanism proposed will be summarized.

(a) Adsorption of OFMs on the contact surfaces

The adsorption ability of OFMs on PEEK and steel surfaces was investigated in section 5.1.3. The tribological test results in the PEEK-PEEK and steel-steel contacts indicate OFMs can adsorb on both PEEK and steel surfaces. Based on the experimental results, OSa presumably has a much higher adsorption ability on both surfaces than OAm and OAc. The low adsorption ability of OAm and OAc on either PEEK or steel surfaces could be due to the test conditions i.e., the test temperature employed in this study. Although OAm and OAc are widely used OFMs in lubricants for many applications, it has been reported that they generally work better at higher temperature which accelerate the reaction of their polar groups (amine in OAm and carboxyl in OAc) with the surfaces [108,109]. On the contrary, OSa has a superior adsorption ability on both PEEK and steel surfaces at the ambient temperature employed in this study. Sarcosine derivatives of fatty acids have been historically used as a preferred anti-rust additive due to the chelate-forming property of its two polar groups (amine and carboxyl) as seen in Figure 5.35, which interact strongly with metal surfaces [153,154]. Chelation may also enhance the adsorption of OSa on the PEEK surface which contains polar ketone groups in its molecular structure [155–157].

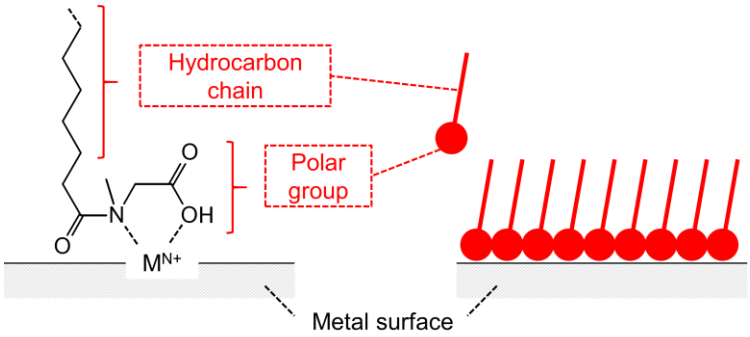

Figure 5.35. Schematic effect of a sarcosine derivative of fatty acids on a metal surface

In terms of the influence of SRR, OFMs, especially OSa, gave superior friction reduction at 200% SRR than at 50% SRR for both PEEK-PEEK and steel-steel contacts, as revealed in section 5.1.3. This indicates that the adsorption of OFMs is greater in 200% SRR (sliding) than 50% SRR (sliding-rolling). As SRR is the ratio of the sliding speed to the entrainment speed, the sliding speeds at each entrainment speed are higher at 200% SRR than 50% SRR, which causes higher frictional heat so accelerating the adsorption of OFMs.

(b) Polymer transfer films on the steel counterparts

As discussed in Chapter 4, base oil lubrication inhibits the formation of polymer transfer films compared to the dry condition. In this chapter, the adsorption of OFM on the steel surfaces was found to inhibit even more the formation of polymer transfer films. The investigation of the polymer transfer films using EPMA was carried out only on the steel balls tested in the PEEK-rough steel contacts, because the polymer transfer films proved difficult to detect on smooth steel balls as they were easily removed from the balls at the end of tests. However, the higher and unstable friction values for PAO4 at 200% SRR (Figure 5.2) imply that the amount of the PEEK transfer film under PAO4 lubrication was larger at 200% SRR than 50% SRR. The polymer transfer films increase the surface roughness, and thus the lubrication regime moves towards boundary lubrication, resulting in higher friction. The outstanding friction reduction with PAO4 + OSa at 200% SRR reported in section 5.1.1 was achieved by the synergistic effect of the OFM adsorption film and the inhibition of excessive polymer transfer films on the steel counterpart (Figure 5.36). The effect of the OFM adsorption film is mainly at lower entrainment speeds where the lubrication regime is more severe. On the contrary, the effect of the inhibition of polymer transfer films by oil lubrication affects the entire range of entrainment speeds, because it works to change the lubrication regime itself.

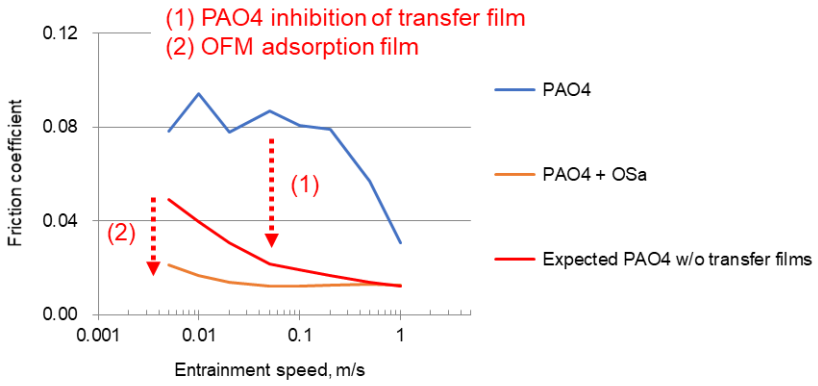

Figure 5.36. Impact of OFM on friction coefficients of PEEK-smooth steel contact at 200% SRR

In PEEK-rough steel contacts, the carbon amounts outside the wear scars were very limited for PAO4 + OSa regardless of SRRs as shown in Figure 5.12. This implies that OSa adsorbed not only inside but also outside the wear scars on the steel balls and thus inhibited the formation of PEEK transfer films. However, thick transfer films were formed inside the wear scars at 200% SRR even in the PAO4 + OSa lubricated test (Figure 5.12(d)). This implies that in the sliding (200% SRR)

condition, the formation of a PEEK transfer film was favoured to the OSa adsorption and thus it controlled the process. Puhan and Wong [90] have reported in-situ observation of the PEEK wear process under dry conditions and proposed that PEEK wear debris, ploughed by the asperities on the counter surface, re-entered the contact surfaces, forming PEEK transfer films. Under lubricated conditions, wear debris particles once formed disperse into the lubricant. The sliding condition (200% SRR) where the steel ball is fixed can help to trap and pile up wear debris near the contact inlet more efficiently than the sliding-rolling condition (50% SRR) where both the steel ball and the PEEK plate rotate and aid the flushing out of wear debris. The accumulation of wear debris near the inlet can contribute to the formation of a PEEK transfer film on the steel surface in sliding (200% SRR) even under lubrication with PAO4 + OSa (Figure 5.12(d)). In addition, PAO4 + OSa showed lower friction and wear (the wear track profile showed almost no wear) than PAO4 at 200% SRR (Figure 5.4, Figure 5.8). This implies that OSa adsorbed on both the PEEK plate and the PEEK transfer film formed on the steel ball, thus mitigating the severity of the contact conditions between the two sliding surfaces. The above discussion has been mainly focused on OSa, but presumably it can be generalized for OFMs as most OFMs are considered to work essentially in the same way as OSa, although the extent depends on their adsorption abilities.

(c) Proposed mechanism of action

Taking into account the factors discussed above, the proposed mechanism of lubrication with OFMs in the PEEK-steel contact is summarized in Figure 5.37 and Figure 5.38. OFMs adsorb on both steel and PEEK surfaces with their polar groups. The lubrication mechanism in the PEEK-smooth steel contact is similar to that of the steel-steel contact: the OFM adsorption film mitigates the direct contact between the two surfaces and thus reduces friction. Furthermore, the adsorption of OFMs on the smooth steel surface inhibits the formation of excessive PEEK transfer films which would increase friction by increasing surface roughness. The adsorption of OFMs is greater in sliding than in sliding-rolling, resulting in superior friction reduction. For the PEEK-smooth steel contact, OFMs show positive effects in both sliding and sliding-rolling. By contrast, in the PEEK-rough steel contact, OFMs show either a positive or negative effect on friction and wear depending on the type of contact motion. In sliding, a thick and stable PEEK transfer film is formed on the rough steel surface even under lubrication with PAO + OFM. OFM adsorbs on the PEEK transfer film and the PEEK plate surface, reducing friction and wear. However, this scenario changes in sliding-rolling where OFM adsorption on the rough steel inhibits the formation of the PEEK transfer film, thus preserving the ball roughness. As a result, abrasive wear between the surface asperities of the steel ball and the PEEK plate causes increased friction and wear of PEEK.

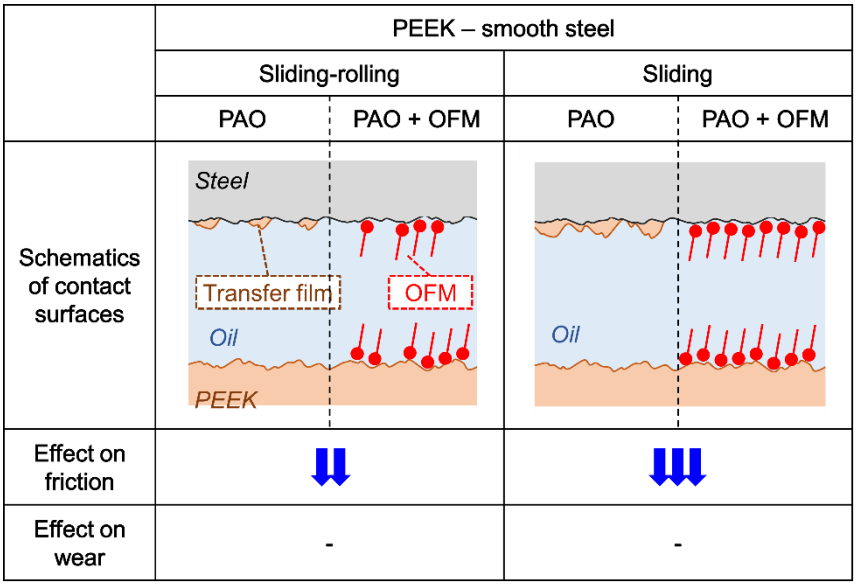

Figure 5.37. Proposed mechanism of lubrication with OFM in PEEK-smooth steel contact

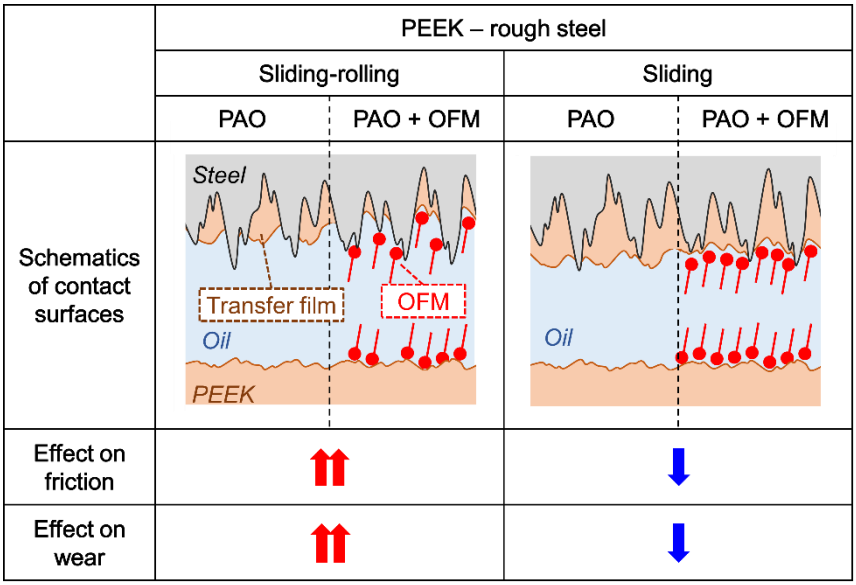

Figure 5.38. Proposed mechanism of lubrication with OFM in PEEK-rough steel contact

5.3.2 Working mechanism of AW additives

Compared to OFMs, the effect of AW additives on the friction and wear properties of the PEEK-steel contact was limited irrespective of the SRRs or roughness of the steel specimens as reported in section 5.2.1. Having said that, PAO4 + AW additives did give different results compared to PAO4, indicating AW additives, especially ZDDP, influenced the tribological properties of PEEK-steel

contacts to some extent. Therefore, the working mechanism in the PEEK-smooth steel contact and in the PEEK-rough steel contact will be discussed.

(a) In PEEK-smooth steel contact

In PEEK-smooth steel contacts, AW additives reduced friction especially at 200% SRR (sliding condition). In steel-steel contacts, the effect of AW additives on friction behaviour depends on the thickness of the reaction films formed: thin reaction films reduce friction while thick and rough reaction films increase friction. In the PEEK-smooth steel contact, a thin reaction films of AW additives may have been formed on the contact surfaces at 200% SRR. However, another possibility is that the adsorption films formed by AW additives inhibited excessive PEEK transfer films on the steel counterparts similar to the case of OFMs discussed in section 5.3.1. AW additives commonly have polar groups in their molecular structures and can adsorb on the contact surfaces despite their adsorption ability being lower than that of OFMs [39,113]. The fact that PAO4 + OAm and PAO4 + OAc gave similar friction results to PAO4 + ZDDP and PAO4 + TCP in the PEEK-smooth steel contacts at both 50% SRR (sliding-rolling condition) and 200% SRR (sliding condition) suggests that the AW additives work similarly to OFMs in the PEEK-smooth steel contact. Given that the operating condition in the PEEK-smooth steel contact was mild as wear of PEEK plates was not observed even when lubricated with PAO4 only, the AW additives plausibly worked by forming adsorption films, not reaction films. The discussion above is summarized in Figure 5.39.

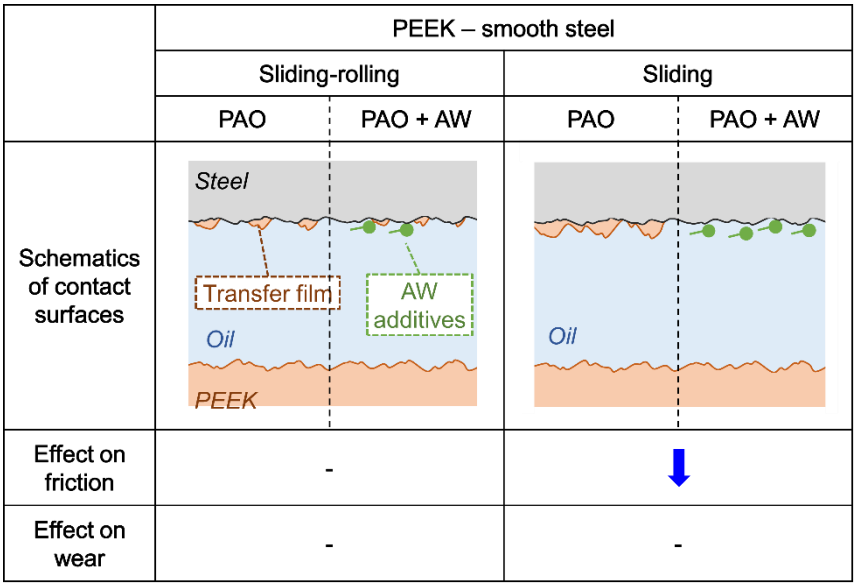

Figure 5.39. Proposed mechanism of lubrication with AW additive in PEEK-smooth steel contact

(b) In PEEK-rough steel contact

In the PEEK-rough steel contact, ZDDP and TCP had a similar effect on friction as OAm and OAc, indicating that AW additives worked by forming an adsorption film as in PEEK-smooth steel contacts. OAm and OAc had less impact on wear performance at both 50% SRR (sliding-rolling condition) and 200% SRR (sliding condition) as shown in Figure 5.7 and Figure 5.8, because their adsorption ability on steel and PEEK surfaces is not as high as OSa. On the other hand, ZDDP slightly reduced the wear of the PEEK plate at 200% SRR (sliding condition) compared to PAO4, although the amount of polymer transfer film on the steel surface (which strongly influence the tribological performance of the PEEK-steel contact) was almost the same for PAO4 and PAO4 + ZDDP. Based on the results of the EPMA phosphorus and sulphur maps in section 5.2.2.2, the ZDDP reaction film formed on the PEEK surface evidently contributed to the improvement of wear of PEEK. In this study, the investigation of the ZDDP reaction film was limited to EPMA phosphorus and sulphur maps. Other research reported that ZDDP forms glassy viscous reaction films [39,113] and in the PEEK-rough steel contact, this type of film can mitigate the severity of the contact condition between the two surfaces and reduce friction and wear of PEEK. As seen in section 5.2.3, the formation of the ZDDP reaction film is accelerated more at 200% SRR (sliding condition) than at 50% SRR (sliding-rolling condition). As the sliding speeds at each entrainment speed are higher at 200% SRR than at 50% SRR, this causes higher frictional heat which accelerates the reaction of ZDDP. This explains why a ZDDP reaction film was detected only on the specimens tested at 200% SRR (sliding condition) in the PEEK-rough steel contact in section 5.2.2.2. However, the reason why the ZDDP reaction film was only detected on the PEEK surface is unclear as section 5.2.3 indicated that the reaction film formation ability of AW additives is supposed to be much higher on a steel surface than on a PEEK surface. A plausible explanation is as follows: the ZDDP reaction film was formed on the steel surface, then part of the film transferred to the PEEK surface. These processes were followed by the formation of the PEEK transfer film on the steel surface, resulting in less of the ZDDP reaction film being detected on the steel surface. The discussion above is summarized in Figure 5.40. Note that there is a possibility that part of the ZDDP reaction film existed on the steel surface but was covered by the PEEK transfer film.

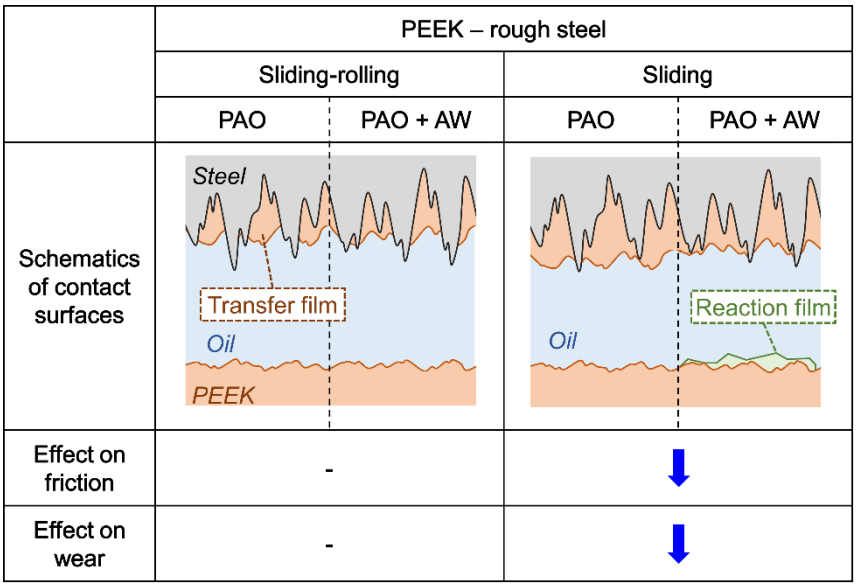

Figure 5.40. Proposed mechanism of lubrication with AW additive in PEEK-rough steel contact

5.4 Summary

Among the various types of lubricant additives, organic friction modifiers (OFMs) and anti-wear (AW) additives are known to strongly affect the tribological properties of the steel-steel contact. Therefore, they are considered to be essential in formulating optimal lubricants and developing ideally suited and efficient PEEK-based systems for tribological applications. This chapter investigated the effect of OFMs and AW additives on the lubrication of PEEK paired with a steel counterpart. The working mechanism was discussed based on the results of the tribological tests and the surface analyses of after-test specimens.

Firstly, tribological tests using a MTM were performed in a PEEK-steel contact at 50% SRR (sliding-rolling condition) and 200% SRR (sliding condition) under lubrication with PAO4 and PAO + OFMs e.g., oleylamine (OAm), oleic acid (OAc) and N-oleoyl sarcosine (OSa). Surface analyses of after-test specimens by nanoindentation, EPMA and Raman spectroscopy were conducted to ascertain any hardness modification of the polymer surfaces and the formation of polymer transfer films on steel counterparts. In addition, tribological testing of PEEK-PEEK and steel-steel contacts was carried out to investigate the adsorption ability of OFMs on the PEEK and steel surfaces in similar operating conditions. The following conclusions have been drawn:

(1) Compared with OAm and OAc, OSa showed a significant friction reduction in the PEEK-smooth steel contact at both 50% SRR (sliding-rolling condition) and 200% SRR (sliding condition). A similar friction reducing effect of OSa was observed in the PEEK-PEEK and steel-steel contacts, indicating the superior adsorption ability of OSa on both the PEEK and steel surfaces;

(2) In the PEEK-rough steel contact, OFMs, most significantly OSa, showed opposite effects depending on SRRs, reducing friction and wear at 200% SRR (sliding condition) while increasing them at 50% SRR (sliding-rolling condition);

(3) The hardness of PEEK surfaces was affected by the addition of OSa, but no correlation was observed between the PEEK hardness and the tribological properties of the PEEK-steel contact. However, a good correlation was observed between the amount of PEEK transfer films on the steel counterparts and the tribological properties of the PEEK-steel contact when lubricated with PAO4 and PAO4 + OSa;

(4) The working mechanism of OFMs is explained by the adsorption of OFMs on the contact surfaces and the formation of the PEEK transfer films on the steel surfaces. As these two phenomena are related to each other, the effect of OFMs depends on the test conditions, and therefore, OFMs can have either a positive or negative effect on the tribological properties.

Secondly, to evaluate the effects of the AW additives, tribological tests were conducted with PAO4 and PAO4 + AW additives, e.g., ZDDP and TCP. In addition to EPMA carbon maps of the after-test steel balls employed to evaluate the amount of PEEK transfer films, EPMA phosphorous and sulphur maps of the after-test steel balls and PEEK plates were obtained to investigate the reaction films formed by ZDDP. Tribological testing of the PEEK-PEEK and steel-steel contacts was also carried out to estimate the reaction film formation ability of AW additives on PEEK and steel surfaces in similar operating conditions. The following conclusions have been drawn:

(1) The addition of ZDDP and TCP slightly reduced friction in the PEEK-smooth steel contact at 200% SRR (sliding condition), but less influence was seen at 50% SRR (sliding-rolling condition). Both ZDDP and TCP did not affect the friction in the PEEK-PEEK contact regardless of SRRs, while their influence on friction in the steel-steel contacts depended on SRRs, indicating that the reaction film formation ability of AW additives is higher on the steel surface than on the PEEK surface;

(2) Compared to OFMs, AW additives had less impact on the friction and wear performance in the PEEK-rough steel contact except for ZDDP at 200% SRR (sliding condition) where a slight improvement in the wear of the PEEK plate was seen;

(3) PAO4 and PAO4 + ZDDP produced the similar amount of polymer transfer films on the steel countersurface at both 50% SRR (sliding-rolling condition) and 200% SRR (sliding condition) in the PEEK-rough steel contact. At 200% SRR, PAO4 + ZDDP slightly improved the wear of the PEEK plate, probably due to the formation of a ZDDP reaction film;

(4) The working mechanism of AW additives is explained by the formation of adsorption films and/or reaction films. The ability of AW additives to form adsorption/reaction films is not as high as OFMs in the PEEK-steel contact. Therefore, both films are thin and only formed at 200% SRR (sliding condition) which can provide higher frictional heat to accelerate the adsorption/reaction of AW additives.

Chapter 6 Base oil lubrication of PEEK composites

The base oil lubrication of two typical PEEK composites, carbon fibre reinforced (CFR) PEEK and glass fibre reinforced (GFR) PEEK, paired with steel counterparts is presented in this chapter. Similar to the study of pure PEEK reported in Chapter 4, the friction and wear performance under base oil lubrication was investigated and compared with that under dry conditions, followed by an investigation of the effect of lubricant oil viscosity. The surface analyses of after-test PEEK specimens were modified so as to focus on the role of the reinforcement fibres.

6.1 Results: Comparison of dry and base oil lubrication

As reviewed in Chapter 2, fibre reinforced PEEK composites such as CFR PEEK and GFR PEEK are widely used for tribological applications due to their superior mechanical performance to pure PEEK. However, the tribological performance under lubrication is still unclear. Therefore, this chapter aims to investigate base oil lubrication of CFR PEEK and GFR PEEK paired with steel counterparts in comparison with dry conditions.

The detailed methodology described in Chapter 3 was followed. Although there are many types of PEEK composites with specific fillers, this study focused on CFR PEEK and GFR PEEK blended with 30 wt.% of carbon fibres and glass fibres, respectively. This is because they are the most typical formulations of PEEK composites in terms of type and composition of fillers. In this chapter, PAO4 and rough steel balls with a Ra of approximately 0.5 µm were used as a test oil and steel specimens. The tribological testing was carried out using a MTM with the constant speed routine as described in section 3.2.3. The test conditions were the standard conditions given in Table 3.5.

6.1.1 Friction and wear performance

The friction performance of the tribological tests under dry and PAO4 lubricated conditions are illustrated in Figure 6.1. Friction coefficient values are plotted as a function of time. CFR PEEK and GFR PEEK showed almost the same friction coefficients in dry conditions. As these values are close to those of pure PEEK tested in the same operating condition (Figure 4.1 in Chapter 4), the addition of reinforcement fibres of CF and GF thus did not affect the friction coefficients in dry conditions. In dry conditions, the friction coefficients of CFR PEEK-steel and GFR PEEK-steel contacts reported

in literature were between 0.2 to 0.4 depending on the test conditions [3,20,93,142,158]. The friction coefficient values measured in this study are in the middle of this range. PAO4 lubrication reduced friction compared to the dry condition for both CFR PEEK and GFR PEEK. In PAO4 lubricated conditions CFR PEEK gave higher friction coefficients than GFR PEEK. Both start with almost the same friction coefficients of approximately 0.07. Then, the friction coefficients of CFR PEEK gradually increased to a plateau value of 0.10 after approximately 20 minutes. In contrast, those of GFR PEEK gradually decreased to approximately 0.04. As reported in Chapter 4, pure PEEK in PAO4 lubricated condition gave friction coefficients of approximately 0.07 placing them between those of CFR PEEK and GFR PEEK. This indicates that the addition of reinforcement fibres affected the friction performance in PAO4 lubricated conditions but the effect depended on the type of fibres.

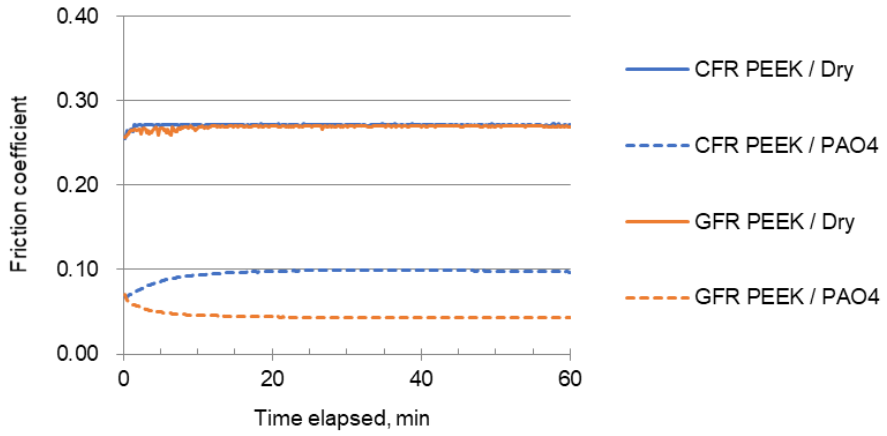

Figure 6.1. Friction coefficients in dry and PAO4 lubricated conditions

The optical images of the wear tracks and the corresponding wear profiles of after-test polymer plates are summarized in Figure 6.2 and Figure 6.3. The wear tracks in dry conditions looked distinctively different from those in PAO4 lubrication. The dry conditions gave wear tracks with a patchy appearance for both CFR PEEK and GFR PEEK (Figure 6.2(a, c)), while PAO4 lubrication generated wear tracks with a uniform appearance (Figure 6.2(b, d)). The same trend was also observed in the wear profiles. The wear profiles in dry conditions were more jagged than those in PAO4 lubricated conditions for both CFR PEEK and GFR PEEK. In terms of the wear volumes, CFR PEEK and GFR PEEK exhibited almost the same wear volumes in dry conditions. Conversely, in the PAO4 lubricated condition the wear volume of GFR PEEK was much lower than that of CFR PEEK. These results indicate that the reinforcement fibres greatly influence both the friction and wear performance of PEEK composites under PAO4 lubricated conditions.

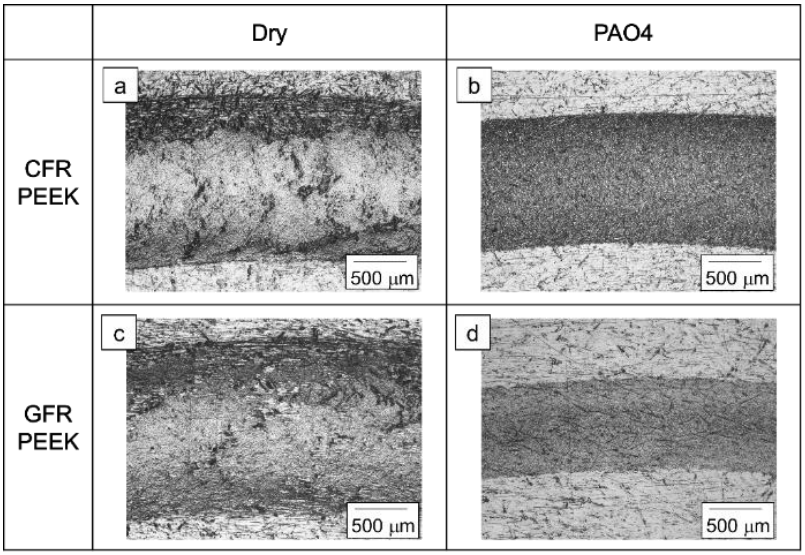

Figure 6.2. Optical images of after-test polymer plates in (a, c) dry and (b, d) PAO4 lubricated conditions

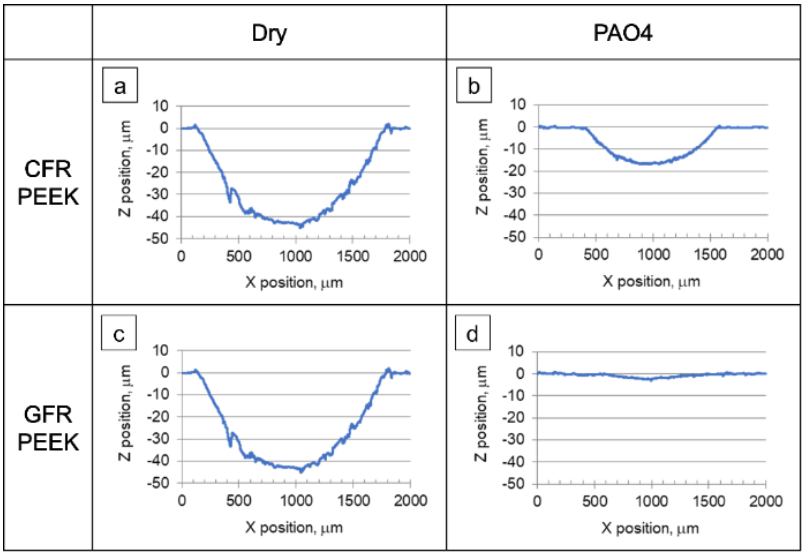

Figure 6.3. Wear profiles of polymer plates in (a, c) dry and (b, d) PAO4 lubricated conditions

6.1.2 Surface analyses

As mentioned in section 6.1.1, the wear tracks of CFR PEEK and GFR PEEK plates were distinctively different under dry conditions and PAO4 lubricated conditions. Therefore, the 3D surface profiles of polymer plates were investigated by Alicona optical profilometry. Hardness mapping of the polymer plates was also carried out by nanoindentation to estimate the influence of the

reinforcement fibres on the contact surfaces. As Chapter 4 demonstrated that the polymer transfer films on the steel counterparts had significant impact on the tribological behaviour of pure PEEK, the polymer transfer films derived from the PEEK composites were also analysed by EPMA in this chapter.

6.1.2.1 3D Profilometry

The wear tracks of polymer plates were investigated with Alicona optical profilometry which provides optical images and 3D surface profiles as described in section 3.3.1. Figure 6.4 and Figure 6.5 show the optical images and the corresponding 3D surface profiles of the wear tracks on the polymer plates. The CFR and GFR PEEK tested in dry conditions produced similar wear tracks which showed piled up wear debris containing fractured fibres (Figure 6.4 (a, c) and Figure 6.5 (a, c)). This explains the patchy appearance of the wear tracks and the jagged wear profiles observed for CFR PEEK and GFR PEEK in dry conditions presented in section 6.1.1. In addition, these results support the hypothesis that three-body abrasion by wear debris containing hard reinforcement fibres caused the large wear of CFR and GFR PEEK plates in dry conditions. However, as the oil-lubrication flushed wear debris out from the contact surfaces, the wear tracks then had a relatively smooth appearance as shown in Figure 6.5 (b, d). CFR PEEK and GFR PEEK contain the same weight percentage of carbon fibres and glass fibres, respectively, but the volume percentage is about 1.4 times higher for carbon fibres in CFR PEEK than that of glass fibres in GFR PEEK due to the difference in the specific weights of carbon fibres (approximately 1.8) and glass fibres (approximately 2.5). Interestingly, the amount of fibres observed on the wear tracks of CFR PEEK in PAO4 lubricated condition was much larger than that of GFR PEEK, even after taking into account the difference in fibre volume percentages. In addition, in PAO4 lubricated conditions, the carbon fibres observed on the wear tracks of CFR PEEK were finely fractured resulting in sizes less than 20 μm (Figure 6.4 (b)), while the glass fibres observed on the wear tracks of GFR PEEK were less damaged (Figure 6.4 (d)). Furthermore, the 3D surface profiles suggest that there is a difference in their distributions. Most of the fractured carbon fibres were placed on top of the PEEK matrix (Figure 6.45 (b)). In contrast, the glass fibres were well embedded in the PEEK matrix (Figure 6.45 (b)).

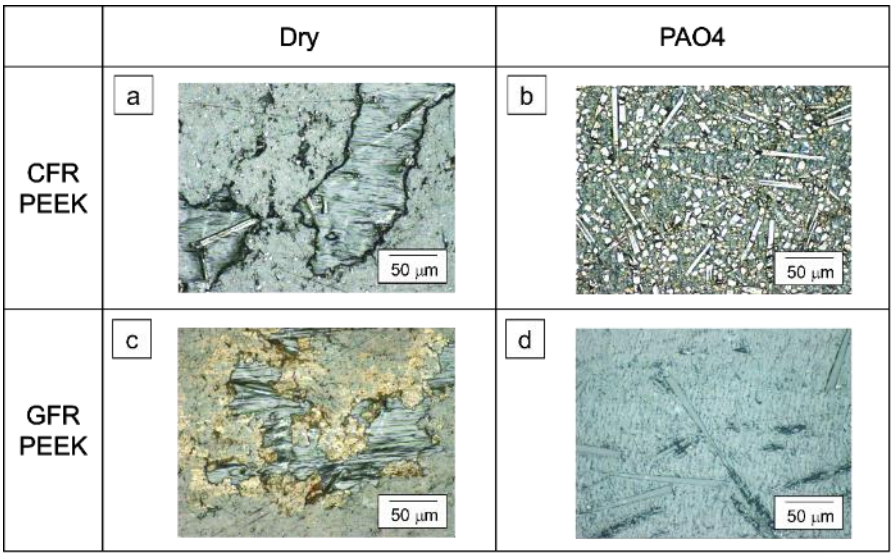

Figure 6.4. Optical images of wear tracks on polymer plates in (a, c) dry and (b, d) PAO4 lubricated conditions

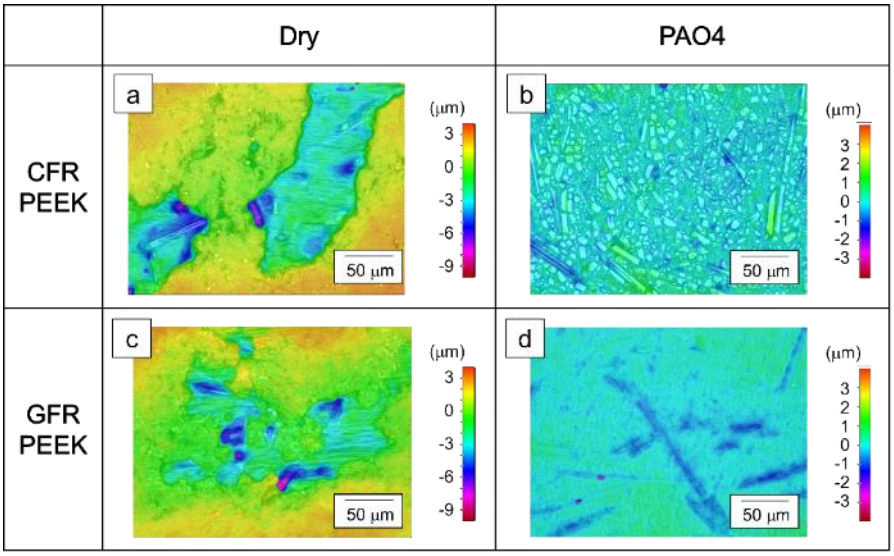

Figure 6.5. 3D surface profiles of wear tracks on polymer plates in (a, c) dry and (b, d) PAO4 lubricated conditions

6.1.2.2 Nanoindentation

As shown in section 6.1.2.1, the carbon fibres and glass fibres on the wear tracks tested in PAO4 lubrication showed distinctively different distributions. These results suggest a possible difference in hardness distribution on the wear tracks on CFR PEEK and GFR PEEK. To confirm this, hardness mapping was carried out by using nanoindentation as described in section 3.3.2. Figure 6.6 and Figure 6.7 show optical images of the polymer plates and their corresponding hardness maps,

where the colour scale indicates the hardness values. Small nanoindentation indents are observed over the entire surface of the optical images, because these images were acquired after indentation. For comparison with the wear tracks lubricated with PAO4, a nanoindentation study of new plates of CFR PEEK and GFR PEEK was also carried out (Figure 6.6 (a, c) and Figure 6.7 (a, c)). The hardness map of the new plates showed a uniform hardness with values mostly below 0.5 GPa. This indicates that the CFR and GFR fibres were not exposed from the PEEK matrix, except for small areas of the CFR PEEK surface (Figure 6.7 (a)). Numerous areas of high hardness (values over 1.0 GPa) were detected on the wear tracks of CFR and GFR PEEK lubricated with PAO4 (Figure 6.7 (b, d)). These areas matched well the distributions of the fibres observed in the corresponding optical images (Figure 6.6 (b, d)). As discussed in section 6.1.2.1, fractured fibres were observed to be densely distributed on the wear tracks of PAO4 lubricated CFR PEEK. The hardness map in Figure 6.7 (b) confirmed that these more or less damaged fibres contributed to the hardness values of the wear tracks.

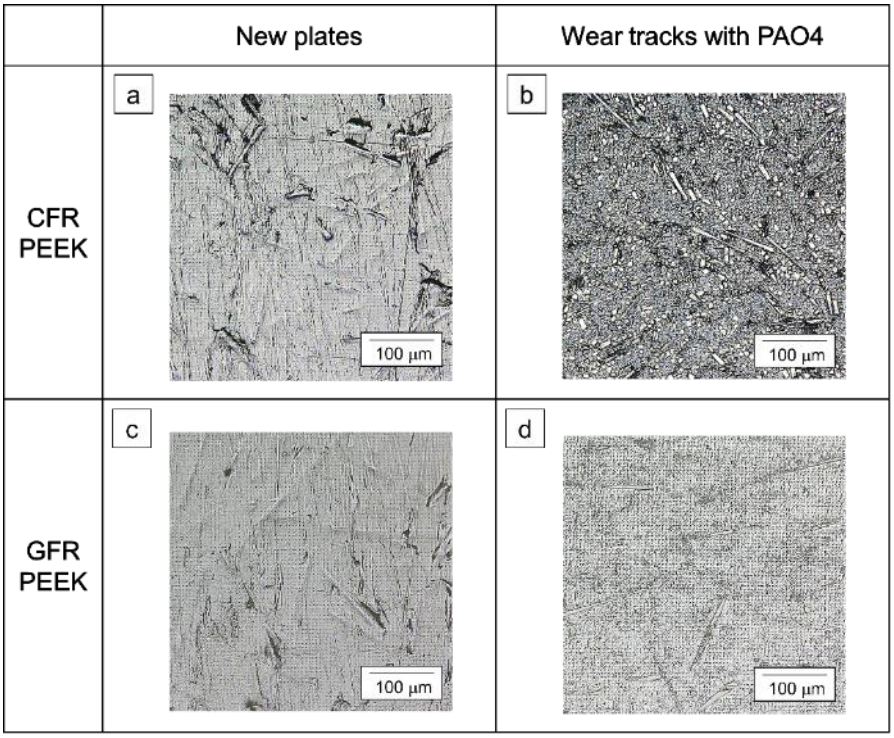

Figure 6.6. Optical images of new polymer plates and wear tracks on polymer plates in (a, c) dry and (b, d) PAO4 lubricated conditions

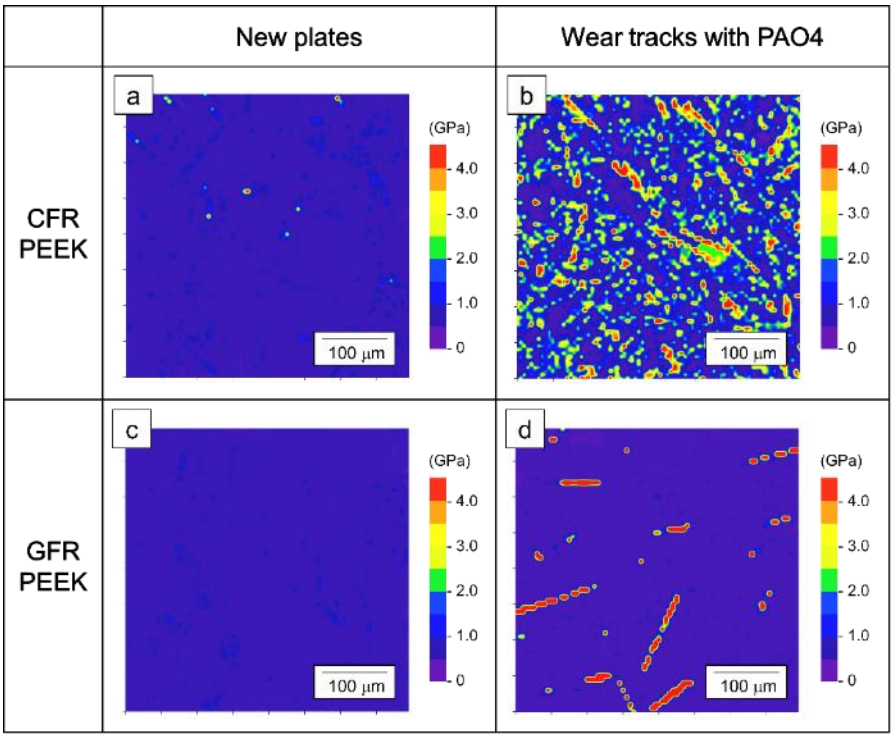

Figure 6.7. Nanoindentation hardness maps of (a, c) new polymer plates and (b, d) wear tracks on polymer plates in PAO4 lubricated condition

6.1.2.3 EPMA

In the base-oil lubrication of pure PEEK investigated in Chapter 4, the formation of polymer transfer films on steel counterparts was one of the most important parameters that controlled the wear of the polymer. Figure 6.8 shows the optical images of the wear tracks on the steel balls paired with CFR and GFR PEEK; the tracks looked polished with barely any polymer transfer film present. A large volume of wear debris was observed piled up at the sides of the steel ball wear tracks in the CFR and GFR PEEK tests in dry conditions (Figure 6.8 (a, c)), supporting the hypothesis that three-body abrasion by wear debris containing the hard fibres caused the large wear of polymer plates (Figure 6.3 (a, c)). The amount of polymer transfer films on the wear track in PAO4 lubrication was difficult to estimate from the optical images so EPMA carbon mapping was employed as was the case for pure PEEK investigated in section 4.1.2.2.

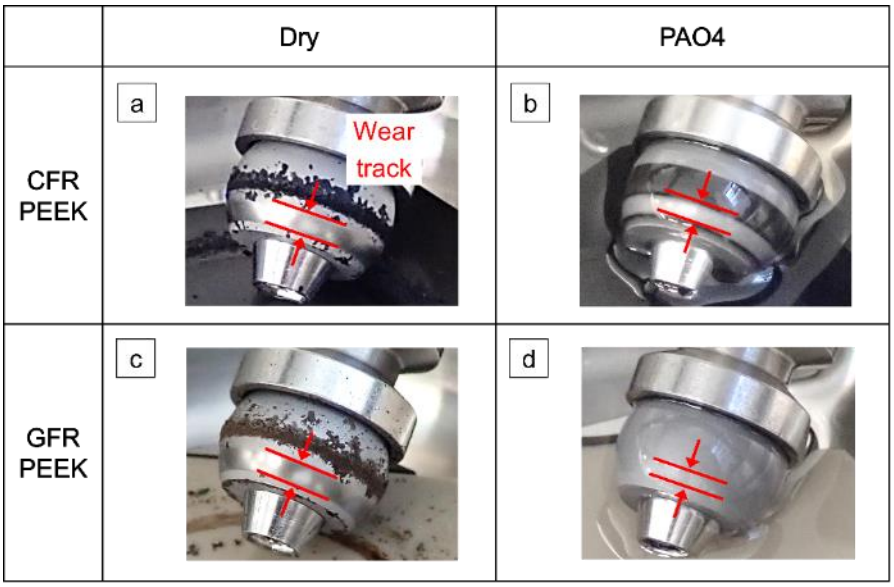

Figure 6.8. Optical images of after-test steel balls paired with CFR and GFR PEEK in (a, c) dry and (b, d) PAO4 lubricated conditions

By following the procedure described in section 3.3.3, SE images and EPMA carbon maps on after-test steel balls were obtained as shown in Figure 6.9 and Figure 6.10. The amount of carbon in the transfer film is indicated by the colour scale on the EPMA map. In dry conditions, the SE images and EPMA carbon maps show that there was no transfer film on the steel balls paired with both CFR PEEK and GFR PEEK. In PAO4 lubricated conditions, a polymer transfer film was observed on the wear track produced with GFR PEEK, while no film was detected on the one produced with CFR PEEK. As previously investigated in sections 4.1.2.2 and 4.1.2.3, the carbon detected with EPMA arises from PEEK, which in Figure 6.10 (d) originates from the PEEK matrix in GFR PEEK plates. Although the EPMA measured carbon can be derived from the carbon fibres in CFR PEEK, in Figure 6.10 (b) no carbon was detected on the wear tracks which simplifies the interpretation. The SE images and EPMA carbon maps show a good correlation between the polymer transfer films on the wear track of steel balls and the wear volumes of polymer plates (Figure 6.3) e.g. for the GFR PEEK PAO4 lubricated test the polymer transfer film on the wear track of steel ball (Figure 6.10 (d)) was conducive to the lower wear volume of the polymer plate (Figure 6.3 (d)). This emphasizes the importance of the polymer transfer film in reducing polymer wear not only for pure PEEK but also for PEEK composites.

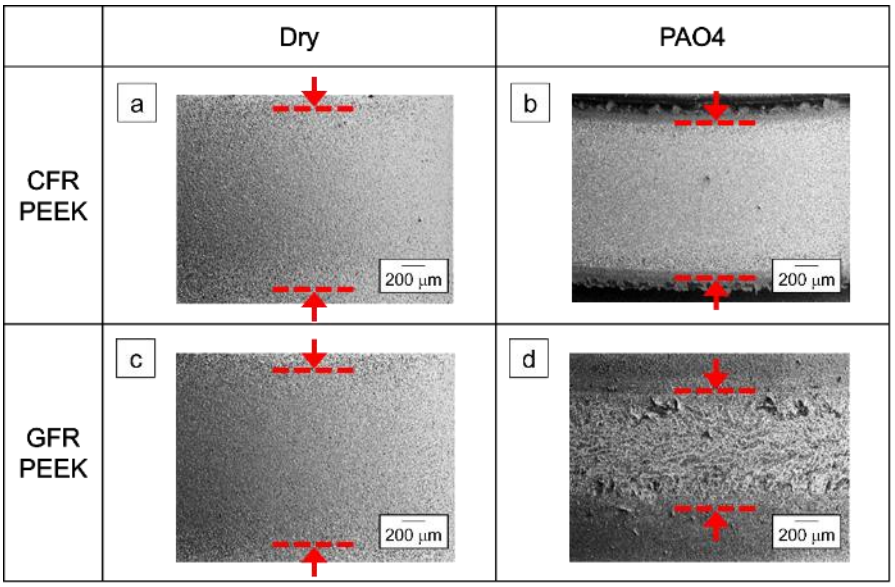

Figure 6.9. SE images of after-test steel balls paired with CFR and GFR PEEK in (a, c) dry and (b, d) PAO4 lubricated conditions

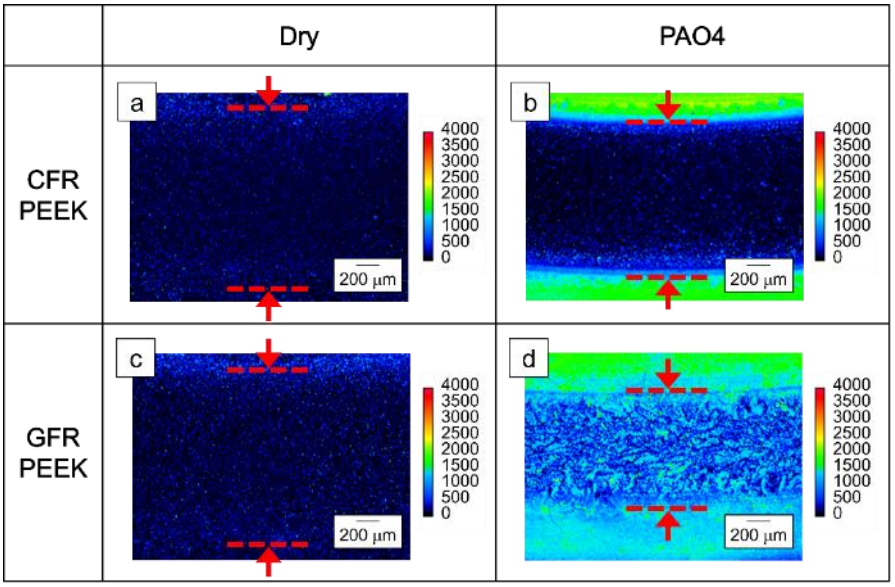

Figure 6.10. EMPA carbon maps of after-test steel balls paired with CFR and GFR PEEK in (a, c) dry and (b, d) PAO4 lubricated conditions

The distribution of reinforcement fibres on the wear tracks of polymer plates was considered to play an important role in terms of the difference in the formation of transfer films between CFR PEEK and GFR PEEK in PAO4 lubricated conditions. This will be discussed further in section 6.3.3.

6.1.3 Testing with base oil containing wear debris

The results from section 6.1.2 suggest that the reinforcement fibres exposed on the wear tracks on the polymer plates play an important role in determining the tribological properties in PAO4 lubricated conditions. However, the mechanism of action remains unclear e.g. what is the influence of wear debris under oil-lubrication? As mentioned in section 6.1.2.1, wear debris from CFR and GFR PEEK containing hard reinforcement fibres caused the large amount of wear found on the polymer plates in dry conditions. Although the wear debris was flushed out from the contact surfaces by the oil, this debris remained dispersed in the oils possibly influencing the tribological performance directly and/or indirectly. Therefore, an additional test was devised to investigate the influence of wear debris. This test was performed on GFR PEEK lubricated with the PAO4 oil containing the CFR PEEK wear debris. The test oil was prepared by collecting the PAO4 oil previously used in a CFR PEEK test which contained dispersed CFR PEEK wear debris with sizes up to 20 μm (Figure 6.11). The appearance of the oil containing CFR PEEK wear debris was slightly darker in colour and opaques as shown in Figure 6.12.

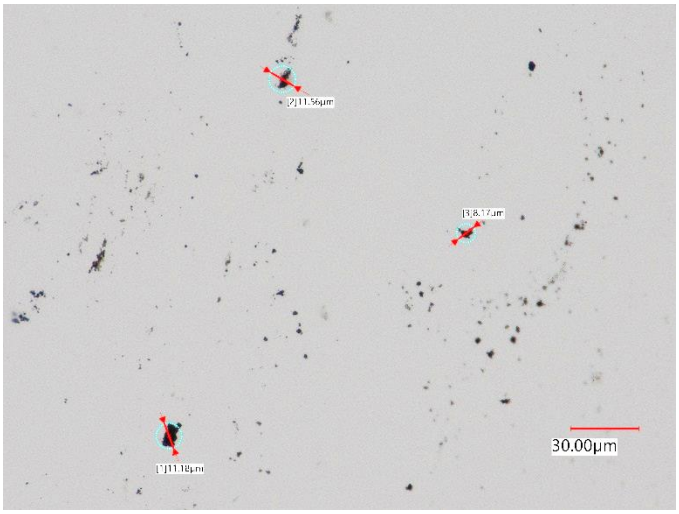

Figure 6.11. Optical image of dispersed CFR PEEK wear debris contained in PAO4 oil

Figure 6.12. PAO4 oil containing CFR PEEK wear debris

Figure 6.13 shows the friction coefficient values as a function of time for this test in comparison with CFR and GFR PEEK lubricated with pristine PAO4. If CFR PEEK wear debris has an important role on the friction performance, the GFR PEEK lubricated with PAO4 containing CFR PEEK wear debris (the red line) was expected to show similar values to the CFR PEEK lubricated with pristine PAO4 (the blue dotted line). However, the wear-debris-containing PAO4 gave slightly higher friction than pristine PAO4 lubricated GFR PEEK (the orange dotted line), but much lower friction than pristine PAO4 lubricated CFR PEEK.

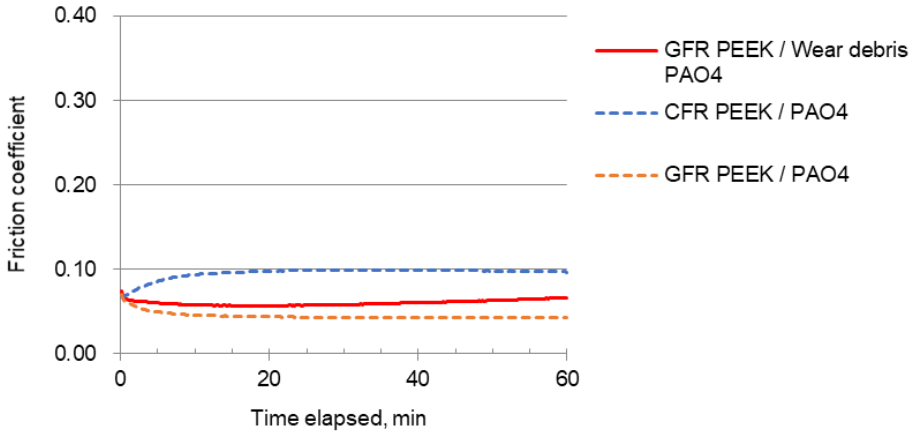

Figure 6.13. Friction coefficients in wear debris PAO4 lubricated condition

Optical images and wear profiles of GFR PEEK plate lubricated with wear-debris-containing PAO4 are shown in Figure 6.14. A similar trend as the friction coefficients was observed for the wear of the polymer plates (Figure 6.14(b)): the wear-debris PAO4 slightly increased the wear of the GFR PEEK plate compared to pristine PAO4 (Figure 6.3(d)), but the wear was still distinctively lower than that of CFR PEEK lubricated with pristine PAO4 (Figure 6.3(b)). Similar results have been reported by Kunishima et al. [159] who studied the effect of glass fibre wear debris contained in grease lubricant on the tribological properties of GFR polyamide 66 paired with steel counterparts. They concluded that the wear debris contained in the grease did not affect the friction and wear of the polymer composite.

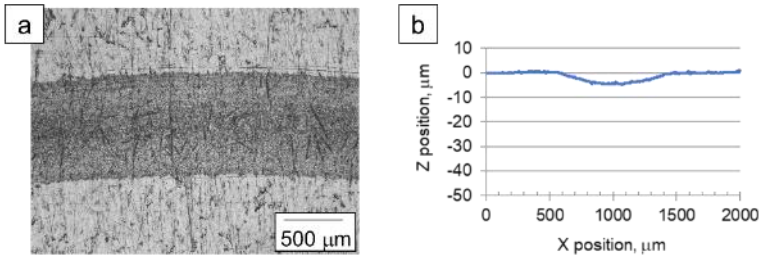

Figure 6.14. (a) Optical image and (b) wear profile of polymer plate in wear debris PAO4 lubricated condition

GFR PEEK lubricated with wear-debris-containing PAO4 gave an almost similar optical image and 3D surface profile (Figure 6.15) to pristine PAO4 (Figure 6.4 (d), Figure 6.5 (d)); fractured carbon fibres were hardly ever observed on the wear track. This implies that the fractured carbon fibres formed on the CFR PEEK wear tracks (Figure 6.4 (b)) once flushed out from the polymer contact surfaces by the oils as wear debris, would not re-enter the tribological contact and adhere to the contact surfaces again. Taking into account the wear debris sizes up to 20 µm, as shown in Figure 6.11, was larger than the oil film thickness (calculated as approximately 0.1 µm at the condition tested), the wear debris once dispersed in oils is expected to flow mainly outside the contact area.

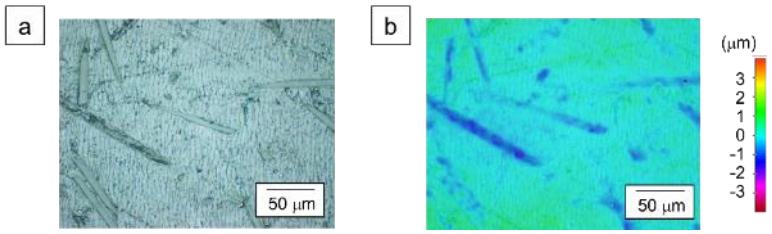

Figure 6.15. (a) Optical image and (b) 3D surface profile of wear tracks on polymer plate in wear debris PAO4 lubricated condition

Figure 6.16 shows the polymer transfer film on the steel ball wear track analyzed with EPMA as described in section 6.1.2.3. The wear-debris-containing PAO4 led to less transfer film than pristine PAO4 in GFR PEEK tests (Figure 6.9 (d), Figure 6.10 (d)). This indicates CFR PEEK wear debris inhibited the formation of the polymer transfer film. However, PAO4 lubricated CFR PEEK generated an even thinner transfer film (Figure 6.9 (b), Figure 6.10 (b)). These results show that the wear debris containing hard reinforcement fibres is detrimental to friction and wear but not as much as

the exposed fibres on the wear tracks of polymer plates as discussed in sections 6.1.2.1 and 6.1.2.2. The working mechanism will be discussed in section 6.3.3.

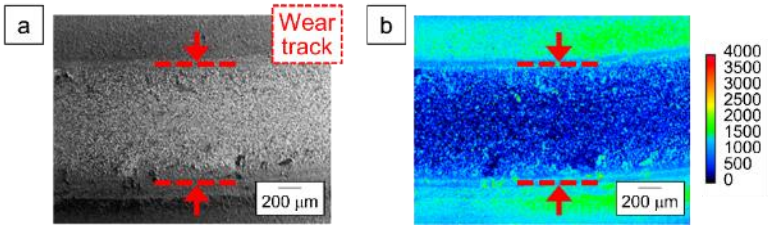

Figure 6.16. (a) SE image and (b) EPMA carbon map of after-test steel balls in wear debris PAO4 lubricated condition

6.2 Results: Effect of lubricant oil viscosity

The lubricant oil viscosity is one of the most important parameters in designing a suitable lubricant for each application. In pure PEEK-steel contacts, the effect of base oil viscosity shows different trends depending on the roughness of the steel counterparts as described in section 4.2. In PEEK-smooth steel contacts, PAOs with higher viscosity gave lower friction and less damage to the PEEK surfaces, while in PEEK-rough steel contacts they resulted in higher friction and larger wear of PEEK. This section aims to investigate the effect of base oil viscosity in PEEK composites-steel contacts.

As in section 6.1, CFR PEEK and GFR PEEK blended with 30 wt.% of carbon fibres and glass fibres were used as PEEK composites because they are the most typical formulations. The detailed methodology was described in Chapter 3. In this section, PAOs with different viscosity grades, PAO2, PAO4 and PAO10 were used as test oils (Table 3.2). Additionally, steel balls with smooth surfaces (Ra of 0.01-0.02 µm) and rough surfaces (Ra of approximately 0.5 µm) were used as described in section 3.1.2. The combination of PAOs with different viscosity grades and the steel balls with different surface roughness enables the tribological tests in this section to cover a wide range of lubrication regime (from hydrodynamic lubrication to mixed and boundary lubrication). The tribological testing was carried out using a MTM with the constant speed routine described in section 3.2.3. The test conditions were based on the standard conditions given in Table 3.5.

6.2.1 Friction and wear performance

(a) PEEK composites-smooth steel contact

Figure 6.17 illustrates the friction coefficients of the CFR PEEK-smooth steel contact lubricated with PAO2, PAO4 and PAO10. All PAOs gave very low and constant values of friction coefficients of approximately 0.02 during the entire period of testing. From the optical images of the after-test CFR PEEK plates (Figure 6.18), wear tracks were hardly observed regardless of the oil viscosity. Similar to CFR PEEK-smooth steel contact the fiction coefficients of GFR PEEK-smooth steel contacts exhibited the same trend and values (of approximately 0.02 for all PAOs) as shown in Figure 6.19. The optical images of the after-test GFR PEEK plates (Figure 6.20) also showed less damaged wear tracks regardless of the oil viscosity. In terms of the comparison with pure PEEK, PAO4 and PAO10 gave almost the same friction coefficients (of approximately 0.02) for pure PEEK (Figure 4.15), CFR PEEK (Figure 6.17) and GFR PEEK (Figure 6.19). Interestingly, PAO2 gave higher friction coefficients of around 0.03 than PAO4 and PAO10 for pure PEEK, while there was no significant difference between PAO2, PAO4 and PAO10 for CFR PEEK and GFR PEEK. In addition, the after-test pure PEEK plate lubricated with PAO2 showed more damaged wear tracks than PAO4 and PAO10 lubricated plates (Figure 4.16), while CFR PEEK and GFR PEEK lubricated with PAO2, PAO4 and PAO10 gave less-damaged wear tracks. The numerous marks like scratches which were observed on the entire surface (inside/outside wear tracks) of CFR PEEK plates and GFR PEEK plates are due to the reinforcement fibres contained. Note that no transfer film was detected on the smooth steel balls paired with both CFR PEEK and GFR PEEK.

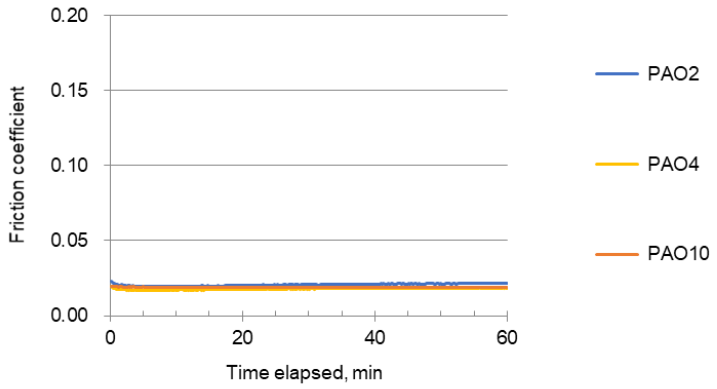

Figure 6.17. Friction coefficients of CFR PEEK paired with smooth steel balls and lubricated with PAOs

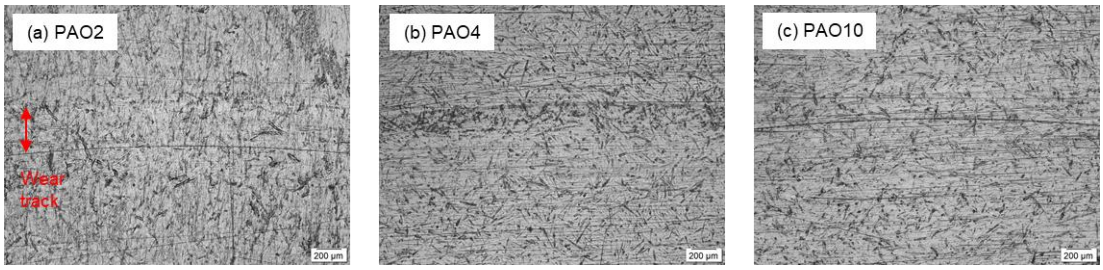

Figure 6.18. Optical images of after-test CFR PEEK plates paired with smooth steel balls and lubricated with (a) PAO2, (b) PAO4 and (c) PAO10

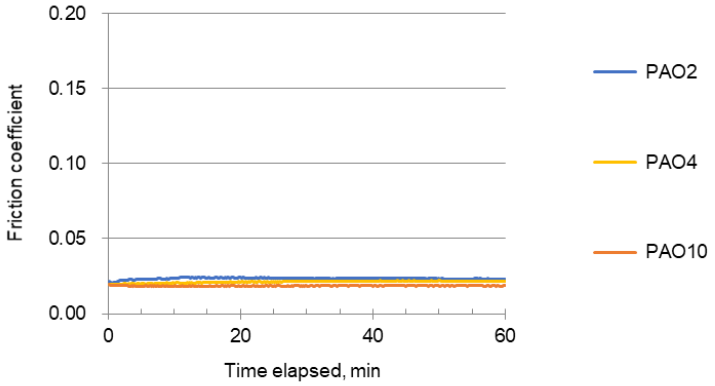

Figure 6.19. Friction coefficients of GFR PEEK paired with smooth steel balls and lubricated with PAOs

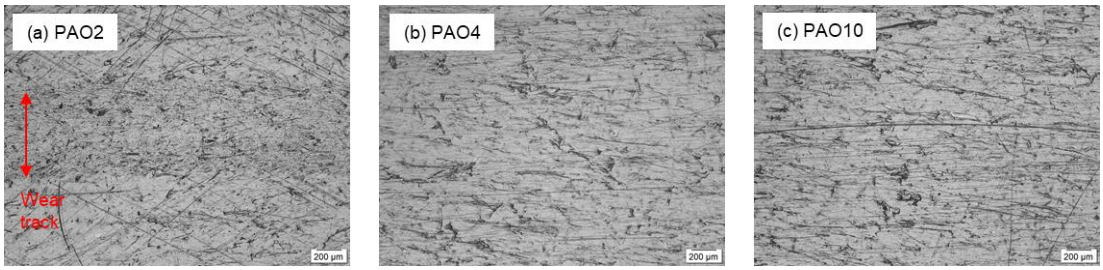

Figure 6.20. Optical images of after-test GFR PEEK plates paired with smooth steel balls and lubricated with (a) PAO2, (b) PAO4 and (c) PAO10

(b) PEEK composites-rough steel contact

Figure 6.21 illustrates the friction coefficients of CFR PEEK-rough steel contact lubricated with PAO2, PAO4 and PAO10. The lower viscosity PAOs gave the higher friction coefficients. The friction coefficients of CFR PEEK lubricated with PAO2 and PAO4 gradually increased as the time elapsed,

while those lubricated with PAO10 were relatively stable around 0.07. The friction coefficients of GFR PEEK- paired with rough steel contacts followed a completely different trend compared with CFR PEEK as shown in Figure 6.22. PAO2, PAO4 and PAO10 resulted in almost the same friction coefficients which were stable around 0.05 throughout the testing. In pure PEEK-rough steel contact PAO2, PAO4 and PAO10 showed friction coefficients between 0.06 to 0.10 (Figure 4.17). GFR PEEK provided lower friction than pure PEEK regardless of the viscosity of PAO oils, while CFR PEEK gave lower friction than pure PEEK only when lubricated with PAO10. Additionally, the effect of the viscosity grade of PAO on friction was found to depend on the polymer material. Lower friction was achieved when lubricating pure PEEK with lower viscosity PAO and CFR PEEK with higher viscosity PAO. The viscosity grades did not make much difference to friction in the GFR PEEK tests, where almost the same friction values were measured for all three PAO oils.

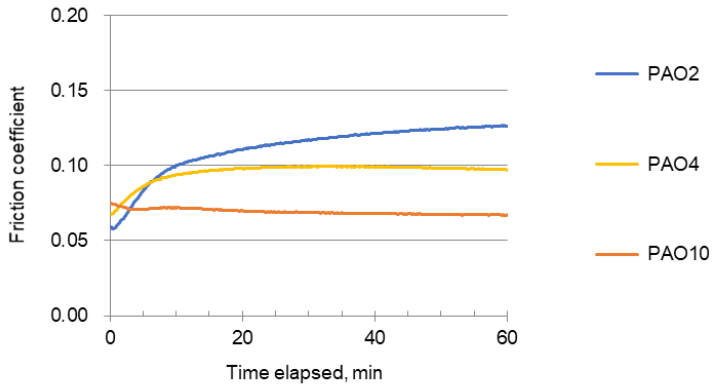

Figure 6.21. Friction coefficients of CFR PEEK paired with rough steel balls and lubricated with PAOs

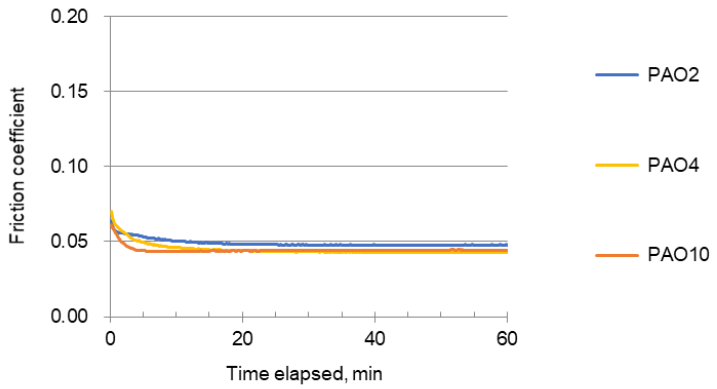

Figure 6.22. Friction coefficients of GFR PEEK paired with rough steel balls and lubricated with PAOs

The optical images of the wear tracks and the corresponding wear profiles of after-test polymer plates are summarized in Figure 6.23 and Figure 6.24 for CFR PEEK and Figure 6.25 and Figure 6.26 for GFR PEEK, respectively. The lower viscosity PAOs resulted in larger wear of CFR PEEK. In contrast, the viscosity grades of PAO had less influence on wear of GFR PEEK, though PAO10 provided a slightly less damaged appearance as shown in Figure 6.25 (c). As a matter of course, there was a good correlation between wear performance and friction performance, i.e. lower friction leads to lower wear of polymers.

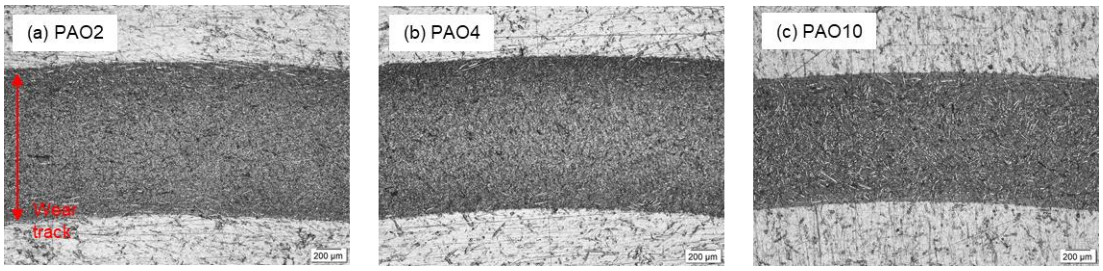

Figure 6.23. Optical images of after-test CFR PEEK plates paired with rough steel balls and lubricated with (a) PAO2, (b) PAO4 and (c) PAO10

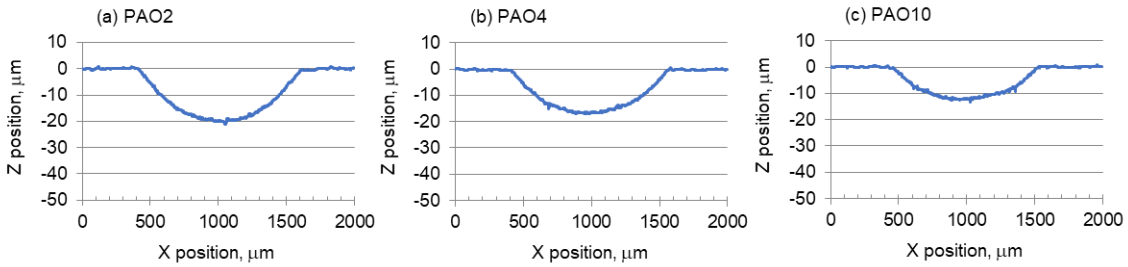

Figure 6.24. Wear profiles of CFR PEEK plates paired with rough steel balls and lubricated with with (a) PAO2, (b) PAO4 and (c) PAO10

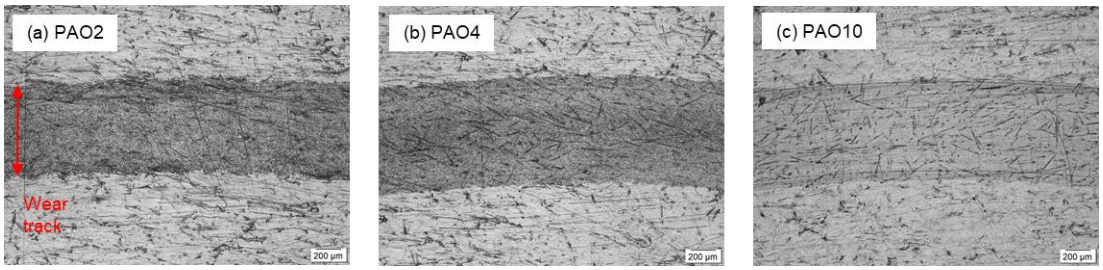

Figure 6.25. Optical images of after-test GFR PEEK plates paired with rough steel balls and lubricated with (a) PAO2, (b) PAO4 and (c) PAO10

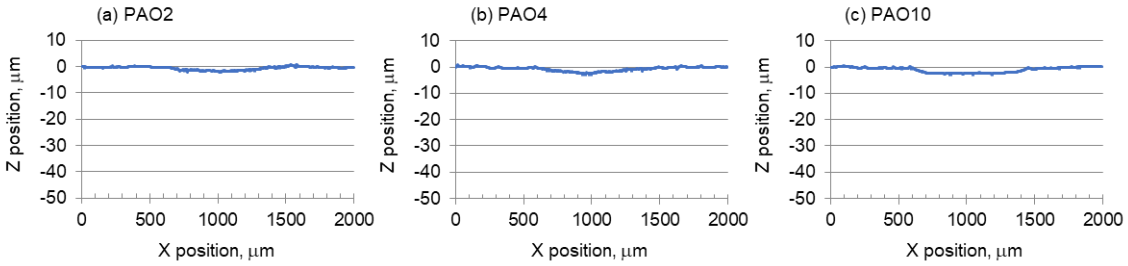

Figure 6.26. Wear profiles of GFR PEEK plates paired with rough steel balls and lubricated with (a) PAO2, (b) PAO4 and (c) PAO10

6.2.2 Surface analyses

As investigated in section 6.1, the reinforcement fibre distributions on the polymer wear tracks and the polymer transfer films on steel counterparts are important factors dominating the tribological behaviour of PEEK composites under oil-lubrication. To investigate further the mechanism of action, these factors were also analysed on after-test specimens lubricated with different grades of PAO. The tribological tests were carried out PEEK composites paired with smooth and rough steel balls, but surface analyses were conducted only with the specimens tested with rough steel balls. This is because the wear tracks on polymer plates and the polymer transfer films on steel balls were difficult to detect in the PEEK composites-smooth steel contacts as described in section 6.2.1.

6.2.2.1 3D Profilometry

The wear tracks of polymer plates were investigated by Alicona optical profilometry which provides optical images and 3D surface profiles as described in section 3.3.1. The optical images and the corresponding 3D surface profiles of the wear tracks are shown in Figure 6.27 and Figure 6.28 for

CFR PEEK and Figure 6.29 and Figure 6.30 for GFR PEEK. CFR PEEK and GFR PEEK gave distinctively different appearances regardless of the viscosity grades of PAO. On the wear tracks of CFR PEEK, finely fractured fibres (with sizes less than 20 μm) compared to the 100-200 μm fibres present in new plates were present in larger amounts under lubrication with lower viscosity PAOs (Figure 6.27). Additionally, from the corresponding 3D surface profiles (Figure 6.28) these fractured carbon fibres were located on the top of the PEEK matrix of the wear tracks regardless of the viscosity grades of PAO. The glass fibres observed on the wear tracks of GFR PEEK were less damaged and were well embedded in the PEEK matrix. PAO2, PAO4 and PAO10 showed the same trend, and there was no clear difference with the viscosity grades. Although the hardness mapping measurements were only carried out for the wear tracks lubricated with PAO4 as described in section 6.1.2.2, the results for the wear tracks lubricated with PAO2 and PAO10 are expected to show the same trend based on the fibre distributions observed in the optical images (Figure 6.27, Figure 6.29).

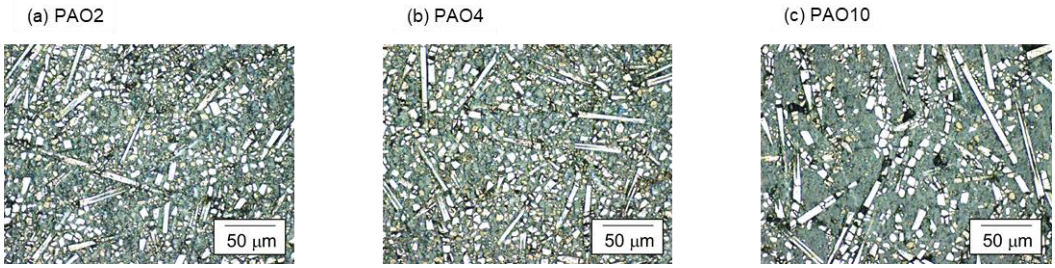

Figure 6.27. Optical images of wear tracks on CFR PEEK plates paired with rough steel balls and lubricated with (a) PAO2, (b) PAO4 and (c) PAO10

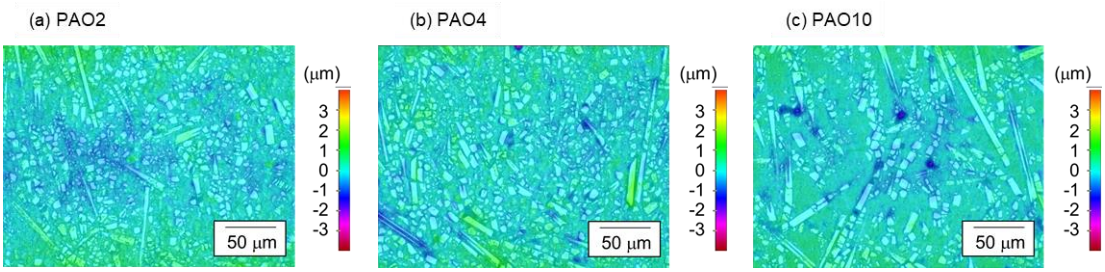

Figure 6.28. 3D surface profiles of wear tracks on CFR PEEK plates paired with rough steel balls and lubricated with (a) PAO2, (b) PAO4 and (c) PAO10

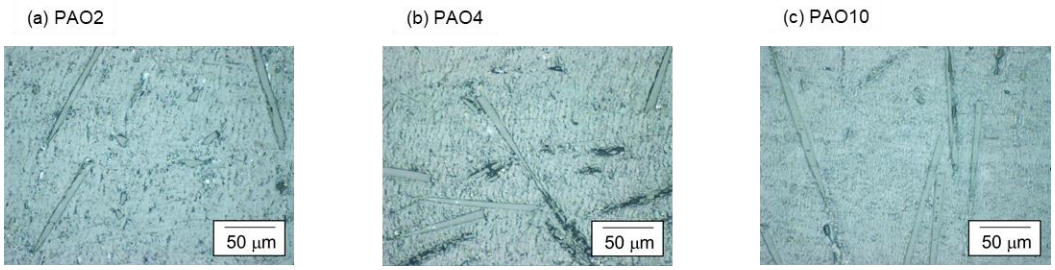

Figure 6.29. Optical images of wear tracks on GFR PEEK plates paired with rough steel balls and lubricated with (a) PAO2, (b) PAO4 and (c) PAO10

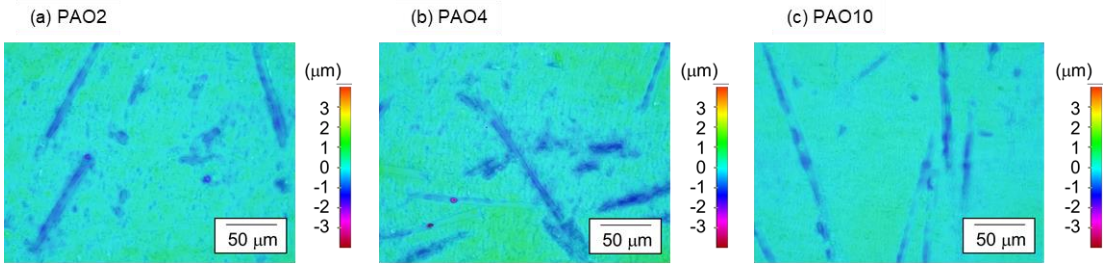

Figure 6.30. 3D surface profiles of wear tracks on GFR PEEK plates paired with rough steel balls and lubricated with (a) PAO2, (b) PAO4 and (c) PAO10

6.2.2.2 EPMA

As shown in section 6.1.2.3, polymer transfer films on steel counterparts are an important factor in reducing polymer wear not only for pure PEEK but also for PEEK composites. Therefore, the effect of oil viscosity on the formation of polymer transfer films was investigated. By following the procedure described in section 3.3.3, SE images and EPMA carbon maps on after-test steel balls were obtained as shown in Figure 6.31 and Figure 6.32 for CFR PEEK and Figure 6.33 and Figure 6.34 for GFR PEEK. The amount of carbon in the transfer film is indicated by the colour scale on the EPMA map. For CFR PEEK, regardless of the viscosity grades of PAO, transfer films were hardly observed on SE images and almost no carbon was detected on the wear tracks in EPMA carbon maps. As already mentioned in section 6.1.2.3, EPMA measured carbon could also be derived from the carbon fibres in CFR PEEK but as no carbon was detected on the wear tracks this simplifies the interpretation. For GFR PEEK, polymer transfer films were observed from SE images for all three PAOs. EPMA carbon maps show PAO2 and PAO4 provided a larger amount of transfer films than PAO10. This trend is similar to pure PEEK (Figure 4.23), as investigated in section 4.2.2.2. In terms of the correlation with wear performance, thinner transfer films for CFR PEEK could lead to higher wear compared to GFR PEEK. For pure PEEK, PAO10 resulted in less transfer films, and thus higher

wear than PAO2 and PAO4 which formed thicker transfer films (Figure 4.19, Figure 4.23). In contrast, the wear of GFR PEEK lubricated with PAO10 was very low, similar to that of samples lubricated with PAO2 and PAO4 (Figure 6.26), although PAO10 provided less transfer films than PAO2 and PAO4 (Figure 6.34). The synergistic contribution of oil film thickness which is advantageous for the more viscous oil PAO10 can explain this, i.e. the thicker oil film generated by the more viscous PAO10 can compensate for the thinner transfer film in terms of wear performance. The working mechanism of the lubrication of PEEK composites will be discussed more in section 6.3.3.

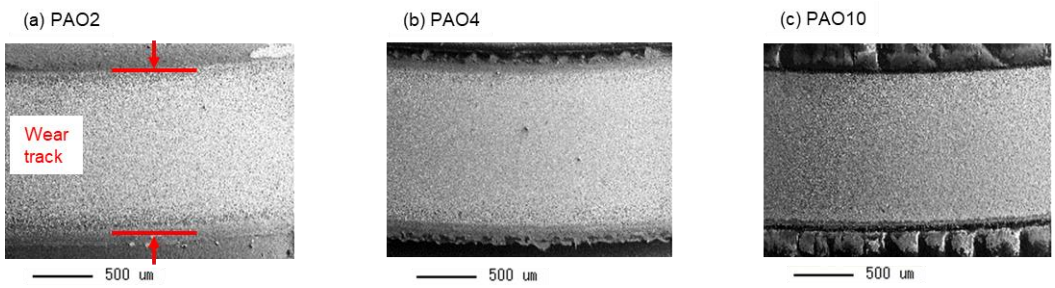

Figure 6.31. SE images of after-test rough steel balls paired with CFR PEEK and lubricated with (a) PAO2, (b) PAO4 and (c) PAO10

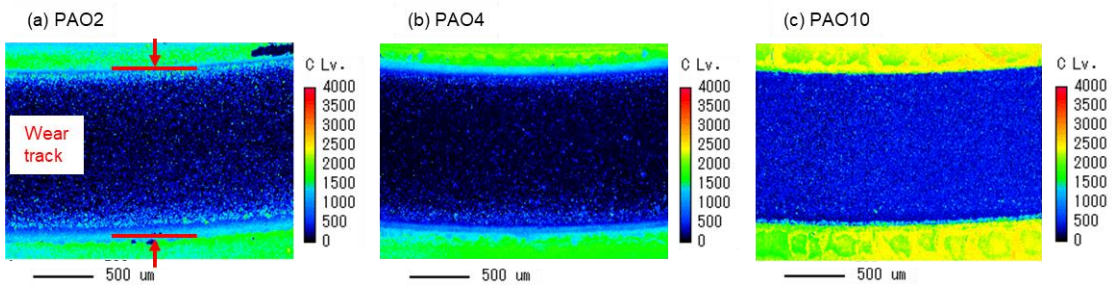

Figure 6.32. EPMA carbon maps of after-test rough steel balls paired with CFR PEEK and lubricated with (a) PAO2, (b) PAO, and (c) PAO10

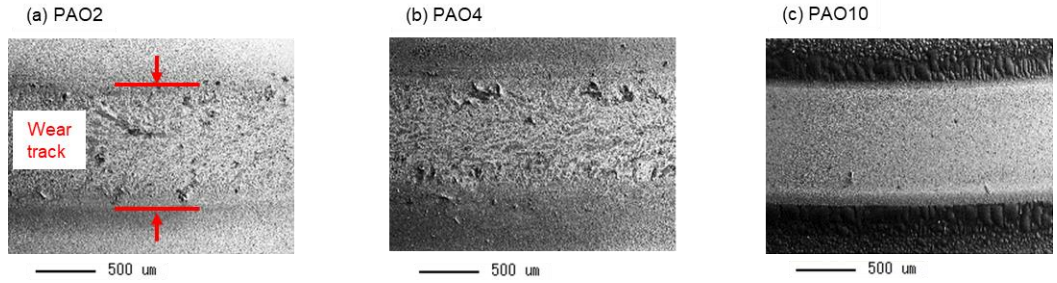

Figure 6.33. SE images of after-test rough steel balls paired with GFR PEEK and lubricated with (a) PAO2, (b) PAO4 and (c) PAO10

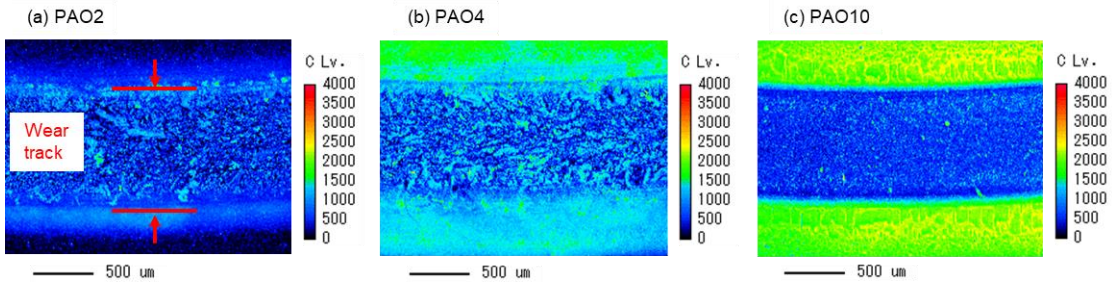

Figure 6.34. EPMA carbon maps of after-test rough steel balls paired with GFR PEEK and lubricated with (a) PAO2, (b) PAO4 and (c) PAO10

6.3 Discussion

In Chapter 4, the working mechanism of base oil lubrication of pure PEEK was discussed based on two factors: hardness modification of polymer surfaces and polymer transfer films on the steel balls. The experimental results obtained in sections 6.1 and 6.2 show the effect of base oil lubrication on the tribological performance of PEEK composites-steel contacts was different from that of pure PEEK-steel contacts. There was less damage on the CFR PEEK and GFR PEEK plates paired with smooth steel balls under base oil lubrication, and no transfer film was detected on the smooth steel balls. In the PEEK composites-rough steel contact, the results of surface analyses indicate that the polymer transfer film on the rough steel ball was the dominant factor controlling the friction and wear performance and was well correlated to the hardness modification of polymer surfaces. Therefore, this section discusses these factors for the PEEK composites-rough steel contacts.

6.3.1 Hardness modification of polymer surface

As discussed in section 4.3, despite base oil lubrication causing the softening of pure PEEK surfaces rubbed with steel counterparts, this hardness modification was not the main factor controlling the tribological behaviour of the lubricated pure PEEK-steel contact. However, the situation differs for the PEEK composites due to the reinforcement fibres present. As discussed in section 6.1.2.2, the reinforcement fibres exposed on the wear tracks when rubbed with rough steel balls gave a much higher hardness to the matrix PEEK. Interestingly, CFR PEEK and GFR PEEK gave distinctively different distributions of the exposed reinforcement fibres. Figure 6.35 summarizes the hardness distributions of new polymer plates and wear tracks on polymer plates in PAO4 lubricated conditions which correspond to the nanoindentation hardness maps shown in Figure 6.7 (b, d). On new plates, the hardness values of approximately 0.3-0.4 GPa were derived from the PEEK matrix and those above 0.8 GPa were derived from carbon fibres and glass fibres. The carbon fibres covered about 40% of the wear tracks (Figure 6.35 (a)), while the glass fibres covered less than 5% (Figure 6.35 (b)). The hardness values of approximately 0.3-0.4 GPa in new plates were reduced to approximately 0.2-0.3 GPa at the wear tracks lubricated with PAO4. Considering that these values were derived from the PEEK matrix, the softening of the PEEK matrix in the composites was seemed to occur by the same mechanism as the softening of pure PEEK discussed in section 4.3.1.

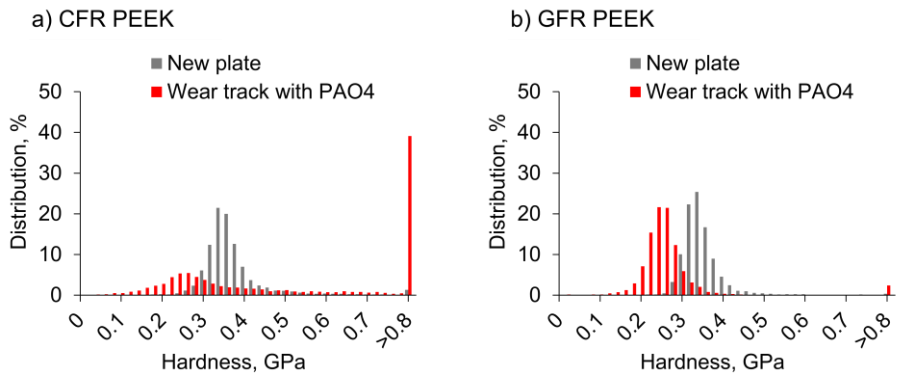

Figure 6.35. Hardness distribution of new polymer plates and wear tracks on polymer plates for (a) CFR PEEK and (b) GFR PEEK in PAO4 lubricated conditions

As already mentioned, although the hardness mapping measurements were only carried out for the wear tracks lubricated with PAO4, the results for the wear tracks lubricated with PAO2 and PAO10 are expected to show the same trend based on the fibre distributions observed in the optical images (Figure 6.27, Figure 6.29). Reinforcement fibres added to the PEEK matrix are expected to improve mechanical properties. Despite that many carbon fibres were detected on the wear tracks,

CFR PEEK paired with rough steel balls gave much larger wear volumes than GFR PEEK, regardless of the viscosity grades of PAO (Figure 6.24, Figure 6.26). This implies the fractured carbon fibres did not contribute to the wear resistance. Chen et al. [126] also reported that the fractured carbon fibres may decrease the load carrying capacity. Furthermore, these fractured fibres can be detrimental to the formation of polymer transfer films on steel counterparts, further increasing friction and wear.

6.3.2 Polymer transfer films on steel counterparts

For the base oil lubrication of pure PEEK, discussed in Chapter 4, the amount of the polymer transfer films on the steel counter surfaces was found to be the main parameter controlling tribological performance in not only dry conditions but also lubricated conditions. In PEEK composites-rough steel contacts the thickness of polymer transfer films was also well correlated with the tribological behaviour as discussed in section 6.2.2.2. Under base oil lubrication, CFR PEEK provided less transfer films on steel counterparts, resulting in higher friction and larger wear. In contrast, GFR PEEK provided a much larger amount of transfer films, resulting in lower friction and wear. These results indicate that the polymer transfer film on the steel counterpart is also the main parameter that controls the tribological performance of the PEEK composites-steel contacts. The difference in amount of polymer transfer films between CFR PEEK and GFR PEEK was explained by the difference in the fibre distribution on the wear tracks of the polymer plates. Figure 6.36 illustrates the schematic of the contact surfaces for pure PEEK, CFR PEEK and GFR PEEK paired with rough steel. When comparing dry and base oil lubrication, wear debris is found to play a key role. In the pure PEEK-steel contact in the dry condition, wear debris contributed to the formation of polymer transfer films and thus provides thick films. Oil-lubrication flushes out wear debris from the contact surfaces, increasing friction and wear in the pure PEEK tests. On the other hand, in the CFR and GFR PEEK tests, wear debris, which contains hard reinforcement fibres, causes three-body abrasion under dry conditions. In this case, base oil lubrication flushed out wear debris from the contact surfaces and reduced friction and wear. When comparing the polymer types under base oil lubrication, the formation of polymer transfer films is inhibited in oil lubricated pure PEEK. On the other hand, in the CFR PEEK tests, the fractured carbon fibres exposed on the polymer surface wear off, by abrasion, the polymer transfer film on the steel counterparts and thus inhibit transfer film formation even more strongly than oil-lubrication. Notably, compared to these exposed fibres, wear debris flushed out from the contact surfaces seems to be less influential on friction and wear, even though it is carried around/circulated in the oil. In the GFR PEEK tests, the polymer transfer film is formed even under base oil lubrication. The glass fibres on the wear tracks are less damaged

and better embedded in the PEEK matrix, therefore not impeding the transfer film formation, as seen in the case of exposed/broken carbon fibres. In addition, due to the superior mechanical strength of GFR PEEK, its friction and wear performance is far superior to that of pure PEEK.

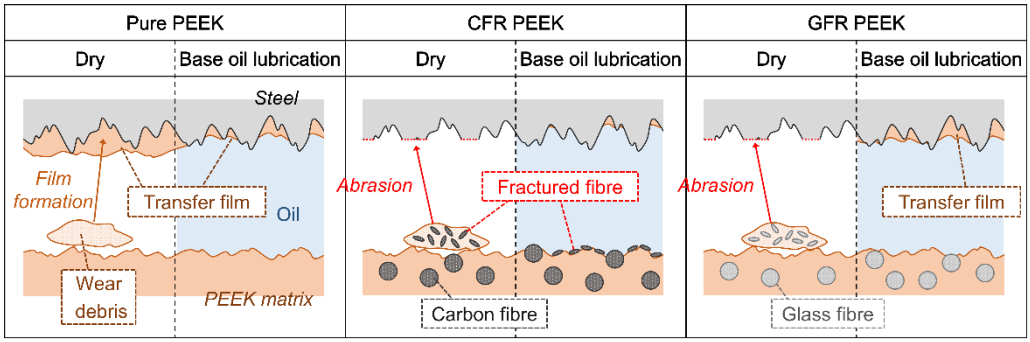

Figure 6.36. Schematic of contact surfaces in dry and base oil lubricated conditions

6.3.3 Working mechanism of base oil lubrication of PEEK composites

As discussed in section 4.3.3, in pure PEEK-steel contacts the working mechanism of base oil lubrication depends on the surface roughness of the steel counterparts. In PEEK-smooth steel contacts, the working mechanism of base oil lubrication basically follows the traditional theory after taking into account the modification of the surface roughness by removal (through wear) and/or compression of PEEK asperities. On the other hand, the working mechanism of base oil lubrication in PEEK-rough steel contacts does not follow the traditional theory due to the presence of PEEK transfer films on the steel counterparts. The above discussion is based on the estimation of the lubrication regimes using the modified Lambda ratio "Λ_{mod}" calculated by Equation 4-2:

$$\Lambda_{mod} = h/\sigma_{steel} \qquad \text{(Eq. 4-2)}$$

where h is the oil film thickness under operating conditions and σ_{steel} is the surface roughness of steel specimens. The values of the oil film thickness were estimated from the expression presented by Hamrock and Dowson [150,151] described in Appendix A. In this section, the same method was applied to the results obtained in sections 6.1 and 6.2 for CFR PEEK-steel contacts and GFR PEEK-steel contacts, respectively. Figure 6.37 shows the friction coefficients of PEEK composites-steel contacts as a function of the modified Lambda ratios. Similar to the pure PEEK-smooth steel contacts (Figure 4.31), the friction coefficients of PEEK composites-smooth steel contacts match the expected trend that friction coefficients gradually increase around Lambda ratios of 1-5 corresponding to mixed lubrication regime. This indicates that the working mechanism of base oil

lubrication in PEEK composites-smooth steel contacts follows the traditional theory. In contrast, the CFR PEEK-rough steel contacts and GFR PEEK-rough steel contacts give different trends, and they were also different from the trend of pure PEEK-rough steel contacts (Figure 4.31). The friction coefficients of CFR PEEK-rough steel contacts gradually increase as the modified Lambda ratios decrease below one corresponding to boundary lubrication. This trend matches the traditional theory of lubrication regime. However, the friction coefficients of the GFR PEEK-rough steel contacts do not follow this trend and exhibited stable values around 0.05.

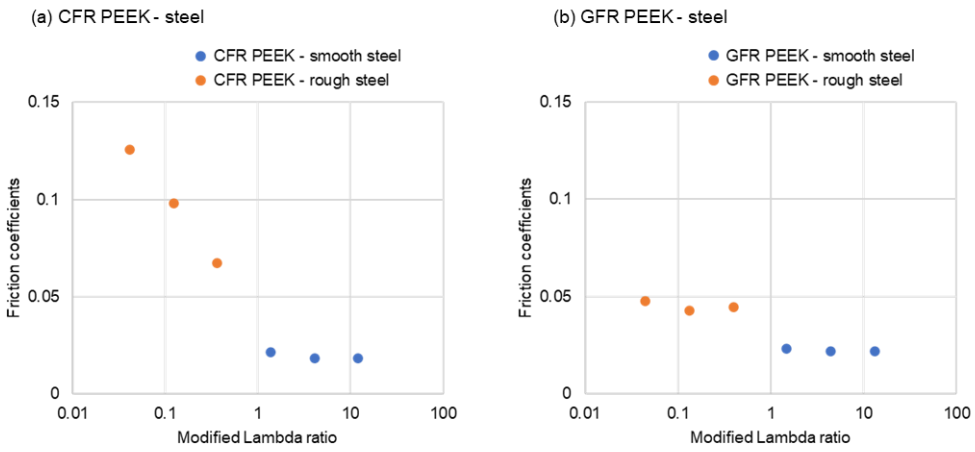

Figure 6.37. Friction coefficients of (a) CFR PEEK-steel and (b) GFR PEEK-steel contacts as a function of modified Lambda ratios

To clarify the effect of polymer types, the friction coefficients of polymer-steel contacts and wear volumes of polymer plates are summarized as a function of modified Lambda ratios in Figure 6.38 and Figure 6.39. The friction coefficients at modified Lambda ratios above one had similar values and no wear of polymer plates was observed under these conditions regardless of polymer types. As the reinforcement fibres contained in PEEK composites were not exposed on the surfaces of pristine plates as shown in Figure 6.7 investigated in section 6.1.2.2, the reinforcement fibres are assumed not to influence the tribological performance in the range of the Lambda ratios 1-10 which correspond to mixed to hydrodynamic lubrication regimes. In contrast, the polymer types distinctively affect the friction and wear performance in the range of the Lambda ratios below one which correspond to the boundary lubrication regime. As mentioned in section 6.3.2, the polymer transfer films on steel counterparts controlled the tribological performance of pure PEEK and PEEK composites paired with rough steel balls, i.e. tested under boundary lubrication. The friction coefficients and the wear volumes showed the same trend with modified Lambda ratios, indicating higher friction leads to greater wear of polymers. Pure PEEK exhibited much larger wear than CFR

PEEK and GFR PEEK at the modified Lambda ratio of around 0.5, while pure PEEK provided smaller wear than CFR PEEK at the modified Lambda ratio of around 0.05. As discussed in section 4.3.3, pure PEEK formed thicker transfer films in more severe conditions, and therefore resulted in lower friction and wear at lower modified Lambda ratios. CFR PEEK did not form any transfer films regardless of the viscosity of PAOs, i.e. regardless of the modified Lambda ratios. As a result, the friction coefficients and wear volumes gradually increase as the modified Lambda ratio decreases, well matching the traditional theory. Comparing at a modified Lambda ratio of around 0.5 in tests with rough steel balls under PAO10 lubrication, both pure PEEK and CFR PEEK had almost no transfer films on the steel counterparts as shown in Figure 4.23 and Figure 6.32. Therefore, the difference in the friction coefficients and the wear volumes reflected the difference in the mechanical properties of pure PEEK and CFR PEEK, implying superior mechanical properties potentially lead to lower friction and wear. Thus, the lower friction and wear of GFR PEEK-steel contacts at modified Lambda ratios below one were derived from the combination of thick transfer films and the superior mechanical properties.

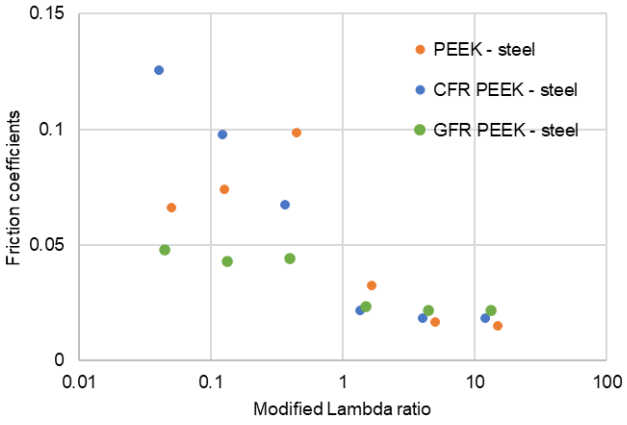

Figure 6.38. Friction coefficients of polymer-steel contacts as a function of modified Lambda ratios

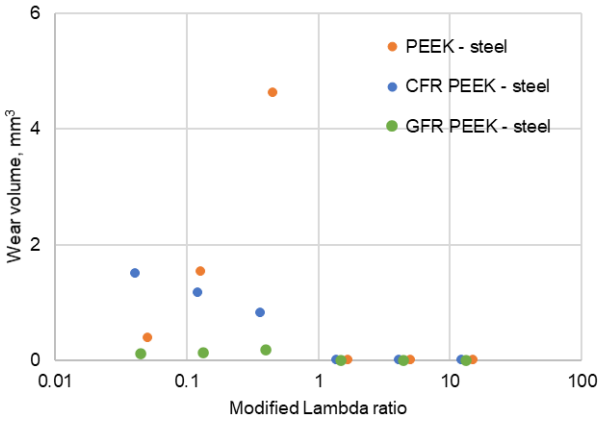

Figure 6.39. Wear volumes of polymer plates as a function of modified Lambda ratios

Finally, schematics of contact surfaces as a function of the modified Lambda ratios are summarized in Figure 6.40 based on the above discussion. Under hydrodynamic lubrication at modified Lambda ratios over 5, the reinforcement fibres contained in CFR PEEK and GFR PEEK are less influential, therefore CFR PEEK and GFR PEEK show a similar tribological performance to pure PEEK. Under mixed to boundary lubrication at modified Lambda ratios of around 0.5, CFR PEEK and GFR PEEK show lower friction and wear than pure PEEK due to their superior mechanical properties arising from the reinforcement fibres. Polymer transfer films form less under this lubrication regime, therefore the mechanical properties of polymers strongly affect their tribological performance. Under boundary lubrication at Lambda ratios around 0.05, the formation of polymer transfer films occurs for pure PEEK and GFR PEEK. As a result, they give lower friction and wear than expected from the traditional theory. In contrast, for CFR PEEK the exposed and fractured carbon fibres on the wear track of CFR PEEK inhibit the formation of polymer transfer films. Therefore, the tribological performance of CFR PEEK follows the traditional theory. Note that the glass fibres contained in GFR PEEK are well embedded in the PEEK matrix and inhibit less the formation of polymer transfer films.

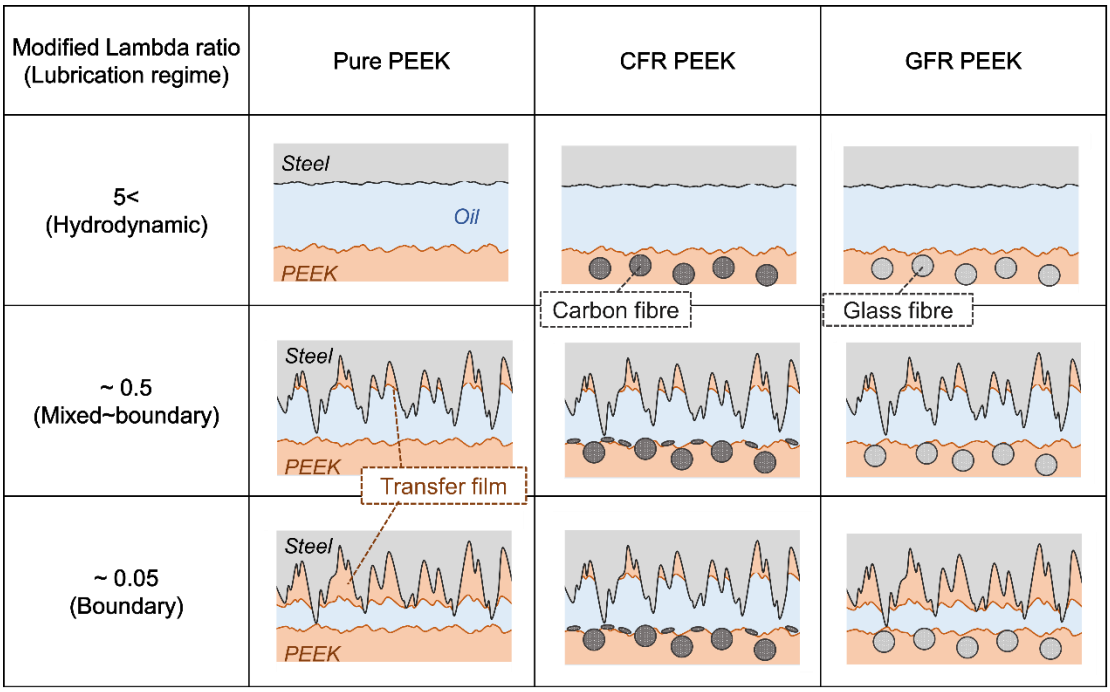

Figure 6.40. Schematic of contact surfaces depending on the modified Lambda ratios

As regards the design of polymer composites suitable under lubrication, the mechanism discussed above suggests that the adhesion force between reinforcement fibres and PEEK matrix is very important to provide thick polymer transfer films by keeping fibres well embedded in the PEEK matrix. SE images of the inner surfaces of CFR PEEK and GFR PEEK, which are prepared by mechanically breaking new plates, support this idea (Figure 6.41). The carbon fibres and the glass fibres are embedded in the PEEK matrix, and no specific orientation of the fibres is observed. The diameter of the glass fibres (approximately 9-11 µm) is slightly more than that of the carbon fibre (approximately 6-8 µm). Furthermore, the PEEK matrix appeared more adhered to the glass fibres than to the carbon fibres. To increase the adhesion between reinforcement fibres and the polymer matrix, surface treatment of reinforcement fibres is commonly carried out. Detailed information on the surface treatment of the CFR PEEK and GFR PEEK used in this study was not disclosed by the supplier. However, as the glass fibres were well adhered to the PEEK matrix shown in Figure 6.41, some surface treatments of glass fibres, e.g. with coupling agents, might have been applied to the GFR PEEK to increase hydrophobicity and as a result contribute to its superior tribological performance under lubrication.

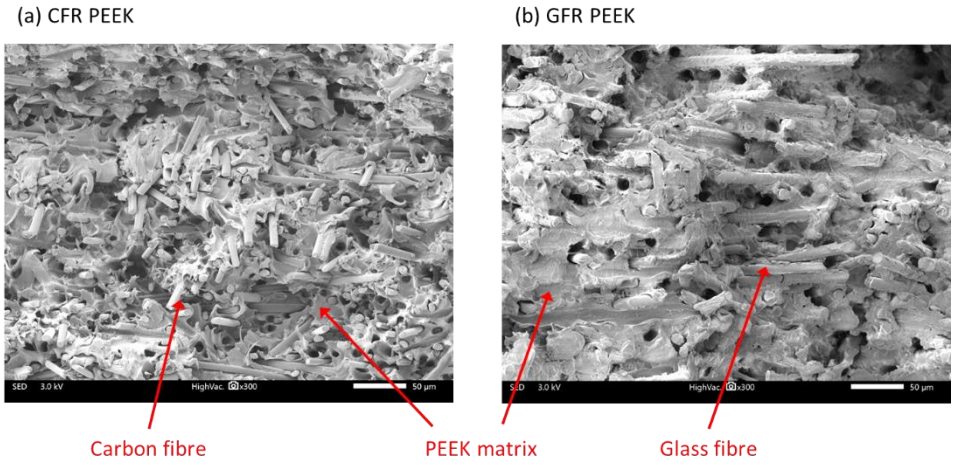

Figure 6.41. SE images of the inner surfaces of (a) CFR PEEK and (b) GFR PEEK plates

6.4 Summary

Carbon fibre reinforced (CFR) PEEK and glass fibre reinforced (GFR) PEEK are the most typical PEEK composites. Therefore, this chapter investigated their tribological performance and working mechanism under base oil lubrication. The working mechanism was discussed based on the tribological results and the surface analyses of after-test specimens.

Firstly, tribological testing using the MTM was performed to compare dry and PAO4 oil lubricated conditions. Surface analyses of after-test specimens with Alicona, Nanoindentation and EPMA were carried out focusing on the hardness modification of polymer surfaces and the formation of polymer transfer films on the steel counterparts. The following conclusions are drawn:

(1) Although lubrication with PAO4 reduced the friction of both CFR PEEK and GFR PEEK paired with rough steel compared to dry condition, GFR PEEK gave significantly lower friction and wear than CFR PEEK;

(2) In dry conditions, the CFR and GFR PEEK gave similar wear tracks with piled up wear debris containing fractured fibres. In PAO4 lubricated conditions, the reinforcement fibres were observed on the wear tracks, especially and in greater amount for CFR PEEK. The carbon fibres on the wear tracks of CFR PEEK were exposed and fractured, while the glass fibres on the GFR PEEK were less damaged and well embedded in the matrix;

(3) Both the carbon and glass fibres distributed on the wear tracks were much harder than the PEEK matrix. There was a large difference in the area covered by the reinforcement fibres e.g. the carbon fibres covered about 40% of the wear tracks, while the glass fibres covered less than 5%;

(4) In PAO4 lubricated conditions, the amount of the polymer transfer films on the steel counter surfaces correlated well with the tribological performance. No transfer film was observed for the CFR PEEK test, while a thick transfer film was detected for the GFR PEEK test which imparted a lower friction and wear.

Secondly, the effect of base oil viscosity, one of the most important parameters of lubrication, was investigated by using PAOs with different viscosities: PAO2, PAO4 and PAO10. The CFR and GFR PEEK plates were paired with smooth and rough steel balls. The following conclusions are drawn:

(1) In PEEK composites-smooth steel contacts, PAOs gave almost the same friction coefficients for both CFR PEEK and GFR PEEK. When paired with rough steel, the effect of base oil viscosity shows different trends depending on the polymer types. The friction and wear of the CFR PEEK tests showed lower values when lubricated with higher viscosity PAOs, while the friction and wear of the GFR PEEK tests were less influenced by the PAO viscosity;

(2) In PEEK composites-rough steel contacts, fractured and exposed carbon fibres on the wear tracks of CFR PEEK were detected in larger amounts under lubrication with lower viscosity PAO. The less damaged and well embedded glass fibres on the GFR PEEK were observed similarly regardless of the PAO viscosity;

(3) In PEEK composites-rough steel contacts, the thickness of the polymer transfer films on the steel counter surfaces correlated well with the tribological performance. No transfer film was observed for the CFR PEEK test regardless of the PAO viscosity, while a thick transfer film was detected for the GFR PEEK test especially when lubricated with PAO2 and PAO4.

Finally, the working mechanism of base oil lubrication of PEEK composites was discussed based on two factors: hardness modification of polymer surfaces and polymer transfer films on steel balls. The following mechanisms are summarized:

(1) There were more fractured fibres on the wear tracks of CFR PEEK than GFR PEEK. The fractured carbon fibres had a detrimental effect on the wear resistance of the composite by inhibiting the formation of polymer transfer films on steel counterparts;

(2) The polymer transfer film on steel counterparts was also the main parameter that controlled the tribological performance of PEEK composites-steel contacts. Hardness modification of polymer surfaces and polymer transfer films formed on the steel counter surfaces were related to each other. Fractured fibres exposed on the wear tracks of CFR PEEK plates after testing possibly inhibited the formation of polymer transfer films on steel counterparts. In contrast, the wear tracks on GFR PEEK plates showed the fibres were well matrix embedded and less damaged, enabling the formation of transfer films similar to those found on pure PEEK;

(3) The working mechanism of base oil lubrication depends on the surface roughness of the steel counterparts. In PEEK composites-smooth steel contacts, the mechanism follows the traditional theory after evaluating the modified Lambda ratios, as discussed for the pure PEEK-smooth steel contacts. In PEEK composites-rough steel contacts, CFR PEEK and GFR PEEK showed different trends depending on the thickness of the polymer transfer films formed. Owing to the lack of formation of transfer films, CFR PEEK still followed the traditional theory, showing higher friction and larger wear at lower modified Lambda ratios. On the other hand, GFR PEEK formed thick transfer films on the steel counter surfaces and gave lower friction and wear than expected from the traditional theory regardless of the values of the modified Lambda ratios.

Chapter 7 Effect of lubricant additives on lubrication of PEEK composites

This chapter investigates the effects of the lubricant additives, namely organic friction modifiers (OFMs) and anti-wear (AW) additives, on the lubrication of the PEEK composites, specifically carbon fibre reinforced (CFR) PEEK and glass fibre reinforced (GFR) PEEK, paired with steel counterparts. Tribological testing was performed with lubricants containing OFMs and AW additives, followed by surface analyses of the after-test specimens. In addition to the tests at ambient temperature (approximately 25 °C), high temperature tests at 80 °C were conducted to investigate the working mechanism of lubricant additives.

7.1 Results: Effect of organic friction modifiers

In Chapter 5, the effect of OFMs on the lubrication of pure PEEK paired with steel counterpart was reported. This chapter adds to that study by addressing the case of PEEK composites, CFR PEEK and GFR PEEK blended with 30 wt.% of carbon fibres and glass fibres. The detailed methodology described in Chapter 3 was followed. As in the investigation of pure PEEK in section 5.1, three types of OFMs, oleylamine (OAm), oleic acid (OAc) and N-oleoyl sarcosine (OSa) were added at 1.0 wt.% to PAO4 as listed in Table 3.3. The tribological testing was carried out using a MTM with the Stribeck routine as described in section 3.2.3. The test conditions were the standard conditions given in Table 3.6. In Chapter 5, the tribological tests were conducted at 50% SRR (sliding-rolling) and 200% SRR (sliding); this chapter focuses on the standard condition of 50% SRR (sliding-rolling) as encountered in gears, one of the main expected applications. Steel balls with smooth surfaces (Ra of 0.01-0.02 μm) and rough surfaces (Ra of approximately 0.5 μm) were used as described in section 3.1.2.

7.1.1 Friction and wear performance

(a) PEEK composites-smooth steel contact

The Stribeck curves, representing friction coefficient values as a function of entrainment speed, in the PEEK composites-smooth steel contact lubricated with PAO4 and PAO4 + OFMs are presented in Figure 7.1 and Figure 7.2. As stated in section 5.1.1, the effect of OFMs is expected to be seen at

lower entrainment speeds in Stribeck curves when the lubrication regime changes from hydrodynamic lubrication to boundary lubrication. In the PEEK composites-smooth steel contacts, OFMs reduced friction more at entrainment speeds below 0.1 m/s. Among the three types of OFMs, a significant friction reduction was achieved by the addition of OSa (N-oleoyl sarcosine), while the impact of the addition of OAm (oleylamine) and OAc (oleic acid) was much lower especially for the CFR PEEK-smooth steel contact. Note that when the tribological tests were conducted with smooth steel balls, there was almost no wear on the polymer plates, regardless of the polymer types or lubricant formulations. These results are similar to those with the pure PEEK-smooth steel contact reported in Figure 5.1 in section 5.1.1, although the impact for CFR PEEK is less. These results indicate that OFMs work similarly both on pure PEEK and PEEK composites when paired with smooth steel.

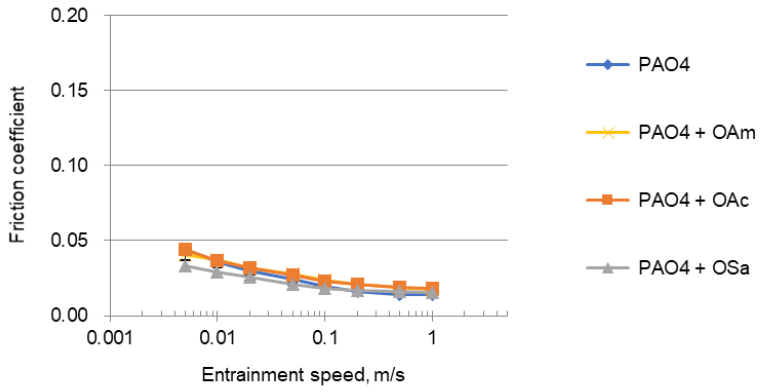

Figure 7.1. Stribeck curves of CFR PEEK paired with smooth steel balls for PAO4 and PAO4 + OFMs

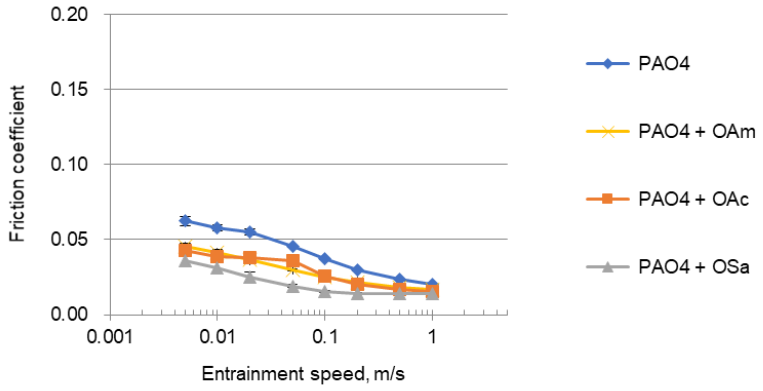

Figure 7.2. Stribeck curves of GFR PEEK paired with smooth steel balls for PAO4 and PAO4 + OFMs

(b) PEEK composites-rough steel contact

To complement the investigation of pure PEEK in section 5.1.1, the effect of OFMs was investigated in the PEEK composites-rough steel contact. The calculated Lambda ratios of below one indicate that the tests were performed in the boundary lubrication regime. The Stribeck curves lubricated with PAO4 and PAO4 + OFMs are shown in Figure 7.3 and Figure 7.4. The addition of OFMs, especially OSa, increased friction between 0.5-0.05 m/s for CFR PEEK and 1-0.05 m/s for GFR PEEK. This damaging effect of OFMs on friction was also observed in the pure PEEK-rough steel contact (Figure 5.3).

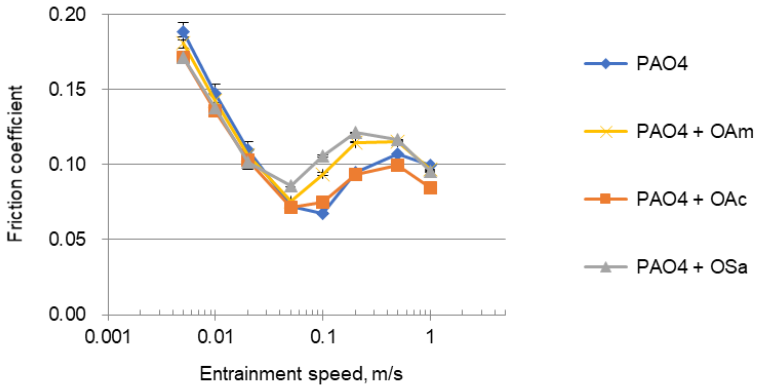

Figure 7.3. Stribeck curves of CFR PEEK paired with rough steel balls for PAO4 and PAO4 + OFMs

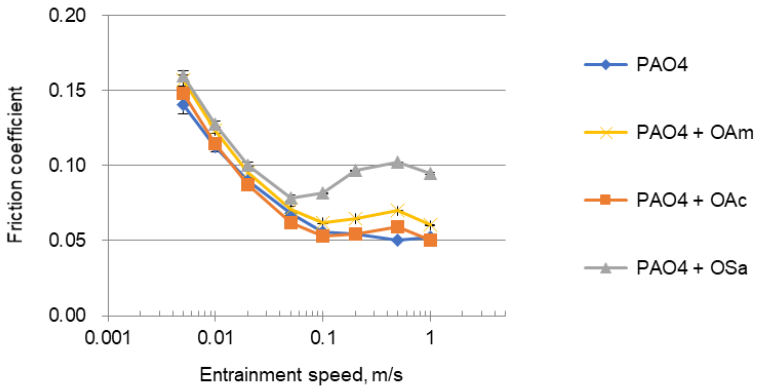

Figure 7.4. Stribeck curves of GFR PEEK paired with rough steel balls for PAO4 and PAO4 + OFMs

The optical images of after-test polymer plates are shown in Figure 7.5 and Figure 7.6. The influence of the addition of OFMs is not clear from the appearance of the four wear tracks, but PAO4 + OSa

gave a wear track with a slightly larger width than the others for both CFR PEEK and GFR PEEK. This was also confirmed by the wear profiles of the after-test PEEK plates shown in Figure 7.7 and Figure 7.8. The wear volumes of the polymer plates correlate well with the friction behaviour. PAO4 + OAm and PAO4 + OSa, which showed higher friction in the CFR PEEK-rough steel contact (Figure 7.3), gave larger wear of the polymer plate. OSa also increased the friction and wear of the GFR PEEK paired with rough steel (Figure 7.4). The wear volumes are lower for GFR PEEK than for CFR PEEK with the same lubricants. The same trend was reported in section 6.1 which investigated the effect of PAO4 lubrication in PEEK composites-rough steel contacts using the constant speed routine (Figure 6.3).

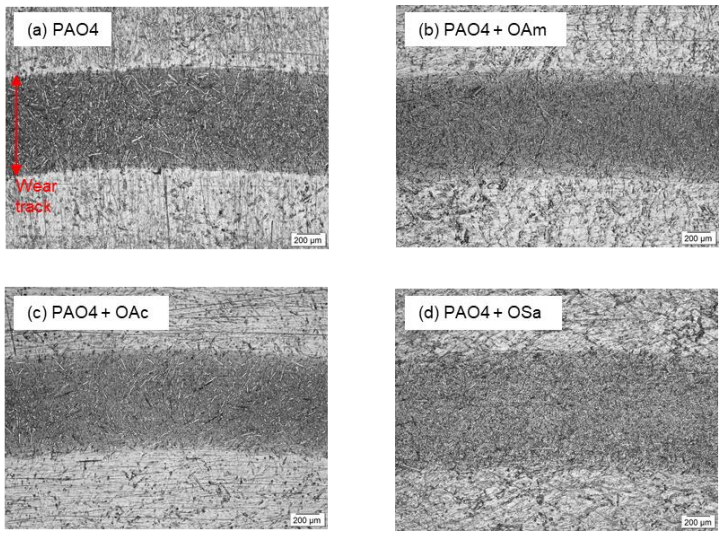

Figure 7.5. Optical images of after-test CFR PEEK plates paired with rough steel balls for (a) PAO4 and (b-d) PAO4 + OFMs

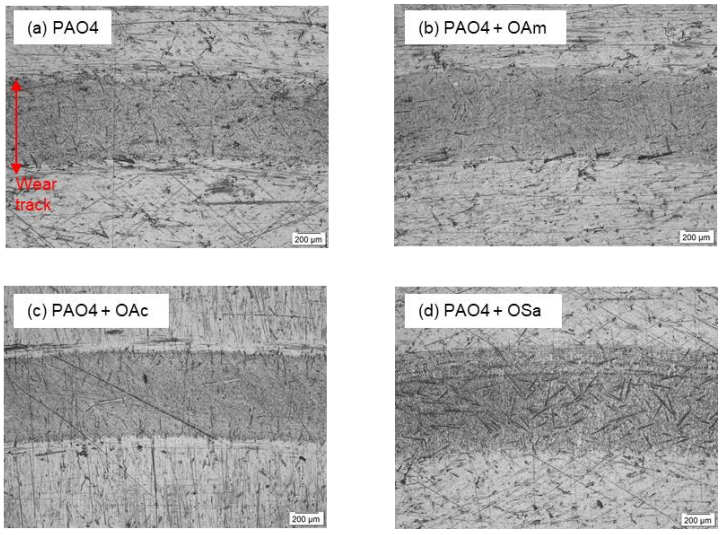

Figure 7.6. Optical images of after-test GFR PEEK plates paired with rough steel balls for (a) PAO4 and (b-d) PAO4 + OFMs

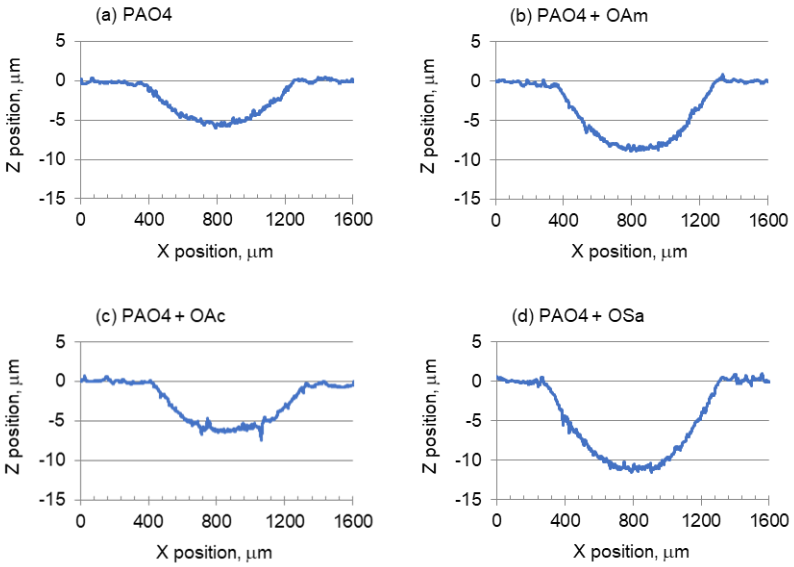

Figure 7.7. Wear profiles of CFR PEEK plates paired with rough steel balls for (a) PAO4 and (b-d) PAO4 + OFMs

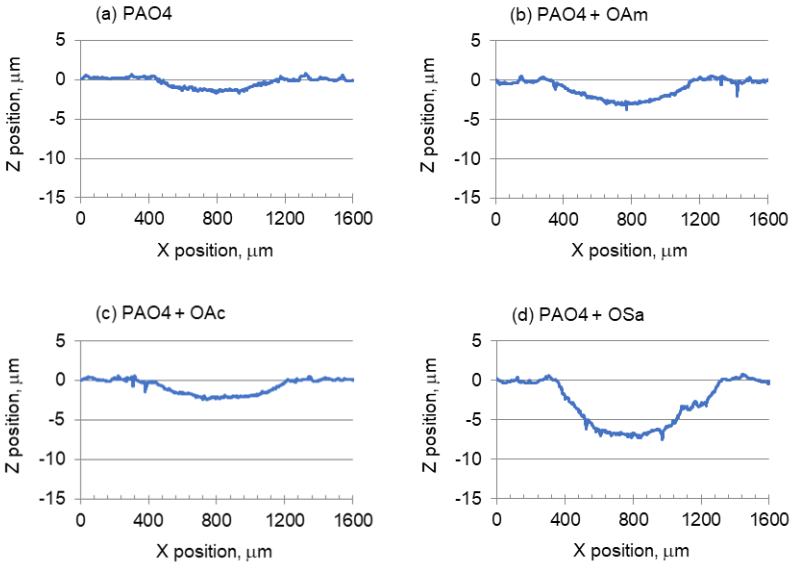

Figure 7.8. Wear profiles of GFR PEEK plates paired with rough steel balls for (a) PAO4 and (b-d) PAO4 + OFMs

7.1.2 Surface analyses

As reported in Chapter 6, both the distribution of the reinforcement fibres on the polymer wear tracks and the polymer transfer films on the steel counterparts are important factors influencing the tribological behaviour of PEEK composites under oil-lubrication. To investigate further the

mechanism of action, these factors were also analysed on after-test specimens lubricated with PAO and PAO + OSa, OSa showing a greater effect on friction and wear behaviour than other OFMs. Surface analyses were conducted only with the specimens tested with rough steel balls, because the wear tracks on the polymer plates and the polymer transfer films on the steel balls were difficult to detect on the PEEK composites-smooth steel contacts.

7.1.2.1 3D Profilometry

The wear tracks of polymer plates were investigated by Alicona optical profilometry as described in section 3.3.1. The optical images and the corresponding 3D surface profiles of the wear tracks are shown in Figure 7.9 and Figure 7.10. When lubricated with both PAO4 and PAO4 + OSa, a large amount of finely fractured fibres was observed on the wear tracks of CFR PEEK, while a lesser number of fibres was observed on the wear tracks of GFR PEEK and these were less damaged. Additionally, the 3D surface profiles indicate that most of the fractured carbon fibres were located on top of the PEEK matrix, while the glass fibres were well embedded in the PEEK matrix. These features were also observed on the wear tracks of polymer plates lubricated with PAOs with different viscosity grades as reported in Chapter 6. PAO4 and PAO4 + OSa provided almost the same optical images and 3D surface profiles for both CFR PEEK and GFR PEEK despite the addition of OSa increasing friction and wear as described in section 7.1.1. This indicates that OFMs do not influence the distribution of fractured reinforcement fibres on the polymer wear tracks which was one of the important factors influencing the tribological behaviour of PEEK composites under oil-lubrication revealed in Chapter 6. The working mechanism of OFMs will be discussed in more detail in section 7.3.1.

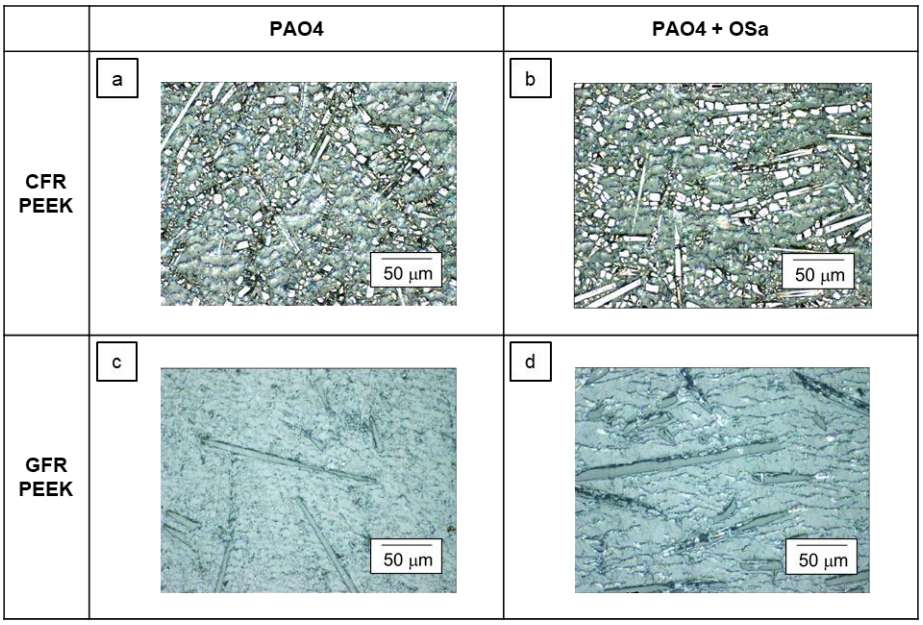

Figure 7.9. Optical images of wear tracks on polymer plates with rough steel balls for (a, c) PAO4 and (b, d) PAO4 + OSa

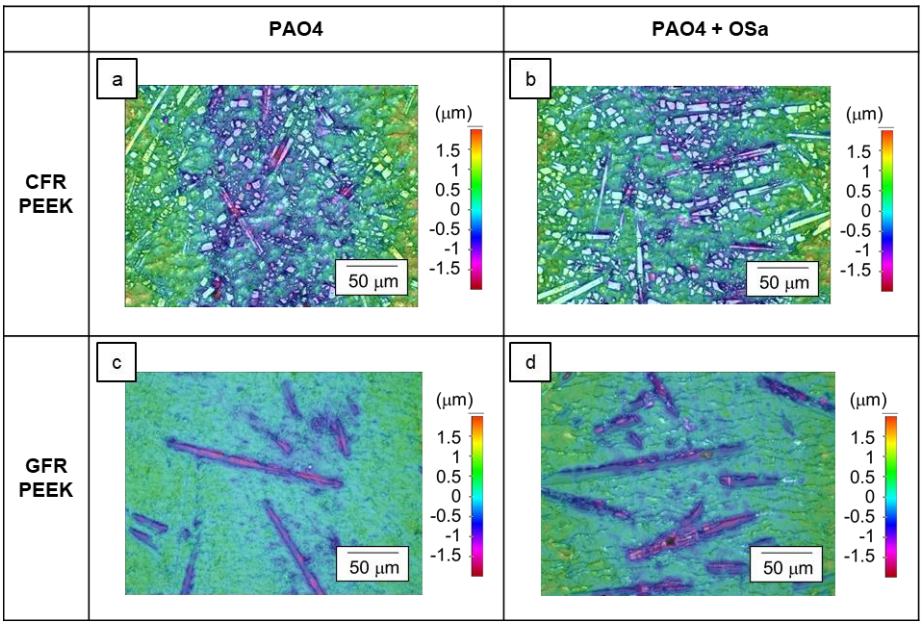

Figure 7.10. 3D surface profiles of wear tracks on polymer plates with rough steel balls for (a, c) PAO4 and (b, d) PAO4 + OSa

7.1.2.2 EPMA

As reported in Chapter 6, polymer transfer films on steel counterparts are an important factor in reducing polymer wear not only for pure PEEK but also for PEEK composites. Therefore, the effect

of OFMs on the formation of polymer transfer films was investigated. By following the procedure described in section 3.3.3, SE images and EPMA carbon maps on after-test steel balls were obtained as shown in Figure 7.11 and Figure 7.12. The amount of carbon in the transfer film is indicated by the colour scale on the EPMA map. For CFR PEEK under lubrication with both PAO4 and PAO4 + OSa, transfer films were hardly observed on SE images and almost no carbon was detected on the wear tracks in EPMA carbon maps. A polymer transfer film was observed on the wear track produced with GFR PEEK under PAO4 lubrication (Figure 7.11 (c) and Figure 7.12 (c)), but the amount of this film was less with PAO4 + OSa (Figure 7.11 (d) and Figure 7.12 (d)). The addition of OSa reduced the amount of carbon outside the wear tracks for both CFR PEEK and GFR PEEK. These results indicate that OSa adsorbed on the steel surface and inhibited the formation of polymer transfer films, resulting in larger wear of the polymer plates. This mechanism of action is similar to that for pure PEEK shown in section 5.1. As the amount of wear of CFR PEEK increased on adding OSa, the formation of the polymer transfer film is hypothesised to occur under PAO4 lubrication to some extent and contribute to mitigating the direct contact between CFR PEEK and steel surfaces. The working mechanism of OFMs will be discussed in more detail in section 7.3.1.

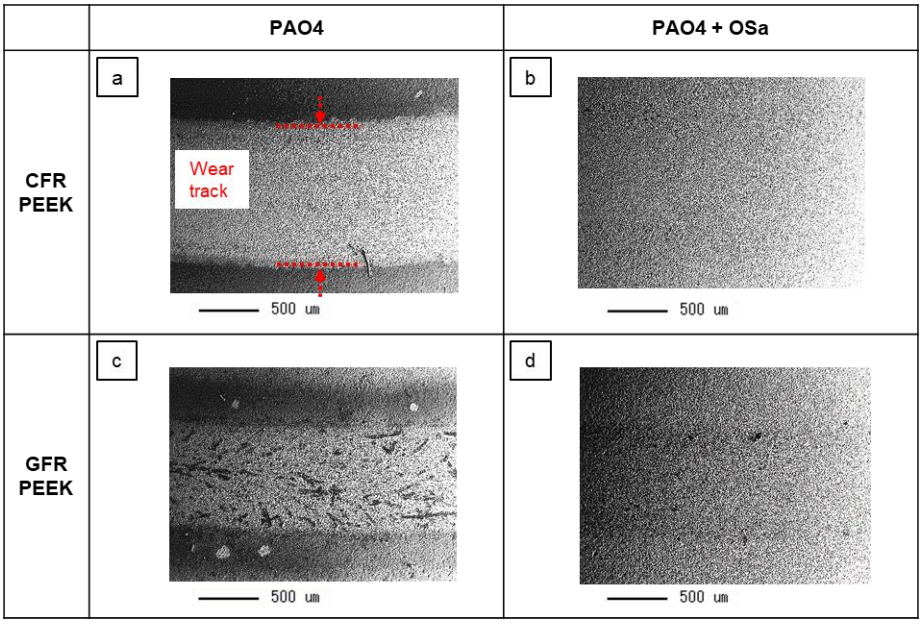

Figure 7.11. SE images of after-test rough steel balls paired with CFR and GFR PEEK lubricated with (a, c) PAO4 and (b, d) PAO4 + OSa

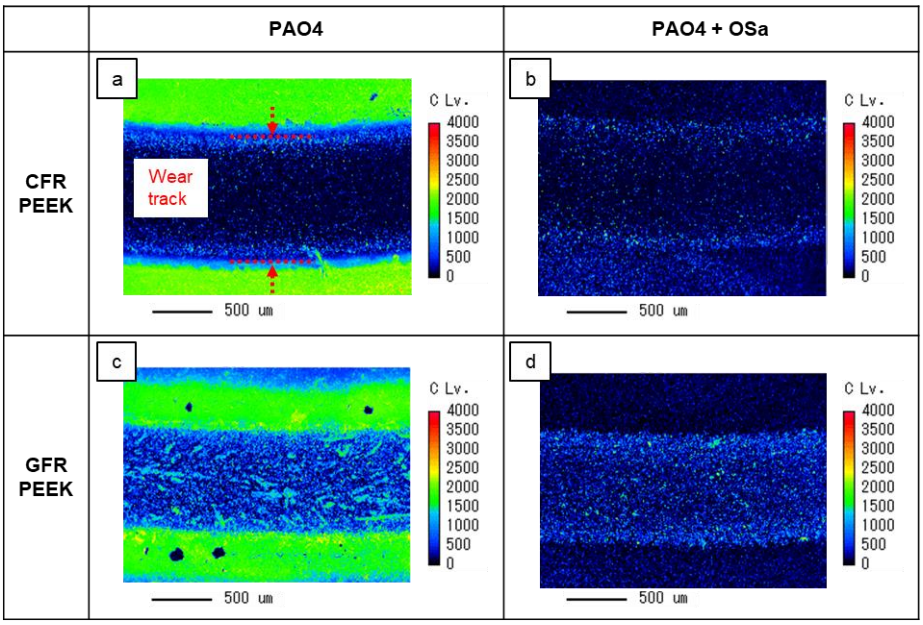

Figure 7.12. EPMA carbon maps of after-test rough steel balls paired with CFR and GFR PEEK lubricated with (a, c) PAO4 and (b, d) PAO4 + OSa

7.1.3 Testing at higher temperature

In the standard test condition of this study described in section 3.2.3, tribological tests were carried out at ambient temperature (approximately 25 °C). However, as frictional heat can accelerate the adsorption of OFMs, test temperature is an important parameter influencing the working mechanism of OFMs. This becomes more important in the polymer-rough steel contact where the formation of the polymer transfer film on the steel surface greatly affects tribological performance, because the adsorption of OFMs and the formation of transfer films are related, as reported in section 5.3.1. Therefore, this section investigates the effect of OFMs at a higher temperature (80 °C). OSa was studied in this section because it exhibited a greater effect on friction and wear behaviour than other OFMs in the ambient temperature tests reported in section 7.1.1.

(a) Friction and wear performance

The tribological test conditions were the same as those in section 7.1.1 except for the test temperature. Although this chapter focuses principally on the PEEK composites, the higher temperature tests were performed on both pure PEEK and PEEK composites, CFR PEEK and GFR PEEK, paired with rough steel balls. The Stribeck curves for the tests lubricated with PAO4 and PAO4 + OSa are presented in Figure 7.13, Figure 7.14 and Figure 7.15. In each figure, the Stribeck curves

obtained at ambient temperature (approximately 25 °C) and 80 °C are shown with grey and orange lines, respectively.

In the pure PEEK-rough steel contact (Figure 7.13), OSa increased friction at ambient temperature, while it decreased friction at 80 °C. Over the whole range of entrainment speeds friction coefficients under PAO4 lubrication showed higher values at 80 °C than at ambient temperature. In contrast, friction coefficients under PAO4 + OSa showed lower values at 80 °C especially at entrainment speeds above 0.1 m/s.

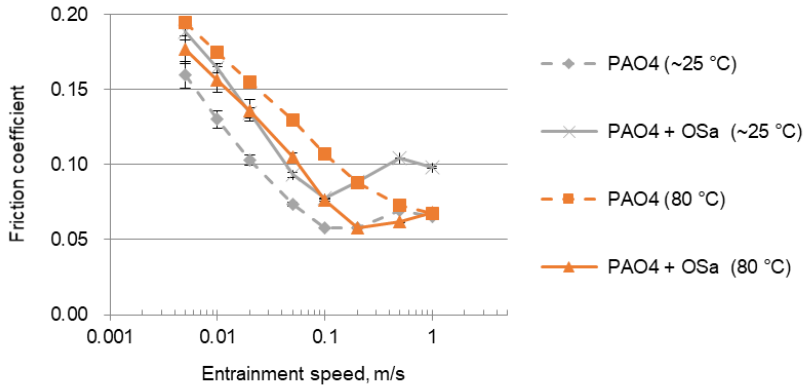

Figure 7.13. Stribeck curves of pure PEEK paired with rough steel balls for PAO4 and PAO4 + OSa at ambient temperature (approximately 25 °C) and 80 °C

In the CFR PEEK-rough steel contact (Figure 7.14), OSa increased friction at ambient temperature and 80 °C especially at entrainment speeds above 0.1 m/s. Tests at 80 °C gave lower friction at entrainment speeds above 0.1 m/s under both PAO4 and PAO4 + OSa, while the friction coefficients at entrainment speeds below 0.1 m/s showed similar values regardless of lubricant or temperature tested.

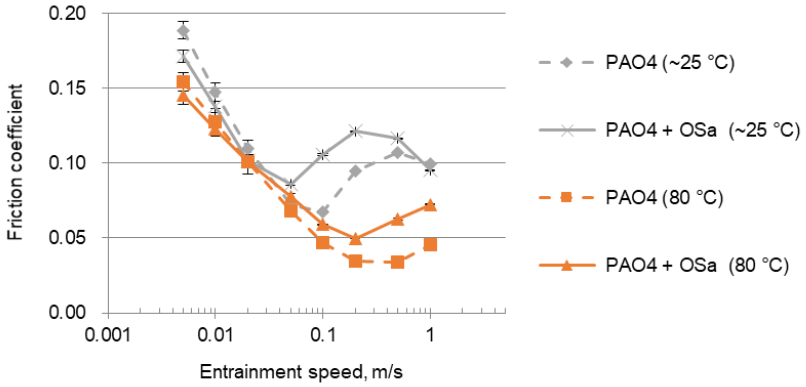

Figure 7.14. Stribeck curves of CFR PEEK paired with rough steel balls for PAO4 and PAO4 + OSa at ambient temperature (approximately 25 °C) and 80 °C

In the GFR PEEK-rough steel contact (Figure 7.15), OSa increased friction at both ambient temperature and 80 °C especially at entrainment speeds above 0.1 m/s, however, at these entrainment speeds the increase at 80 °C was much less than at ambient temperature. Under PAO4 lubrication, tests at ambient temperature and 80 °C gave almost the same friction curves.

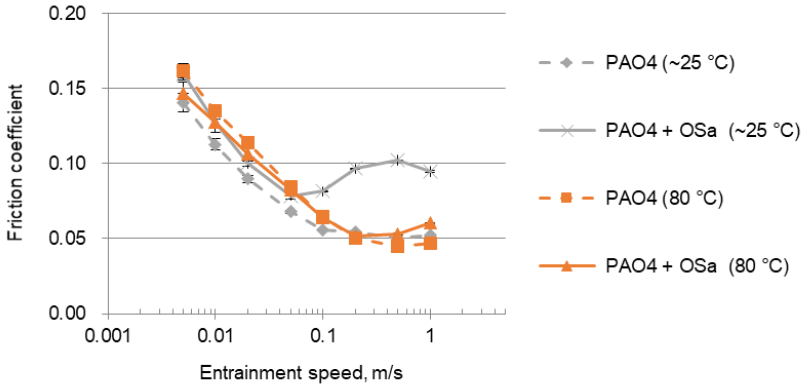

Figure 7.15. Stribeck curves of GFR PEEK paired with rough steel balls for PAO4 and PAO4 + OSa at ambient temperature (approximately 25 °C) and 80 °C

The optical images and wear profiles of after-test polymer plates tested at 80 °C are presented in Figure 7.16 and Figure 7.17. As already reported in sections 5.1.1. and 7.1.1, the addition of OSa increased the wear of the polymer plates when tested at ambient temperature regardless of the polymer type (Figure 5.7, Figure 7.7, Figure 7.8). In contrast, PAO4 and PAO4 + OSa gave similar wear profiles for each after-test polymer plate when tested at 80 °C (Figure 7.17), although they

produced wear tracks with a slightly different appearance (Figure 7.16). As discussed in section 5.3.1, in the sliding-rolling contact used the adsorption of OFMs on the rough steel surface causes a negative effect on the wear of polymer plate by inhibiting the formation of polymer transfer films. The adsorption of OFMs is expected to be accelerated at higher temperature, suggesting that the negative effect of OFMs on the wear of the polymer plate would possibly become more significant at higher temperature. However, contrary to this expectation, the addition of OSa had less impact on the wear of the polymer plates at 80 °C. This may be because not only the adsorption of OFMs, but also the formation of polymer transfer films is accelerated at higher temperature and thus the amount of polymer transfer film, which controls the tribological behaviour, is determined by the interplay of these two factors. Therefore, the polymer transfer films formed in higher temperature tests were investigated using EPMA.

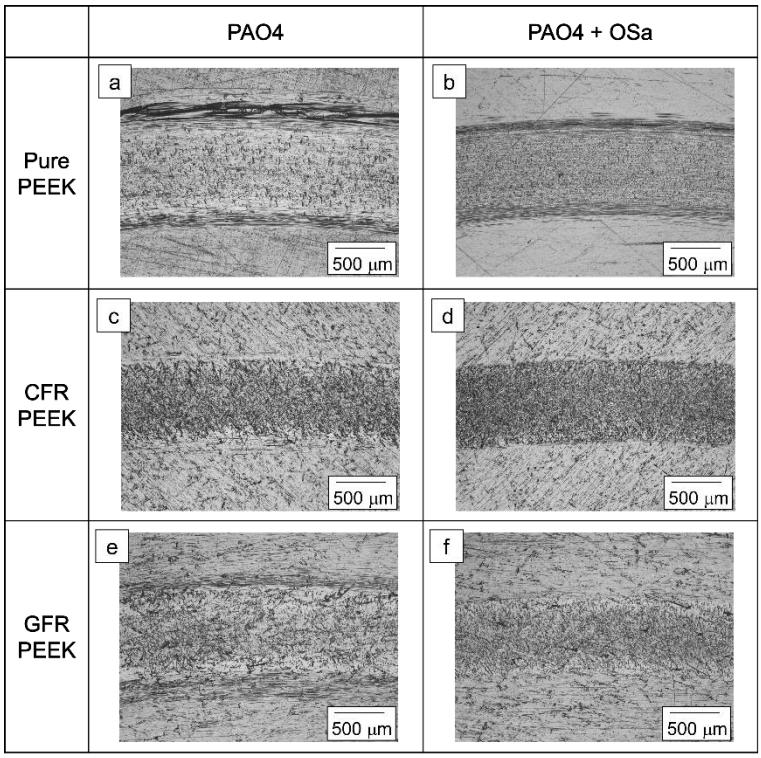

Figure 7.16. Optical images of after-test polymer plates paired with rough steel balls and lubricated with (a, c, e) PAO4 and (b, d, f) PAO4 + OSa at 80 °C

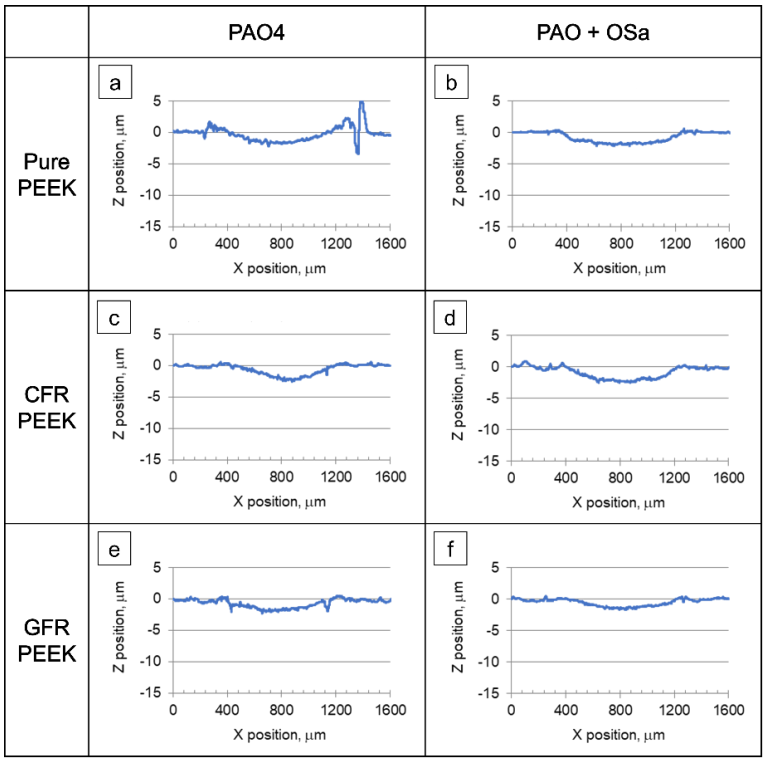

Figure 7.17. Wear profiles of after-test polymer plates paired with rough steel balls and lubricated with (a, c, e) PAO4 and (b, d, f) PAO4 + OSa at 80 °C

(b) EPMA

Polymer transfer films formed on the steel surfaces in the higher temperature tests were investigated by following the procedure described in section 3.3.3. SE images and EPMA carbon maps on after-test steel balls were obtained as shown in Figure 7.18 and Figure 7.19. Compared with the test at ambient temperature (approximately 25 °C) reported in section 5.1.2.2 and 7.1.2.2, thicker transfer films were formed at 80 °C under lubrication with both PAO4 and PAO4 + OSa regardless of polymer types. As described in section 2.1.3, Kurdi et al. reported that for PEEK and PEEK composites, which show a more ductile behaviour at higher temperature, the amount of polymer transfer films increases with the softening of the polymer surfaces caused by heat [19]. The EPMA results suggest that the same mechanism applies even under lubrication. OSa inhibited the formation of polymer transfer films at 80 °C as well as at ambient temperature, but sufficient polymer transfer films were formed at 80 °C even under lubrication with PAO4 + OSa. These results correlate well with the friction and wear performance found at 80 °C, which indicate that even when lubricated at higher temperature, the mechanism of action is basically the same as that at ambient temperature.

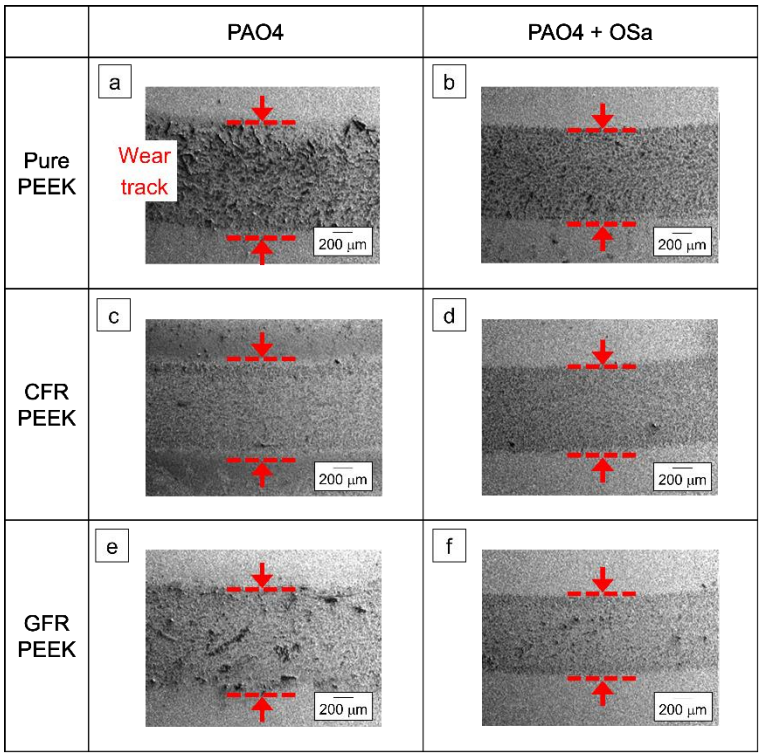

Figure 7.18. SE images of after-test rough steel balls lubricated with (a, c, e) PAO4 and (b, d, f) PAO4 + OSa at 80 °C

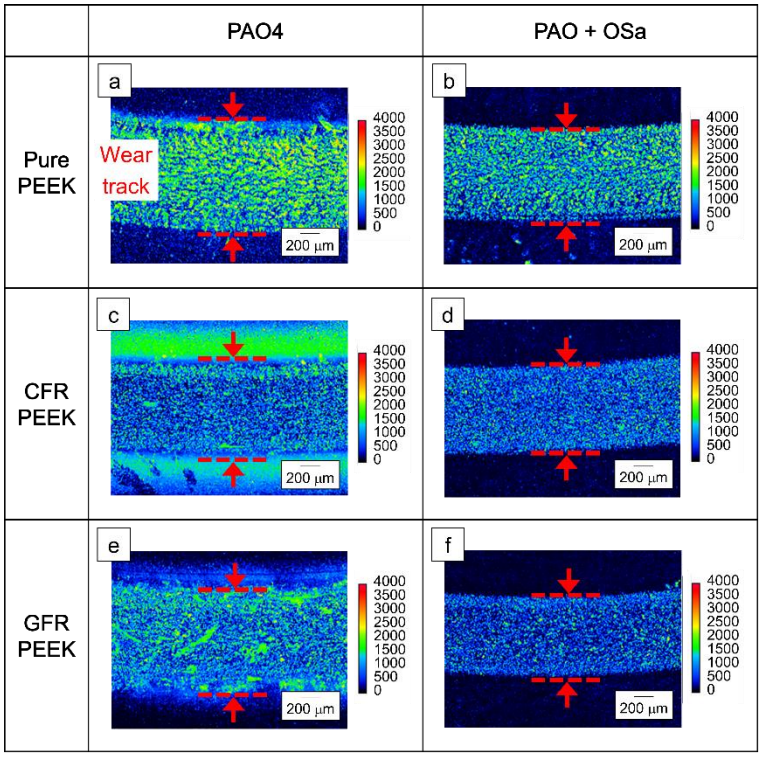

Figure 7.19. EPMA carbon maps of after-test rough steel balls lubricated with (a, c, e) PAO4 and (b, d, f) PAO4 + OSa at 80 °C

7.2 Results: Effect of anti-wear additives

In Chapter 5, the effect of AW additives on the lubrication of pure PEEK paired with steel counterpart was reported. This chapter reports a similar study on PEEK composites, CFR PEEK and GFR PEEK blended with 30 wt.% of carbon fibres and glass fibres.

The detailed methodology described in Chapter 3 was followed. As in the investigation of pure PEEK contained in section 5.2, the typical anti-wear (AW) additives, Zinc dialkyldithiophosphate (ZDDP) and tricresyl phosphate (TCP) were added at 1.0 wt.% to PAO4 as listed in Table 3.4. The tribological tests were carried out using a MTM with the Stribeck routine as described in section 3.2.3. The test conditions were the standard conditions given in Table 3.6, i.e. with a 50% SRR (sliding-rolling). Steel balls with smooth surfaces (Ra of 0.01-0.02 μm) and rough surfaces (Ra of approximately 0.5 μm) were used as described in section 3.1.2.

7.2.1 Friction and wear performance

(a) PEEK composites-smooth steel contact

The Stribeck curves in the PEEK composites-smooth steel contact lubricated with PAO4 and PAO4 + AW additives are presented in Figure 7.20 and Figure 7.21. For both CFR PEEK and GFR PEEK, AW additives had little impact on the friction performance, although ZDDP slightly increased friction. As reported in section 5.2.1, AW additives also had little influence on the friction coefficients of the pure PEEK-smooth contact. These results imply that the test conditions were too mild for AW additive reaction films to form.

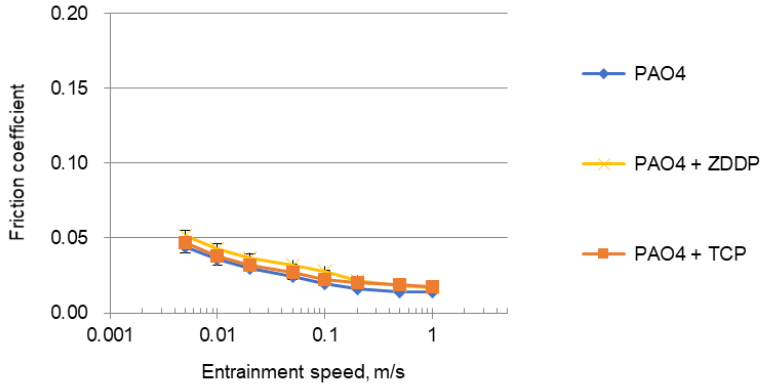

Figure 7.20. Stribeck curves of CFR PEEK paired with smooth steel balls for PAO4 and PAO4 + AW additives

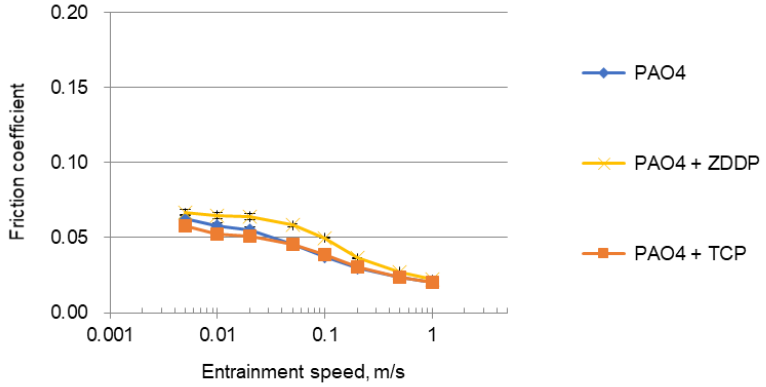

Figure 7.21. Stribeck curves of GFR PEEK paired with smooth steel balls for PAO4 and PAO4 + AW additives

(b) PEEK composites-rough steel contact

The effect of AW additives was investigated in the PEEK composites-rough steel contacts where the calculated Lambda ratios of below one indicate that the tests were performed in the boundary lubrication regime. The Stribeck curves lubricated with PAO4 and PAO4 + AW additives are shown in Figure 7.22 and Figure 7.23. Similar to the PEEK composites-smooth steel contacts, AW additives have little effect on the friction coefficients for both CFR PEEK and GFR PEEK.

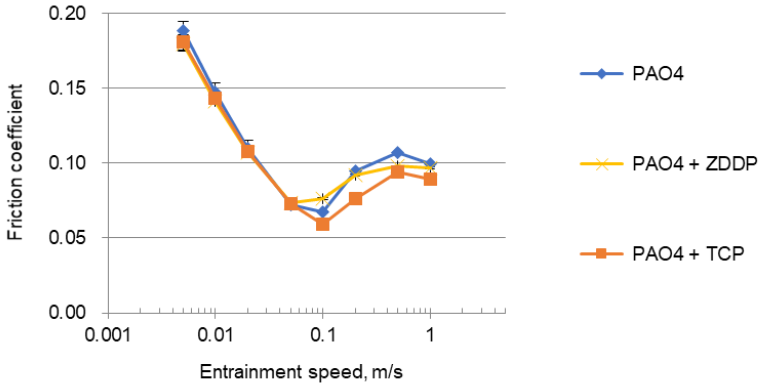

Figure 7.22. Stribeck curves of CFR PEEK paired with rough steel balls for PAO4 and PAO4 + AW additives

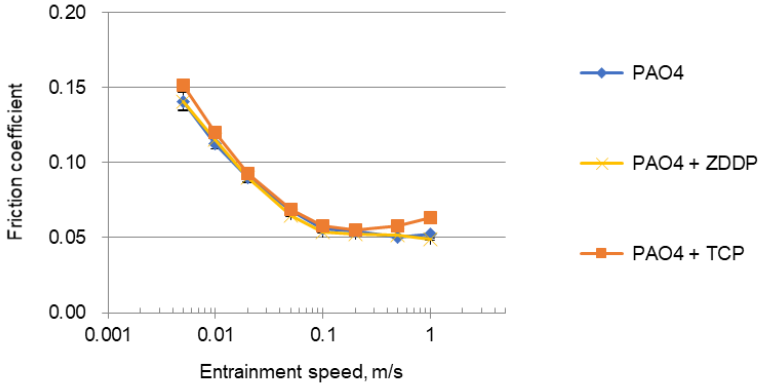

Figure 7.23. Stribeck curves of GFR PEEK paired with rough steel balls for PAO4 and PAO4 + AW additives

The optical images of the after-test polymer plates are presented in Figure 7.24 and Figure 7.25. The influence of the addition of AW additives is not clear from the appearance of wear tracks for both CFR PEEK and GFR PEEK. This was also the case for the wear profiles of the after-test PEEK plates shown in Figure 7.26 and Figure 7.27. These results suggest that AW additives did not work well both in the PEEK composites-rough steel contacts and in the PEEK composites-smooth steel contacts.

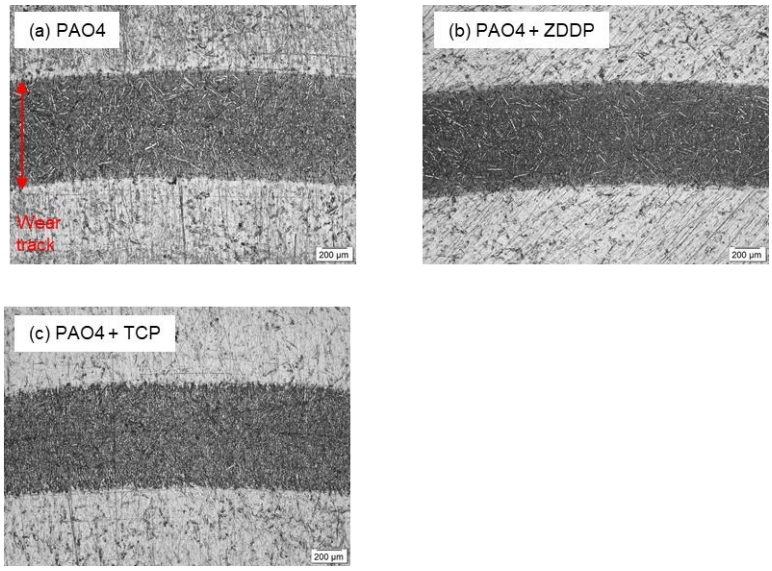

Figure 7.24. Optical images of after-test CFR PEEK plates paired with rough steel balls lubricated with (a) PAO4 and (b, c) PAO4 + AW additives

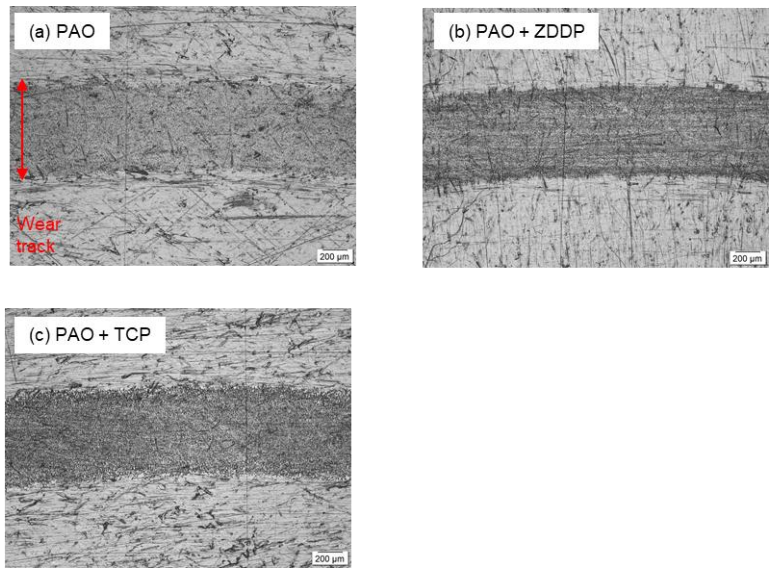

Figure 7.25. Optical images of after-test GFR PEEK plates paired with rough steel balls lubricated with (a) PAO4 and (b, c) PAO4 + AW additives

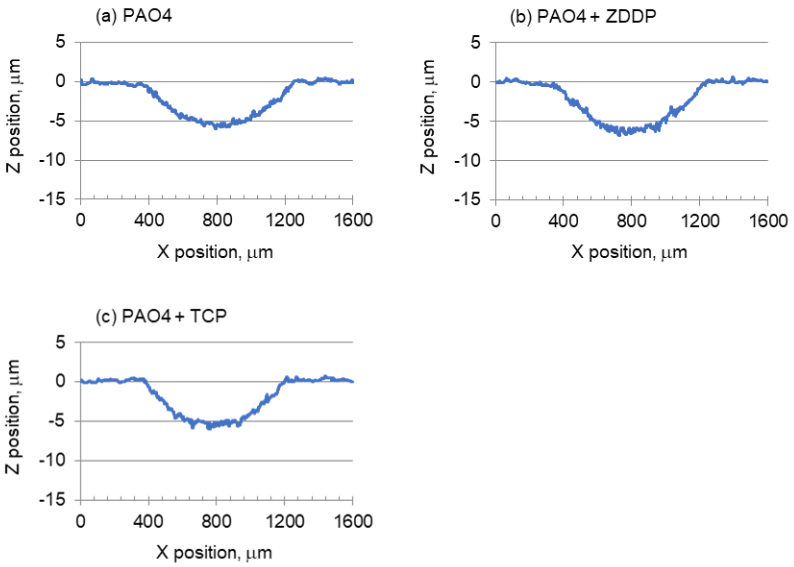

Figure 7.26. Wear profiles of CFR PEEK plates paired with rough steel balls lubricated with (a) PAO4 and (b, c) PAO4 + AW additives

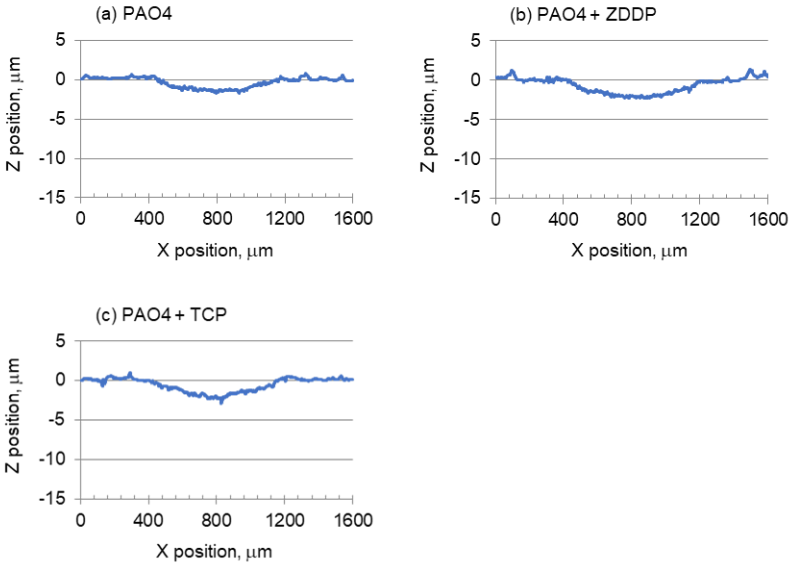

Figure 7.27. Wear profiles of GFR PEEK plates paired with rough steel balls lubricated with (a) PAO4 and (b, c) PAO4 + AW additives

7.2.2 Surface analyses

As seen in section 7.2.1, the addition of the AW additives, ZDDP and TCP, did not influence the friction and wear performance of the PEEK composites-steel contact. This indicate that AW additives did not work well under the test conditions. To confirm this, polymer transfer films on the

steel balls and reaction films formed on the steel balls and the polymer plates were investigated on after-test specimens lubricated with PAO and PAO + ZDDP. Surface analyses were conducted only on the specimens tested with rough steel balls as the wear tracks on the polymer plates and the polymer transfer films on the steel balls were difficult to detect in the PEEK composites-smooth steel contacts.

7.2.2.1 EPMA of polymer transfer films

EPMA of after-test steel ball specimens was performed to investigate the polymer transfer films following the procedure described in section 3.3.3. Secondary Electron (SE) images and EPMA carbon maps on the after-test rough steel balls are shown in Figure 7.28 and Figure 7.29. For CFR PEEK under lubrication with both PAO4 and PAO4 + ZDDP, transfer films were hardly observed on SE images and almost no carbon was detected on the wear tracks in the EPMA carbon maps. For GFR PEEK, the addition of ZDDP had a small impact; it slightly decreased the amount of transfer films on the wear track in both the SE image and the EPMA carbon map. These results correlated well with the wear behaviour that PAO4 and PAO4 + ZDDP gave almost the same wear of both CFR PEEK and GFR PEEK (Figure 7.26 and Figure 7.27).

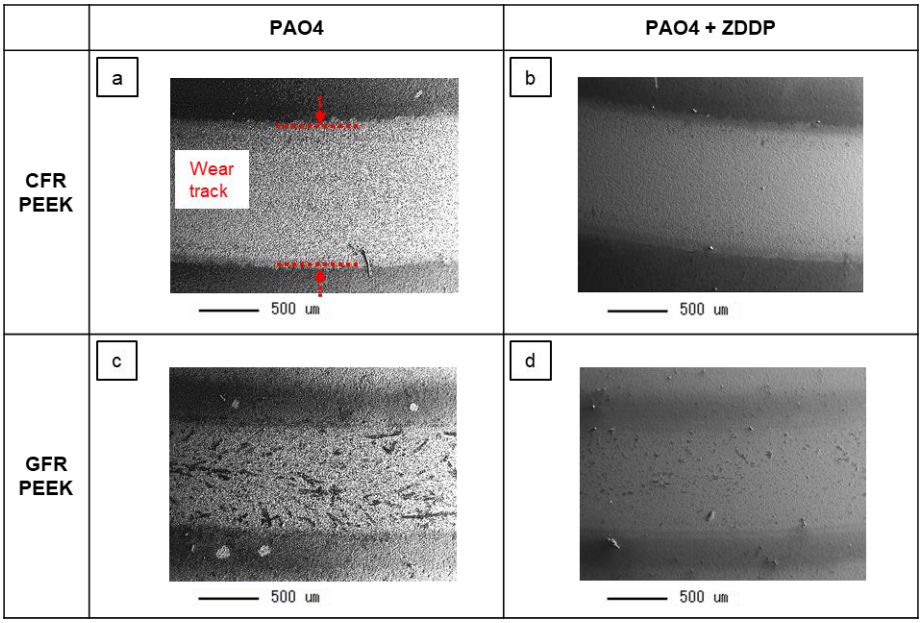

Figure 7.28. SE images of after-test rough steel balls lubricated with (a, c) PAO4 and (b, d) PAO4 + ZDDP

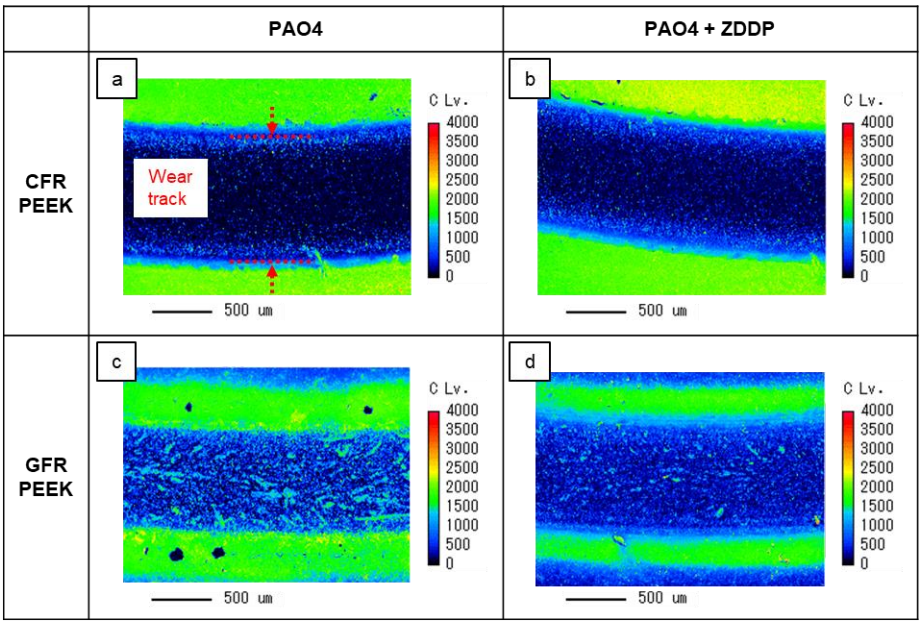

Figure 7.29. EMPA carbon maps of after-test rough steel balls lubricated with (a, c) PAO4 and (b, d) PAO4 + ZDDP

7.2.2.2 EPMA of AW additive reaction films

As described in section 5.2.2.2, if ZDDP reaction films are formed on the steel and/or polymer surfaces, these films may contribute to reducing the wear of the polymer plate. To investigate the presence of ZDDP reaction films, which consist of phosphorus and sulphur atoms, EPMA phosphorus and sulphur mapping was conducted on the after-test steel balls and polymer plates in the PEEK composites-rough steel contact following the procedure described in section 3.3.3.

Figure 7.30 shows the SE images and corresponding EPMA phosphorus and sulphur maps of the after-test rough steel balls lubricated with PAO4 + ZDDP. The amount of phosphorus and sulphur was very low on the steel balls paired with both CFR PEEK and GFR PEEK. This indicates that there was almost no reaction film on the steel surface regardless of the types of PEEK composites.

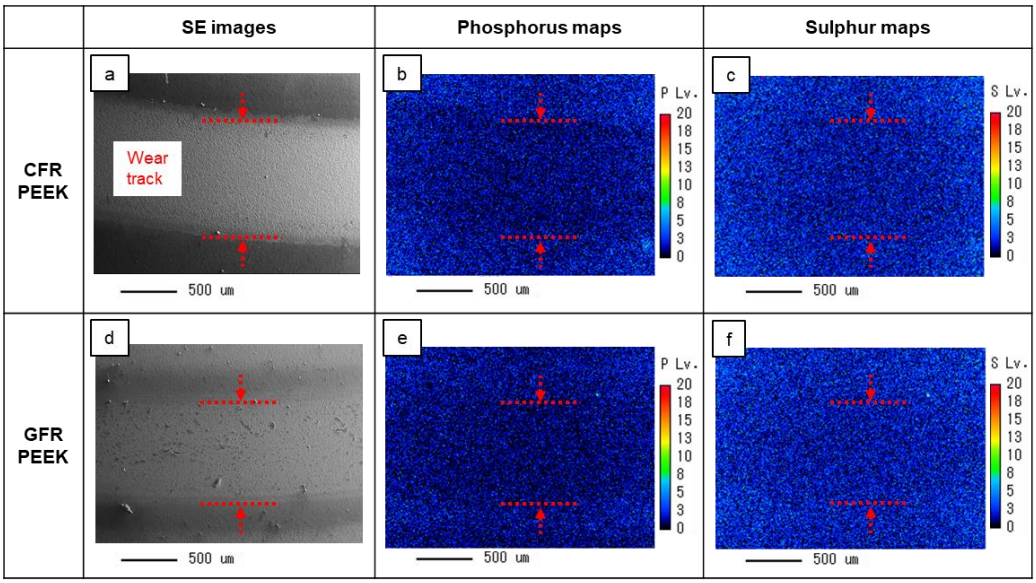

Figure 7.30. (a, d) SE images and corresponding EPMA (b, e) phosphorus and (c, f) sulphur maps of after-test rough steel balls lubricated with PAO4 + ZDDP

The EPMA phosphorus and sulphur maps were also obtained for the after-test polymer plates as shown in Figure 7.31. Similar to the steel balls, the amount of phosphorus and sulphur was very low on both the CFR PEEK and GFR PEEK plates. As phosphorus and sulphur were not detected on both the steel balls and polymer plates, it is concluded that ZDDP did not form a reaction film on the PEEK composites-rough steel contacts under the test conditions applied in section 7.2.1.

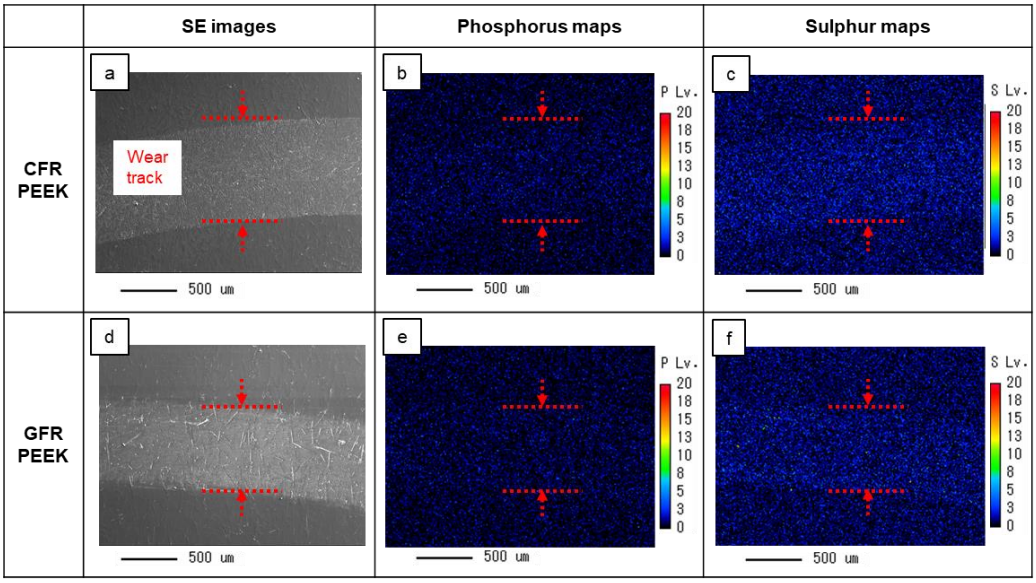

Figure 7.31. (a, d) SE images and corresponding EPMA (b, e) phosphorus and (c, f) sulphur maps of after-test polymer plates lubricated with PAO4 + ZDDP

7.2.3 Testing at higher temperature

As reported in section 7.1.3, the test temperature is an important parameter which influences the effect of OFMs on the tribological performance of pure PEEK and PEEK composites paired with rough steel. AW additives are also known to be more active under more severe operating conditions such as higher temperature [39,113,115,160]. Therefore, this section investigates the effect of ZDDP, the most typical AW additive, at a higher temperature (80 °C).

(a) Friction and wear performance

The tribological test conditions were the same as in section 7.2.1 except for the test temperature. Although this chapter focuses on the PEEK composites, for completeness higher temperature tests were also carried out on pure PEEK as well as on the PEEK composites, CFR PEEK and GFR PEEK, paired with rough steel balls. The Stribeck curves when lubricated with PAO4 and PAO4 + ZDDP are given in Figure 7.32, Figure 7.33 and Figure 7.34. In each figure, the Stribeck curves obtained at ambient temperature (approximately 25 °C) and 80 °C are shown with grey and orange lines, respectively. Irrespective of the polymer types, the addition of ZDDP had little effect on the friction performance at both ambient temperature and 80 °C, i.e., PAO4 and PAO4 + ZDDP gave almost the same Stribeck curves. As already described in section 7.1.3, with the same lubricant, the friction coefficients of pure PEEK showed higher values at 80 °C than at ambient temperature (Figure 7.32), while those of CFR PEEK gave lower values at 80 °C (Figure 7.33). The friction coefficients of GFR PEEK had almost the same values regardless of lubricants or test temperature (Figure 7.34).

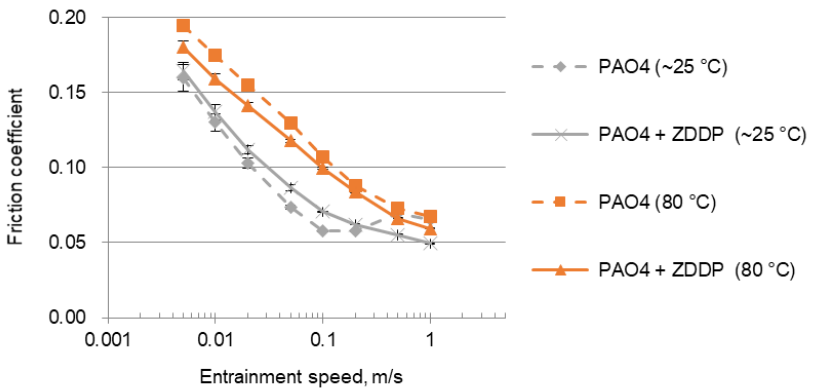

Figure 7.32. Stribeck curves of pure PEEK paired with rough steel balls for PAO4 and PAO4 + ZDDP at ambient temperature (approximately 25 °C) and 80 °C

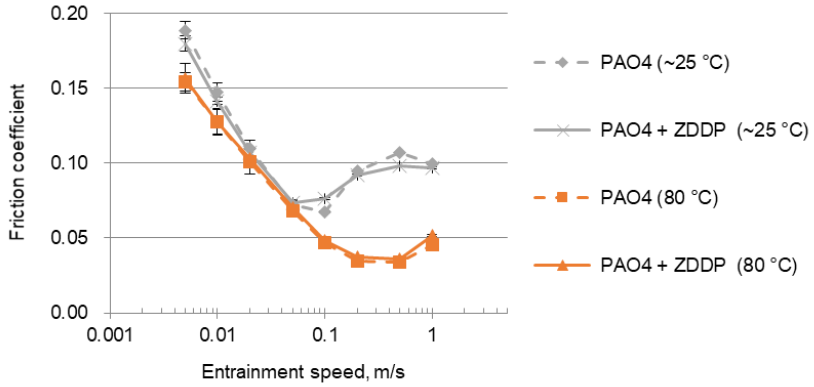

Figure 7.33. Stribeck curves of CFR PEEK paired with rough steel balls for PAO4 and PAO4 + ZDDP at ambient temperature (approximately 25 °C) and 80 °C

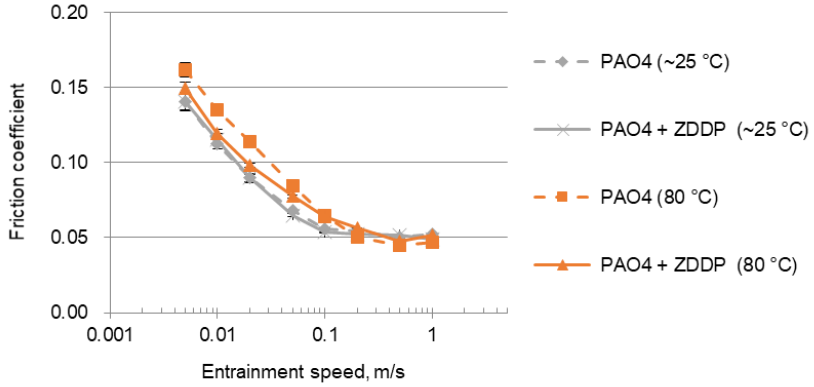

Figure 7.34. Stribeck curves of GFR PEEK paired with rough steel balls for PAO4 and PAO4 + ZDDP at ambient temperature (approximately 25 °C) and 80 °C

The optical images and wear profiles of the after-test polymer plates tested at 80 °C are presented in Figure 7.35 and Figure 7.36. Similar to the friction coefficient results, the addition of ZDDP had little impact on the wear performance at 80 °C, i.e., PAO4 and PAO4 + ZDDP produced almost the same wear profiles for pure PEEK, CFR PEEK and GFR PEEK. These results indicate that ZDDP did not work in the PEEK composites-rough steel contacts even at a higher temperature. This was confirmed by the investigation with EPMA.

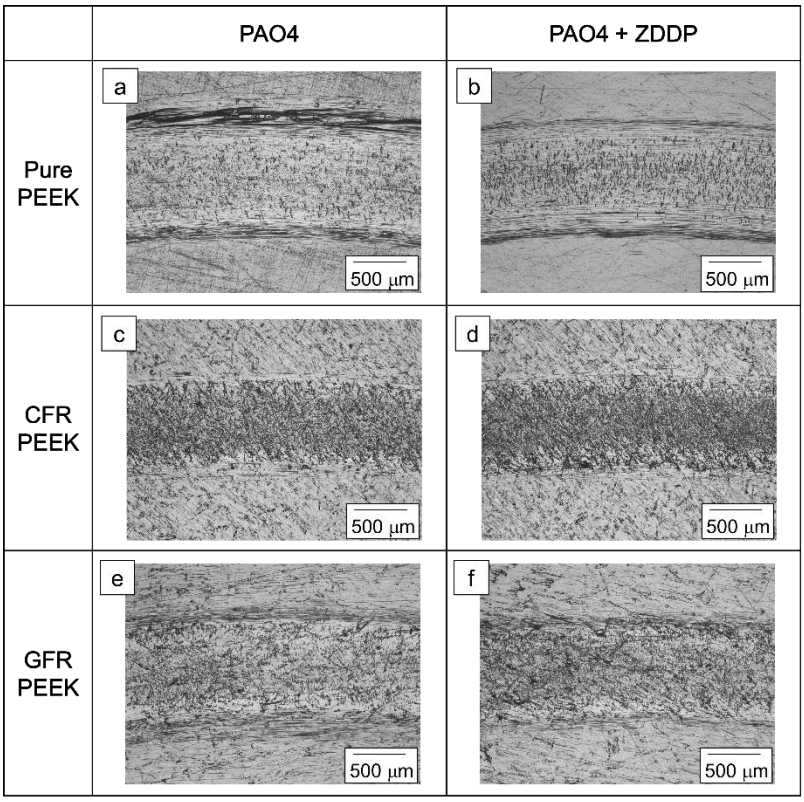

Figure 7.35. Optical images of after-test polymer plates paired with rough steel balls and lubricated with (a, c, e) PAO4 and (b, d, f) PAO4 + ZDDP at 80 °C

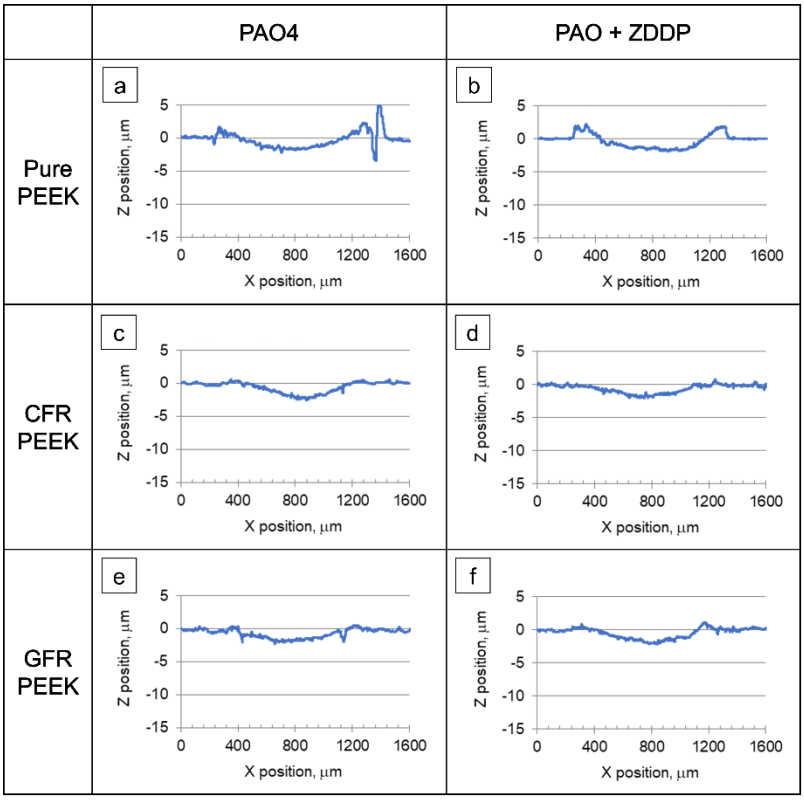

Figure 7.36. Wear profiles of after-test polymer plates paired with rough steel balls and lubricated with (a, c, e) PAO4 and (b, d, f) PAO4 + ZDDP at 80 °C

(b) EPMA

EPMA on the after-test steel ball specimens was performed to investigate both the polymer transfer films and the ZDDP reaction films following the procedure described in section 3.3.3. Secondary Electron (SE) images and EPMA carbon maps on the after-test rough steel balls are shown in Figure 7.37 and Figure 7.38. Regardless of the type of polymer, the addition of ZDDP had little influence on the amount of transfer films detected on the wear tracks. In the case of GFR PEEK, PAO4 + ZDDP produced slightly less film than PAO4, but the influence of this AW additive was much less than that of the OFM (OSa) reported in section 7.1.3. Bearing in mind that a slight inhibition of the formation of polymer transfer films by ZDDP was also observed at ambient temperature in section 7.2.2.1, the addition of ZDDP is thought to slightly inhibit the formation of polymer transfer films. However, as this inhibiting effect is small compared with the acceleration of the formation of polymer transfer films at high temperature, the effect of ZDDP was hardly noticeable for pure PEEK and CFR PEEK.

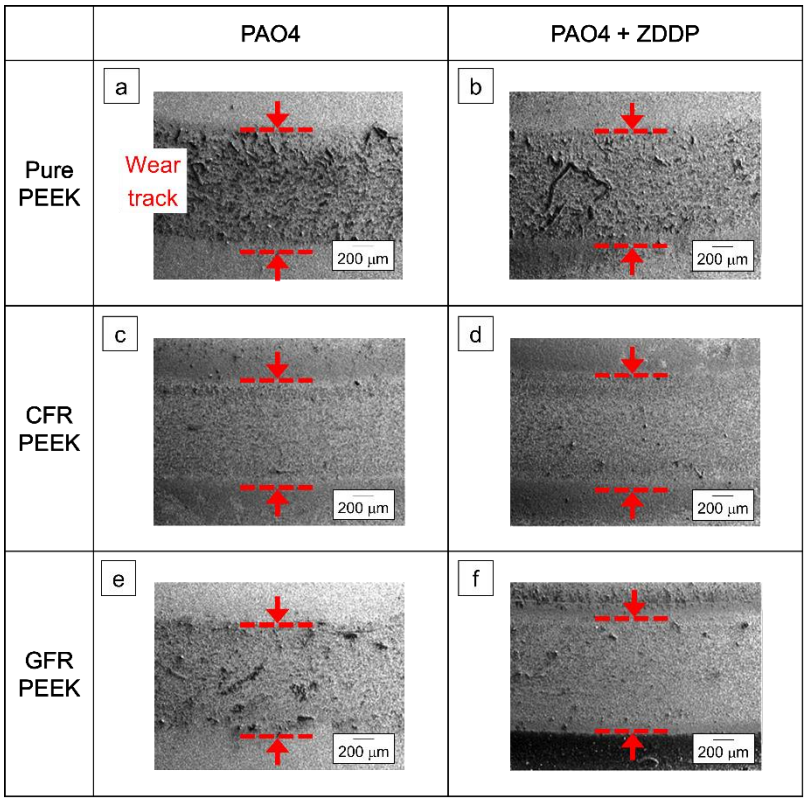

Figure 7.37. SE images of after-test rough steel balls lubricated with PAO4 and PAO4 + ZDDP at 80 °C

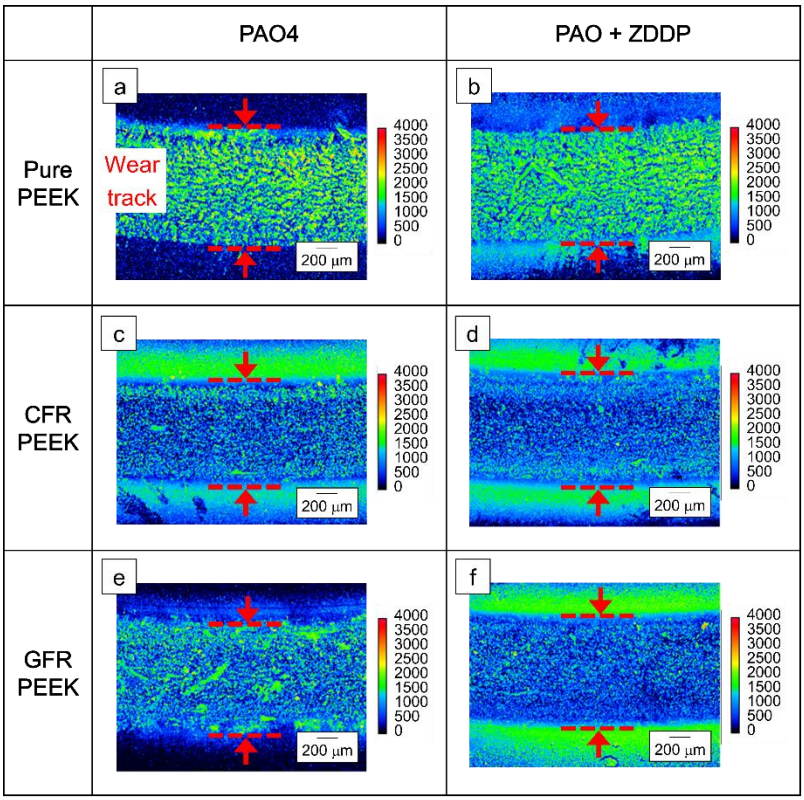

Figure 7.38. EPMA carbon maps of after-test rough steel balls lubricated with (a, c, e) PAO4 and (b, d, f) PAO4 + OSa at 80 °C

Figure 7.39 shows the SE images and corresponding EPMA phosphorus and sulphur maps of the after-test rough steel balls lubricated with PAO4 + ZDDP at 80 °C. There was very little phosphorus and sulphur on the steel balls regardless of the type of polymers tested. This indicates that there was almost no reaction film on the steel surface. There was also very little phosphorus and sulphur on the polymer plates as shown in Figure 7.40. Together these results indicate that ZDDP did not form a reaction film on the polymer-rough steel contacts even when tested at 80 °C. The working mechanism of the AW additives (ZDDP) will be further discussed in section 7.3.2.

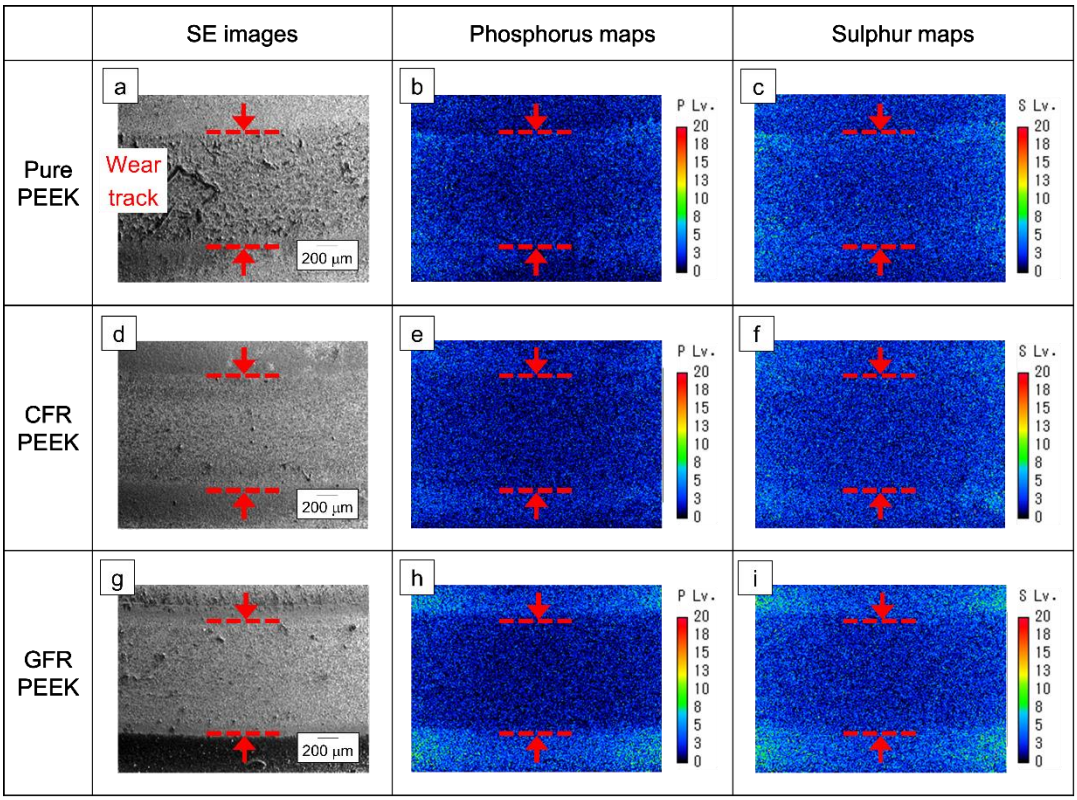

Figure 7.39. (a, d, g) SE images and corresponding EPMA (b, e, h) phosphorus and (c, f, i) sulphur maps of after-test rough steel balls lubricated with PAO4 + ZDDP at 80 °C

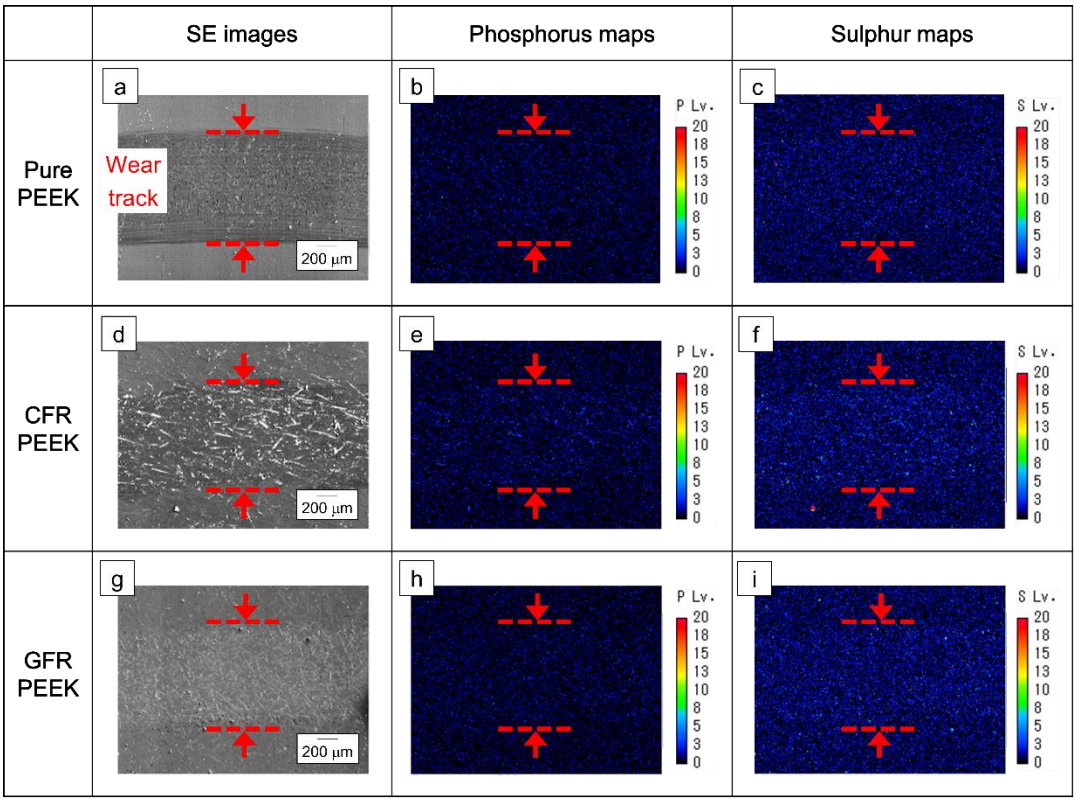

Figure 7.40. (a, d, g) SE images and corresponding EPMA (b, e, h) phosphorus and (c, f, i) sulphur maps of after-test PEEK plates lubricated with PAO4 + ZDDP at 80 °C

7.3 Discussion

As reported in Chapter 5, OFMs, especially OSa, greatly affected the friction and wear properties of the pure PEEK-steel contact, while the effect of AW additives was limited compared to that of the OFMs. A similar trend was observed for the PEEK composites-steel contacts investigated in this chapter. Based on the experimental results of tribological testing and surface analyses, this section discusses the working mechanisms of OFMs and AW additives in more detail.

7.3.1 Working mechanism of OFMs

As indicated in section 7.1.1, the effect of OFMs on the friction and wear performance of the PEEK composites-steel contacts were similar to that of the pure PEEK-steel contact when tested in the sliding-rolling condition reported in Chapter 5, i.e., OFMs reduced friction in the polymer-smooth steel contacts, while they increased friction and wear of the polymer when paired with the rough steel. These results suggest that the working mechanism of OFMs in the PEEK composites-steel contacts is similar to that in the pure PEEK-steel contact discussed in section 5.3.1. Chapter 6 indicated that the reinforcement fibres contained in the PEEK composites changed the working mechanism when paired with rough steel. Taking these aspects into account, the working mechanism of OFMs in the PEEK composites-steel contacts is summarized below.

(a) PEEK composite-smooth steel contact

As reported in section 7.1.1, when paired with smooth steel, the effect of OFMs on CFR PEEK and GFR PEEK is similar to that on pure PEEK. This suggests that OFMs work similarly regardless of polymer types, as shown in Figure 7.41. The nanoindentation measurement results in section 6.1.2.2 reveal that the surfaces of pristine CFR PEEK and GFR PEEK plates consist almost entirely of the PEEK matrix. As there was almost no wear of the CFR PEEK and GFR PEEK plates when paired with smooth steel under lubrication with both PAO4 and PAO4 + OFMs as reported in section 7.1.1, OFMs are assumed to adsorb on both the steel surface and the PEEK matrix of CFR PEEK and GFR PEEK and so reducing friction.

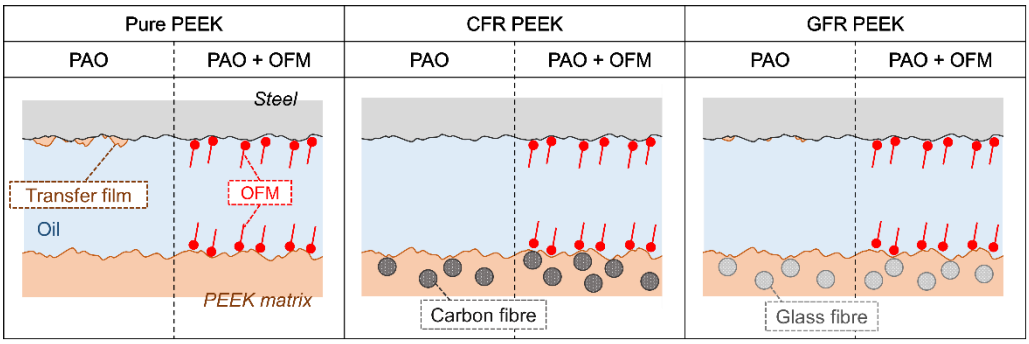

Figure 7.41. Schematic of contact surfaces in polymer-smooth steel contacts lubricated with PAO and PAO + OFM

(b) PEEK composite-rough steel contact

Section 5.3.1 reported that in the PEEK-rough steel contact, OFMs inhibit the formation of PEEK transfer films on the steel counterparts, thus increasing friction and wear of PEEK. Based on the results of the tribological testing and surface analyses presented in section 7.1, the mechanism of action of PEEK composites-rough steel contact is as shown in Figure 7.42. As discussed in section 6.3.2, in the CFR PEEK tests, the fractured carbon fibres exposed on the polymer surface wear off, by abrasion, the polymer transfer films on the steel counterparts and thus inhibit film formation even under PAO lubrication. Therefore, it is difficult to observe any further inhibition of polymer transfer films by OFMs. However, the fact that the addition of OFMs increased friction and wear supports the following: some polymer transfer films are formed on the rough steel surface even when paired with CFR PEEK, but they are removed immediately, resulting in less film being detected at the end of the test. Despite these films being temporary, they can contribute to reducing friction and wear. The addition of OFM inhibits the formation process of these films, and thus increases friction and wear of CFR PEEK. In the GFR PEEK tests, the polymer transfer film formed is thick even under PAO lubrication as was the case for pure PEEK. The glass fibres on the wear tracks were less damaged and better embedded in the PEEK matrix, therefore not causing the negative effect on film formation seen for the exposed carbon fibres. OFM inhibits the formation of polymer transfer films on the steel counterparts, thus increasing friction and wear of GFR PEEK.

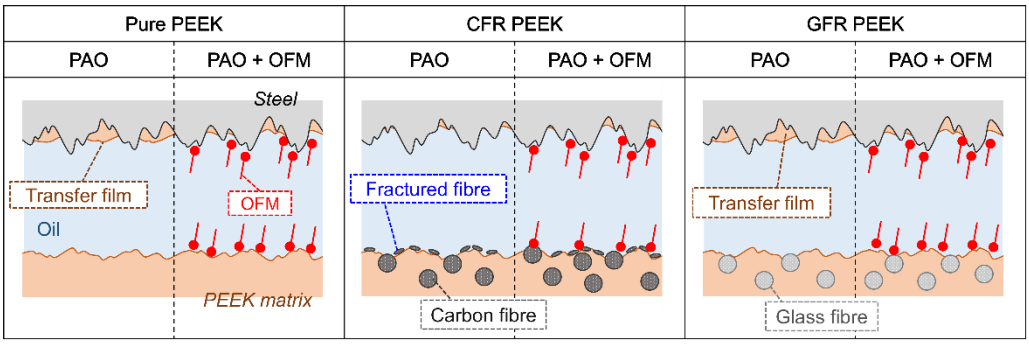

Figure 7.42. Schematic of contact surfaces in polymer-rough steel contacts lubricated with PAO and PAO + OFM

Even when lubricated at a higher temperature, the mechanism of action is basically the same as that at ambient temperature (approximately 25 °C). As discussed in section 4.3.2, the total amount of polymer transfer films is determined by the balance between the formation and removal processes which depends on the tribological test conditions. At a higher temperature, the formation of the polymer transfer films is enhanced by the softening of the polymer surfaces caused by heat [19]. As a result, the formation process of the polymer transfer film is faster than the removal process, resulting in thicker transfer films than at ambient temperature. Taking this into account, the schematic of the contact surfaces in the polymer-rough steel contacts lubricated with PAO and PAO + OFM at a higher temperature is modified as shown in Figure 7.43. As shown in section 7.1.3, thick transfer films are formed at a higher temperature irrespective of polymer types. In the pure PEEK-steel contact, the friction coefficient under PAO4 lubrication had higher values at a high temperature than those at ambient temperature as reported in Figure 7.13. EPMA carbon maps (Figure 7.19) support the idea that the excessively thick transfer film increases friction. OFM (OSa) inhibits the formation of polymer transfer films at a high temperature as well as at ambient temperature, but sufficient polymer transfer films are still formed at a high temperature, due to the acceleration of the formation of these films, resulting in low wear of polymers even under lubrication with PAO + OFM. In the CFR PEEK-steel contact, many fractured carbon fibres are found on the polymer surface when tested at ambient temperature as shown in Figure 7.42. However, the amount of fractured fibres was much less in the high temperature tests under lubrication with both PAO and PAO + OFM due to the polymer transfer films mitigating contact.

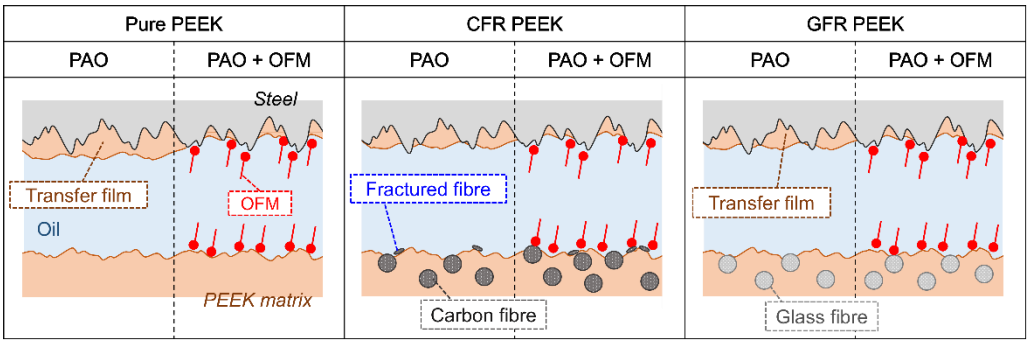

Figure 7.43. Schematic of contact surfaces in polymer-rough steel contacts lubricated with PAO and PAO + OFM at high temperature

7.3.2 Working mechanism of AW additives

In this study, the effect of AW additives on the tribological performance of CFR PEEK and GFR PEEK paired with steel counterparts were not readily apparent at both ambient temperature (approximately 25 °C) and at high temperature (80 °C) as reported in section 7.2.1 and section 7.2.3. As no reaction film was detected on both the steel and the polymer surfaces irrespective of the test temperature, AW additives are assumed not to work in the PEEK composites-steel contacts at least under the sliding-rolling condition (50% SRR) used in this chapter. As reported in Chapter 5, ZDDP did form a thin reaction film on the PEEK surface in the sliding condition (200% SRR), resulting in a slight improvement in the wear of the PEEK plate. However, the impact of ZDDP was much less than that of OFMs.

The above might be explained by the fact that Fujita and Spikes reported that thermal action alone cannot explain the formation of a ZDDP reaction film and suggested that the ZDDP reaction film formation is strongly catalysed by species released during rubbing, such as soluble Fe^{2+} or Fe^{3+} [160]. In the PEEK-steel and PEEK composite-steel contacts, no wear of the steel surface was observed under lubricated conditions and thus there were no catalyst species to accelerate the formation of the ZDDP reaction film. Most AW additives such as TCP also need this kind of surface catalysis to form reaction films [114], while OFMs can work by physically adsorbing on the surfaces [98,99].

Based on the discussion above, in both PEEK-steel and PEEK composites-steel contacts AW additives have less influence on tribological performance due to their lack of ability to form the reaction films. Although AW additives can affect the friction and wear performance under limited condition, their impact is much lower than that of OFMs.

7.4 Summary

This chapter investigated the effect of organic friction modifiers (OFMs) and anti-wear (AW) additives on the lubrication of carbon fibre reinforced (CFR) PEEK and glass fibre reinforced (GFR) PEEK paired with steel counterparts. In addition to the tests carried at ambient temperature (approximately 25 °C), tests at 80 °C were also conducted to investigate the working mechanism of these lubricant additives.

Firstly, tribological tests using a MTM were performed on CFR PEEK-steel and GFR PEEK-steel contacts under lubrication with PAO4 and PAO + OFMs, oleylamine (OAm), oleic acid (OAc) and N-oleoyl sarcosine (OSa). Surface analyses of after-test specimens by Alicona and EPMA were conducted, focusing both on the distribution of the reinforcement fibres on polymer surfaces and on the formation of polymer transfer films on the steel counterparts. In addition, tribological testing at a higher temperature (80 °C) was carried out to investigate the mechanism of action of OFMs. The following conclusions have been drawn:

(1) In PEEK composites-smooth steel contacts, OFMs, especially OSa, reduced friction both for CFR PEEK and GFR PEEK. Although their impact was less for CFR PEEK, this friction reducing effect for PEEK composites is similar to that found for pure PEEK. In the PEEK composites-rough steel contact, OFMs, most significantly OSa, increased friction and wear for both CFR PEEK and GFR PEEK as well as for pure PEEK;

(2) When paired with rough steel, a large amount of fractured and exposed carbon fibres was detected on the wear tracks of CFR PEEK, while less damaged and well embedded glass fibres were observed on the GFR PEEK wear track. PAO4 and PAO4 + OFM (OSa) produced almost the same wear track features for both PEEK composites;

(3) The addition of OFM (OSa) inhibited the formation of polymer transfer films on the steel counterparts causing an increased wear of both CFR PEEK and GFR PEEK, as well as pure PEEK;

(4) When tested at a higher temperature (80 °C), thicker polymer transfer films were formed on the steel surface irrespective of the type of polymers, resulting in low wear of the polymers even under lubrication with PAO + OFM;

(5) The working mechanism of OFMs in the PEEK composites-steel contacts is thought to be similar to that of the pure PEEK-steel contact. The adsorption of OFMs on the contact surfaces and the formation of the polymer transfer films on the steel surfaces are the key factors controlling tribological performance and these two phenomena are interdependent.

Secondly, tribological tests were conducted with PAO4 and PAO4 + AW additives, ZDDP and TCP. In addition to EPMA carbon maps of the after-test steel balls to evaluate the amount of PEEK transfer films present, EPMA phosphorous and sulphur maps of the after-test steel balls and PEEK plates were obtained to investigate any reaction films formed by the AW additive (ZDDP). Tribological tests at 80 °C were also carried out to investigate the mechanism of action of AW additives:

(1) The addition of ZDDP and TCP had little impact on the friction and wear performance of the PEEK composites-steel contacts irrespective of the polymer types or surface roughness of the steel balls. This was also found in the high temperature tests;

(2) No reaction film derived from ZDDP was detected on both the steel and polymer surfaces even when tested at 80 °C;

(3) In PEEK composites-steel contacts, AW additives have less effect on tribological performance than OFMs due to their lack of ability to form reaction films.

.

Chapter 8 Conclusions and future work

8.1 Conclusions

The aim of this study was to elucidate the effect of lubrication on the tribological properties of PEEK and its composites and thus ascertain the lubrication mechanism. Tribological tests were mainly performed on PEEK, carbon fibre reinforced (CFR)PEEK and glass fibre reinforced (GFR) PEEK paired with steel using a Mini Traction Machine (MTM) which simulates the sliding-rolling contact motion encountered in gears, one of the main expected applications of this study. Base oils with/without lubricant additives, namely organic friction modifiers (OFMs) and anti-wear (AW) additives, were employed as test lubricants. To further investigate the mechanism of action, after-test specimens were analysed using various surface analysis techniques e.g., 3D surface profilometer, nanoindentation, Electron Probe Micro Analysis (EPMA), X-ray Photoelectron Spectroscopy (XPS) and Raman spectroscopy.

The main conclusions from the results of this study are as follows:

(a) The effect and working mechanism of base oil lubrication on the tribological properties of PEEK

Compared with dry conditions, lubrication with PAO4, as a base oil, reduced the friction of the PEEK-steel contact regardless of the operating conditions (i.e. SRR). By contrast, lubrication has a positive or negative effect on the wear of PEEK, depending on SRR. Lubrication with PAO4 resulted in a softening of the PEEK wear track, but no correlation was established between this and wear performance. The thickness of the PEEK transfer films on the steel counter surfaces was the main parameter that controlled PEEK wear in not only dry conditions but also lubricated conditions. Lubrication with PAO4 inhibited both the formation and the removal of the PEEK transfer films and the resulting balance between these opposing processes explains why lubrication can have both a positive and negative effect on the wear of PEEK, depending on the operating conditions.

The effect of base oil viscosity, one of the most important parameters when designing lubricants suitable for various applications, shows different trends depending on the roughness of the steel counterparts. In PEEK-smooth steel contacts, PAOs with higher viscosity gave lower friction and less damage to the PEEK surfaces, while in PEEK-rough steel contacts higher viscosities resulted in higher friction and greater wear of PEEK. The softening of PEEK wear tracks was observed under some conditions, but little correlation was found with tribological performance. The amount of PEEK transfer films on the steel counterparts correlated well with the tribological properties of the PEEK-

rough steel contact. PAOs with lower viscosity gave more transfer films, resulting in better tribological performance.

By considering the two factors proposed in previous studies to play decisive roles in PEEK-steel contacts, namely hardness modification of PEEK and the presence of PEEK transfer films on steel balls, the working mechanism of base oil lubrication of PEEK can be deduced. Hardness modification of PEEK is caused by the permeation of base oil molecules through the damaged surface and does not directly affect the tribological properties of the PEEK-steel contact. Base oil lubrication inhibits both the formation and removal of the PEEK films. The balance between these processes is controlled by the severity of the tribological conditions, causing both a positive and negative effect on the tribological properties of PEEK. The working mechanism of base oil lubrication depends on the surface roughness of the steel counterparts. In PEEK-smooth steel contacts, the working mechanism of base oil lubrication basically follows the traditional theory after taking into account the modification of the surface roughness by removal (through wear) and/or compression of PEEK asperities. However, base oil lubrication of PEEK-rough steel contacts does not follow the traditional theory due to the PEEK transfer films formed on the steel counterparts.

(b) The effect and working mechanism of lubricant additives (OFMs and AW additives) on the lubrication of PEEK

Of the three types of OFMs which have been widely used in commercial lubricants namely oleylamine (OAm), oleic acid (OAc) and N-oleoyl sarcosine (OSa), OSa gave a significant friction reduction in the PEEK-smooth steel contact at both 50% SRR (sliding-rolling condition) and 200% SRR (sliding condition). A similar friction reducing effect of OSa was observed in the PEEK-PEEK and steel-steel contacts, demonstrating the superior adsorption ability of OSa on both PEEK and steel surfaces. In the PEEK-rough steel contact, OFMs, most significantly OSa, showed opposite effects depending on SRRs, reducing friction and wear at 200% SRR (sliding condition) while increasing them at 50% SRR (sliding-rolling condition). The hardness of the PEEK surfaces was affected by the addition of OSa, but no correlation was observed between the PEEK hardness and the tribological properties of the PEEK-steel contact. However, a good correlation was observed between the amount of PEEK transfer films on the steel counterparts and the tribological properties of the PEEK-steel contact when lubricated with PAO4 and PAO4 + OSa. The working mechanism of OFMs is explained by the adsorption of OFMs on the contact surfaces and the formation of the PEEK transfer films on the steel surfaces. As these two phenomena are interrelated, the effect of OFMs depends on the test conditions, which explains why OFMs can have either a positive or negative effect on the tribological properties.

The addition of ZDDP and TCP slightly reduced friction in the PEEK-smooth steel contact at 200% SRR (sliding condition), but less influence was seen at 50% SRR (sliding-rolling condition). Both ZDDP and TCP did not affect the friction in the PEEK-PEEK contact regardless of SRRs, while their influence on friction in the steel-steel contacts depended on SRRs, indicating that the reaction film formation ability of AW additives is higher on the steel surface than on the PEEK surface. Compared to OFMs, AW additives had less impact on the friction and wear performance in the PEEK-rough steel contact except for ZDDP at 200% SRR (sliding condition) where a slight improvement in the wear of the PEEK plate was seen. PAO4 and PAO4 + ZDDP produced similar amounts of polymer transfer films on the steel countersurface at both 50% SRR (sliding-rolling condition) and 200% SRR (sliding condition) in the PEEK-rough steel contact. At 200% SRR, PAO4 + ZDDP slightly improved the wear of the PEEK plate, probably due to the formation of a ZDDP reaction film. The working mechanism of AW additives is explained by the formation of adsorption films and/or reaction films. The ability of AW additives to form adsorption/reaction films is not as high as OFMs in the PEEK-steel contact. Therefore, AW additives formed thin films only at 200% SRR (sliding condition) which can provide higher frictional heat to accelerate the adsorption/reaction of AW additives.

(c) The effect and working mechanism of base oil lubrication on the tribological properties of CFR PEEK and GFR PEEK

Although lubrication with PAO4 reduced the friction of both CFR PEEK and GFR PEEK paired with rough steel compared to dry condition, GFR PEEK gave significantly lower friction and wear than CFR PEEK. In dry conditions, the CFR and GFR PEEK gave similar wear tracks with piled up wear debris containing fractured fibres. In PAO4 lubricated conditions, the reinforcement fibres were observed on the wear tracks, especially and in greater amount for CFR PEEK. On the wear tracks the carbon fibres of CFR PEEK were exposed and fractured, while the glass fibres of the GFR PEEK were less damaged and well embedded in the matrix. Both the carbon and glass fibres distributed on the wear tracks were much harder than the PEEK matrix. There was a large difference in the area covered by the reinforcement fibres e.g. the carbon fibres covered about 40% of the wear tracks, while the glass fibres covered less than 5%. In PAO4 lubricated conditions, the amount of the polymer transfer films on the steel counter surfaces correlated well with the tribological performance. No transfer film was observed for the CFR PEEK test, while a thick transfer film was detected for the GFR PEEK test which imparted a lower friction and wear.

In PEEK composites-smooth steel contacts, the PAOs gave almost the same friction coefficients for both CFR PEEK and GFR PEEK. When paired with rough steel, the effect of base oil viscosity shows different trends depending on the polymer types. The friction and wear in the CFR PEEK tests

showed lower values when lubricated with higher viscosity PAOs, while the friction and wear in the GFR PEEK tests were less influenced by the PAO viscosity. In PEEK composites-rough steel contacts, fractured and exposed carbon fibres on the wear tracks of CFR PEEK were detected in larger amounts under lubrication with lower viscosity PAO. The less damaged and well embedded glass fibres on the GFR PEEK were observed similarly regardless of the PAO viscosity. In PEEK composites-rough steel contacts, the thickness of the polymer transfer films on the steel counter surfaces correlated well with the tribological performance. No transfer film was observed for the CFR PEEK test regardless of the PAO viscosity, while a thick transfer film was detected for the GFR PEEK test especially when lubricated with PAO2 and PAO4.

There were more fractured fibres on the wear tracks of CFR PEEK than GFR PEEK. The fractured carbon fibres did not contribute to improving wear resistance. In fact, it reduced it by inhibiting the formation of polymer transfer films on steel counterparts. The polymer transfer film on steel counterparts was also the main parameter that controlled the tribological performance of PEEK composites-steel contacts. Hardness modification of polymer surfaces and the formation of polymer transfer films on the steel counter surfaces were interrelated. Fractured fibres exposed on the wear tracks of CFR PEEK plates after testing possibly inhibited the formation of polymer transfer films on steel counterparts. In contrast, the wear tracks on GFR PEEK plates showed the fibres were well matrix embedded and less damaged, enabling the formation of transfer films similar to those found on pure PEEK. The working mechanism of base oil lubrication depends on the surface roughness of the steel counterparts. Similar to pure PEEK-smooth stell, in PEEK composites-smooth steel contacts, the mechanism follows the traditional theory after taking into account the modification of the surface roughness by removal (through wear) and/or compression of polymer asperities. In PEEK composites-rough steel contacts, CFR PEEK and GFR PEEK showed different trends depending on the thickness of the polymer transfer films formed. Owing to the lack of formation of transfer films, CFR PEEK continued to follow the traditional theory. On the other hand, GFR PEEK formed thick transfer films on the steel counter surfaces and gave lower friction and wear than that expected from the traditional theory.

(d) The effect and working mechanism of lubricant additives (OFMs and AW additives) on lubrication of CFR PEEK and GFR PEEK

In PEEK composites-smooth steel contacts, OFMs, especially OSa, reduced friction both for CFR PEEK and GFR PEEK. Although their impact was less noteworthy for CFR PEEK, this friction reducing effect for PEEK composites is similar to that found for pure PEEK. In the PEEK composites-rough steel contact, OFMs, most significantly OSa, increased friction and wear for both CFR PEEK and GFR

PEEK as well as for pure PEEK. When paired with rough steel, a large amount of fractured and exposed carbon fibres was detected on the wear tracks of CFR PEEK, while less damaged and well embedded glass fibres were observed on the GFR PEEK wear track. PAO4 and PAO4 + OFM (OSa) produced almost the same wear track features for both PEEK composites. The addition of OFM (OSa) inhibited the formation of polymer transfer films on the steel counterparts causing an increased wear of both CFR PEEK and GFR PEEK as well as pure PEEK. When tested at a higher temperature (80 °C), thicker polymer transfer films were formed on the steel surface irrespective of the type of polymers, resulting in low wear of the polymers even under lubrication with PAO + OFM. The working mechanism of OFMs in the PEEK composites-steel contacts is thought to be similar to that of the pure PEEK-steel contact. The adsorption of OFMs on the contact surfaces and the formation of the polymer transfer films on the steel surfaces are the key factors controlling tribological performance and these two phenomena are interdependent.

The addition of the AW additives, ZDDP and TCP, had little impact on the friction and wear performance of the PEEK composites-steel contacts irrespective of the polymer types or surface roughness of the steel balls. This was also found in the high temperature tests. No reaction film derived from ZDDP was detected on both the steel and polymer surfaces even when tested at 80 °C. In PEEK composites-steel contacts, AW additives have less effect on tribological performance than OFMs due to their lack of ability to form reaction films.

Table 8.1 summarizes the impact of SRR, oil viscosity, OFMs and AW additives on the tribological properties along with the two key parameters: polymer transfer film formation and hardness modification of polymer surface. The criterion of high impact especially for tribological properties, friction and wear is set to approximately $\pm$30%.

Table 8.1. Impact of SRR, oil viscosity, OFM and AW additive on tribological properties of PEEK and PEEK composites when paired with smooth and rough steel

Material pairing		PEEK-steel		CFR PEEK-steel		GFR PEEK-steel	
Steel roughness		Smooth	Rough	Smooth	Rough	Smooth	Rough
Impact of SRR	Tribological properties	Medium	High	-	-	-	-
	Polymer transfer film formation	Medium	High	-	-	-	-
	Hardness modification of polymer surface	Medium	Low	-	-	-	-
Impact of oil viscosity	Tribological properties	Medium	High	Low	High	Low	Low
	Polymer transfer film formation	Low	High	Low	Low	Low	Medium
	Hardness modification of polymer surface	Medium	Low	-	Low	-	Low
Impact of OFM	Tribological properties	High	High	Medium	Medium	High	High
	Polymer transfer film formation	Low	High	Low	Medium	Low	High
	Hardness modification of polymer surface	Medium	Medium	-	Low	-	Low
Impact of AW additive	Tribological properties	Medium	Medium	Low	Low	Low	Low
	Polymer transfer film formation	Low	Low	Low	Low	Low	Low
	Hardness modification of polymer surface	-	-	-	-	-	-

The overall results indicate that the polymer transfer film that forms on the steel counterparts is the dominant factor controlling the tribological properties of the PEEK-steel and PEEK composites-steel contacts, especially when the steel has a rough surface. The polymer transfer films are assumed to act as protective films, thus preventing the direct contact of the relatively soft polymer surfaces with the hard asperities of the steel surfaces and so reducing the wear of the polymers. Although this contribution of polymer transfer films has been previously found in dry conditions, this study reveals their significance under lubrication and the mechanism of action. Furthermore, the novelty of this study is that the effect and working mechanism of lubricant oil viscosity and lubricant additives (OFMs and AW additives) were examined based on the tribological test results and surface analyses of after-test specimens. Although they work in a similar manner to that in the steel-steel contact to some extent, their effect on the formation of polymer transfer films should be taken into account in the PEEK-steel and PEEK composites-steel contacts. The knowledge obtained in this study will aid the development of appropriately formulated lubricants which will help to improve the efficiency and durability of the tribological applications envisaged for PEEK and

its composites, and promote their adoption in green technologies which will contribute to reducing CO_2 emission, e.g. by reducing weight through replacement of metallic gears with polymeric ones in automobiles which contain a large number of gears to transmit engine/motor power to the wheels.

8.2 Future work

This study, which focuses on the lubrication of PEEK and its composites, could contribute to our understanding of the tribological properties of other polymers under lubrication, because the fundamental mechanism of action is expected to be common to some extent. However, as the current work has only covered limited types of polymers and lubricants, further investigation is necessary to obtain more generalized knowledge of the lubrication of polymers. In addition, the development of lubricants and lubricant additives for polymers is required. Future work should address the following topics:

(a) Lubrication of various types of polymers

PEEK and its composites have superior mechanical properties and higher thermal stabilities to conventional polymers, therefore they are preferably used for tribological applications under severe conditions. On the other hand, the material costs of PEEK and its composites are much more expensive compared to conventional polymers such as PA (Polyamides, 'Nylon') and POM (Polyoxymethylene or Polyacetal) [52]. The fundamental mechanism of lubrication is expected to be somewhat similar in these polymers. However, the amount of polymer transfer films formed on steel counterparts, which is revealed as the dominant factor controlling the tribological properties in this study, might be different in PEEK to other polymers, because the energy needed for their transfer depends on chemical structures of the polymers [81]. As found for PEEK and its composites in this thesis, lubrication affects the formation and removal processes of polymer transfer films and shows a positive or negative effect depending on their balance. These aspects should be investigated for other polymers.

In addition, the effect of the solid lubricants contained in polymer composites under lubrication also warrants attention. Polymer composites envisaged for tribological applications under dry conditions often contain both reinforcement fibres and solid lubricants such as graphite, PTFE and MoS_2. This study used PEEK composites with only reinforcement fibres, because lubrication is expected to improve the tribological properties of these polymers which do not have additions of

expensive solid lubricants. However, to maximize the tribological performance of polymers under lubrication, the effect of solid lubricants under lubrication should be investigated.

(b) Development of lubricants and lubricant additives for polymers

This study aimed to obtain fundamental knowledge on the lubrication of polymers, and therefore the lubricants tested had simple formulations consisting of a base oil or a base oil with one type of lubricant additive and focused on OFMs and AW additives which are known to strongly affect tribological properties. Lubricants for practical usage for steel-steel contacts commonly contain a number of lubricant additives, and in some cases, they work synergistically or antagonistically [152,161–163]. This might be the same for polymer-steel contacts, and therefore the interaction between multiple lubricant additives should be investigated to develop desirably formulated lubricants for polymers.

Furthermore, the development of lubricant additives for polymers will be expected to be based on the working mechanisms obtained in this study. Existing lubricant additives have been developed for use in steel-steel contacts and are not designed to work effectively in polymer-steel contacts as was the case of ZDDP. On the other hand, the fact that OSa, an OFM, had a significant positive or negative impact on the tribological performance of lubricated PEEK and its composite depending on the operating conditions suggests that a specially designed lubricant additive for polymers achieved through the optimisation of the modification of the chemical structure of OSa should be considered.

Appendix A Oil film thickness estimation

In section 4.3.3 and section 6.3.3, the values of oil film thickness were used to determine the Lambda ratios under the operating conditions. They were estimated from the equations presented by Hamrock and Dowson [150,151] as described in this appendix.

In general, there are four lubrication regimes in EHL contacts:

(a) Isoviscous-Rigid

(b) Piezoviscous-Rigid

(c) Isoviscous-Elastic (soft EHL)

(d) Piezoviscous-Elastic (hard EHL)

As shown in Figure A.1, each of these regimes is characterized by the operating conditions and the properties of the material by using the parameters G_V and G_E given by Equations A-1 and A-2:

$$G_v = G\frac{W^3}{U^2} \quad \text{(Eq. A-1)}$$

$$G_E = \frac{W^{8/3}}{U^2} \quad \text{(Eq. A-2)}$$

where U, G, and W are dimensionless parameters given by Equations A-3, A-4 and A-5:

$$U = u\eta_0/E'R_x \quad (\textit{Speed parameter}) \quad \text{(Eq. A-3)}$$

$$G = \alpha \mathrm{E}' \quad (\textit{Materials parameter}) \quad \text{(Eq. A-4)}$$

$$\mathrm{W} = w/E'R_x^2 \quad (\textit{Load parameter}) \quad \text{(Eq. A-5)}$$

where u is the *entrainment velocity* defined as the average of surface velocities with respect to the contact, w is the normal load, α is the viscosity–pressure coefficient of lubricants, η_0 is the dynamic viscosity of lubricants at ambient pressure, E' is *reduced Young's modulus* defined as Equation A-6:

$$\frac{2}{E'} = \frac{1-v_A^2}{E_A} + \frac{1-v_B^2}{E_B} \quad \text{(Eq. A-6)}$$

where υ_A and υ_B are the Poisson's ratio of the contacting bodies 'A' and 'B', respectively, E_A and E_B are the Young's modulus of the contacting bodies 'A' and 'B', respectively.

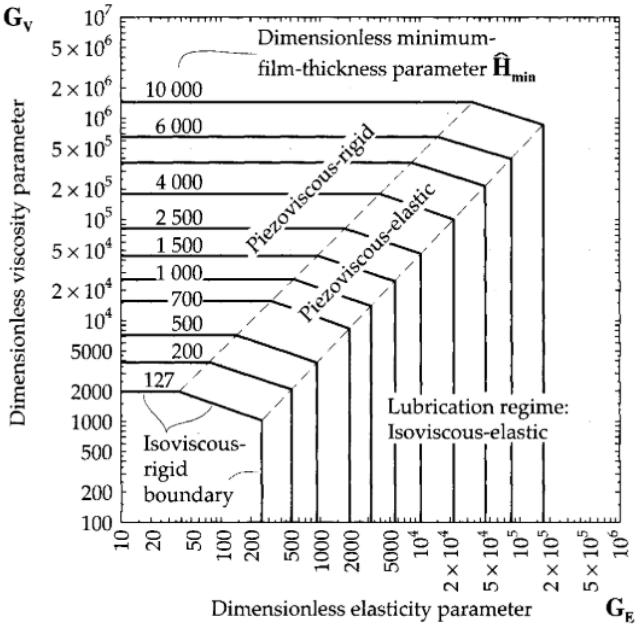

Figure A.1. Map of lubrication regimes for an ellipticity (parameter k = 1) (adapted from [99])

Based on the numerical results for Piezoviscous-Elastic (hard EHL) contacts with two rigid spheres (or an equivalent sphere and plane), Hamrock and Dowson presented Equations A-7 and A-8 for the minimum and centre film thicknesses in hard EHL contacts [150]:

$$h_{min}/R_x = 3.63\, U^{0.68}\, G^{0.49}\, W^{-0.073}\left(1 - e^{-0.68k}\right) \qquad \text{(Eq. A-7)}$$

$$h_c/R_x = 2.69\, U^{0.67}\, G^{0.53}\, W^{-0.067}\left(1 - 0.61e^{-0.73k}\right) \qquad \text{(Eq. A-8)}$$

where k is the *ellipticity parameter* defined as R_y/R_x, R_y and R_x are the effective radii in the y and x directions, respectively (x is the moving or sliding/rolling direction). As described above, U, G, and W are dimensionless parameters given by Equations A-3, A-4 and A-5.

Hamrock and Dowson also proposed Equations A-9 and A-10 for the film thicknesses at Isoviscous-Elastic (soft EHL) contacts for materials of low elastic modulus such as polymers [151]:

$$h_{min}/R_x = 7.43\left(1 - 0.85e^{-0.31k}\right) U^{0.65}\, W^{-0.21} \qquad \text{(Eq. A-9)}$$

$$h_c/R_x = 7.32\left(1 - 0.73e^{-0.28k}\right)U^{0.64}\,W^{-0.22} \qquad \text{(Eq. A-10)}$$

The tribological test conditions employed in Chapter 4 and Chapter 6 are located at the borderline between Piezoviscous-Elastic lubrication (hard EHL) and Isoviscous-Elastic lubrication (soft EHL). Therefore, the minimum oil film thicknesses were estimated from Eq. A-7 for hard EHL contacts and Eq. A-9 for soft EHL contacts, as shown in Table A.1 and Table A.2. From both equations, the values of the oil film thickness gradually increase with the higher viscosity grades of PAOs. Pure PEEK-steel contacts give similar values from both equations, while CFR PEEK-steel and GFR PEEK-steel contacts provide higher values from Eq. A-7 for hard EHL contacts than from Eq. A-9 for soft EHL contacts. The higher Young's modulus of CFR PEEK and GFR PEEK makes their contacts with steel more like at hard EHL contacts and thus Eq. A-7 for hard EHL contacts is more appropriate in this study. Therefore, the values of oil film thickness listed in Table A.1 were used to determine the Lambda ratios at the operating conditions in section 4.3.3 and section 6.3.3.

Table A.1. Minimum oil film thicknesses estimated from Eq. A-7 for hard EHL contacts

Material pairing		PAO2	PAO4	PAO10
Pure PEEK	Steel	25 nm	75 nm	224 nm
CFR PEEK	Steel	20 nm	61 nm	182 nm
GFR PEEK	Steel	22 nm	67 nm	198 nm

Table A.2. Minimum oil film thicknesses estimated from Eq. A-9 for soft EHL contacts

Material pairing		PAO2	PAO4	PAO10
Pure PEEK	Steel	25 nm	64 nm	168 nm
CFR PEEK	Steel	11 nm	29 nm	77 nm
GFR PEEK	Steel	16 nm	40 nm	106 nm

List of References

[1] Sinha, S. K., and Briscoe, B. J., eds., 2009, *Polymer Tribology*, Imperial College Press, London, UK.

[2] Myshkin, N. K., Pesetskii, S. S., and Grigoriev, A. Y., 2015, "Polymer Tribology: Current State and Applications," Tribology in Industry, 37, 3, 284–290.

[3] Friedrich, K., 2018, "Polymer Composites for Tribological Applications," Advanced Industrial and Engineering Polymer Research, 1, 1, 3–39.

[4] Kurdi, A., and Chang, L., 2018, "Recent Advances in High Performance Polymers – Tribological Aspects," Lubricants, 7, 1, 2–10.

[5] Gandhi, R., Jayawant, A., Bhalerao, A., and Dandagwhal, R., 2018, "Applicability of Composite Polymer Gear in Low RPM Applications – a Review," International Journal of Engineering Science Invention, 7, 4, 36–41.

[6] Nunez, E. E., Gheisari, R., and Polycarpou, A. A., 2019, "Tribology Review of Blended Bulk Polymers and Their Coatings for High-Load Bearing Applications," Tribology International, 129, July 2018, 92–111.

[7] Cole, G. S., and Sherman, A. M., 1995, "Light Weight Materials for Automotive Applications," Materials Characterization, 35, 1, 3–9.

[8] Immarigeon, J. P., Holt, R. T., Koul, A. K., Zhao, L., Wallace, W., and Beddoes, J. C., 1995, "Lightweight Materials for Aircraft Applications," Materials Characterization, 35, 1, 41–67.

[9] Volpe, V., Lanzillo, S., Affinita, G., Villacci, B., Macchiarolo, I., and Pantani, R., 2019, "Lightweight High-Performance Polymer Composite for Automotive Applications," 1–16.

[10] Tung, S. C., and McMillan, M. L., 2004, "Automotive Tribology Overview of Current Advances and Challenges for the Future," Tribology International, 37, 7, 517–536.

[11] Taywade, A. N., and Arajpure, V. G., 2014, "Design and Development of Nylon 66 Plastic Helical Gears in Automobile Application," International Journal of Engineering Research & Technology (IJERT) ISSN: 2278-0181, 3, 9, 1330–1334.

[12] Walton, D., and Shi, Y. W., 1989, "A Comparison of Ratings for Plastic Gears," Proceedings of the Institution of Mechanical Engineers, Part C: Journal of Mechanical Engineering Science, 203, 1, 31–38.

[13] Li, W., Wood, A., Weidig, R., and Mao, K., 2011, “An Investigation on the Wear Behaviour of Dissimilar Polymer Gear Engagements,” Wear, 271, 9–10, 2176–2183.

[14] Mertens, A. J., and Senthilvelan, S., 2015, “Durability Enhancement of Polymer Gear Using Compressed Air Cooling,” Proceedings of the Institution of Mechanical Engineers, Part L: Journal of Materials: Design and Applications, 230, 2, 515–525.

[15] Singh, A. K., Siddhartha, and Singh, P. K., 2018, “Polymer Spur Gears Behaviors under Different Loading Conditions: A Review,” Proceedings of the Institution of Mechanical Engineers, Part J: Journal of Engineering Tribology, 232, 2, 210–228.

[16] Avanzini, A., Donzella, G., Mazzù, A., and Petrogalli, C., 2013, “Wear and Rolling Contact Fatigue of PEEK and PEEK Composites,” Tribology International, 57, 22–30.

[17] Kalin, M., and Kupec, A., 2017, “The Dominant Effect of Temperature on the Fatigue Behaviour of Polymer Gears,” Wear, 376–377, 1339–1346.

[18] Harrass, M., Friedrich, K., and Almajid, A. A., 2010, “Tribological Behavior of Selected Engineering Polymers under Rolling Contact,” Tribology International, 43, 3, 635–646.

[19] Kurdi, A., Kan, W. H., and Chang, L., 2019, “Tribological Behaviour of High Performance Polymers and Polymer Composites at Elevated Temperature,” Tribology International, 130, June 2018, 94–105.

[20] Lu, Z. P., and Friedrich, K., 1995, “On Sliding Friction and Wear of PEEK and Its Composites,” Wear, 181–183, 624–631.

[21] Moder, J., Grün, F., Summer, F., Kohlhauser, M., and Wohlfahrt, M., 2018, “Application of High Performance Composite Polymers with Steel Counterparts in Dry Rolling/Sliding Contacts,” Polymer Testing, 66, January, 371–382.

[22] Greco, A. C., Erck, R., Ajayi, O., and Fenske, G., 2011, “Effect of Reinforcement Morphology on High-Speed Sliding Friction and Wear of PEEK Polymers,” Wear, 271, 9–10, 2222–2229.

[23] Rodriguez, V., Sukumaran, J., Schlarb, A. K., and De Baets, P., 2016, “Influence of Solid Lubricants on Tribological Properties of Polyetheretherketone (PEEK),” Tribology International, 103, 45–57.

[24] Kumar, D., Rajmohan, T., and Venkatachalapathi, S., 2018, “Wear Behavior of PEEK Matrix Composites: A Review,” Materials Today: Proceedings, 5, 6, 14583–14589.

[25] Dickens, P. M., Sullivan, J. L., and Lancaster, J. K., 1986, “Speed Effects on the Dry and Lubricated Wear of Polymers,” Wear, 112, 3–4, 273–289.

[26] Jia, J., Chen, J., Zhou, H., and Hu, L., 2004, “Comparative Study on Tribological Behaviors of Polyetheretherketone Composite Reinforced with Carbon Fiber and Polytetrafluoroethylene under Water-Lubricated and Dry-Sliding against Stainless Steel,” Tribology Letters, 17, 2, 231–238.

[27] Sumer, M., Unal, H., and Mimaroglu, A., 2008, “Evaluation of Tribological Behaviour of PEEK and Glass Fibre Reinforced PEEK Composite under Dry Sliding and Water Lubricated Conditions,” Wear, 265, 7–8, 1061–1065.

[28] Zhang, D., Qi, H., Zhao, F., Zhang, G., Wang, T., and Wang, Q., 2017, “Tribological Performance of PPS Composites under Diesel Lubrication Conditions,” Tribology International, 115, May, 338–347.

[29] Samad, M. A., and Sinha, S. K., 2011, “Dry Sliding and Boundary Lubrication Performance of a UHMWPE/CNTs Nanocomposite Coating on Steel Substrates at Elevated Temperatures,” Wear, 270, 5–6, 395–402.

[30] Lancaster, J. K., 1972, “Lubrication of Carbon Fibre-Reinforced Polymers Part I - Water and Aqueous Solutions,” Wear, 20, 315–333.

[31] Yamamoto, Y., and Hashimoto, M., 2002, “Friction and Wear of Water Lubricated PEEK and PPS Sliding Contacts,” Wear, 253, 7–8, 820–826.

[32] Kurdi, A., Wang, H., and Chang, L., 2018, “Effect of Nano-Sized TiO2 Addition on Tribological Behaviour of Poly Ether Ether Ketone Composite,” Tribology International, 117, August 2017, 225–235.

[33] Zhang, G., Wetzel, B., and Wang, Q., 2015, “Tribological Behavior of PEEK-Based Materials under Mixed and Boundary Lubrication Conditions,” Tribology International, 88, 153–161.

[34] Jacobs, O., Jaskulka, R., Yan, C., and Wu, W., 2005, “On the Effect of Counterface Material and Aqueous Environment on the Sliding Wear of Carbon Fibre Reinforced Polyetheretherketone (PEEK),” Tribology Letters, 19, 4, 319–329.

[35] Loy, X. Z. K., and Sinha, S. K., 2012, “Lubrication of Polyether Ether Ketone (PEEK) Surface by Liquid Ultrathin Films for High Wear Durability,” Wear, 296, 1–2, 681–692.

[36] Brown, S. F., 2015, “Base Oil Groups: Manufacture, Properties, and Performance,” Tribology and Lubrication Technology, 71, 4, 32–35.

[37] Johnson, D. W., 2016, “Lubricants for Turbine Engines,” Recent Progress in Some Aircraft Technologies, September.

[38] Sniderman, D., 2017, “The Chemistry and Function of Lubricant Additives,” Tribology and Lubrication Technology, 73, 11, 18–28.

[39] Spikes, H. A., 2004, “The History and Mechanisms of ZDDP,” Tribology Letters, 17, 3, 469–489.

[40] Spikes, H., 2015, “Friction Modifier Additives,” Tribology Letters, 60, 1, 1–26.

[41] Jost, H. P., 1990, “Tribology - Origen and Future,” Wear, 136, 1–17.

[42] Holmberg, K., and Erdemir, A., 2017, “Influence of Tribology on Global Energy Consumption, Costs and Emissions,” Friction, 5, 3, 263–284.

[43] Jensen, W. B., 2009, “The Origin of the Polymer Concept,” Journal of Chemical Education, 85, 5, 624.

[44] Klein, R., 2011, “Material Properties of Plastics,” *Laser Welding of Plastics*, Wiley-VCH Verlag GmbH, Weinheim, Germany, 3–69.

[45] Scott, D., Blackwell, J., McCullagh, P. J., and Mills, G. H., 1970, “Composite Materials for Rolling Bearing Cages,” Wear, 15, 4, 257–269.

[46] Koike, H., Kida, K., Santos, E. C., Rozwadowska, J., Kashima, Y., and Kanemasu, K., 2012, “Self-Lubrication of PEEK Polymer Bearings in Rolling Contact Fatigue under Radial Loads,” Tribology International, 49, June 2014, 30–38.

[47] Sreenilayam-Raveendran, R. K., Azarian, M. H., Morillo, C., Pecht, M. G., Kida, K., Santos, E. C., Honda, T., and Koike, H., 2013, “Comparative Evaluation of Metal and Polymer Ball Bearings,” Wear, 302, 1–2, 1499–1505.

[48] Kleiss, B. R., 2011, “Take a PEEK at Polymer,” Gear Solutions, January, 32–37.

[49] Small, G., 2014, “Outstanding Physical Properties Make PEEK Ideal for Sealing Applications,” Sealing Technology, 2014, 4, 9–12.

[50] Thomas Krause, 2016, *SKF Polymer Products and Components*.

[51] Friedrich, K., Chang, L., and Haupert, F., 2011, “Current and Future Applicaitons of Polymer Composites in the Field of Tribology,” *Composite Materials, A Vision for the Future*, Springer-Verlag London, London, UK, 129–167.

[52] Fox, M., 2016, “Polymer Tribology,” Lube Magazine, 135, 32–37.

[53] Sinha, S. K., Chong, W. L. M., and Lim, S. C., 2007, “Scratching of Polymers-Modeling Abrasive Wear,” Wear, 262, 9–10, 1038–1047.

[54] Myshkin, N. K., Petrokovets, M. I., and Kovalev, A. V., 2005, “Tribology of Polymers: Adhesion, Friction, Wear, and Mass-Transfer,” Tribology International, 38, 11-12 SPEC. ISS., 910–921.

[55] Brostow, W., Kovacevic, V., Vrsaljko, D., Kovačević, V., and Whitworth, J., 2010, “Tribology of Polymers and Polymer-Based Composites,” Journal of Materials Education, 32, 6, 5–6.

[56] Kalácska, G., 2013, “An Engineering Approach to Dry Friction Behaviour of Numerous Engineering Plastics with Respect to the Mechanical Properties,” Express Polymer Letters, 7, 2, 199–210.

[57] Myshkin, N., and Kovalev, A., 2018, “Adhesion and Surface Forces in Polymer Tribology—A Review,” Friction, 6, 2, 143–155.

[58] Prabhakar, K., Debnath, S., Ganesan, R., and Palanikumar, K., 2018, “A Review of Mechanical and Tribological Behaviour of Polymer Composite Materials,” IOP Conference Series: Materials Science and Engineering, 344, 1.

[59] Aldousiri, B., Shalwan, A., and C.W., C., 2013, “A Review on Tribological Behaviour of Natural Reinforced Composites,” Advances in Materials Science and Engineering, 2013, 1–8.

[60] Theiler, G., and Gradt, T., 2015, “Friction and Wear Behaviour of Graphite Filled Polymer Composites in Hydrogen Environment,” Tribology Online, 10, 2, 207–212.

[61] Pogačnik, A., Kupec, A., and Kalin, M., 2017, “Tribological Properties of Polyamide (PA6) in Self-Mated Contacts and against Steel as a Stationary and Moving Body,” Wear, 378–379, 17–26.

[62] Theiler, G., Harsha, A. P., and Gradt, T., 2019, “On the Sliding Wear Behavior of PAEK Composites in Vacuum Environment,” Journal of Tribology, 141, 4, 1–7.

[63] Kumar, V., Sinha, S. K., and Agarwal, A. K., 2017, “Tribological Studies of Epoxy Composites with Solid and Liquid Fillers,” Tribology International, 105, May 2016, 27–36.

[64] Minami, I., Kubo, T., Nanao, H., Mori, S., Iwata, H., and Fujita, M., 2008, “Surface Chemistry for Improvement in Load-Carrying Capacity of Poly(Ether-Ether-Ketone)-Based Materials by Poly(Tetrafluoroethylene),” Tribology Online, 3, 3, 190–194.

[65] Burris, D. L., Boesl, B., Bourne, G. R., and Sawyer, W. G., 2007, “Polymeric Nanocomposites for Tribological Applications,” Macromolecular Materials and Engineering, 292, 4, 387–402.

[66] Chang, L., and Friedrich, K., 2010, “Enhancement Effect of Nanoparticles on the Sliding Wear of Short Fiber-Reinforced Polymer Composites: A Critical Discussion of Wear Mechanisms,” Tribology International, 43, 12, 2355–2364.

[67] Zhang, G., Sebastian, R., Burkhart, T., and Friedrich, K., 2012, “Role of Monodispersed Nanoparticles on the Tribological Behavior of Conventional Epoxy Composites Filled with Carbon Fibers and Graphite Lubricants,” Wear, 292–293, 176–187.

[68] J. K. Lancaster, 1978, “Dry Bearings: A Survey of Materials and Factors Affecting Their Performance,” TRIBOLOGY, 6, 6, 219–251.

[69] Pogačnik, A., and Tavčar, J., 2015, “An Accelerated Multilevel Test and Design Procedure for Polymer Gears,” Materials and Design, 65, 961–973.

[70] Gurunathan, C., Kirupasankar, S., and Gnanamoorthy, R., 2011, “Wear Characteristics of Polyamide Nanocomposite Spur Gears,” Proceedings of the Institution of Mechanical Engineers, Part J: Journal of Engineering Tribology, 225, 5, 299–306.

[71] Zorko, D., Kulovec, S., Duhovnik, J., and Tavčar, J., 2019, “Durability and Design Parameters of a Steel/PEEK Gear Pair,” Mechanism and Machine Theory, 140, 825–846.

[72] Düzcükoğlu, H., 2009, “PA 66 Spur Gear Durability Improvement with Tooth Width Modification,” Materials and Design, 30, 4, 1060–1067.

[73] Mao, K., Langlois, P., Hu, Z., Alharbi, K., Xu, X., Milson, M., Li, W., Hooke, C. J., and Chetwynd, D., 2015, “The Wear and Thermal Mechanical Contact Behaviour of Machine Cut Polymer Gears,” Wear, 332–333, 822–826.

[74] Terashima, K., Tukamoto, N., and Nishida, N., 1986, “Development of Plastic Gears for Power Transmission (Design on Load-Carrying Capacity),” Bulletin of JSME, 29, 250, 1326.

[75] Mao, K., 2007, “A New Approach for Polymer Composite Gear Design,” Wear, 262, 3–4, 432–441.

[76] Shooter, K. V., and Tabor, D., 1952, “The Frictional Properties of Plastics,” Proceedings of the Physical Society. Section B, 65, 9, 661–671.

[77] Ludema, K. C., and TABOR, D., 1966, “THE FRICTION AND VISCO-ELASTIC PROPERTIES OF POLYMERIC SOLIDS,” Wear, 9, 329–348.

[78] Pogačnik, A., and Kalin, M., 2012, “Parameters Influencing the Running-in and Long-Term Tribological Behaviour of Polyamide (PA) against Polyacetal (POM) and Steel,” Wear, 290–291, 140–148.

[79] Wang, M., Zhang, C., and Wang, X., 2017, “The Wear Behavior of Textured Steel Sliding against Polymers,” Materials, 10, 4.

[80] Rhee, S. H., and Ludema, K. C., 1978, “Mechanism of Formation of Polymeric Transfer Films,” Wear, 46, 231–240.

[81] Bahadur, S., 2000, “The Development of Transfer Layers and Their Role in Polymer Tribology,” Wear, 245, 1–2, 92–99.

[82] Briscoe, B. J., and Sinha, S. K., 2002, “Wear of Polymers,” Proceedings of the Institution of Mechanical Engineers, Part J: Journal of Engineering Tribology, 216, 6, 401–413.

[83] Nunez, E. E., and Polycarpou, A. A., 2015, “The Effect of Surface Roughness on the Transfer of Polymer Films under Unlubricated Testing Conditions,” Wear, 326–327, 74–83.

[84] Chang, L., Friedrich, K., and Ye, L., 2013, “Study on the Transfer Film Layer in Sliding Contact Between Polymer Composites and Steel Disks Using Nanoindentation,” Journal of Tribology, 136, 2, 021602.

[85] Stuart, B. H., and Briscoe, B. J., 1996, “Scratch Hardness Studies of Poly(Ether Ether Ketone),” Polymer, 37, 17, 3819–3824.

[86] Patel, P., Hull, T. R., McCabe, R. W., Flath, D., Grasmeder, J., and Percy, M., 2010, “Mechanism of Thermal Decomposition of Poly(Ether Ether Ketone) (PEEK) from a Review of Decomposition Studies,” Polymer Degradation and Stability, 95, 5, 709–718.

[87] Shukla, D., Negi, Y. S., Uppadhyaya, J. Sen, and Kumar, V., 2012, “Synthesis and Modification of Poly(Ether Ether Ketone) and Their Properties: A Review,” Polymer Reviews, 52, 2, 189–228.

[88] Zhang, L. Z., Li, M., and Hu, H., 2012, “Study on Mechanical Properties of PEEK Composites,” Advanced Materials Research, 476–478, 519–525.

[89] Sarasua, J. R., Remiro, P. M., and Pouyet, J., 1995, “The Mechanical Behaviour of PEEK Short Fibre Composites,” Journal of Materials Science, 30, 13, 3501–3508.

[90] Puhan, D., and Wong, J. S. S., 2019, “Properties of Polyetheretherketone (PEEK) Transferred Materials in a PEEK-Steel Contact,” Tribology International, 135, February, 189–199.

[91] Laux, K. A., and Schwartz, C. J., 2013, “Influence of Linear Reciprocating and Multi-Directional Sliding on PEEK Wear Performance and Transfer Film Formation,” Wear, 301, 1–2, 727–734.

[92] Ovaert, T. C., and Cheng, S. C., 1991, “Counterface Topographical Effects on the Wear of Polyetheretherketone and a Polyetheretherketone-Carbon Fiber Composite,” Wear, 150, 1–2, 275–287.

[93] Friedrich, K., Karger-Kocsis, J., and Lu, Z., 1991, “Effects of Steel Counterface Roughness and Temperature on the Friction and Wear of PE(E)K Composites under Dry Sliding Conditions,” Wear, 148, 2, 235–247.

[94] Pei, X. Q., Bennewitz, R., and Schlarb, A. K., 2015, “Mechanisms of Friction and Wear Reduction by Carbon Fiber Reinforcement of PEEK,” Tribology Letters, 58, 3.

[95] Zhang, G., Rasheva, Z., and Schlarb, A. K., 2010, “Friction and Wear Variations of Short Carbon Fiber (SCF)/PTFE/Graphite (10 Vol.%) Filled PEEK: Effects of Fiber Orientation and Nominal Contact Pressure,” Wear, 268, 7–8, 893–899.

[96] Zalaznik, M., Kalin, M., Novak, S., and Jakša, G., 2016, “Effect of the Type, Size and Concentration of Solid Lubricants on the Tribological Properties of the Polymer PEEK,” Wear, 364–365, 31–39.

[97] Kalin, M., Zalaznik, M., and Novak, S., 2015, “Wear and Friction Behaviour of Poly-Ether-Ether-Ketone (PEEK) Filled with Graphene, WS2 and CNT Nanoparticles,” Wear, 332–333, 855–862.

[98] Bhushan, B., 2013, *Introduction to Tribology, Second Edition*.

[99] Stachowiak, G. W., and Batchelor, A. W., 2006, *Engineering Tribology, Third Edition*.

[100] Miller, A., 2009, “The Chemistry of Lubricating Oil Additives,” Journal of Chemical Education, 33, 7, 308.

[101] Minami, I., 2017, “Molecular Science of Lubricant Additives,” Applied Sciences, 7, 5, 445–477.

[102] Tang, Z., and Li, S., 2014, “A Review of Recent Developments of Friction Modifiers for Liquid Lubricants (2007-Present),” Current Opinion in Solid State and Materials Science, 18, 3, 119–139.

[103] Beltzer, M., and Jahanmir, S., 1988, “Effect of Additive Molecular Structure on Friction,” Lubrication Science, 1, 1, 3–26.

[104] Studt, P., 1989, “Boundary Lubrication: Adsorption of Oil Additives on Steel and Ceramic Surfaces and Its Influence on Friction and Wear,” Tribology International, 22, 2, 111–119.

[105] Ratoi, M., Anghel, V., Bovington, C., and Spikes, H. A., 2000, “Mechanisms of Oiliness Additives,” Tribology International, 33, 3–4, 241–247.

[106] Ratoi, M., Bovington, C., and Spikes, H., 2003, “In Situ Study of Metal Oleate Friction Modifier Additives,” Tribology Letters, 14, 1, 33–40.

[107] Hirayama, T., Torii, T., Konishi, Y., Maeda, M., Matsuoka, T., Inoue, K., Hino, M., Yamazaki, D., and Takeda, M., 2012, “Thickness and Density of Adsorbed Additive Layer on Metal Surface in Lubricant by Neutron Reflectometry,” Tribology International, 54, 100–105.

[108] Simič, R., and Kalin, M., 2013, “Adsorption Mechanisms for Fatty Acids on DLC and Steel Studied by AFM and Tribological Experiments,” Applied Surface Science, 283, 460–470.

[109] Loehle, S., Matta, C., Minfray, C., Mogne, T. Le, Martin, J. M., Iovine, R., Obara, Y., Miura, R., and Miyamoto, A., 2014, “Mixed Lubrication with C18 Fatty Acids: Effect of Unsaturation,” Tribology Letters, 53, 1, 319–328.

[110] Nakano, K., and Spikes, H. A., 2012, “Process of Boundary Film Formation from Fatty Acid Solution,” Tribology Online, 7, 1, 1–7.

[111] Nalam, P. C., Pham, A., Castillo, R. V., and Espinosa-Marzal, R. M., 2019, “Adsorption Behavior and Nanotribology of Amine-Based Friction Modifiers on Steel Surfaces,” Journal of Physical Chemistry C, 123, 22, 13672–13680.

[112] Bec, S., Tonck, A., Georges, J. M., Coy, R. C., Bell, J. C., and Roper, G. W., 1999, “Relationship between Mechanical Properties and Structures of Zinc Dithiophosphate Anti-

Wear Films," Proceedings of the Royal Society A: Mathematical, Physical and Engineering Sciences, 455, 1992, 4181–4203.

[113] Nicholls, M. A., Do, T., Norton, P. R., Kasrai, M., and Bancroft, G. M., 2005, "Review of the Lubrication of Metallic Surfaces by Zinc Dialkyl-Dithiophosphates," Tribology International, 38, 1, 15–39.

[114] Guan, B., Pochopien, B. A., and Wright, D. S., 2016, "The Chemistry, Mechanism and Function of Tricresyl Phosphate (TCP) as an Anti-Wear Lubricant Additive," Lubrication Science, 28, 257–265.

[115] Papay, A. G., 1998, "Antiwear and Extreme-Pressure Additives in Lubricants," Lubrication Science, 10, 3, 209–224.

[116] Ueda, M., Spikes, H., and Kadiric, A., 2019, "In-Situ Observations of the Effect of the ZDDP Tribofilm Growth on Micropitting," Tribology International, 138, May, 342–352.

[117] Stolarski, T. A., 1992, "Tribology of Polyetheretherketone," Wear, 158, 1–2, 71–78.

[118] Yamamoto, Y., and Hashimoto, M., 2004, "Friction and Wear of Water Lubricated PEEK and PPS Sliding Contacts Part 2. Composites with Carbon or Glass Fibre," Wear, 257, 1–2, 181–189.

[119] Jia, B. Bin, Li, T. S., Liu, X. J., and Cong, P. H., 2007, "Tribological Behaviors of Several Polymer-Polymer Sliding Combinations under Dry Friction and Oil-Lubricated Conditions," Wear, 262, 11–12, 1353–1359.

[120] Chen, B., Yang, J., Wang, J., Liu, N., and Yan, F., 2015, "Comparative Investigation on the Friction and Wear Behaviors of Carbon Fabric–Reinforced Phenolic Composites under Seawater Lubrication," Tribology Transactions, 58, 1, 140–147.

[121] Gao, C., Fan, S., Zhang, S., Zhang, P., and Wang, Q., 2018, "Enhancement of Tribofilm Formation from Water Lubricated PEEK Composites by Copper Nanowires," Applied Surface Science, 444, 364–376.

[122] Sarita, B., and Senthilvelan, S., 2019, "Effects of Lubricant on the Surface Durability of an Injection Molded Polyamide 66 Spur Gear Paired with a Steel Gear," Tribology International, 137, February, 193–211.

[123] Lu, Z., Liu, H., Zhu, C., Song, H., and Yu, G., 2019, "Identification of Failure Modes of a PEEK-Steel Gear Pair under Lubrication," International Journal of Fatigue, 125, April, 342–348.

[124] Zhang, G., Burkhart, T., and Wetzel, B., 2013, “Tribological Behavior of Epoxy Composites under Diesel-Lubricated Conditions,” Wear, 307, 1–2, 174–181.

[125] Zhao, F., Li, G., Österle, W., Häusler, I., Zhang, G., Wang, T., and Wang, Q., 2016, “Tribological Investigations of Glass Fiber Reinforced Epoxy Composites under Oil Lubrication Conditions,” Tribology International, 103, 208–217.

[126] Chen, B., Wang, J., and Yan, F., 2012, “Comparative Investigation on the Tribological Behaviors of CF/PEEK Composites under Sea Water Lubrication,” Tribology International, 52, 170–177.

[127] Chen, B., Wang, J., and Yan, F., 2011, “Friction and Wear Behaviors of Several Polymers Sliding against GCr15 and 316 Steel under the Lubrication of Sea Water,” Tribology Letters, 42, 1, 17–25.

[128] Yamaguchi, T., and Hokkirigawa, K., 2016, “Friction and Wear Properties of Peek Resin Filled with RB Ceramics Particles under Water Lubricated Condition,” Tribology O, 11, 6, 653–660.

[129] Wang, A., Yan, S., Lin, B., Zhang, X., and Zhou, X., 2017, “Aqueous Lubrication and Surface Microstructures of Engineering Polymer Materials (PEEK and PI) When Sliding against Si3N4,” Friction, 5, 4, 414–428.

[130] Al-Jeboori, Y., Kosarieh, S., Morina, A., and Neville, A., 2018, “Investigation of Pure Sliding and Sliding/Rolling Contacts in a DLC/Cast Iron System When Lubricated in Oils Containing MoDTC-Type Friction Modifier,” Tribology International, 122, December 2017, 23–37.

[131] Haque, T., Korres, S., Carey, J. T., Jacobs, P. W., Loos, J., and Franke, J., 2018, “Lubricant Effects on White Etching Cracking Failures in Thrust Bearing Rig Tests,” Tribology Transactions, 61, 6, 979–990.

[132] Wright, N. A., and Kukureka, S. N., 2001, “Wear Testing and Measurement Techniques for Polymer Composite Gears,” Wear, 250–251, PART 2, 1567–1578.

[133] Rycerz, P., and Kadiric, A., 2019, “The Influence of Slide–Roll Ratio on the Extent of Micropitting Damage in Rolling–Sliding Contacts Pertinent to Gear Applications,” Tribology Letters, 67, 2, 1–20.

[134] Li, X., and Bhushan, B., 2002, “A Review of Nanoindentation Continuous Stiffness Measurement Technique and Its Applications,” Materials Characterization, 48, 11–36.

[135] Iqbal, T., Briscoe, B. J., and Luckham, P. F., 2011, “Surface Plasticization of Poly(Ether Ether Ketone),” European Polymer Journal, 47, 12, 2244–2258.

[136] Voyiadjis, G. Z., Samadi-Dooki, A., and Malekmotiei, L., 2017, “Nanoindentation of High Performance Semicrystalline Polymers: A Case Study on PEEK,” Polymer Testing, 61, 57–64.

[137] Laigo, J., Christien, F., Le Gall, R., Tancret, F., and Furtado, J., 2008, “SEM, EDS, EPMA-WDS and EBSD Characterization of Carbides in HP Type Heat Resistant Alloys,” Materials Characterization, 59, 11, 1580–1586.

[138] Newbury, D. E., and Ritchie, N. W. M., 2014, “Performing Elemental Microanalysis with High Accuracy and High Precision by Scanning Electron Microscopy/Silicon Drift Detector Energy-Dispersive X-Ray Spectrometry (SEM/SDD-EDS),” Journal of Materials Science, 50, 2, 493–518.

[139] Ellis, G., Naffakh, M., Marco, C., and Hendra, P. J., 1997, “Fourier Transform Raman Spectroscopy in the Study of Technological Polymers Part 1: Poly(Aryl Ether Ketones), Their Composites and Blends,” Spectrochimica Acta - Part A: Molecular and Biomolecular Spectroscopy, 53, 13, 2279–2294.

[140] Stuart, B. H., 1998, “Application of Raman Spectroscopy to the Tribology of Polymers,” Tribology International, 31, 11, 687–693.

[141] Zimmerman, D. A., Koenig, J. L., and Ishida, H., 1999, “Infrared and Raman Spectroscopy of Cyclohexa(p-Phenylene Sulfide) and the Polymer Obtained Therefrom,” Polymer, 40, 17, 4723–4731.

[142] Doumeng, M., Ferry, F., Delbé, K., Mérian, T., Chabert, F., Berthet, F., Marsan, O., Nassiet, V., and Denape, J., 2019, “Evolution of Crystallinity of PEEK and Glass-Fibre Reinforced PEEK under Tribological Conditions Using Raman Spectroscopy,” Wear, 426–427, September 2018, 1040–1046.

[143] Schallamach, A., 1958, “Friction and Abrasion of Rubber,” Wear, 1, 5, 384–417.

[144] Persson, B. N. J., 2001, “Theory of Rubber Friction and Contact Mechanics,” Journal of Chemical Physics, 115, 8, 3840–3861.

[145] Maegawa, S., Itoigawa, F., and Nakamura, T., 2015, “Effect of Normal Load on Friction Coefficient for Sliding Contact between Rough Rubber Surface and Rigid Smooth Plane,” Tribology International, 92, September, 335–343.

[146] Bonne, M., Briscoe, B. J., Lawrence, C. J., Manimaaran, S., Parsonage, D., and Allan, A., 2005, “Nano-Indentation of Scratched Poly(Methyl Methacrylate) Surfaces,” Tribology Letters, 18, 2, 125–133.

[147] Li, T. Q., Zhang, M. Q., Song, L., and Zeng, H. M., 1999, “Friction Induced Mechanochemical and Mechanophysical Changes in High Performance Semicrystalline Polymer,” Polymer, 40, 16, 4451–4458.

[148] Pei, X. Q., Lin, L., Schlarb, A. K., and Bennewitz, R., 2019, “Correlation of Friction and Wear across Length Scales for PEEK Sliding against Steel,” Tribology International, 136, April, 462–468.

[149] Pei, X. Q., Lin, L. Y., Schlarb, A. K., and Bennewitz, R., 2016, “Novel Experiments Reveal Scratching and Transfer Film Mechanisms in the Sliding of the PEEK/Steel Tribosystem,” Tribology Letters, 63, 3, 1–9.

[150] Hamrock, B. J., and Dowson, D., 1976, “Isothermal Elastohydrodynamic Lubrication of Point Contacts III - Fully Flooded Results,” NASA Technical Note, D-8317.

[151] Hamrock, B. J., and Dowson, D., 1977, “Elastohydrodynamic Lubrication of Elliptical Contacts for Materials of Low Elastic Modulus. 1-Fully Flooded Conjunction.,” NASA Technical Note, D-8528.

[152] Ratoi, M., Niste, V. B., Alghawel, H., Suen, Y. F., and Nelson, K., 2014, “The Impact of Organic Friction Modifiers on Engine Oil Tribofilms,” RSC Advances, 4, 9, 4278–4285.

[153] Salensky, G. A., Cobb, M. G., and Everhart, D. S., 1986, “Corrosion-Inhibitor Orientation on Steel,” Industrial and Engineering Chemistry Product Research and Development, 25, 2, 133–140.

[154] Kaskah, S. E., Pfeiffer, M., Klock, H., Bergen, H., Ehrenhaft, G., Ferreira, P., Gollnick, J., and Fischer, C. B., 2017, “Surface Protection of Low Carbon Steel with N-Acyl Sarcosine Derivatives as Green Corrosion Inhibitors,” Surfaces and Interfaces, 9, August, 70–78.

[155] Chen, H. L., You, J. W., and Porter, R. S., 1996, “Intermolecular Interaction and Conformation in Poly(Ether Ether Ketone)/Poly(Ether Imide) Blends - an Infrared Spectroscopic Investigation,” Journal of Polymer Research, 3, 3, 151–158.

[156] Roy, S., Sahoo, N. G., Kuo, H., Cheng, F., Das, C. K., Chan, S. H., and Li, L., 2011, “Molecular Interaction and Properties of Poly(Ether Ether Ketone)/Liquid Crystalline Polymer Blends

Incorporated with Functionalized Carbon Nanotubes," Journal of Nanoscience and Nanotechnology, 11, 12, 10408–10416.

[157] Li, D., Shi, D., Feng, K., Li, X., and Zhang, H., 2017, "Poly(Ether Ether Ketone) (PEEK) Porous Membranes with Super High Thermal Stability and High Rate Capability for Lithium-Ion Batteries," Journal of Membrane Science, 530, 125–131.

[158] Davim, J. P., and Cardoso, R., 2009, "Effect of the Reinforcement (Carbon or Glass Fibres) on Friction and Wear Behaviour of the PEEK against Steel Surface at Long Dry Sliding," Wear, 266, 7–8, 795–799.

[159] Kunishima, T., Nagai, Y., Kurokawa, T., Bouvard, G., Abry, J. C., Fridrici, V., and Kapsa, P., 2020, "Tribological Behavior of Glass Fiber Reinforced-PA66 in Contact with Carbon Steel under High Contact Pressure, Sliding and Grease Lubricated Conditions," Wear, 456–457, March.

[160] Fujita, H., and Spikes, H. A., 2004, "The Formation of Zinc Dithiophosphate Antiwear Films," Proceedings of the Institution of Mechanical Engineers, Part J: Journal of Engineering Tribology, 218, 4, 265–277.

[161] Smith, G. C., and Bell, J. C., 1999, "Multi-Technique Surface Analytical Studies of Automotive Anti-Wear Films," Applied Surface Science, 144–145, 222–227.

[162] Onumata, Y., Zhao, H., Wang, C., Morina, A., and Neville, A., 2018, "Interactive Effect between Organic Friction Modifiers and Additives on Friction at Metal Pushing V-Belt CVT Components," Tribology Transactions, 61, 3, 474–481.

[163] Guegan, J., Southby, M., and Spikes, H., 2019, "Friction Modifier Additives, Synergies and Antagonisms," Tribology Letters, 67, 3, 1–12.